TECHNISCHE UNIVERSITÄT MÜNCHEN

Ingenieurfakultät Bau Geo Umwelt
Lehrstuhl für Verkehrswegebau

Road Infrastructure Design towards Passenger Ride Comfort for Autonomous Public Transport

Te Ron Nguyen Van

"Out of clutter, find Simplicity. From discord, find Harmony. In the middle of difficulty lies Opportunity."

– Albert Einstein

PREFACE

In fulfilment of the requirements for the degree of Dr.-Ing, this publication-based dissertation, entitled "Road Infrastructure Design towards Passenger Ride Comfort for Autonomous Public Transport", was submitted to the Technische Universität München. I am the first author, under the name **Teron Nguyen,** in the five accompanying journal papers. For most of the work, I am responsible for the conceptual design of the research, data acquisition and analysis, and drafting all manuscripts. The co-authors provided the supervision of the project, knowledge discussion, revision of the papers and endorsement of the papers to be published.

The five papers including four published journal articles and one under-review manuscript, are listed below, and with full details in Appendices 1-5.

1. **Nguyen, T.**, Lechner, B., Wong, Y.D. (2019). Response-type methods to evaluate road roughness: a state-of-the-art review. *European Transport Research Review,* 11(1), 43, doi: 10.1186/s12544-019-0380-6.

2. **Nguyen, T.**, Swolana, P., Lechner, B., & Wong, Y.D. An experimental comparison of mathematical heavy-duty city bus models to evaluate passenger ride comfort induced by road roughness. *Mathematical and Computer Modelling of Dynamical Systems* (Under review).

3. **Nguyen, T.**, Lechner, B., Wong, Y.D., & Tan, J. Y. (2019). Bus ride index - A refined approach to evaluating road surface irregularities. *Road Material and Pavement Design*, doi: 10.1080/14680629.2019.1625806.

4. **Nguyen, T.**, NguyenDinh, N., Lechner, B., & Wong, Y.D. (2019). Insight into the lateral ride discomfort of young-adult bus passengers at multiple postures: Case of Singapore. *Case Studies on Transport Policy,* 7(3), 617-627, doi: doi.org/10.1016/j.cstp.2019.07.002.

5. **Nguyen, T.**, Xie, M., Liu, X., Arunachalam, N., Rau, A., Lechner, B., Busch, F., & Wong, Y.D (2019). Platooning of autonomous public transport vehicles: The influence of ride comfort on travel delay. *Sustainability* 2019, 11(19), 5237, doi: https://doi.org/10.3390/su11195237.

Other Relevant Publication

6. **Nguyen T.**, Swolana P., Lechner B., Wong Y.D. (2020) A Comparison of Different Mathematical Bus Dynamics Models to Evaluate Road Roughness and Ride Comfort. In: Klomp M., Bruzelius F., Nielsen J., Hillemyr A. (eds) Advances in Dynamics of Vehicles on Roads and Tracks. IAVSD 2019. *Lecture Notes in Mechanical Engineering.* Springer, Cham, doi: https://doi.org/10.1007/978-3-030-38077-9_191

7. **Nguyen, T.**, Xie, M., Liu, X., Arunachanlam, N., Rau, A., Lechner, B., Busch, F. & Wong, Y.D. (2020). Platooning of Autonomous Public Transport Vehicles: A Trade-off between System Performance and Passenger Ride Comfort. TRB 2020 Annual Meeting, Washington DC, USA, 12-16 January 2020.

8. Rau, A., Jain, M., Meng, X., **Nguyen, T.**, Tao, L., Xiaodong, L., Yuan, Z., Ul-Abedin, Z., (2019). Planning and Design of a New Dynamic Autonomous Public Transport System: The DART System in Singapore. In Proceeding of 26th ITS World Congress, Singapore, 21-25 October 2019.

Other Publication during PhD period 04/2016-02/2020

9. Nguyen-Phuoc, D. Q., Oviedo-Trespalacios, O., **Nguyen, T.**, & Su, D. N. (2020). The effects of unhealthy lifestyle behaviours on risky riding behaviours – A study on app-based motorcycle taxi riders in Vietnam. *Journal of Transport & Health*, *16*, 100666, doi https://doi.org/10.1016/j.jth.2019.100666

10. **T. Nguyen**, N. NguyenDinh, B. Lechner. Traffic microsimulation of roadwork in Singapore - A case study. In Proceedings of the 2nd conference on Transportation Infrastructure with Sustainable Development – TISDC 2016. Danang city, Vietnam, 2016 (ISBN 978-604-82-1809-6).

11. N. NguyenDinh, **T. Nguyen**, E. H. Yang, B. Lechner. Life cycle cost assessment of engineered cementitious composite (ECC) precast pavement in Singapore. In Proceeding of the 11th International Conference on Concrete Pavements. San Antonio, USA, 2016.

ACKNOWLEDGEMENTS

Table of Contents

List of Figures

List of Tables

List of Abbreviations

Terms	Abbreviations	Terms	Abbreviations
APT	Autonomous Public Transport	PI_t	Profile Index for Truck
AV/AB	Autonomous Vehicle/Autonomous Bus	PQI	Pavement Quality Index
BRI	Bus Ride Index	MBS	Multi-Body Simulation
BSEP	Bus Service Enhancement Programme	MRT	Mass Rapid Transit
C_w	Corrected Unevenness Index	NQI	Ride Quality Index
DART	Dynamic Autonomous Road Transit	NR	Novel Roughness
DLI	Dynamic Load Index	NTU	Nanyang Technological University Singapore
DOF	Degree of Freedom	PD	Potholes detection
FBM	Full-Bus Model	PR	Road Profile Reconstruction/Estimation
FCM	Full-Car Model	PSD	Power Spectral Density
FEM	Finite Element Method	QBM/QBS	Quarter-Bus Model/ Quarter-Bus Simulation
FRI	Full-car Roughness Index	QCM/QCS	Quarter-Car Model/ Quarter-Car Simulation
HATI	Heavy Articulated Truck Index	R.M.S./r.m.s.	Root Mean Squared
HBM/ HCM	Half-Bus Model/ Half-Car Model	RE	Roughness Index Estimation
HI	Health Index	SEI	Spectrum Evenness Index
HRI	Half-car Roughness Index	SRT	Semi Rapid Transit
HST	High-Speed Train	TRI	Truck Ride Index
HVRBI	Heavy Vehicle Roughness Band Index	TUM	Technical University of Munich
IMVS	Individual Mobility Vehicles and Services	TUMCREATE	TUM Campus for Research Excellence and Technological Enterprise
IRI	International Roughness Index	VDV	Vibration Dose Value
LTA	Land Transport Authority	VRI	Vehicle Response Index
LRT	Light Rail Transit	WLP	Weighted Longitudinal Profile
LWI	Longitudinal Evenness Index		

SUMMARY

The rapid developments of smart technology and the vision to smart cities have led to parallel developments of various innovative transport means. Among them, road-based autonomous public transport (APT) is being planned, designed and developed worldwide such as the Dynamic Autonomous Road Transit (DART) in the city of Singapore. Innovative vehicle configuration and operation in the APT shall demand new requirements for design and construction of the infrastructure concerning the ride comfort of onboard passengers. This study aims at supporting the required update of guidelines for the design of roadway (e.g. horizontal alignment design), for vehicle speed recommendation along existing infrastructure and for pavement maintenance concerning passenger ride comfort in which DART is considered as a case study for APT application. Bottom-up and top-down approaches are used, in which the former method uses existing bus vehicles and network as a base-line reference while the latter method is based on APT's vehicle specification and operation.

At first, this study starts with a comprehensive review of ride comfort thresholds, recent approaches to evaluate passenger ride comfort onboard and to assess road surface irregularity, where research gaps are pointed out for further study. The interaction between passenger-vehicle-pavement is studied through numerical analysis. Given the similarities between regular bus and APT, the former system has been investigated and detailed bus mathematical models are constructed and validated to evaluate the pavement quality that affects passenger ride comfort. Based on the comparison of different bus models regarding their simulation complexity and performance, a refined Bus Ride Index (BRI) is proposed as a key achievement of this research study. At the same time, regression relationships are established between road geometrical design (e.g. horizontal curve radius) and passenger perceptions at different postures onboard the bus. Herein, experimental study with analytical analysis is carried out to evaluate principal factors (e.g. lateral acceleration, lateral jerk and duration of turning movement) affecting passenger-vehicle-road interaction and ride discomfort based on existing bus fleet and road network. Finally, the DART concept is examined from different perspectives such as network analysis, traffic operation and road infrastructure design.

The findings indicate that research on geometry design and road maintenance based on passenger ride comfort for APT is important to support the new vehicle concept. In the urban context, while road geometry concerning the horizontal curve is contributing to the upper range (*uncomfortable*, *very uncomfortable* to *extremely uncomfortable*), road roughness is the principal factor affecting passenger ride quality in the lower range of discomfort (*not uncomfortable*, *a little uncomfortable*, *fairly uncomfortable* to *uncomfortable*). The developed BRI offers a faster, inexpensive, convenient and more suitable method for evaluating bus lane roughness regarding passenger ride comfort and can be used as a supporting measure for the conventional Pavement Management System using Automated Pavement Profiler. From the experimental study, the newly established ride comfort thresholds provide the

recommendations for vehicle speeds within turning curves, as well as recommendations for the design of horizontal curves that ensure passenger ride comfort.

ZUSAMMENFASSUNG

Die rasante Entwicklung intelligenter Technologien und die Vision von Smart Cities haben zur parallelen Entwicklung verschiedener innovativer Transportsysteme geführt. Unter anderem wird der autonome öffentliche Straßenverkehr (APT) weltweit entwickelt, beispielsweise das Dynamic Autonomous Road Transit (DART) System in Singapur. Die innovative Fahrzeugkonfiguration und der neuartige Fahrzeugbetrieb im APT werden neue Anforderungen an die geometrische Gestaltung und an den Bau der Infrastruktur in Bezug auf den Fahrkomfort der Fahrgäste an Bord stellen. Diese Studie zielt darauf ab, Empfehlungen für die Gestaltung neuer Fahrwege (Linienführung) sowie Empfehlungen zur Instandhaltung bzw. zur Anpassung der Fahrzeuggeschwindigkeit bei bestehenden Fahrwegen für das neue APT bezogen auf den Fahrkomfort der Fahrgäste festzulegen. Hierbei wird das DART als Fallstudie für die Anwendung betrachtet. Bei der Studie kommen Bottom-Up- und Top-Down-Ansätze zur Anwendung, wobei zunächst vorhandene Busfahrzeuge sowie das bestehende Straßennetz als Ausgangspunkt verwendet werden (Bottom-Up). Der zweite Schritt basiert auf den neuen Fahrzeugspezifikationen und den Betriebsanforderung für APT.

Zunächst wird eine umfassende Überprüfung der Schwellenwerte für den Fahrkomfort vorgenommen. Es werden neue Ansätze zur Bewertung des Fahrkomforts an Bord sowie der Fahrbahnunebenheiten vorgestellt und der Forschungsbedarf für die weiteren Untersuchungen identifiziert. Die Wechselwirkung zwischen Passagier, Fahrzeug und Fahrbahn wird durch numerische Analysen untersucht. Angesichts der Vergleichbarkeit zwischen aktuell eingesetzten Bussen und den APTs wurden auf deren Basis detaillierte mathematische Busmodelle erstellt, um auch die Fahrbahnqualität hinsichtlich der Auswirkung auf den Fahrkomfort der Fahrgäste zu bewerten. Basierend auf verschiedenen Modellierungsansätzen für die Busse (hinsichtlich Simulationskomplexität und Leistungsfähigkeit) wird ein verfeinerter Bus Ride Index (BRI) vorgeschlagen. Ebenso werden Regressionsbeziehungen zwischen der geometrischen Straßengestaltung (z.B. dem horizontalen Kurvenradius) und der Wahrnehmung durch die Fahrgäste in verschiedenen Positionen an Bord des Busses hergestellt. Dazu wird eine experimentelle Studie analysiert, um die maßgebenden Faktoren (z.B. Querbeschleunigung, lateraler Ruck und Dauer der Kurvenfahrt) zu bewerten, die die Interaktion zwischen Passagier, Fahrzeug und Straße auf der Grundlage der vorhandenen Busflotte und des Straßennetzes beeinflussen. Abschließend wird das DART-Konzept unter verschiedenen Gesichtspunkten wie Netzgestaltung, Verkehrsbetrieb und Entwurf der Straßeninfrastruktur untersucht.

Die Ergebnisse zeigen, dass Untersuchungen zur Gestaltung der Straßengeometrie sowie zur Straßeninstandhaltung auf Grundlage des Fahrkomforts für APT wichtig sind, um die Akzeptanz für das neue Fahrzeugkonzept zu unterstützen. Im vorliegenden städtischen Kontext (Singapur) kann die horizontale Linienführung wesentlich zu einer negativen Komfortbewertung beitragen (unangenehm, sehr unangenehm bis extrem unangenehm), während die Fahrbahnunebenheiten den Fahrkomfort nur geringfügig beeinflussen (nicht unangenehm, ein wenig unangenehm, ziemlich unangenehm bis

unangenehm). Der entwickelte Bus Ride Index (BRI) bietet eine schnelle und kostengünstige Methode zur Bewertung der Fahrbahnunebenheiten in Bezug auf den Fahrkomfort von Fahrgästen und kann als unterstützende Maßnahme für das herkömmliche Fahrbahnmanagementsystem mit Längsprofilmessung (Automated Pavement Profiler) verwendet werden. Aus der experimentellen Studie ergeben sich aus den neu festgelegten Schwellenwerten für den Fahrkomfort Empfehlungen für die Fahrzeuggeschwindigkeit in Kurven sowie Empfehlungen für die Gestaltung der horizontalen Linienführung.

Keywords: *Horizontale Linienführung, Fahrbahn-Instandhaltung, Fahrkomfort für Passagiere; autonomer öffentlicher Straßenverkehr; Singapur.*

1. INTRODUCTION

1.1 Research background

In recent years, big cities are increasingly becoming overcrowded from protracted urbanisation and globalisation that result in burdens on the infrastructure system, especially the transportation network. The higher the population, the more travel demands are generated. In Singapore, the population has been rapidly increasing from 2.074 million in 1970 to 5.638 million in 2018 [1] and expected to reach 6.9 million by 2030 [2]. To tackle the mobility challenges in Singapore, transport demand management strategies have been proposed and implemented such as the well-known Electronic Road Pricing (ERP) to manage road usage, and the Certificate of Entitlement (COE) to control car-ownership. There is a massive expansion of the Mass Rapid Transit (MRT) system, which shall double from 180km in 2015 to 360km by 2030 [3]. The implementation of the Bus Service Enhancement Programme (BSEP) which involves the addition of 1,000 buses also increases fleet size which allows more frequent services, thereby attracting more passengers to the public transport (PT) [3]. There are also concerted efforts in improving active mobility infrastructure such as sharing of walking facilities and expansion of cycling network [4]. Singapore city has gained numerous achievements in balancing travel demand and transport supply to ensure a good quality of life and to improve the liveability of the megacity.

Existing PT system has achieved a high service satisfaction in Singapore. PT customer satisfaction survey is conducted every year to analyse commuters' expectations on many service attributes such as waiting time, reliability, comfort, travel time, safety and security. The PT system in Singapore is overall ranked top among high-density compact centres (including Singapore, Hong Kong and Beijing) regarding the economic cost of transport according to the Mobility Opportunities report by Siemens [5] or McKinsey [6]. The efficiency, broad coverage, integration and precise transport planning are also common PT attributes among leading cities like Copenhagen and Singapore.

However, like many megacities worldwide, Singapore is frequently facing "bus-train" or bus bunching problem during peak periods that result in inefficient bus operation. The research proposition in TUMCREATE [7] is to develop an innovative semi-rapid transit (SRT) system aimed at ameliorating this critical problem. The rights-of-way (ROW) infrastructures are critical components in the development of the SRT. As classified by Vuchic [8, 9] there are two broad types of mode suitable for SRT namely bus semi-rapid transit (BST) and light rail transit (LRT). The fundamental infrastructure change is to replace many bus lines with SRT through upgrading public transport ROW to offer preferential treatment, from mixed traffic streets to partially segregated streets where public transport vehicles have dedicated lane along the route but sharing the lane at intersections. Figure 1-1 shows an example in Sacramento where many bus lines were replaced by a higher capacity and performance LRT

to solve the "bus-train" problem. Redesign of intersections, separate stops or station areas as well as roadways are also prioritisation methods for SRT but tend to be costly.
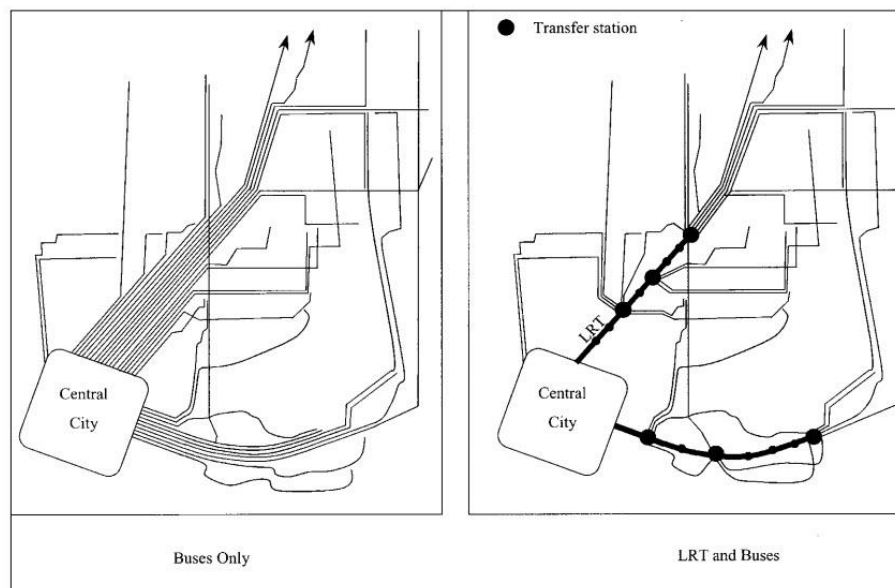
Figure 1-1: Example of upgrading branch lines into a trunk with feeders [9]

There is a need for the development of an "Ultimate Public Transport System" where the new SRT will bridge the capacity gap between Regular Transit and Rapid Transit. The conducive conditions for SRT in Singapore are:

1) Besides the high capacity transport of MRT and LRT, public bus service is one of the leading PT mode. Bus ridership has a high share of 3.9 million passenger trips out of 7.9 million PT passenger trips per day [10], for a resident population of 5.5 million in the small (719km^2 land area) island nation. The rail network for the future aims at "eight in 10 households will be within a 10-minute walk to a train station" by 2030 [3]. Therefore, the new SRT system can be a good alternative that offers complementary connectivity to the train system.

2) The gap in PT supply is in the accessibility of the road network, from local roads, collector roads to the arterial highway, each at the different level of functional classification and capacity [11]. In Singapore, the PT system encompasses 5 MRT lines, 3 LRT lines, over 5,000 buses and 28,000 taxis [10]. About 1,000 buses were added to existing PT fleet from 2012-2017 according to the Bus Service Enhancement Programme (BSEP), resulting in 90% bus services being operated within 2-10 minute headways. The MRT network is being expanded to 360km length by 2030. However, the application of SRT in Singapore's travel demand is still at the middle ROW B category transit as illustrated in Figure 1-2 (where ROW C is defined as street with mixed traffic, ROW A is fully separated driveway while ROW B is partially separated street).
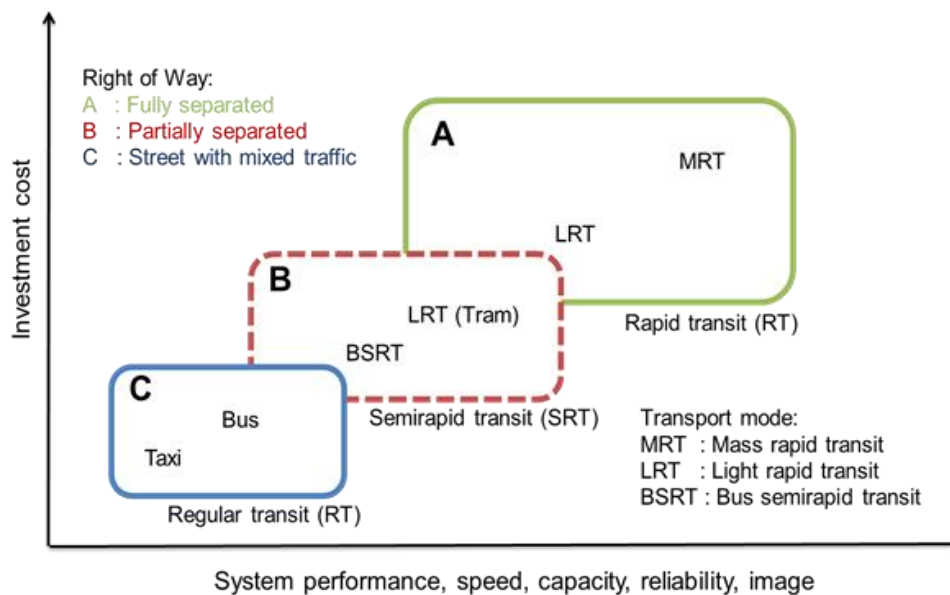
Figure 1-2: Performance/investment cost of modes in which ROW B category is missing in Singapore (adapted based on [9])

3) Bus bunching problem, where two or more buses serving the same route arrive at the same bus stop at about the same time, is currently a big issue raised by commuters during the survey of Public Transport Council [10]. The Land Transport Authority (LTA) announced in 2014 the Bus Service Reliability Framework (BSRF) as a carrot-and-stick approach aimed at dealing with bus bunching. The simulation study by Future Cities Laboratory has shown that bus reliability can increase by 35% when splitting a long bus route into two parts [12].

4) Bus train problem is a problem where many buses form a long bus queue on a street segment. This problem occurs daily in Singapore where more than 5,000 buses are being operated at the same time. Many busy bus stops are shared to cater around 20 bus lines stopping for passenger boarding and alighting.

5) The relocation of container terminals to the industrial hub of Tuas [13] will increase travel demand to/from Tuas peninsula significantly. The resultant big gap in transport demand-supply is possible to be a test-bed for DART, especially that there was an extension of MRT Green line to Tuas checkpoint.

Infrastructure upgrading from ROW C to ROW A will be costly in the investment cost shown in Figure 1-2, which applies to conventional LRT and BSRT. Fortunately, this cost can be reduced thanks to recent advances in engineering, computing, as well as information and communication technologies. For example, state-of-the-art development in vehicle-to-vehicle and vehicle-to-infrastructure communication mechanisms have enabled the vehicles to formulate platooning on the streets, resulting in increasing of traffic flow capacity and reduction in unutilised road spaces. On the other hand, electromobility has reached the readiness of mass production that reduces vehicle emission significantly

with increases in passenger ride comfort thanks to its quiet electric engines and regenerative braking. Electrified vehicle (EV) is a prerequisite condition for autonomous vehicles (AV).

Furthermore, the development of Intelligent Technology System (ITS) has brought intelligent traffic control and management that can prioritise PT at every intersection as well as providing actual travel time information to passengers. These technologies together with innovative vehicle design, data analytics, and crowdsourcing have reshaped the ways and patterns of passenger mobility and transport services soon. The proposed Dynamic Autonomous Road Transit (DART) as an SRT layer for Singapore transport system will inevitably be among innovative public transport modes that extensively utilise these emerging state-of-the-art technologies.

1.2 Specification and operation of autonomous public transport

Autonomous public transport (APT) using autonomous bus is being planned and implemented worldwide. A rail-bus Autonomous Rail Rapid Transit (ART) network in Zhuzhou, China was set to become operational in early 2018 [14]. While the autonomous shuttle is in small size of 15 passengers per module for the first and last mile connection [15], a full electric-autonomous bus capacity of 80 passengers was first launched in Singapore [16]. Other than that, the idea of coupling different modules into a platoon has emerged not only in DART in Singapore, but also the autonomous pods in Dubai in its drive for a smart city [17–20]. A brief comparison of DART and autonomous pods are shown in Table 1-1.

Table 1-1: Comparison of DART and Autonomous pods

APT system	DART – Singapore	Autonomous pods – Dubai
Capacity (passengers/module)	30	10
Dimensions: length, width, height (m)	7 x 2.7 x 3.1	2.87 x 2.24 x 2.82
Design speed (km/h)	70	60
Average speed (km/h)	30-40	20
Dedicated lanes	Not required	Required
Coupling/decoupling functions	Non-mechanical	Mechanical
Time to couple/decouple (second)	N/A	15/5
Maximum coupling (modules)	10	N/A
Plan to hit the road	N/A	Early 2019
Real prototype	In progress	Two pods at real size
Distance travel	Long	Short and medium

DART offers much higher capacity than autonomous pods. However, DART is neither BST nor LRT, but a new tyre-based mode characterised with different types of AV, vehicle configurations with electric propulsion as well as different types of operation. As a trade-off between high capacity and flexibility, DART module (7m length, a capacity of 30 passengers) is designed to be smaller than a bus and able

to couple into a platoon on the streets for demand-based operation. For example, a platoon during peak period can include 7-10 modules while a non-peak period platoon needs only 3-4 modules. The controls of platoon's non-mechanical coupling/decoupling together with ITS technology (on-demand virtual lane, adaptive signal control) are the most critical aspects for the success of DART operation. Other operational characteristics are conductive charging at terminals and depots, minimum noise emission of 50dB, one driving direction with average design occupancy of 60%. Suitable corridors for DART have been analysed and studied from the perspective of the larger PT network to identify routes with insufficient transport supply to meet travel demand [21].

The APT operation may require adaptation of existing physical street design and layout to offer higher travel speed and capacity. For example, higher operating speeds of DART platoons (capacity of 30 passengers for each module) as compared to regular buses (able to carry 80-143 passengers) will be a trade-off against DART smaller vehicle size and capacity. However, higher vehicle speed will result in higher acceleration while turning, and results in higher adverse effects on passengers' ride comfort. This uncontroversial compromise between travel time and ride comfort has been pointed out in many studies [22]. On the other hand, smoother quality on the road surface is required to ensure adequate ride quality and safe operation of AV technology, where APT vehicles are coupled to each other at a close distance to formulate platoons.

1.3 Road infrastructure design for APT towards passenger ride comfort

APT requires dedicated road infrastructure especially for its state-of-the-art electrification and automation. Intensive research related to pavement structure has been conducted to support the electrification of APT such as electrified roadway [23], the engineered cementitious composite (ECC) precast pavement [24] and its construction [25], as well as energy demand for large-scale PT network [26]. Still, little is known about the relation between APT automation and road infrastructure performance such as road surface condition and road alignment. Regular bus and APT vehicles are sharing similar operational characteristics which mean the regular bus can be considered as a reference for the APT system. Both are tyre-based public transport modes operating on urban streets, sharing spaces with other private vehicles as ROW B or ROW C, being prioritised by intelligent traffic control and dedicated lane allocation. It is worth emphasising that there is no dedicated physical lane but the DART will be prioritised by the new concept of Virtual ROW such as the dynamic bus lanes in Figure 1-3 [27–31]. The concept of dynamic bus lanes was initially proposed to optimise bus lane usage, which are dedicated to buses and general traffic in some instances. Therefore, studying the road infrastructure for bus operation will be useful for the planning and design of APT operation.
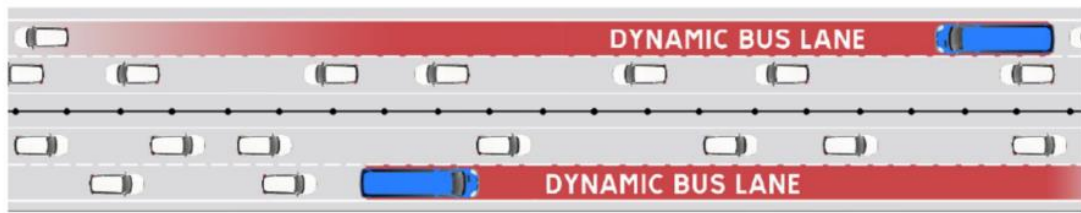
Figure 1-3: An illustration of the dynamic bus lane concept [32]

Bus lane or busway is the most common measure to offer priority for bus worldwide where there is sufficient demand; they are installed by setting aside a dedicated lane for the bus where there is enough cross-section width. The bus lanes are usually located near the kerbside for passengers to board and alight quickly, though another option is in the central median like BRT lanes, and some are run on contra-flow. Dedicated bus lanes can also be operated on specific road segments for part of the day, like during peak periods (e.g. there are 100 such street segments so far in Singapore [33]) or full day from 7.30am to 11.00pm, when motorists are not allowed to access the full-day bus lane at all. In Singapore, the total length of full-day bus lanes is 23km on 30 streets and are operated according to LTA regulations [34]. Bus lane enforcement is performed via CCTV cameras. LTA is planning to provide more bus lanes for existing road network as well as for new road infrastructure, such as 21.5km dedicated bus lane on the forthcoming North-South Corridor (Lim, 2016). Bus lane plays a vital role in improving Singapore's traffic condition concerning efficient, reliable and fast public transport service [36]. Figure 1-4 shows examples of existing and planned bus lanes in Singapore.

Bus lane in Singapore   North-South Corridor [35]
Figure 1-4: Existing and planned bus lanes in Singapore
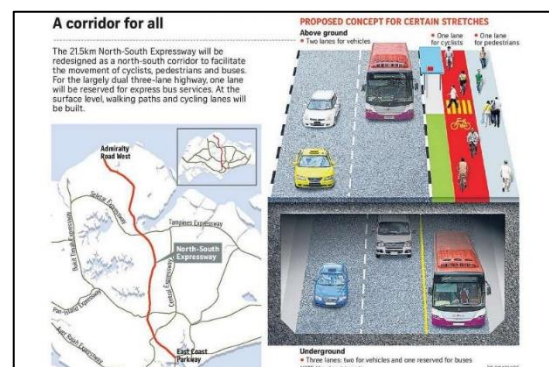
Despite the excellent bus services, there has always been a strong motivation to make the bus system in Singapore better to offer even higher riding quality in meeting high passenger expectation. The following is an example of a participant's perception in the survey of the Public Transport Council [10]:

"I think there is improvement but as Singaporeans…we want perfect, not just improved. So, we hope that it will improve further." Working adult, male

Ride comfort is both subjective and objective in nature, spanning operational attributes such as accelerations (in 3 dimensions: vertical, lateral and longitudinal), vibration, noise, and lighting to human user perceptions. Among them, road alignment, vehicle condition and pavement quality are important extrinsic factors impacting on passengers' riding discomfort, which is a crucial human-centric focus in recent infrastructure design approaches [37]. With the increasing expectation on ride comfort, the new APT vehicles has to offer a higher ride comfort level compared to those of existing bus systems.

1.4 Ride quality in bus systems compared to the railway system

In general, ride quality of bus system is lower than railway system, which has stringent design standards such as lateral acceleration threshold value of 0.1g for LRT [38, 39] or even 0.05g for a high-speed train [40]. To improve ride comfort on the highway, a Clothoid curve is often used whose minimum length of spiral transition curve is calculated based on the standard developed in 1909 for railway track curves [11, 41]. Given the large gaps in ride quality between a conventional bus system and railway system, various guidance technologies for road vehicles have been implemented [42, 43].

Guidance systems can be physical, such as kerb guidance, central rail guidance, optical guidance and magnetic guidance [44]. For physically guided busways, the features of the guideway such as alignment, surface regularity, and surface texture affect the ride quality. Therefore, the construction and configuration of busways are essential to ensure good ride quality. Compared to trams, ride quality of central rail guidance, as a hybrid transport vehicle between a tram and a bus [45], is reduced due to the four-wheeled design, whereas trams have bogies [46].

On the other hand, the alignment and pavement surface of the bus lane are the main external factor affecting ride quality of a conventional bus. As different from guided busways, the bus can manoeuvre laterally with higher tolerance and with less comfort. These issues are probably similar to the autonomous bus (AB) without guided busways but following lane detection [47]. The tyre-based design of AB will be less comfortable compared to tramways.

Based on the above analysis, Figure 1-5 illustrates different levels of ride quality according to different guidance technologies. AB's ride quality is still unknown but probably ranging from mixed traffic operation to magnetic and optical guidance depending on whether there is dedicated lane (for the operation of AB fleet) or not (in case of single AB such as the current trial worldwide) and the accuracy of AB's guidance technologies. The assumption in [22] that AB can be operated based on the passenger comfort lateral acceleration threshold of the railway system is, thus, not feasible in reality of urban road traffic. Therefore, this study on road infrastructure for APT is crucial to improve the passenger ride comfort towards the direction of the high ride quality of railway systems.
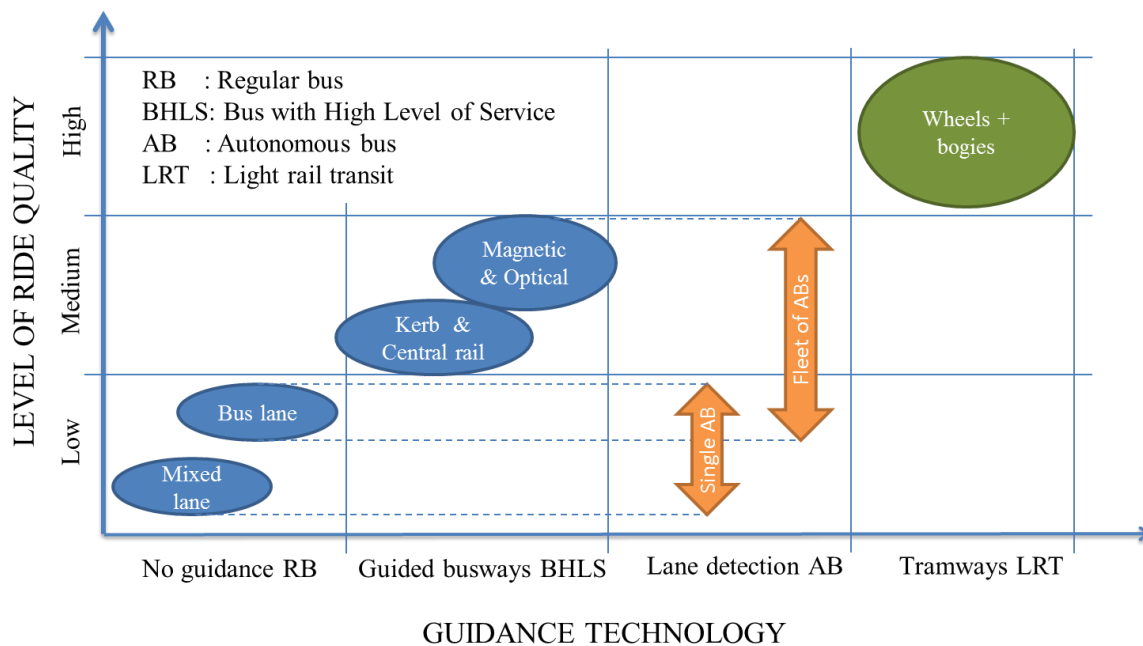
Figure 1-5: Level of ride quality according to guidance technology

1.5 Research objectives

This study focuses on road infrastructure design based on passenger ride comfort with consideration of the dynamic characteristics of APT vehicles as well as bus vehicles. The road pavement quality and geometric alignment at the corridor scale are emphasised. The specific objectives are as follows:

1) To review the development of response-type methods for road surface irregularity and propose research gaps for study, resulting in the requirements of different bus mathematical models to estimate road roughness index.

2) To develop different bus mathematical models to evaluate the effect of road roughness on passenger ride comfort, in which these models can be adapted to simulate any APT concept by taking vehicle conditions into account.

3) To establish a new evaluation method/index for pavement maintenance that is more appropriate for public transport roadways such as bus/APT and BRT lanes.

4) To propose speed recommendation for existing bus operation and develop design criteria for new road infrastructure based on passenger ride comfort requirement.

5) To evaluate the APT platooning system performance (e.g. average speed, delay, number of coupling modules) following different ride comfort criteria: three bus comfort and two railway criteria.

1.6 Structure of the dissertation

The structure of the dissertation is shown in Figure 1-6. The "methods" and "outcomes" described in the diagram are mainly from the contents of the five papers.

Regarding **objective 1**, Paper I (and Section 2) reviewed recent studies within the last decade to provide an overview of the state-of-the-art response-type methods, to highlight fundamental differences between studies and thereby to propose key focus areas for conducting research. The development of bus mathematical models is essential to assess road roughness condition, in general, and to evaluate ride comfort of bus passengers, in particular.

Two numerical studies were conducted to address **objectives 2 and 3** by exploring in detail the vertical-direction interaction between passenger, vehicle and pavement conditions. Various mathematical bus models were built, and their performance was compared based on existing technical parameters of the bus fleet and bus lane profiles in Singapore. Conclusions were drawn for the applicability of those bus models which have been presented in Paper II. As a result, the most appropriate bus model was selected for the establishment of the Bus Ride Index (BRI). Road longitudinal profiles, both artificial and measured, were used to develop and validate the quarter-bus model. The results are presented in Paper III.

Research **objective 4**, on the other hand, employed descriptive and multivariate analyses of passenger rating data, bus operating characteristics (speeds, accelerations, and jerks) and horizontal curve radii. This approach characterises the effects of road conditions on passenger ride comfort, in which road roughness mostly causes passenger ride quality in the lower range of discomfort levels (*not uncomfortable*, *a little uncomfortable*, *fairly uncomfortable* to *uncomfortable*) while road geometry in terms of horizontal curve can lead to the upper range of discomfort levels (*uncomfortable*, *very uncomfortable* to *extremely uncomfortable*). The results are presented in Paper IV. Research **objective 5** is an extension of the established ride discomfort levels to evaluate the performance of the APT system. The results are presented in Paper V showing the feasibility to operate the DART system following the bus standing comfort criterion ($a_y = 1.5$ m/s^2) without any significant impact on system travel time.

In this dissertation, a literature review in Section 2 provides the theoretical background for the research. The methodological framework of the research is summarised in Section 3, where multiple methods were applied in Papers I to V. Furthermore, Section 4 summarises and synthesises the results of Papers I to V regarding the research questions. Section 5 discusses the overall results and presents recommendations to improve vehicle speed profiles and maintain road surface to ensure ride quality on APT. The conclusions and outlook section from this research are also drawn in this last chapter.

Paper I (Literature review) + Section 2

Obj. 1

Methods
- Review on **response-type methods** for road surface irregularity evaluation

Outcomes
- Research gaps for studies using bus mathematical vehicle models

Paper II (Numerical study)

Obj. 2

Methods
- Development and comparison of **different mathematical bus models**
- MATLAB/Simulink numerical simulation
- Testing with 2km measured bus lane profiles

Outcomes
- Advantage and disadvantages of different bus models
- Selection of the best model to develop Bus Ride Index

Paper III (Numerical study)

Obj. 3

Methods
- Refining the quarter-bus-model
- Testing with large amount of artificial and measured road profiles

Outcomes
- The refined Bus Ride Index is more appropriate to **evaluate bus lane roughness**

Paper IV (Experimental study)

Obj. 4

Methods
- Development of new mobile applications
- Statistical analysis
- Correlation between subjective and objective factors

Outcomes
- Regression relationship between passenger ratings and lateral accelerations, jerks and turning durations
- Different ride discomfort levels for **road alignment design**

Paper V (Traffic simulation)

Obj. 5

Methods
- Development of a new platooning protocol for DART
- Investigation the delay of DART system following various ride comfort

Outcomes
- Feasible operation of the system following **bus standing comfort criterion**
- Delay of platooning is high in case of railway ride comfort

Section 5

Methods
- **Summary of findings** from 5 studies

Outcomes
- Recommendation for road infrastructure design for APT
- Suggestion for further study

Figure 1-6: Structure and overview of the dissertation

2. STATE-OF-THE-ART

2.1 Standards for ride comfort evaluation

During regular vehicle operation, the interaction between road and wheel generates vibration, resulting in discomfort, fatigue or even severe injury to passengers. ISO 2631-1:1997 [48] provides a popular method for "Evaluation of human exposure to whole-body vibration". Depending on the range of vibration frequency, there are different effects on health, comfort and perception (0.5Hz to 80Hz) or for motion sickness (0.1Hz to 0.5Hz). Vibration measurements will be at different body positions (seated, standing or recumbent), directions (x, y and z-axis), and locations (seat surface, seat-back and the feet).

Similar to ISO 2631-1:1997, BS 6841:1987 [49] recommends measuring four axes of vibration on the seat and combine them in a vibration severity evaluation. The main factors which influence human response to vibration can be intrinsic variables (such as passenger types, experiences, body postures, and activities) and extrinsic variables (such as vibration magnitude, frequency, axis, input position, and duration). Figure 2-1 shows different axes to measure vibration on the seat.

Seated position in ISO 2631 | Four-axis vibration of a driver in BS 6841
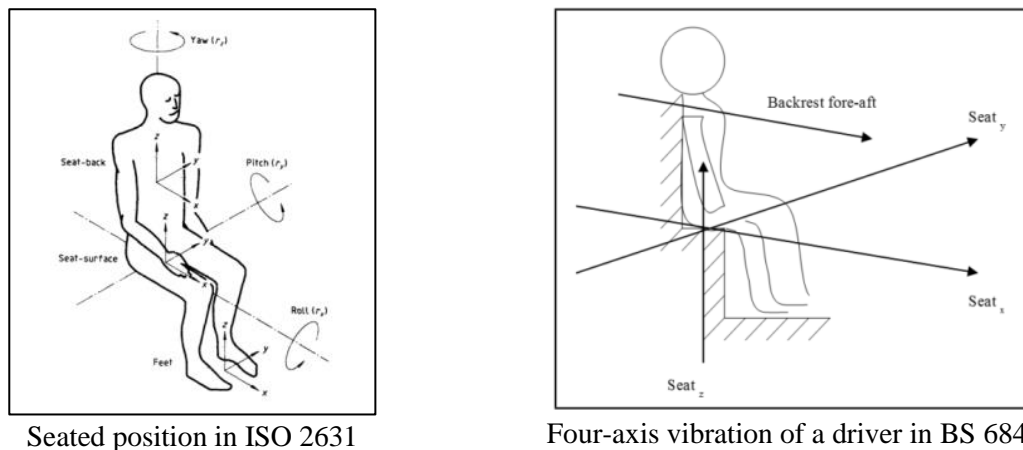
Figure 2-1: Different axes to measure vibration on the seat

Regarding fixed-guideway vehicles (such as railway, MAGLEV and rubber tyre metro-type system), ride comfort of passenger is more complicated which depends on many factors such as motion, class of service, duration of the trip, types of activities as well as other factors such as air quality, seat design and temperature [50]. The human body responds to vibration according to different factors: vibration frequency, acceleration magnitude, exposure time and the direction of vibration. Vibration evaluation can be measured as:

- The weighted-root-mean-square (a_w, unit m/s^2) acceleration as a function of time, and T is the duration of measurement, or

$$a_w = \left[\frac{1}{T} \int_0^T a_w^2(t)\, dt \right]^{\frac{1}{2}}$$

- The Vibration Dose Value (VDV, unit m/s$^{1.75}$) as a fourth power measure which is more sensitive to high amplitude values (jolts/jars). VDV is cumulative and increases with the duration of the measurement.

$$VDV = \left\{ \int_0^T [a_w(t)]^4\, dt \right\}^{\frac{1}{4}}$$

The a_w value can be used as a ride comfort index for some vibration environments (e.g. rail, road vehicles), but only the axis with the highest vibration is used to estimate vibration severity. The relationship between passenger comfort levels and vibration magnitudes in public transport is as shown in Figure 2-2.
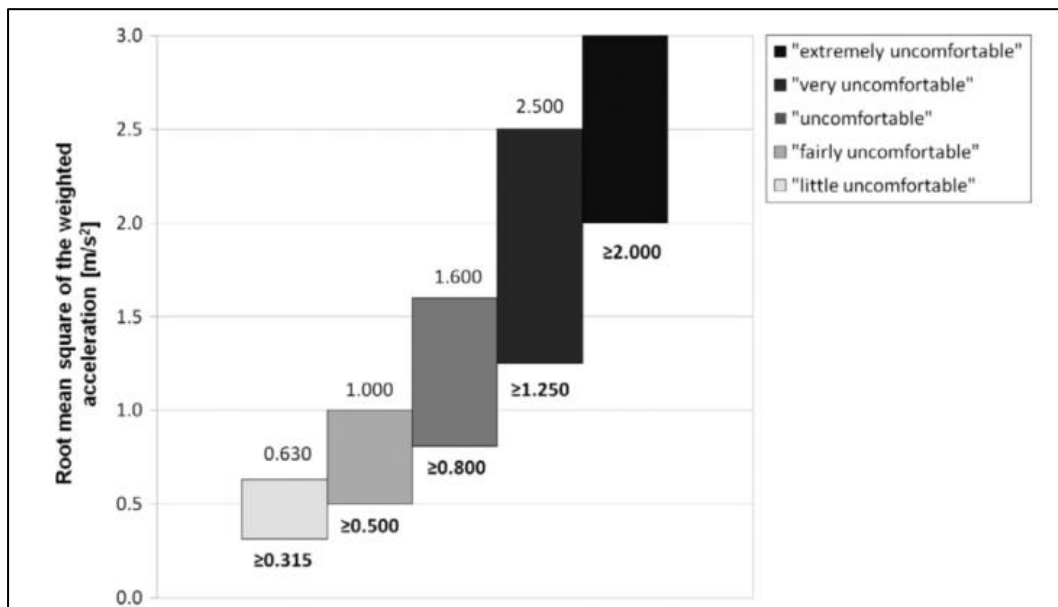
Figure 2-2: Criteria for comfort in public transport according to ISO 2631-1:1997

Besides these standards, many experimental studies have been conducted to establish ride comfort thresholds. In-laboratory research on discomfort caused by the vibration of a floor can be found in [51]. For the real-world experimental study, in [52], the longitudinal acceleration exceeding 1.5m/s^2 and the deceleration below −0.75m/s^2 will make bus passengers feel uncomfortable. The discomfort feeling of standing passengers was investigated in [53] by matching passenger ratings with collected acceleration data, whereas for lateral ride comfort, specific railway ride comfort indicators were adapted in [54].

2.2 Vehicle dynamic response approach for road surface evaluation

For the railway, ride comfort evaluation has been studied for a long time as this is an essential factor for public transport service, especially in railway engineering where increasing train speed will cause more vibration and noise. According to [55], although various evaluation methods have been proposed, a universal evaluation criterion has not been established in Japan concerning ride comfort in Japan's

railway system. Typically Finite Element Method (FEM) and Multi-body Simulation (MBS) models are used for an analytical study on the dynamic performance based on some essential inputs such as track power spectral densities, track irregularities and suspension parameters (stiffness, damping, car mass) [56].

Regarding car and vehicle dynamic response due to pavement roughness, a half-vehicle dynamic model was developed by [57]. Power Spectral Density (PSD) of the unpaved and asphalt-concrete tracks was considered together with numerical vehicle modelling at different speeds to evaluate passenger discomfort. In another study, [58] used 6 degrees-of-freedom (DOFs) multi-body vehicle model to evaluate the ride comfort at different speeds and road conditions. However, most of the recent studies only focused on single-ride comfort indices such as acceleration, heart rate variability or ride speed. Therefore, [59] combined three ride comfort indices: weighted r.m.s. acceleration (α_{wo}), r.m.s. of squared differences of heart rate variability and the weighted value of subjective ride comfort in order to set up a new set of guidelines for ride comfort evaluation. From this latter guideline, the maintenance level for highway pavement can be determined based on ride comfort grade.

The vehicle dynamic response method belongs to "*the effect in distance domain*" approach according to the classification of various indices under four categories [60]. These categories are: geometry in the distance domain, geometry in the spectral domain, the effect in distance domain; and geometry and effect in the distance domain. Among them, the International Roughness Index (IRI) proposed by Sayers in [61] is considered as a standard index for road roughness evaluation. IRI was implemented in several standards such as [62] and [63] and has been recognised worldwide [64]. Figure 2-3 illustrates the 2-DOF quarter-car simulation (QCS) for IRI calculation. IRI (mm/m or m/km) can be interpreted as the output of an "idealised response-type measuring system" (the golden-car) at a speed of 80km/h. The car comfortable ride has been proposed from different IRI levels.

$$c = c_s/m_s = 6.0$$
$$k_1 = k_t/m_s = 653$$
$$k_2 = k_s/m_s = 63.3$$
$$\mu = m_u/m_s = 0.15$$
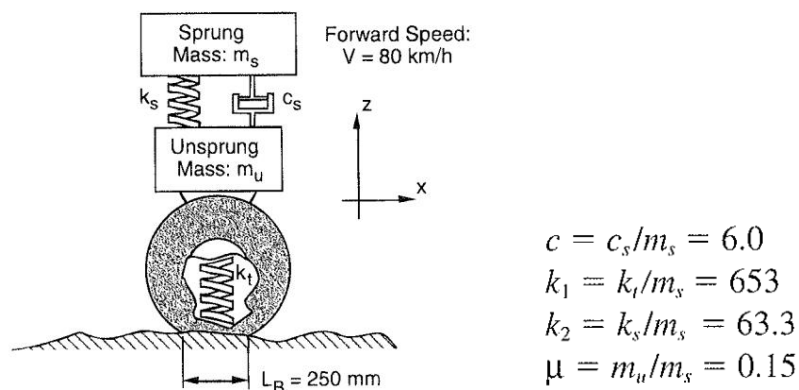
Figure 2-3: IRI model by a 2-DOF QCS [61]

As for the bus, the relationship between road unevenness/vibration and perceived comfort has been the subject of studies over the years [65]. There are many factors affecting passenger perceived comfort,

both objective and subjective, as summarised in Figure 2-4. The most influential factor on ride comfort is pavement condition, followed by vehicle condition and driver/passenger characteristics [59].
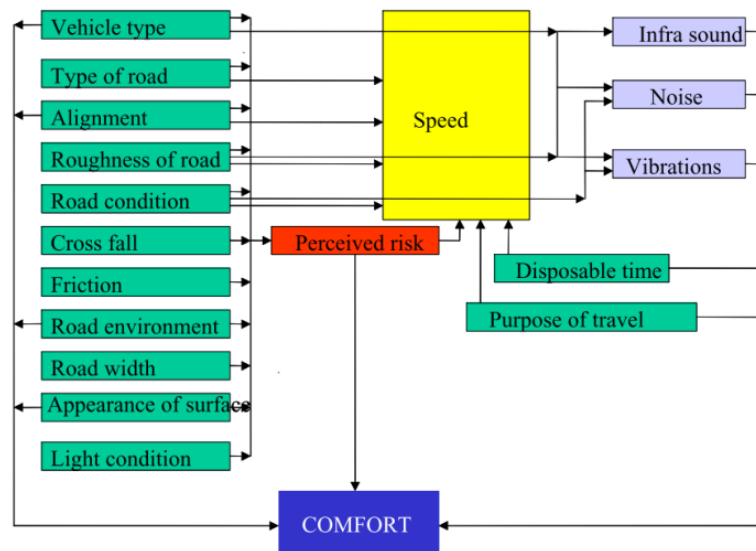
Figure 2-4: The factors contributing to the ride comfort ([65] credited to Georg Magnusson, VTI)

Ride comfort on the bus can be either studied on vehicle performance and running status (vibration, acceleration, jerk magnitude, vehicle noise) or bus operating environments [66]. The 10-DOF bus model was used in [67] where the PSD of asphalt-concrete road roughness was used to generate bus excitation and MATLAB software was used for numerical simulation. The comfort of driver and passengers were assessed based on [48] and vehicle suspension systems (spring stiffness and shock-absorber) were evaluated accordingly. Another study [68] evaluated bus transit in Chinese cities (13 bus routes, 241 measurements, 945 participants) and developed an overall bus comfort model including different parameters on noise, thermal comfort, vibration, acceleration as well as age, gender, the health condition of passengers. Multiple regression analysis was performed to establish the overall bus comfort formula.

2.3 Road roughness indices

Besides the well-known IRI, various indices were developed to evaluate longitudinal road roughness. A summary of 15 indices is given by [69], which includes four ride comfort-related QCS models and three other QCS to measure dynamic suspension (see Table 2-1). There are also two half-car simulation models (C_w), one full-car simulation model (FRI) and the other three indices from in situ measurement (NR, RQI, HVRBI). The last three indices (PI_t, DLI and WLP) do not rely on any vehicle model. Detailed information of these indices is listed in Table 2-1, in which the half-car roughness index (HRI) [70] was also added to make the summary more comprehensive.

Table 2-1: Summary of road roughness indices [69]

	Index	Abbreviation	Vehicle model	Velocity	Response category
1	Half-car Roughness Index	HRI	2 x 2-DOF Quarter-Car Model	80km/h	Dynamic suspension load
2	Full-car Roughness Index	FRI	4 x 2-DOF Quarter-Car Model	80km/h	Dynamic suspension load
3	Pavement Quality Index	PQI	2-DOF Quarter-Car Model (IRI)	80km/h	Dynamic suspension load
4	Heavy Articulated Truck Index	HATI	2-DOF Quarter-Truck Model	100km/h	Dynamic suspension load
5	Vehicle Response Index	VRI	2-DOF Quarter-Car Model (IRI)	adaptable	Dynamic suspension load
6	Spectrum Evenness Index	SEI	3-DOF Quarter-Car Model	80,100km/h (Car) 80km/h (Truck)	Ride comfort Ride safety Dynamic cargo load Dynamic road load
7	Longitudinal Evenness Index	LWI	3-DOF Quarter-Car Model 2-DOF Quarter-Truck Model 5-DOF Five-Axle Semi Trailer Model	100km/h (Car) 80km/h (Truck)	Ride comfort Ride safety Dynamic cargo load Dynamic road load
8	Corrected Unevenness Index	C_w	8-DOF Half-Truck Model 12-DOF Half-Car Model	60km/h (urban) 90km/h (highways) 120km/h (motorways)	Ride comfort Ride safety Dynamic cargo load Dynamic road load
9	Truck Ride Index	TRI	3-DOF Quarter-Truck Model	100km/h	Ride comfort
10	Health Index	HI	2-DOF Quarter-Car Model (IRI)	80km/h	Ride comfort
11	Profile Index for Truck	PI_t	-	-	Ride comfort
12	Dynamic Load Index	DLI	-	-	Ride safety
13	Weighted Longitudinal Profile	WLP	-	-	-
14	Novel Roughness	NR	in situ measurement	-	Ride safety Dynamic load of road
15	Ride Quality Index	NQI	in situ measurement	variable	Ride comfort
16	Heavy Vehicle Roughness Band Index	HVBRI	in situ measurement	variable	Ride comfort

From the summary table, ride comfort is one of the most crucial aspects to be investigated besides the dynamic suspension load and ride safety. The usage of dynamic vehicle models is more popular and more accessible to derive related road roughness indices since it enables the results to be reproducible as compared to in situ measurement. The three indices PI_t, DLI and WLP analyse the longitudinal road profiles directly without consideration of vehicle dynamics model. Some of the indices (PQI, VRI, HI) are based on, and others (HRI, FRI) are derived from the simple QCS model and its calculation procedure, e.g. the IRI. Some indices (SEI, LWI, C_w) include several response categories into their calculations.

2.4 Knowledge gaps for evaluation of the ride quality of bus passengers

From the literature reviews, several knowledge gaps motivating the present study are as follows:

1. *There are few studies on bus dynamics regarding ride comfort and road roughness evaluation, in which insight on different large-size urban bus models has been not investigated.* Several studies were conducted to compare different dynamical vehicle models such as for designing vehicles for ride comfort and vehicle suspension systems [71, 72] using 2-DOF QCS, 4-DOF HCS and 7-DOF FCS with road input as a step-hump of 0.07m height for 0.08s. The results showed that FCS captures the full behaviour of the vehicle body by considering all pitch and roll motions. Another comparative study [73] was conducted by modelling 2-DOF QCS, 4-DOF HCS and 15-DOF FCS using an MBS software with experimental ride comfort data from a vehicle travelling on a Belgian paving road. The FCS gave the most accurate results with errors within 10% of ride comfort indicator, as compared to non-correlated output from simplified vehicle models. However, the vehicle configuration on these studies is for small cars whose characteristics are somewhat different from buses. Vehicle dynamics are modelled inherently and differently, and the study results from car and truck dynamics may not be applicable for bus dynamics which is asymmetric and in larger dimensions, being equipped with air suspension, and able to carry more passengers onboard.

   In the study of [59], the principal focus has been on a passenger car to establish a guideline for the highway with speed from 40-120km/h. The study aimed to propose a ride comfort model with careful consideration of all related factors and proposed a guideline for ride comfort evaluation applicable to pavement maintenance. However, these findings may not be applicable for larger passenger vehicles with more than seven seats.

2. *There is no existing road roughness index to evaluate bus passenger ride comfort on dedicated bus/BRT lane.* From the summary listed in Table 2-1, all the indices are based on car and truck dynamics whose characteristics are different. As for urban buses, the ride comfort aspect is crucial as a single bus vehicle can carry about a hundred passengers, which can lead to significant public concerns if any uncomfortable incident occurs due to road irregularities. Increasing bus ride

comfort will contribute to the strategy of shifting car users to public transport. Vehicle dynamical models for the bus to evaluate road surface irregularities associated with riding comfort are necessary. In Singapore traffic conditions, a new Bus Ride Index (BRI) is essential to propose a suitable maintenance strategy for the widespread bus lane network around the country. Furthermore, to ensure the high degree of leisure or productivity of passenger onboard APT, higher standards of road maintenance are required [22] for which the BRI will be a potential index to consider.

3. *There is no study on the effects of different passenger postures on their ride quality*. The questionnaire method in [52] may not capture the timing of real-time discomfort feelings of bus passengers; their data were smoothed using a 3-second sliding time window technique. The comfort scale used in [54] was based only on passenger movements/sway via video observations but not from direct passenger ratings. The study of [53] used a small sample (12 subjects divided into two groups for two separate bus runs) of standing users to evaluate discomfort feelings and loss of balance. Passengers at sitting positions were not well investigated and the ten buttons that subjects pressed were assembled in 5 handles that limit the number of participants. Besides, another ride comfort threshold used [74, 75] is more appropriate for car passengers, where lateral acceleration $a_y = {} < 1.8m/s^2$ is acceptable, $1.8m/s^2 < a_y < 3.6m/s^2$ is bearable, and $a_y > 5.0m/s^2$ exceeds the human's bearing ability. For AV, [22] used the ride quality from LRT and HST because there is no existing empirical evidence of ride comfort on AV. The experimental study on the real bus in the city can fill this research gap.

The next methodology section will describe the materials and methods that have been used to solve the above-mentioned research gaps.

3. METHODOLOGY

Based on research gaps from reviewing the state-of-the-art, this chapter proposes and discusses two-prolonged methods (bottom-up and top-down approaches) used in the study, including experimental, numerical study, vehicle dynamics, and traffic simulation. The bottom-up (papers I, II, III, IV) and top-down approaches (paper V) complement each other, in which the former approach focuses on bus ride comfort with existing operational and road infrastructure conditions, while the latter considers the implementation of APT vehicle kinematics and dynamics characteristics in the traffic simulations to develop guidelines for comfortable ride. The overall research ideas and methodologies consider two-dimensional accelerations that influence passenger ride quality, in which:

- Vertical acceleration is related to pavement roughness excitation; and
- Lateral acceleration comes from the curve and turning movements.

The effects of braking/longitudinal acceleration have been left out of the study scope since regenerative braking technology of EVs and car following technology of AVs can smooth out the speed and acceleration profiles of APT platoons significantly [76]. The vital research questions are:

1) What are the research gaps for studying response-based methods to evaluate road surface irregularity?
2) What are different mathematical bus models that are applicable for evaluating road surface irregularities and ride comfort?
3) What are the levels of the road roughness to ensure passenger ride quality at different operating speeds of bus/APT vehicles?
4) How do bus/APT vehicles operate within curves and turning movements to ensure passenger ride comfort? What are the design criteria for new road infrastructure for this type of vehicle?
5) What is the performance of the DART system (e.g. average speed, delay, number of coupling modules) following different ride comfort criteria?

Figure 3-1 shows a comprehensive flow-chart of the methodological framework step-by-step from infrastructure inputs to newly developed passenger-vehicle models, ride comfort index analysis, and design guideline outputs. The logical relationships among different elements are clearly illustrated, in which new "passenger-vehicle" models are developed using numerical study and vehicle dynamics simulation while new "comfort level" thresholds are established from an experimental study. To address the main research questions 2, 3 4 and 5, four central studies of this dissertation were conducted.

Each research question (2, 3 4 and 5) was answered by investigating different components in the passenger-vehicle-road interaction from different perspectives. While vehicle model variation is the key aspect of the first numerical study on vehicle dynamics (research question 2), the diversity of

longitudinal road profiles is the focus in the second numerical study (research question 3). The human postures and road alignment are the main factors in the experimental study (research question 4), and various ride comfort levels are the centre of traffic simulation (research question 5). By doing this way, the most critical and sensitive elements were analysed comprehensively.
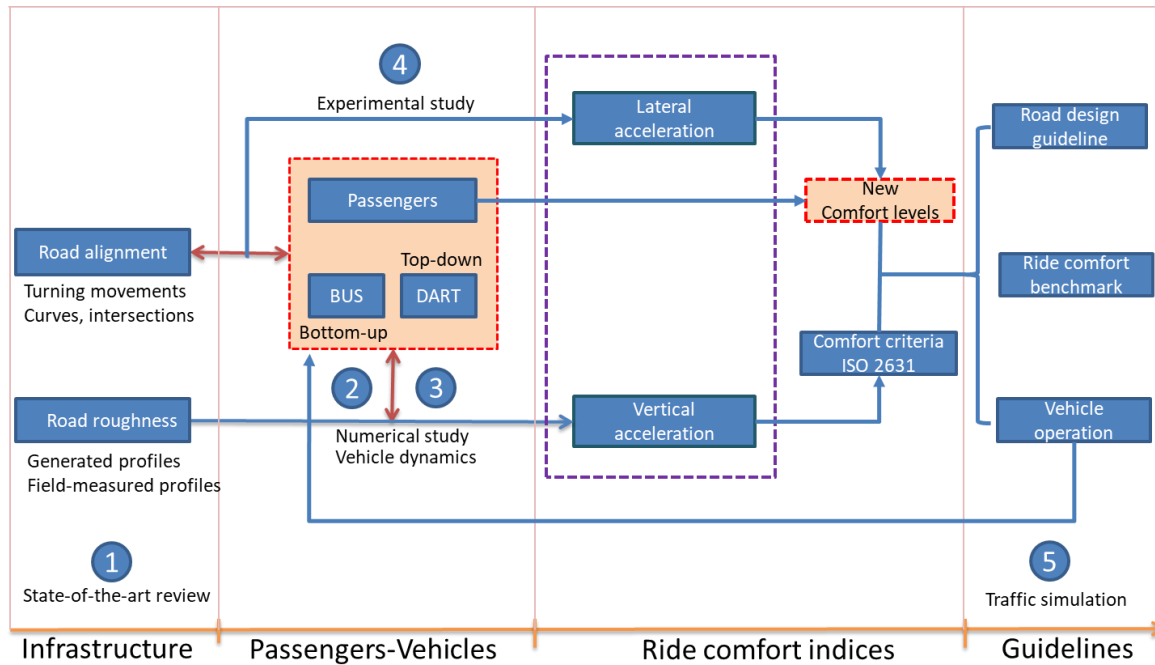
Figure 3-1: Methodological framework of the dissertation with five research focuses

Different methods were applied regarding specific interactions between passenger, vehicle and road conditions (road alignment or pavement roughness) as described in the following sections.

3.1 State-of-the-art methods for road irregularity estimation (Literature review)

This study was presented in Paper I. The study aimed to explore innovative response-based methods to evaluate road surface irregularity.

Available articles regarding response-based methods to measure road roughness condition were collected mainly from "Scopus" database [77] and partially from "Google Scholar" [78]. Articles of focus are those published by international journals and high-quality conferences. The first round of online search was conducted using the following keywords: *(("road roughness" OR "road profile" OR "pothole") AND (accelerometer OR response) AND (estimation OR classification OR detection)) AND PUBYEAR > 2005*, using Scopus' default search settings: article titles, abstracts and/or keywords. The search period is limited to the recent 15 years since an initial investigation found that studies on the topics in view mostly started at around 2006, with predominant numbers within the past ten years.

A total of 161 documents were obtained from the various field of studies, of which 86 are published journal articles, 3 are articles in the press, 1 is a book chapter and 71 are conference papers. All retrieved

documents were further analysed in which 87 documents were removed as being insufficiently related to the main scope of Vehicle Dynamics Control or Vehicle Probe-based Pavement Management nor the primary purposes of system response-based estimation (road profile reconstruction/estimation - PR, Potholes detection – PD or roughness index estimation - RE); these rejected documents are mostly related to bridge-vehicle interaction. Relevant references (56) were retrieved and included in the analysis (see Figure 3-2a). The additional literature that was missed in the direct search is due to various technical terms being used in these documents such as road anomaly, abnormal section, impact, defect, bump, irregularity, failure, damage (instead of 'pothole') or sensing, measurement (instead of estimation, classification, detection). Among the 130 reviewed documents, 37% are for PR, 39% for PD and the rest 24% for RE.
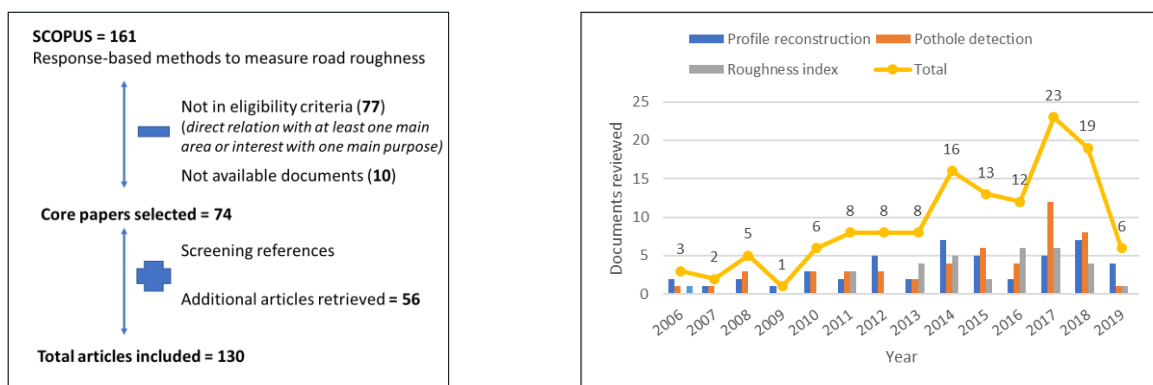
Figure 3-2: Reviewed documents (a) retrieval of 130 articles, and (b) decomposition

3.2 Human-vehicle-road roughness interaction (Numerical study)

This study was presented in Paper II. The study aimed to investigate different mathematical bus models to evaluate road roughness and passenger ride comfort, and to select the most appropriate bus model for further application to develop the new BRI (Bus Ride Index).

The experimental set-up was conducted along with the following steps:

- o Selecting bus lane segments with different road roughness levels (Figure 3-3a);
- o Scanning the bus lane by a multi-laser road profiler;
- o Measuring onboard ride comfort index using a seat-pad accelerometer (Figure 3-3b, c);
- o Developing multiple degrees-of-freedom (DOF) quarter-, half- and full-bus models (QBM, HBM and FBM) to estimate ride comfort index (Figure 3-4); and
- o Comparing the measured and simulated ride comfort levels to evaluate the developed mathematical bus models.

Different mathematical (quarter-, half-, and full-) bus models were developed based on technical data of the existing bus fleet in Singapore. Their performance was compared using measured acceleration data when the bus traverses over a straight segment of 2km in the city-centre road network.

MATLAB/Simulink tool was used for simulation purpose and the seat-pad accelerometer with a sampling rate of 750Hz was used for data collection. Field-measured road profiles were sampled using multi-laser road profiler with a sampling interval of 25mm, collected recently in May 2018.

(a) The selected road segment

(b) The selected single-decker bus

(c) On-cushion accelerometer

Figure 3-3: Experimental set-up
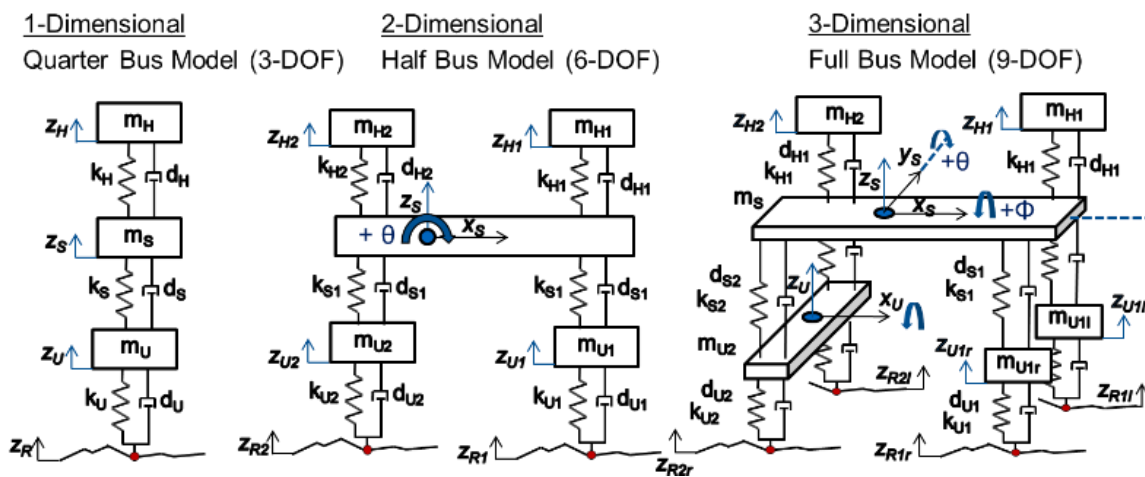
Figure 3-4: Three mathematical bus dynamics models with different DOFs

3.3 The quarter-bus model for Bus Ride Index (Numerical study)

This study was presented in Paper III, aimed to develop the BRI to evaluate road roughness and passenger ride comfort (Figure 3-5), and to develop a maintenance strategy for bus lanes.

Vertical acceleration can be calculated using numerical vehicle models. Field-measured road profiles were sampled using a professional road profiler for roughly 50km bus-lanes. MATLAB/Simulink tools were used throughout the study, from the generation of road profiles to simulation of vehicle models and calculation of frequency-weighted root-mean-square acceleration based on ISO 2631. From the results, the correlation between IRI and ride comfort index was established at different speed levels.

$m_p = M_p/M_s$; $k_p = K_p/M_s$; $c_p = C_p/M_s$
$M_s = 1$; $K_2 = K_s/M_s$; $C = C_s/M_s$;
$\mu = M_u/M_s$; $K_1 = K_t/M_s$
M in kg; K in N/m; C in N/m^2
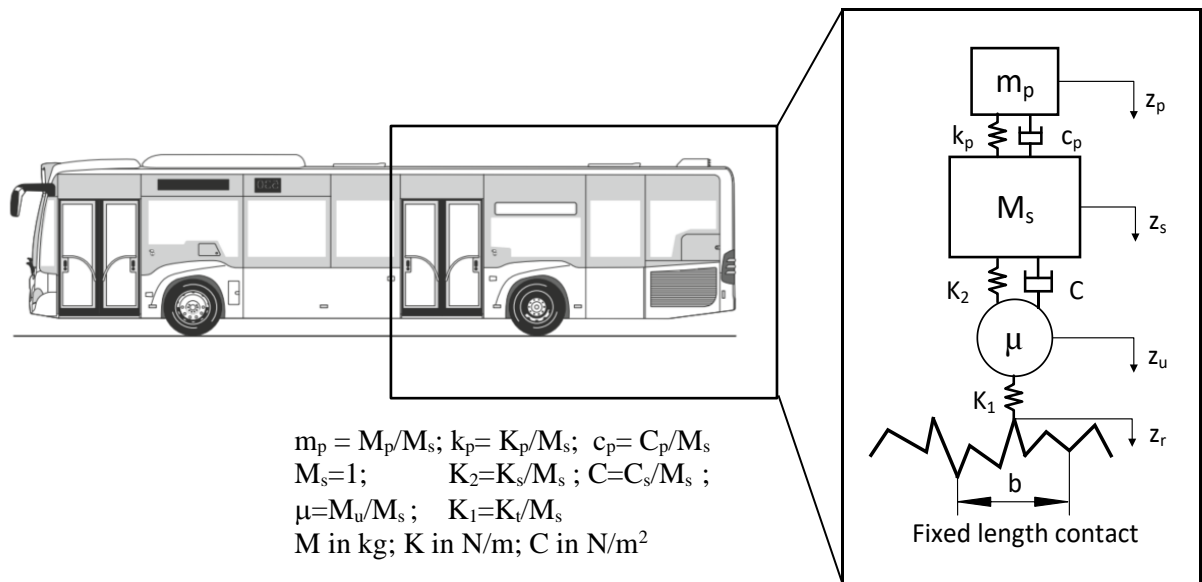
Figure 3-5: The 3-DOF QCS for BRI based on Citaro bus model

Since not all data are available, some of them were referenced from the literature. On the other hand, the field measurement of bus lanes in the city (Figure 3-6) was challenging to be conducted using the professional instrument from industry collaborator. The first run of measurements contained inaccurate GPS data, hence, a second run was performed to correct the problem. All these processes take time and effort in collecting credible data for downstream processing.
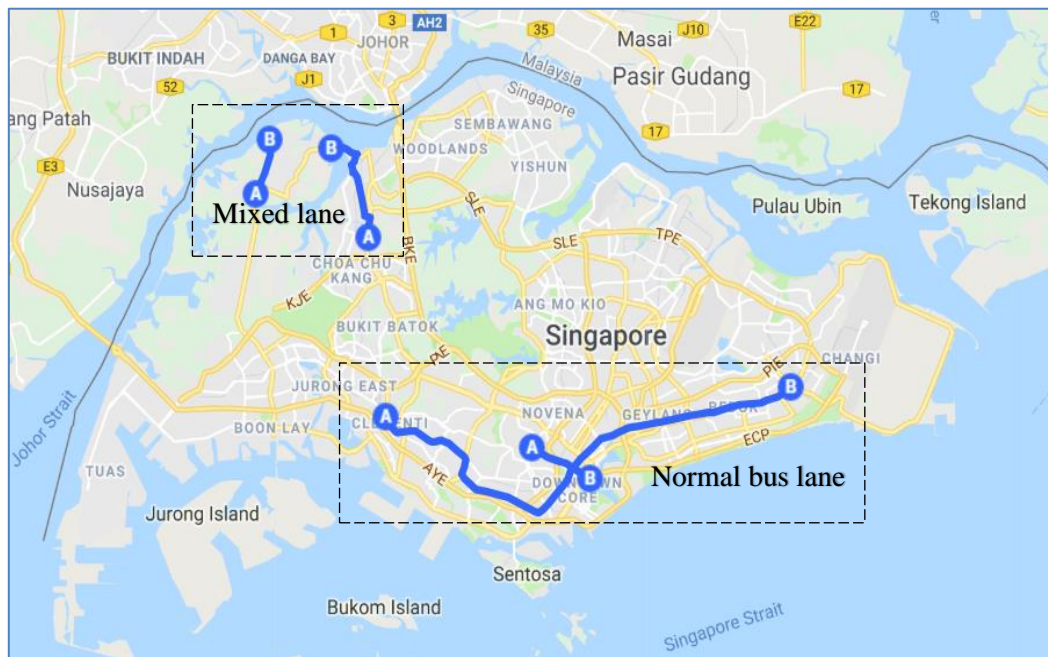
Figure 3-6: Locations of the field-measured bus lanes in Singapore

3.4 Human-vehicle-road alignment interaction (Experimental study)

This study was presented in Paper IV, aimed to investigate how sharp turning radius affected bus passenger ride comfort, and to define the ride comfort thresholds for vehicle operating speeds.

In this experimental study, the focus was a participant group comprising subjects deployed at different postures and locations onboard the bus. To collect passenger ratings, a mobile phone application was designed including a 5-point rating scale from 1 to 5 as *not uncomfortable (1), a little uncomfortable, uncomfortable, very uncomfortable* and *extremely uncomfortable (5),* respectively (see Figure 3-7). Objective indicators (duration of movements, accelerations, jerks) were collected by the commercial and highly accurate seat-pad accelerometer SV100A. Linear multiple regression and classification methods were used to correlate appropriate ride comfort thresholds according to various indicators.

The experiment includes four parts for the participant to follow. Firstly, the mobile application was downloaded by all participants for practice and familiarisation beforehand. Secondly, the whole experimental process was introduced to all participants before the actual experiment. Thirdly, the real experiment was conducted in which participants rated any uncomfortable feelings during the 45 minutes of the bus run. The reason for discomfort can be the vehicle's vibration, swerving, acceleration and deceleration. Lastly, some questions regarding the overall ride comfort were evaluated by all participants at the end of the journey.
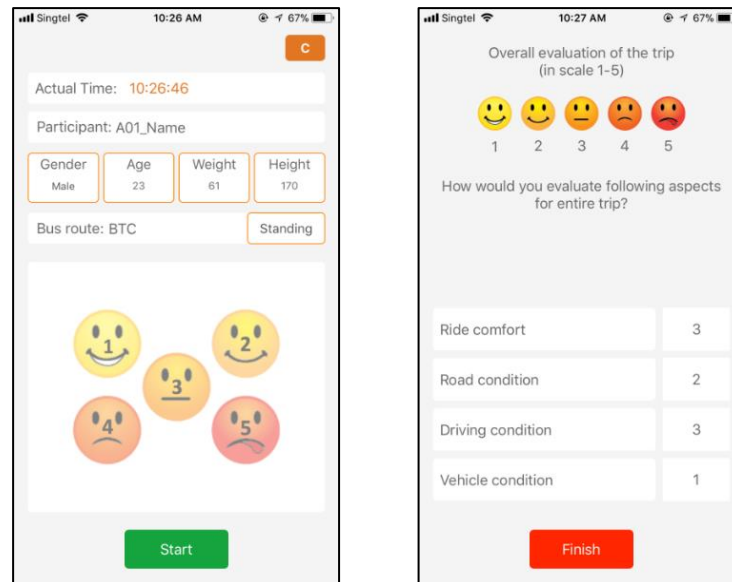
Figure 3-7: Two user interfaces of the mobile application to collect passenger ratings

3.5 Evaluation of APT platooning performance (Traffic simulation)

This study was presented in Paper V. This work investigated the platooning performance by using the PTV VISSIM microscopic simulation to model the operation of the DART system in Singapore city as a case study. This study is representative of the top-down approach based on APT's vehicle

specification and operation affecting on road infrastructure, as contrasted to bottom-up approach using conventional bus system as references.

Platooning protocol of autonomous vehicles was first developed for simulating coupling/decoupling process (see Figure 3-8). The platooning performance was then simulated on a VISSIM platform for various scenarios to compare the performance of DART platooning under several ride comfort levels: three bus comfort and two railway criteria.
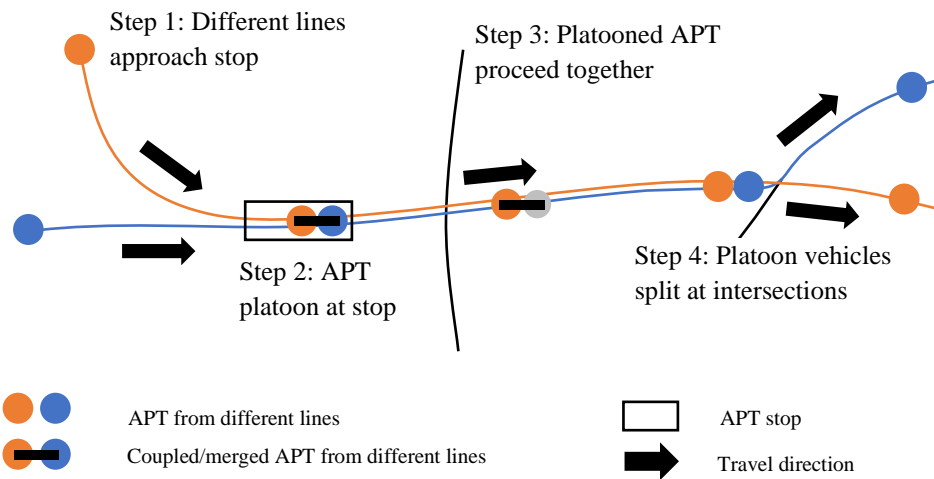
Figure 3-8 Illustration of the DART coupling based on bus platooning

After the platooning protocol has been established, different scenarios were considered to evaluate the DART performance as follows (see the summary in Table 3-1):

-   The long road corridor includes several intersections where the merged-platoons must navigate along sharp turning curves;
-   Apart from LRT and HSR ride comfort criteria, three other lateral thresholds regarding onboard passenger posture are also considered;
-   For longitudinal acceleration and comfort, bus deceleration/braking $a_x = -0.75 m/s^2$ is used to define the "reduced speed areas", which is much lower than the desired deceleration b of the vehicle design;
-   Each merged-platoon includes between 3 to 5 modules running from start to end, where the starting point is a pre-defined merging stop, and the ending point is the last stop before decoupling;
-   In this study, vehicle dynamics behaviour within curves is the focus by using microscopic traffic simulation, where three scenarios are created with the merged-platoons consisting of 5 modules (3+2), 4 modules (2+2) and 3 modules (1+2); and
-   All scenarios are simulated without traffic interference and can be considered as an ideal public transport prioritisation scenario without delay caused by the traffic lights. The operating speed is 49km/h on the straight segments.

Table 3-1: Simulation scenarios

Merged platoon	Number of modules	Platoon formation from		Ride comfort criteria and lateral acceleration thresholds					Traffic conditions
				HST comfort	LRT comfort	Bus standing	Bus leaning	Bus sitting	Dedicated lane
		Platoon A	Platoon B	$a_y = 0.49$ m/s^2	$a_y = 0.98$ m/s^2	$a_y = 1.50$ m/s^2	$a_y = 1.75$ m/s^2	$a_y = 2.0$ m/s^2	without traffic
Platoon1	5	2	3	✔	✔	✔	✔	✔	✔
Platoon2	4	2	2	✔	✔	✔	✔	✔	✔
Platoon3	3	2	1	✔	✔	✔	✔	✔	✔

4. RESULTS AND DISCUSSION

This section summarises the main findings, followed by a discussion of each paper's output. Appendices 1-5 provide further details on the included full papers, which reported the answers to the research questions. Papers II, III, IV and V formed the core research, whereas the review in Paper I documented pertinent research gaps.

4.1 Paper I: State-of-the-art response-type methods to evaluate road roughness

The advent of cheap and available sensors has led to the emergence of response-type methods to evaluate road roughness as supporting methods for existing IRI and Pavement Management System. The knowledge of road profiles, potholes and IRI can be measured using onboard accelerometers via various methods, e.g. inverse calculation by analysing vehicle mathematical models.

This paper reviewed 130 articles to highlight the difference between various methods and proposed research areas for further study on response-type methods. The database was retrieved for a recent decade and data mining was used for analysis. The results showed that machine-learning techniques (data-driven methods) had been used intensively with promising results but the disadvantages on data dependence have limited its application in some instances as compared to analytical/data processing methods (Figure 4-1). Recent algorithms to reconstruct/estimate road profiles (PR) are based mainly on passive suspension and quarter-vehicle model, and trying to utilise as few key parameters as possible, be independent on speed variation, and entails the least computation for real-time/online application. Algorithms for pothole detection (PD) and road roughness index estimation (RE) are increasingly focusing on GPS accuracy, data aggregation and crowdsourcing platform for large-scale application. However, a novel and comprehensive system that is comparable to the existing international roughness index (IRI) and conventional Pavement Management System is not yet finalised/reported.
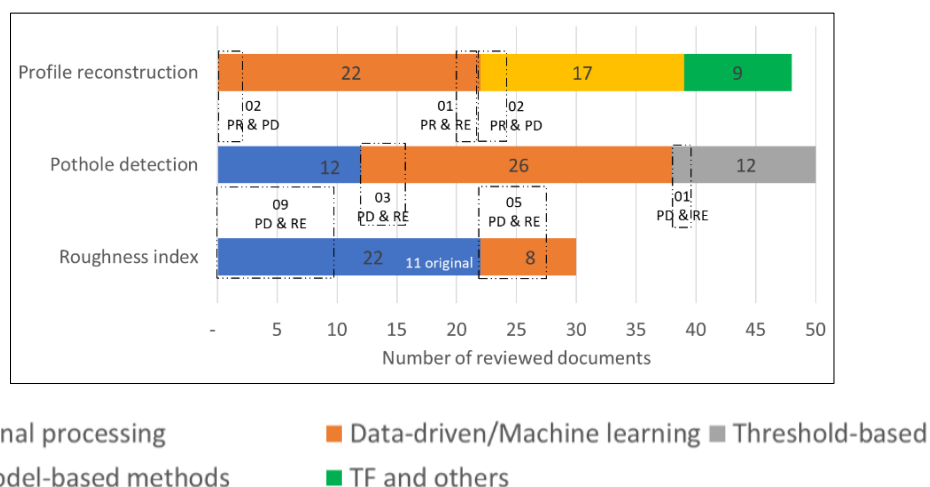
Figure 4-1: Method classification for RE, PD and PR

Moreover, another research gap was also pointed out that further study can focus on the development of machine learning techniques to incorporate all functions (PR, PD, RE) by considering the variance of vehicle parameters and travel speeds within the vehicle connected environment. This potential requires the development of bus mathematical models.

➤ *Discussion on the algorithm for pothole detection and roughness index estimation:*

The complexity, precision and computing intensiveness of each method are different. Regarding PD and RE, various methods have been used and can be classified into three categories: threshold-based, signal processing and machine learning methods. The first threshold-based methods are the most straightforward approaches for pothole or road anomaly detection by processing mainly the vertical acceleration (Z-acc) or in combination with other direction acceleration (x and y) and gyroscopes [79]. Given its simplicity based on the detection rate, be it true positive and false positive, the threshold values may vary due to different factors such as vehicle speeds and suspensions, smartphone types and orientation, which make this method not being feasible to be used in real scenarios and large-scale implementation.

The second signal processing methods overcome these drawbacks by using various filters. Many types of filters were used to develop the vertical acceleration impulse (DVA) to identify a "high-energy event" and to label "anomaly" on the road surface in UNIquALroad [80, 81]. To evaluate road roughness (IRI), the well-known regression relationships between power spectral density (PSD) with IRI was investigated in [82, 83], as were the RMS acceleration and IRI in [84, 85].

Machine learning methods have emerged in recent years due to greater data availability as well as the development of computing technology, which enable the machine to gain self-learning ability. Simple systems such as Nericell [86] and TrafficSense [87] used specific algorithms to filter and to cluster the collected detector data. A sophisticated clustering machine learning (improved Gaussian Mixture Model - iGMM algorithm) was used to cluster potholes with an adaptive detection threshold and learning rate update in CRSM [88, 89] after using pothole filters in Pothole Patrol. CRSM can also estimate IRI data.

This paper has been accepted for publication by the *European Transport Research Review* (see Appendix 1).

4.2 Paper II: A comparison of different mathematical bus dynamics models

Bus configurations are more complex than cars since the buses may be asymmetric, in larger dimensions and able to carry more passengers in different locations onboard. The air-spring suspension is also an important component equipped in the large-size urban bus. The development of accurate bus mathematical models will help to simplify the complicated multi-body vehicle dynamics when evaluating ride comfort and road roughness.

This paper investigated and compared various degrees-of-freedom (DOF) bus model: 3-DOF quarter-, 6-DOF half-, and 9-DOF full-bus dynamics models. Technical data were collected from the operating bus fleet while longitudinal road profiles were sampled from 2 km of the bus lane. The results showed that the full-bus models (FBM) represent most accurately with the minimum difference between simulated and measured acceleration data; however, this model is also the most complicated. The quarter- bus model (QBM) is still plausible to be used to evaluate road roughness condition within a specified error tolerance (around 20% higher than that of the FBM, using only right-wheel track). The half-bus model (HBM) leads to results in the middle of the QBM's and FBM's (Figure 4-3, Figure 4-2).

The findings of this paper are crucial and fundamental for further study to develop the BRI. The justification of quarter-bus model for BRI needs to be conducted for more road profiles in the city road network in the following study on the development of BRI.
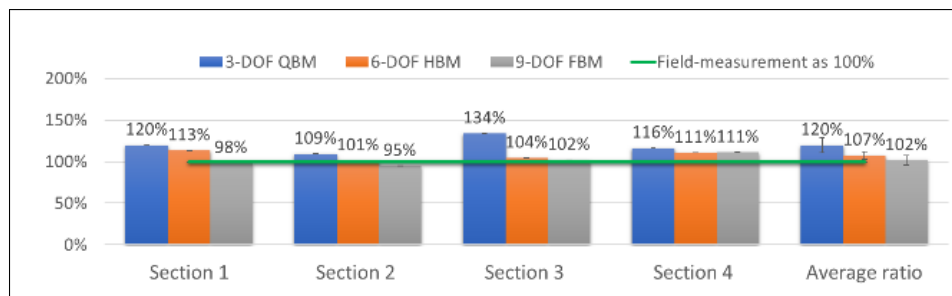
Figure 4-2: $a_{wz\_simulation}/a_{wz\_measurement}$ ratios at different segments and the average ratios using only the right-wheel track where the field measurement was taken

This paper has been submitted to *Mathematical and Computer Modelling of Dynamical Systems* (Appendix 2) and is presently under review.

➢ *Discussion on the developed bus mathematical dynamic models:*

FBM provides the most reliable results and several factors made the outputs from QBM and HBM to be higher than that of FBM. Firstly, QBM only considers vertical oscillation while HBM and FBM take into account pitch motion, and both pitch and roll motion, respectively. This serves to reduce vertical acceleration since when the rear tyres go over the hump the front tyres stay on the ground in the case of HBM and FBM as contrasted to QBM. Secondly, on specific road segments the outputs from the three models can be similar when there are less roll and pitch motions, meaning that the right and left road profiles are quite uniform.

Over the comparison of $a_{wz}(t)$ in the time domain, there is always the trend that the simulated results are higher than field-measured results. This disparity can be explained by the tyre being modelled as a point contact of the mathematical bus models which is different from the dual-wheel rear axle. The real dual-

wheel helps to reduce the impact of road roughness, for example when one tyre goes over a small pothole while another tyre stays on flat ground to keep the whole dual-wheel in the flat, balanced position.
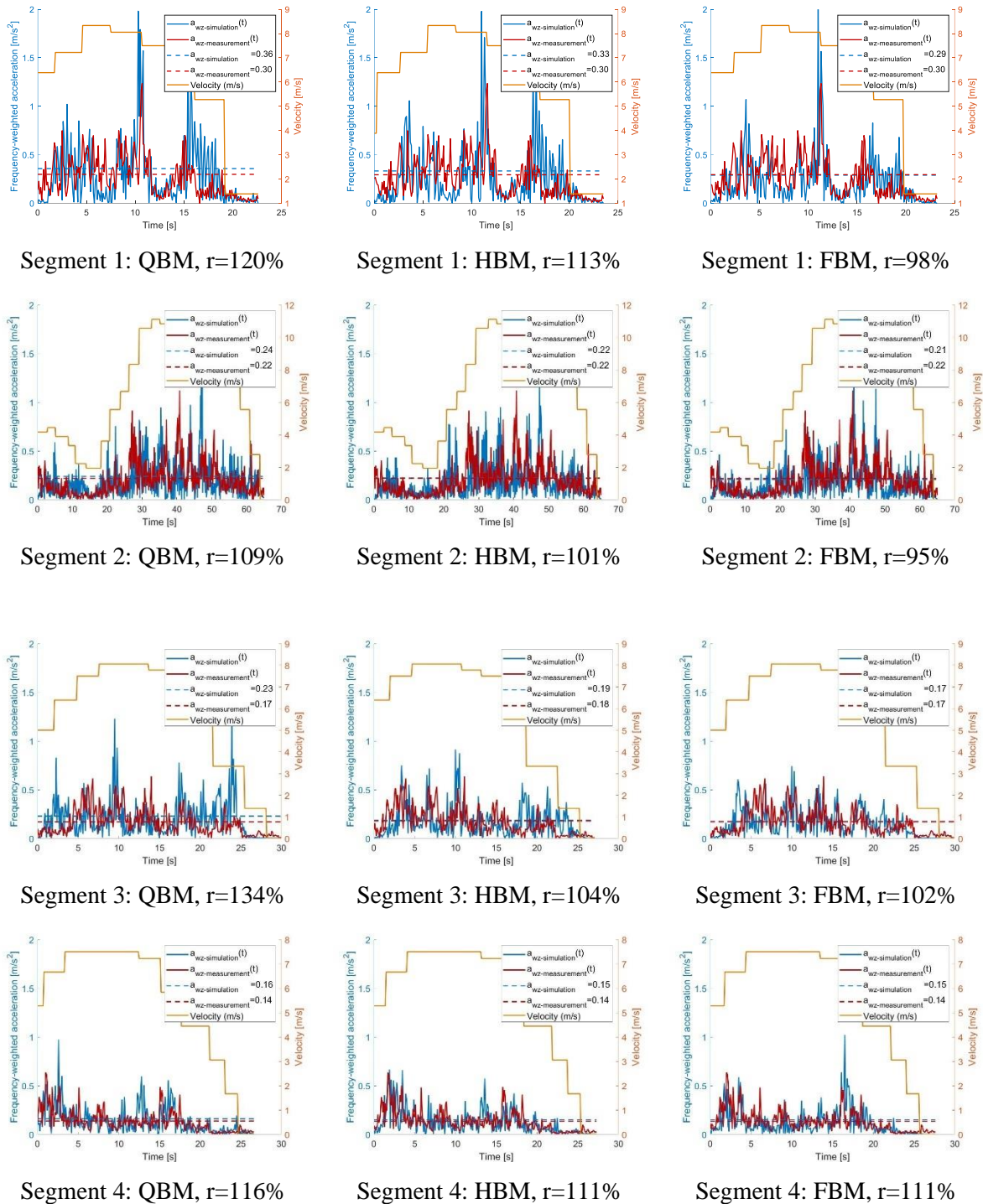
Figure 4-3: The $a_{wz\_simulation}(t)$ and $a_{wz\_measurement}(t)$ at different segments for the right-wheel-track

Even though FBM can provide the highest accuracy, it is still challenging for application in pavement engineering. This is again affirmed by the findings in [69] summary in which there are 4 QCS related to ride comfort evaluation and 3 QCS used to measure dynamic suspension load; two half-car simulation models (Cw), one full-car simulation model (FRI) and the other three indices from in situ measurement.

However, by this comparison study, it is possible to infer the vibration on FBM from QBM or HBM by the established conversion ratios.

4.3 Paper III: Bus Ride Index to evaluate road surface irregularities

In contrast to many developed indices to evaluate ride comfort and road roughness, there are few studies on bus vehicles running on dedicated lanes. The reason probably comes from different traffic conditions in different countries where bus lanes or BRT lanes are not existing everywhere throughout the world.

This paper developed a quarter-bus model for BRI based on the analysis from the previous study on the comparison between different mathematical bus dynamics models. The technical data of buses were collected from regular buses in Singapore as well as from literature reviews. Further longitudinal road profiles were sampled from bus lanes in the urban city. The BRI is a more appropriate tool to evaluate ride comfort of bus passenger. Based on BRI, new IRI threshold levels were proposed to maintain road conditions at different speed levels (Figure 4-4).

The BRI can be considered as the key finding of the whole dissertation, which comes from experimental study to vehicle dynamics and bus mathematical model. It is essential that for transport experts, the easy usage of any tool or index (e.g. IRI) is more helpful instead of complicated models. The BRI has been based on this principle in its development, and it deserves consideration from transport authority in the country.
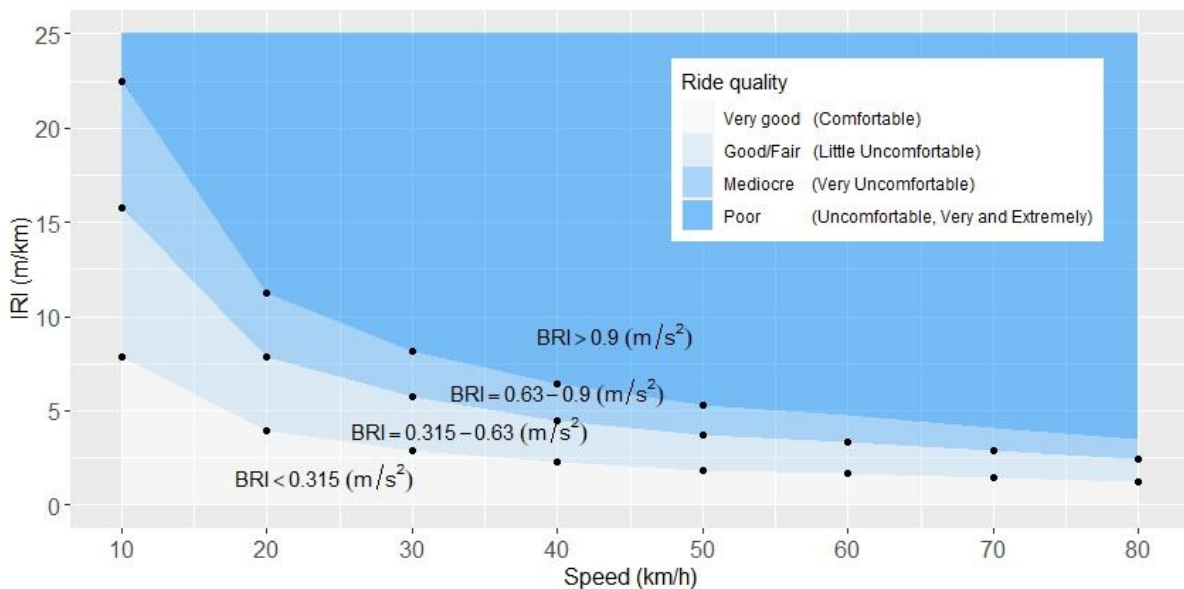
Figure 4-4: Ride quality based on IRI and BRI

This paper is published in *Road Materials and Pavement Design* (Appendix 3).

➢ *Discussion on the developed BRI:*

Notwithstanding the advantages of simple calculation procedures, the novelty of the 3-DOF BRI (bus ride index) model is summarised as follows:

o Applicability to urban heavy-bus dynamics and bus/BRT lane roughness evaluation, where buses are operated at lower speed levels with frequent stop-and-go behaviour, and cars are restricted or prohibited;

o Consideration of air-suspension which is currently a well-developed technology for most urban buses;

o Direct measurement of passenger ride comfort; and

o BRI as an alternative of IRI, in which bus/BRT lane roughness can be evaluated at any time without using professional pavement profiler. BRI has the potential use in the Probe-based Pavement Management where road surface can be up-to-date upon being assessed by every bus that is designed as a probe to detect roughness condition automatically.

Concerning passenger ride comfort and the application of the BRI, the road transport authorities and bus operators can refer to Figure 4-4 for different applications. For example, to offer a certain level of passenger ride comfort at a designed speed, road roughness should be maintained following the proposed IRI thresholds. Alternatively, vehicle speed should be limited when the road is rough to ensure satisfactory onboard ride comfort.

4.4 Paper IV: Ride comfort thresholds of bus passengers on urban roads

Knowledge of how bus passengers perceive ride comfort when the bus is navigating the horizontal curve in urban roads is essential to the design of vehicle speed profiles. Although APT is a brand-new system, it shares the same concerns with existing bus system in terms of ride quality as the high priority for modal choice.

This paper established three levels of ride discomfort by conducting two bus runs with 34 passengers onboard the buses. Lateral acceleration (a_y in m/s^2) has the most influence on passenger ride discomfort from the established relationship between different subjective and objective factors. Figure 4-5 illustrates the ride discomfort level classification when the bus is turning, in which standing passengers experience all levels of ride discomfort (3, 4 and 5) while seated passengers are the most comfortable group. Based on this finding, the classification method was used to categorise ride discomfort into different levels as follows: $a_y \leq 1.5$: *Comfortable*; $1.5 < a_y \leq 1.75$: *Uncomfortable*; $1.75 < a_y \leq 2.0$: *Very Uncomfortable*; and $2.0 < a_y$: *Extremely Uncomfortable*. The results were compared with existing study to justify the reliability of the used method.

The paper has shed light on the posture-dependent ride quality of bus passengers which has not been investigated previously. For commuting and promoting public transport use towards sustainable

mobility, improving passenger satisfaction is the utmost importance. It is recommended that the operation of existing bus fleet should be improved to address passenger perceptions in passenger-centric design.
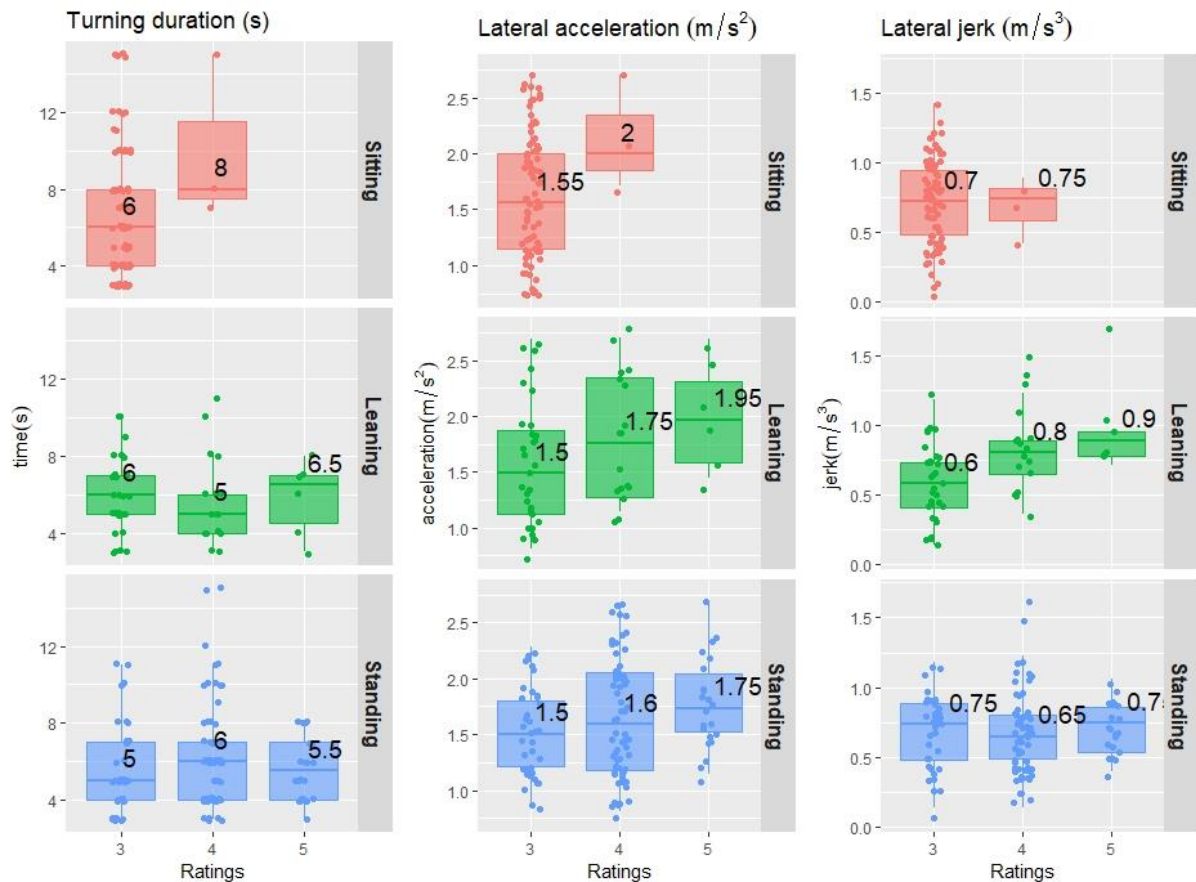
Figure 4-5: Ride discomfort classification when the bus is turning

This paper is published in *Case Studies on Transport Policy* (Appendix 4).

➤ *Discussion on the experimental study:*

By conducting the experimental study and using existing bus technical parameters and field-measured road longitudinal profiles, the study findings have reflected rational cause-and-effect of the influences from road conditions on passenger ride quality. In human perceptions [90], it is worth noting that the study findings on moderate R-squared regression factor are common.

The three ride discomfort levels were compared with values reported in the literature. The average lateral jerks $d_y = 0.6$; 0.75 and 0.9m/s^3 are within the range from 0.3 to 0.9m/s^3 in [11] in design of horizontal alignment such as transition curve. The $a_y = 1.5$m/s^2 (*discomfort* threshold) and $a_y = 2.0$m/s^2 (*extreme discomfort* threshold) is equivalent Level 1 and Level 2 of standing discomfort levels, respectively, from [53]. In another way, the implemented methods have been validated from this consistency and relevance.

4.5 Paper V: APT System Performance and Passenger Ride Comfort

There is always the trade-off between vehicle speed and ride comfort induced by acceleration from road surface/alignment and braking/accelerating that made it difficult to reach the ride comfort levels on LRT or HST, especially in the urban context with frequent stop-and-go imposed by the traffic lights, tight alignment and turning curves along the routes. The investigation in VISSIM has been conducted in [22] on the trade-off between intersection capacity and driver experience. The concern, however, is more critical for AB in an urban area than AV because private AV can travel longer from origin to destination, and passengers will have flexible time to enjoy their leisure/entertainment.

The DART system being researched in Singapore is used as a case study of APT systems, which are configured to accommodate prevailing passenger demand for a peak as well as non-peak periods, by electronic coupling and decoupling of platooned units along travel corridors. Platooning protocol of AVs was first developed for simulating coupling/decoupling process. The platooning performance was then simulated on the VISSIM platform for various scenarios to compare the performance of DART platooning under several ride comfort levels: three bus comfort and two railway criteria. The study revealed that it is feasible to operate the DART system following the bus standing comfort criterion (a_y = 1.5 m/s^2) without any significant impact on system travel time. For DART system operating to maintain a ride comfort of HST and LRT, the delay can constitute up to ≈10% and ≈5% of travel time, respectively. This investigation is crucial for the system delay management towards precisely designed service frequency and improved passenger ride comfort (Figure 4-6).
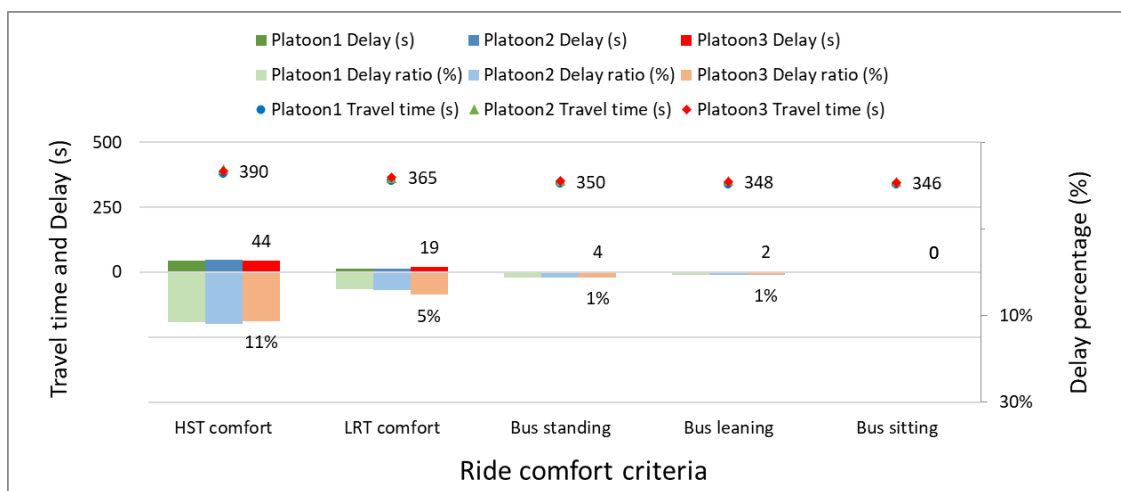

Figure 4-6: Travel time and delay (bus sitting as reference) of 3 platoons at different ride comfort criteria. The value inside the graphs is the travel time and delay of Platoon3 for reference

This paper has been submitted to *Sustainability* journal (Appendix 5) and is presently under second review.

➤ *Discussion on the application of study findings on the planning of the DART system:*

This investigation is crucial for the system delay management towards precisely designed service frequency and improved passenger ride comfort. It is noted that the platooning protocol is designed with maximum waiting time, e.g. of 60s, and the travel delay as 44s for a 3.6km corridor can be extended for a longer travel distance, which can deteriorate the pre-defined platooning sequence. This issue would be scaled up to the more extensive planned network of 18 lines, resulting in delay effects for the whole system. This result has emphasised the importance of pre-emption measures for platooning at the signalised intersections as well as necessary delay management to support APT platooning.

4.6 Analysis of transition curve for APT dedicated roadway

Beside speed recommendation for APT operation, the established ride discomfort thresholds can be investigated to design transition curves as a critical approach to reduce the discomfort of vehicles negotiating horizontal curves at high speed. The design speed is often greater than 60km/h as such in Singapore [38], or Australia [91], whereas in the USA speed requirement is not mentioned [11]. There are two well-known Clothoid and cubic parabola transition curves, for which the former is exclusively used in road alignment and the latter in railway alignment, but only for historical reasons [92]. Except for the simplicity of cubic parabola which is no longer applied thanks to computing technique development nowadays, there is no advantage over the Clothoid [92]. The Clothoid (or Euler spiral) provide many advantages such as a smoother curve, suitable development of super-elevation runoff, widened travelled way and a more gradual change of lateral force [11].

For this reason, Clothoid, though involving more calculation complexity than a cubic parabola, is still used for both roadway [11, 38] and railway alignments in Singapore [38] as well as dedicated bus lane in the UK [41]. Clothoid is also confirmed as the most common type of transition curve for railway application, besides other types such as Helmert curve (or Schramm curve), Bloss curve, Cosine curve and Sine curve (or Klein curve) [93]. The main difference is that the others have nonlinear curvature change with chainage while the Clothoid is linear (Figure 4-7), resulting in jerking at the beginning and end of Clothoid at high speeds (e.g. >160km/h) [94]. Selection among other types of transition curve is based on different aspects, such as the Bloss curve being used for its stricter regulations concerning tilting train for a design speed of 200km/h instead of Clothoid [95].

Key
1 clothoid with linear cant transition (infinite)
2 Helmert (Schramm) transition
3 Bloss transition
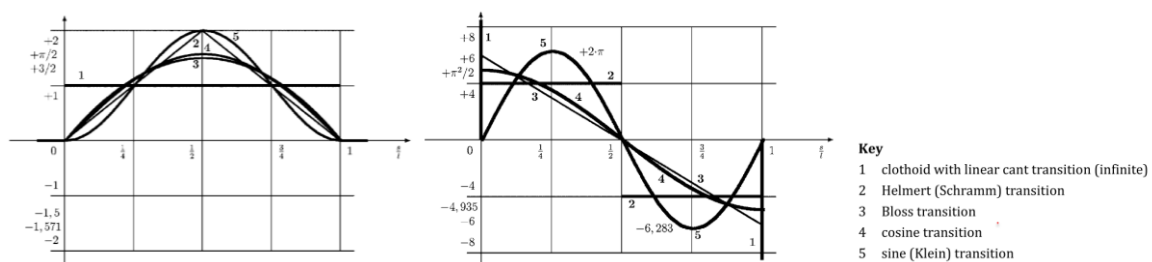4 cosine transition
5 sine (Klein) transition

Figure 4-7: Transition curve comparison (a) first derivatives and (b) second derivatives

The above-mentioned analysis has shown that Clothoid is the most potential for, in case of, APT dedicated lane. Indeed, it is already used for the UK guided busway based on the design speed of 120km/h [41]. The minimum length of spiral transition curve is calculated based on Equation (4.1) developed in 1909 for railway track curves [11, 41]:

$$L = \frac{0.0214V^3}{RC} \qquad (4.1)$$

where L is the minimum length of spiral (m), V is speed (km/h), R is curve radius (m) and C is the rate of increase of lateral acceleration in which C = (0.3-0.9) (m/s^3) has been used for highways.

Table 4-1 compares the limiting values (C, a_y and travel time t at design speed within curve) of ride discomfort thresholds to calculate spiral curve elements (minimum length L_{min} and desirable length L_{des}, maximum radius R_{max} for the use of spiral curve for safety reason). The findings of turning duration of 5-7s are higher than travel time t for desirable length calculation, which can be explained that this duration represents the turning curve characteristics, while passengers may press the button within the curve in a shorter time (e.g. 2-3s). Therefore, this finding does not conflict with the recommendation on the travel time *t*. In Table 4-1 the finding has suggested t=2.4s as a back-calculation from L_{min} which is based on C value. Figure 4-8 shows the values of spiral elements in which the findings on L_{min}, L_{des} and R_{max} are approximate to [11] recommendation for a roadway transition curve.

Table 4-1: Comparison of limiting values to calculate spiral curve elements

Spiral elements	Minimum length	Desirable length	Maximum radius
limiting values	C (m/s^3)	travel time t (s)	a_y (m/s^2)
Roadway [11]	C = 0.3-0.9	t = 2.0 s	a_y = 0.4-**1.3**
[38]	C = 0.3-0.6		
Guided bus lane [41]	C = 0.3-0.6		a_y = 0.6-1.0
Light rapid transit [38]			a_y = 0.5-1.0
Urban bus (finding)	*C = 0.6-0.9*	*t = 2.4 (calculated from L_{min})*	*a_y = **1.5**-2.0*

Note: AASHTO uses a_y = 1.3 to calculate R_{max}, whereas the finding recommends a_y = 1.5 to consider standing passengers.
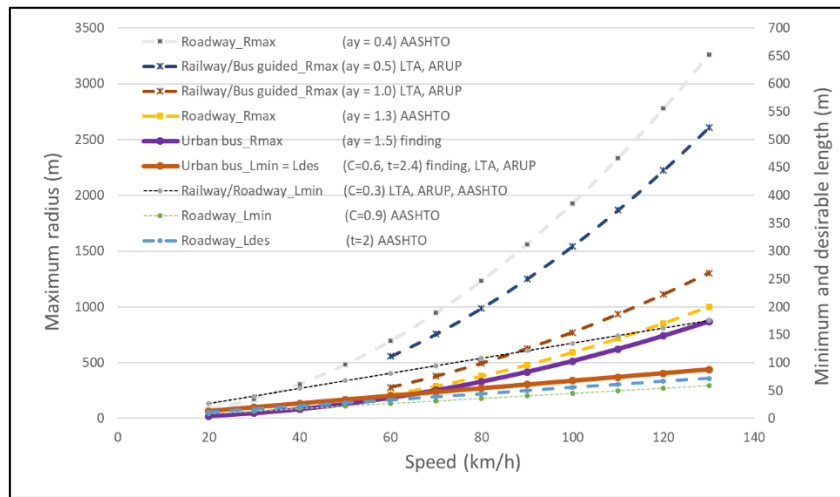
Figure 4-8: Illustration of recommended parameters to calculate spiral elements

In summary, passenger ride comfort has been set as a priority in these standards and guidelines for a long time. L_{min} is calculated from railway track design, and especially in the UK [41] the $a_y = 0.6$-1.0 m/s^2 and $C = 0.3$-0.6 m/s^3 are at the lower limits of AASHTO recommendation. Herein, design speed plays an important role in the difference. The UK guided bus lane has been designed as an independent LRT based on 120km/h design speed for geometry calculation. Therefore, in case of the APT dedicated lane at high speed (e.g. 120km/h), the design guidelines in the UK [41] is suitable to maximise passenger ride comfort. The detailed design handbook for design and construction of busway can be found in [41, 96] with the illustration of the cross-section in Figure 4-9. The study findings and recommendations are more appropriate for APT operation in urban road condition at lower design speed (< 60km/h) and without dedicated lane requirement.
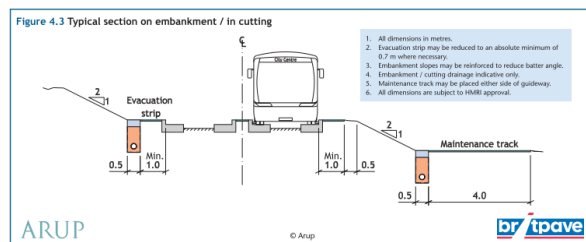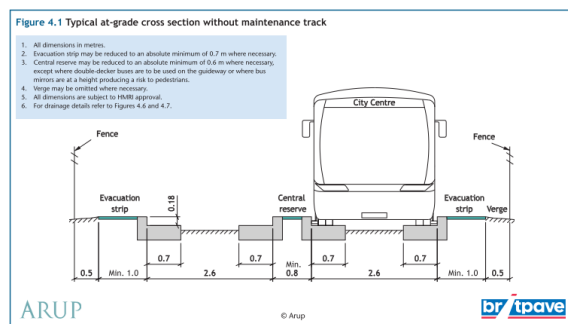
Figure 4-9: Cross section of Guided Busway Design in UK

5. CONCLUSION AND OUTLOOK

5.1 Conclusion

In the new ear of autonomous vehicle (AV) in transportation, challenges have been laid down for transport planners as well as road infrastructure designers to support the implementation of this innovative transport mode. This research was performed to establish road design guidelines for the innovative autonomous public transport (APT) conditioned on passengers' ride comfort and vehicle dynamics characteristics. The study results contribute not only to the operation of buses and APT but also the maintenance of their roadways. This comprehensive study comprises numerical study, experimental study, and traffic simulation, using a two-pronged approach (top-down and bottom-up) for both regular bus and autonomous public transport vehicles. The analysis and evaluation of existing, conventional bus system are considered as the reference for future APT. Table 5-1 summarises the significant contributions to practical implications for road infrastructure managers and planners as well as to the literature by each paper.

Table 5-1: New findings and contributions of the study throughout five papers

| Paper	Contributions

Paper I (bottom-up approach)	- Overview of the state-of-the-art response-based methods to measure road surface irregularity: road profile reconstruction, pothole detection and road roughness index estimation,
	 - Highlighted key differences of approaches: signal processing, model-based, machine learning, threshold-based, transfer function and others,
	 - Key focus areas for future research have been identified as follows:
	     o *Inclusion of the air-suspension system,*
	     o *Improving machine learning technique,*
	     o *Design a comprehensive response-based system for pavement, monitoring of public transport infrastructure, and*
	     o *The potential of Road impact factor (RIF) index as an alternative for IRI in the connected vehicle environment.*

Paper II (bottom-up approach)	- Comprehensive insight into bus dynamics focusing on vertical excitation of road roughness, - Simplified bus mathematical model to evaluate road roughness and passenger ride comfort, - A new method to compare between simulation and field-measurement data by matching GPS locations and speed profiles,

Paper	Contributions
	- Developed algorithms which can incorporate speed changes that replicate the stop-and-go phenomenon of regular bus service, resulting in more reliable outputs, and
	- The quarter-bus model is plausible in evaluating road roughness and can be used for further study.
Paper III (bottom-up approach)	- A refined BRI as a new index to evaluate road roughness which is more appropriate for bus and BRT lanes
	o *Applicability to urban heavy-bus dynamics operated at lower speed levels with frequent stop-and-go behaviour,*
	o *Consideration of the stiffness and damping ratio of air-suspension,*
	o *Direct measurement of ride comfort through the human-seat mass; and*
	o *BRI as an alternative of IRI, in which bus/BRT lane roughness can be evaluated at any time without using professional pavement profiler, and*
	o *New established IRI thresholds for maintenance strategy of bus lanes in the city, which can be adapted for the APT system.*
Paper IV (bottom-up approach)	- A new method to collect and match real-time passenger ratings with vehicle operation parameters,
	- Main factors influencing passenger ride discomfort onboard urban buses,
	- Ride discomfort of bus passenger within curves cannot be evaluated correctly based on RMS lateral acceleration,
	- Newly established ride discomfort thresholds for young-adult bus passengers, which can be used to design vehicle operating speeds:
	o $a_y \leq 1.5$: *Comfortable,*
	o $1.5 < a_y \leq 1.75$: *Uncomfortable,*
	o $1.75 < a_y \leq 2.0$: *Very Uncomfortable, and*
	o $2.0 < a_y$: *Extremely Uncomfortable.*
Paper V (top-down approach)	- New platooning protocol for electronic coupling and decoupling of platooned units,
	- Feasibility to operate the DART system following the bus standing comfort criterion ($a_y = 1.5$ m/s^2) without any significant impact,
	- For DART system operating to maintain a ride comfort of the high-speed train (HST) and light rail transit (LRT), the delay can constitute up to $\approx$10% and $\approx$5% of travel time, respectively.

For the first time, a comprehensive overview of response-type methods to evaluate road surface irregularity has been conducted covering the last decade, to explore state-of-the-art technologies as well as research gaps for study (Appendix 1). Similarly, it is the first time that three nonlinear bus dynamic models were developed and their performance compared regarding ride comfort calculation on a real urban road surface (Appendix 2). Most importantly, the developed BRI has been the first quarter-bus model index for evaluation of ride comfort and road roughness of dedicated bus lanes (Appendix 3). The new method has been developed to include a large number of passengers at multiple postures onboard the bus to explore their ride comfort comprehensively (Appendix 4), followed by the evaluation of APT platooning system performance with different ride comfort criteria (Appendix 5). The results expand the knowledge on the interactions between road infrastructure, vehicle dynamic and passenger characteristics within the context of autonomous vehicle (AV) era. In case of the requirement of dedicated lanes as concrete beams[1] for APT to run on, the design guidelines in the UK [41] is suitable to maximise passenger ride comfort as the LRT design standard. Within the passenger-vehicle-road interaction, each of the three influencing factors has contributed to the overall ride quality of the system as follows:

Firstly, road infrastructure influences significantly on passenger ride comfort. In an urban context where the pavements are often well-maintained in the Class A-B and Class B-C according to [97] classification, the ride quality induced from road surfaces has a common range from *comfortable, little uncomfortable, fairly uncomfortable to uncomfortable*. Whereas, the frequent turning movements of buses with curves, intersections and roundabouts can result in a higher range of ride discomfort from *uncomfortable, very uncomfortable to extremely uncomfortable*. In another context such as rural road or mining roads [98], the effects of the road surface are more significant than urban roads.

Secondly, vehicle dynamics is also important to ride quality as its direct interaction with passengers onboard. The study focus is on the large-size urban buses in the city, in which their configurations and parameters are quite identical. The analysis and development of BRI have demonstrated that this BRI quarter-bus model can represent different large-size urban buses. The analysis and comparison between three mathematical bus models can be considered as a sensitivity analysis of bus dynamics. The results of conversion ratios are beneficial to cross calculation/validation to simplify the high degrees-of-freedom bus models to the BRI for practical pavement engineering application. The use of the higher complicated full-bus model is, on the other hand, essential for vibration analysis regarding seat location variation onboard urban bus besides the investigation for an inter-city bus in [67]. This finding can be a contribution to the literature for any further research interest.

---

[1] However, in this case the autonomous vehicle will become automatic vehicle, which is in lower level of automation. *Levinson says it more plainly: "A truly autonomous car would decide on destination and route as well as control within the lanes. An automated car would follow orders about destination and route, and may only adopt some lane-keeping or car-following guidance."*
https://transportist.org/2017/06/29/on-the-differences-between-autonomous-automated-self-driving-and-driverless-cars/

Lastly, passenger postures are the key factors to consider when operating bus/APT vehicles under the excitation of road infrastructure. There is a clear difference in the perceptions of bus passengers during the same turning movement when the participants were deployed at multiple postures and positions. For urban, low-floor buses with a high proportion of standing position in the middle part of this bus, this area requires more supporting facilities for standing passengers to ensure ride quality. Careful driving behaviours of bus drivers are also necessary during the peak periods when very often seats are not available for all passengers onboard.

Based on the study findings, guidelines and recommendation have been proposed such as for road design and pavement roughness maintenance (Figure 4-4), and the operating speeds for buses and APT concerning passenger ride comfort (Figure 4-6). The recommendations for pavement maintenance (Figure 4-4) are more appropriate for existing large-size bus fleets in the city. This suggestion provides a higher IRI standard for bus dedicated lane than car lanes (e.g. BRI = 0.26IRI as compared to a_{wz} =0.22IRI at a vehicle speed of 80km/h, Appendix 3) which is different from existing maintenance strategies based on car dynamics. The refined BRI is an essential tool as a critical finding in this study and it can be adapted easily to simulate APT dynamics to evaluate the associated passenger ride comfort. However, it is noted that the APT vehicle dimension may be smaller than existing bus and DART configurations are like a small truck or lorry, hence other related findings can also be considered for APT vehicle dynamics simulation. Another study in [99] illustrated the DART ride index – DRI as a modified BRI for a specific application on smaller vehicle dimensions.

Especially for the DART module given its high ratio of standing position and operated at a higher velocity, the recommended speeds within sharp turning curves are essential to ensure proper ride quality. In contrast to highway corridors containing also straight segments and large-radius horizontal curves, the urban context is characterised by a more constrained road layout. Furthermore, the recommendations for APT operating speeds can be achieved more straightforward than for bus since the innovative APT modules are equipped with numerous sensors which can detect passenger positions and postures to provide valuable input for driving the AV. When there is a high number of standing passengers or in case of all seated passengers, the vehicle speeds at discomfort threshold (*uncomfortable*) and great discomfort threshold (*very uncomfortable*) can be suggested, respectively. In any case, the extreme discomfort threshold (*extremely uncomfortable*) must be avoided. The turning radius can also be widened to ensure the designed speeds of APT platoons; however, this is challenging in urban areas with scarce space.

5.2 Outlook

Throughout this study, the dissertation provides insights into the ride quality of passengers on bus/APT in the urban context. The overall contributions are not only in the new methodologies but also detailed specification and recommendation for the design of bus/BRT lanes or APT roadway. In line with the

analysis in [21, 23, 24, 100] the research contributions in the aspect of road infrastructure design have supported the planning and finalisation of the DART concept in Singapore. Cities with a similar condition can also utilise these findings for their potential implementation of the autonomous public transport system. Although this research has been conducted using both experimental and numerical study to consider all three elements (passenger, vehicle and road condition) in the passenger-vehicle-road infrastructure interaction, there are still several research limitations that need to be acknowledged for the benefit of further study.

1. Concerning bus mathematical models and BRI, this is the first time a comprehensive comparison among three mathematical dynamics models of a heavy-duty city bus (19t) has been conducted, resulting in $a_{wz}(QBM) > a_{wz}(HBM) > a_{wz}(FBM)$ over the same road segments. The FBM well captures the correct behaviours of bus dynamics, but this is the most complex model. Therefore, each bus model can be utilised depending on the specific study purpose. Based on that, the refined Bus Ride Index (BRI) was developed that can evaluate more precisely bus passengers ride comfort and road surface irregularity. The study is, however, based on nonlinear but passive suspension and damping vehicle dynamics. Further study can develop an active quarter-bus model coupled with measuring road profiles of the whole city bus lane networks for BRI calculation. Especially from the refined BRI, different alternatives and scenarios can be developed by adapting the BRI quarter-bus simulation for the APT module with a larger/smaller dimension with a capacity of 60, 80, or 120 passengers given its different suspension configuration as in the investigation of [99].

For recent application, more data collection on the bus lane network of the whole city for a comprehensive investigation is necessary. Especially for the full-day bus lanes equipped with Portland cement concrete (versus asphalt concrete) which have been considered, there might be different results between the two types of pavement regarding BRI value. Measurement data were collected in different locations in Singapore in which Figure 5-1 illustrates one such segment for reference. In the figure, time series a_{wz} (red profile) and speed (blue profile) are shown for a selected segment. The green line is a baseline for comparison and can be set up as any threshold (e.g. comfortable or uncomfortable). In case of poor ride quality (established BRI>0.9 m/s^2), several short segments are detected. The figure shows GPS location as well as a_{wz} scale in colour bar (green to red), in which the red segments represent low ride comfort equivalent to poor road roughness. Any small defects such as potholes can be detected easily. From these measurements, transport authority can have a first overview of road condition for further intervention and treatments.

Figure 5-1 indeed shows the functional performance but not technical performance, therefore, it is still unclear as to the roughness level of the road surface. However, the established IRI-BRI

relationship and BRI thresholds will rationally link the "user needs" with "pavement manager" for pavement management to evaluate road roughness as determined from passenger ride comfort.
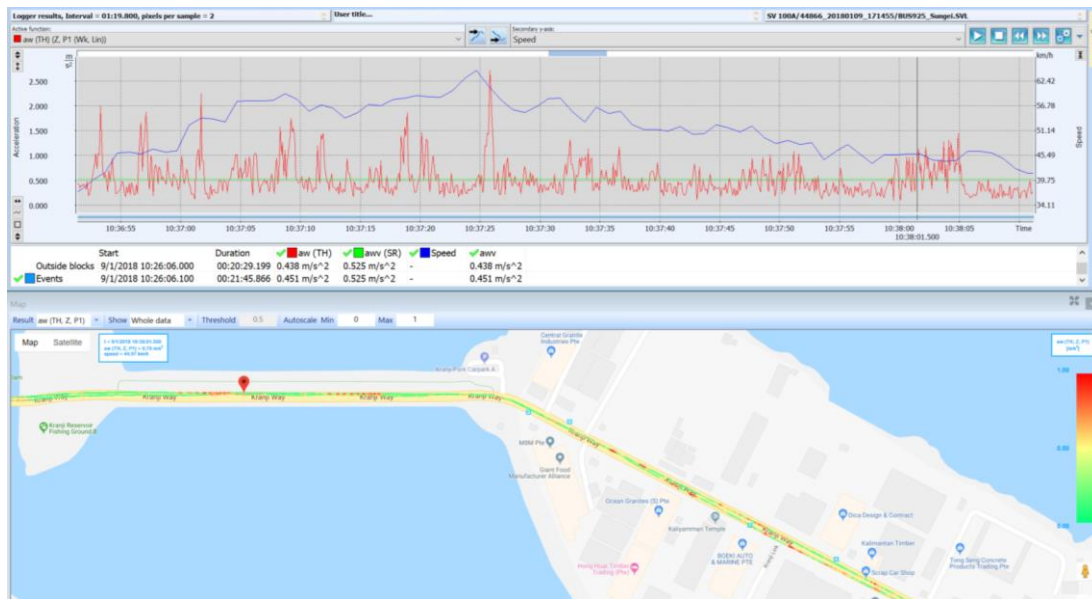

Figure 5-1: Onboard measurement of ride comfort data with time series and GPS data

2. Furthermore, the developed bus mathematical models are potential for future research to reconstruct road profiles for adaptive suspension control. Different methods can be applied where machine learning techniques have demonstrated their capability for multiple functions such as the ANN algorithms for road profile reconstruction and pothole detection in [101], profile reconstruction and roughness index estimation in [102, 103]. Regarding these methods with limitation in the estimation accuracy, vehicle parameters or speed variance can be further studied to develop comprehensive algorithms.

3. Moreover, although efforts have been spent in [104, 105] to develop a new Vehicle Probe-based pavement management (PBPM) for public transport (e.g. bus system only) which is less complicated as compared to a more extensive network, a comprehensive PBPM is still lacking. This fleet vehicle approach faces fewer challenges on data aggregation since vehicle fleets are quite identical, with lower GPS errors caused by lane-by-lane difference and without crowdsourcing platform. Such a system, once developed, will be beneficial in maintaining the road condition for public transport such as the citywide bus lane system in Singapore, London or worldwide BRT lane system, in which the road surfaces often deteriorate quickly due to heavy-loading from heavy-duty vehicles.

4. Lastly, only two bus runs were conducted in the experimental study with good conditions on the road surface and vehicle driving manoeuvres. The study is at first designed to target the passenger groups frequently travelling and commuting using bus transport service during the peak periods

(also the more congested periods). The missing "*mature working age*" group can be a target for further study as well as the world first launched Volvo's full-scale autonomous bus in Singapore [16] which is an excellent opportunity to extend the experimental study. Moreover, a new ride discomfort warning system for regular bus driving can be designed based on the proposed ride discomfort thresholds and the ratio of standing passengers on the bus shall be established, especially during peak periods, as similar to the existing telematics system in Tower Transit [106]. This will be a useful add-in to engender a more comfortable ride in future APT.

REFERENCES

1. Department of Statistics (2018) Population trends 2018. *Department of Statistics, Ministry of Trade & Industry, Republic of Singapore*, Singapore.

2. Sin, Y. (2018) Parliament: Singapore's total population likely to be "significantly below" 6.9 million by 2030. In: The Straits Times. https://www.straitstimes.com/politics/parliament-no-major-changes-expected-to-immigration-policy-josephine-teo. Accessed 9 Jan 2019.

3. LTA (2013) Land transport master plan 2013. *Land Transport Authority Singapore*, Singapore.

4. Menon, G. (2019) Improving Singapore's land transport in 2019. In: Today. https://www.todayonline.com/commentary/improving-singapores-land-transport-2019. Accessed 9 Jan 2019.

5. Credo (2014) The mobility opportunity: improving public transport to drive economic growth. *Siemens AG*, Munich, Germany.

6. Zhu Melissa (2018) Singapore's public transport system among best in the world: Mckinsey report. In: Channel NewsAisa. https://www.channelnewsasia.com/news/singapore/singapore-public-transport-system-among-best-in-the-world-10637978. Accessed 23 Apr 2019.

7. TUMCREATE (2015) Towards the "ultimate public transport system." *TUMCREATE*, Singapore.

8. Vuchic, V. R. (1981) Urban public transportation systems. *Transportation Engineering and Planning*, *I*, 1–26.

9. Vuchic, V. R. (2002) Bus semirapid transit mode development and evaluation. *Journal of Public Transportation*, *5*, 71–95. doi:http://doi.org/10.5038/2375-0901.5.2.4.

10. PTC (2016) Commuters at heart on recommendations to impore commuter's journey. *Public Transport Council*, Singapore.

11. AASHTO (2011) A Policy on Geometric Design of Highways and Streets, 6th ed. *American Association of State Highway and Transportation Officials*, Washington, D.C.

12. Erath, A. (2013) How to solve the problem of bus bunching. In: The Straits Times. http://www.straitstimes.com/the-big-story/case-you-missed-it/story/how-solve-the-problem-bus-bunching-20130324. Accessed 9 Sep 2018.

13. Port Finance International (2013) Singapore confirms transshipment move to Tuas. http://www.portfinanceinternational.com/categories/regulation-policy/item/1010-singapore-confirms-transshipment-move-to-tuas. Accessed 1 Apr 2017.

14. Hitti, N. (2017) Trackless, driverless "rail bus" takes to the roads in China. In: dezeen. https://www.dezeen.com/2017/11/06/worlds-first-driverless-trackless-train-launches-china-zhuzhou-transport-design/. Accessed 23 Apr 2019.

15. Navya (2018) Discover autonom shuttle | Navya. In: Navya. https://navya.tech/en/autonom-shuttle/%0Ahttps://navya.tech/en/autonom-en/autonom-shuttle/. Accessed 23 Apr 2019.

16. CNA (2019) Driverless electric bus launched by NTU and Volvo in "world first." In: CNA. https://www.channelnewsasia.com/news/singapore/driverless-electric-bus-launched-by-ntu-and-volvo-in-world-first-11311838. Accessed 23 Apr 2019.

17. Fahmy, T. (2019) Dubai tests autonomous pods in drive for smart city. In: Reuter.

https://www.reuters.com/article/us-emirates-transportation-autonomous/dubai-tests-autonomous-pods-in-drive-for-smart-city-idUSKCN1GD5G6. Accessed 22 Apr 2019.

18. Galeon, D. (2018) Autonomous transport pods make for a sci-fi commute in Dubai. In: Futurism. https://futurism.com/autonomous-transport-pods-dubai. Accessed 22 Apr 2019.

19. Radcliffe, D. (2019) Driverless air taxis, drones, pods: Dubai puts future tech at heart of transportation. In: zdnet. https://www.zdnet.com/article/driverless-air-taxis-drones-pods-dubai-puts-future-tech-at-heart-of-transportation/. Accessed 22 Apr 2019.

20. Debusmann, B. (2018) World's first autonomous pods unveiled in Dubai. In: Arabianbusiness. https://www.arabianbusiness.com/transport/389656-worlds-first-autonomous-pods-unveiled-in-dubai. Accessed 22 Apr 2019.

21. Rau, A., Tian, L., Jain, M., Xie, M., & Liu, T. (2018) Autonomous road transit (DART) for use-case capacity more than bus. In: *mobil.TUM 2018 "Urban Mobility – Shaping the Future Together" - International Scientific Conference on Mobility and Transport*. TUM, Munich, Germany.

22. Le Vine, S., Zolfaghari, A., & Polak, J. (2015) Autonomous cars: the tension between occupant experience and intersection capacity. *Transportation Research Part C: Emerging Technologies*, *52*, 1–14. doi:10.1016/j.trc.2015.01.002.

23. NguyenDinh, N. (2016) Precast ultra-thin whitetopping (PUTW) in singapore and its application for electrified roadways. PhD Dissertation. *Technische Universität München*, Munich.

24. NguyenDinh, N., Nguyen, T., Yang, E.-H., & Lechner, B. (2016) Life cycle cost assessment of engineered cementitious composite (ECC) precast pavement in Singapore. In: *Proceedings of the 11th International Conference on Concrete Pavements*. International society for concrete pavements, San Antonio, Texas USA.

25. Nguyen, T., NguyenDinh, N., & Lechner, B. (2016) Traffic microsimulation of roadwork in Singapore, a case study. In: *Proceedings of the 2nd Conference on Transport Infrastructure with Sustainable Development*. Danang, Vietnam.

26. Gallet, M., Massier, T., & Hamacher, T. (2018) Estimation of the energy demand of electric buses based on real-world data for large-scale public transport networks. *Applied Energy*, *230*, 344–356. doi:10.1016/j.apenergy.2018.08.086.

27. Viegas, J., & Lu, B. (1997) Traffic control system with intermittent bus lanes. In: *IFAC Proceedings Volumes*. Elsevier, pp 865–870.

28. Viegas, J., & Lu, B. (2001) Widening the scope for bus priority with intermittent bus lanes. *Transportation Planning and Technology*, *24*, 87–110. doi:10.1080/03081060108717662.

29. Viegas, J., Lu, B., Vieira, J., & Roque, R. (2006) Demonstration of the intermittent bus lane in Lisbon. *IFAC Proceedings Volumes (IFAC-PapersOnline)*, *11*, 239–244. doi:10.3182/20060829-3-NL-2908.00042.

30. Currie, G., & Lai, H. (2008) Intermittent and dynamic transit lanes: Melbourne, Australia, experience. *Transportation Research Record: Journal of the Transportation Research Board*, *2072*, 49–56. doi:10.3141/2072-06.

31. Eichler, M., & Daganzo, C. F. (2006) Bus lanes with intermittent priority: strategy formulae and an evaluation. *Transportation Research Part B: Methodological*, *40*, 731–744. doi:10.1016/j.trb.2005.10.001.

32. Olstam, J., Habibovic, A., & Anund, A. (2015) Dynamic bus lanes in Sweden – A pre-study. *Lunds universitet*, Linköping, Sweden.

33. LTA (2016) Bus lane schemes. https://www.onemotoring.com.sg/content/onemotoring/en/on_the_roads/traffic_management/full_day_bus_lanes.html. Accessed 17 Nov 2016.

34. Channelnewsasia (2016) Operating hours of full-day bus lane to be extended. http://www.channelnewsasia.com/news/singapore/operating-hours-of-full/2582442.html. Accessed 17 Nov 2016.

35. Adrian, L. (2016) Experts welcome dedicated bus lane on North-South expressway. http://www.straitstimes.com/singapore/transport/experts-welcome-dedicated-bus-lane-on-north-south-expressway. Accessed 17 Nov 2016.

36. Menon, G., & Kuang, L. C. (2006) Lessons from bus operations. Public Transport Council, Singapore.

37. Mitchell, D., Claris, S., & Edge, D. (2016) Human-centered mobility: a new approach to designing and improving our urban transport infrastructure. *Engineering*, 2, 33–36. doi:10.1016/j.eng.2016.01.030.

38. LTA (2010) Civil design criteria for road and rail transit systems. *Land Transport Authority*, Singapore.

39. Parsons Brinckerhoff, I. (2012) TCRP report 155: Track design handbook for light rail transit (Second edition). *Transportation Research Board*, Washington, D.C.

40. Parsons Brinckerhoff, I. (2009) Technical memorandum: alignment design standards for high-speed train operation. *California High-Speed Rail Authority*, California.

41. ARUP (2017) Guided busway design handbook. *The British Cementitious Paving Association*, Wokingham, Berkshire, UK.

42. Rabuel, S. (2010) Buses with a high level of service (BHLS), the French bus rapid transit (BRT) concept. *DGITM – CERTU - CETE*, France.

43. Hidalgo, D., & Muñoz, J. C. (2014) A review of technological improvements in bus rapid transit (BRT) and buses with high level of service (BHLS). *Public Transport*, 6, 185–213. doi:10.1007/s12469-014-0089-9.

44. COST TU063 BHLS (2011) Buses with high level of service. *European Cooperation in Science and Technology*.

45. Christian (2015) Bus rapid transit and light rail revisited. http://futureuta.blogspot.sg/2015/04/bus-rapid-transit-and-light-rail.html. Accessed 11 Dec 2016.

46. Wikipedia (2016) Bombardier guided light transit. https://en.wikipedia.org/wiki/Bombardier_Guided_Light_Transit#Disadvantages. Accessed 17 Nov 2016.

47. Assidiq, A. A., Khalifa, O. O., Islam, M. R., & Khan, S. (2008) Real time lane detection for autonomous vehicles. In: *2008 International Conference on Computer and Communication Engineering*. Kuala Lumpur, Malaysia, pp 82–88.

48. ISO2631-1:1997 (1997) Mechanical vibration and shock - Evaluation of human exposure to whole body vibration (Part 1: general requirrements). *International Organization for Standardization*, Switzerland.

49.   BS 6841:1987 (1999) Measurement and evaluation of human exposure to whole-body mechanical vibration and repeated shock. *British Standards Institution*.

50.   ISO 2631-4:2001 (2011) Mechanical vibration and shock - Evaluation of human exposure to whole-body vibration. Part 4: Guidelines for the evaluation of the effects of vibration and rotational motion on passenger and crew comfort in fixed-guideway transport systems. *British Standard*.

51.   Thuong, O., & Griffin, M. J. (2012) The vibration discomfort of standing people: relative importance of fore-and-aft, lateral, and vertical vibration. *Applied Ergonomics*, *43*, 902–908. doi:10.1016/j.apergo.2011.12.011.

52.   He, Y., Yan, X., Wu, C., Chu, D., & Peng, L. (2013) Effects of driver's unsafe acceleration behaviors on passengers' comfort for coach buses. *Improving Multimodal Transportation Systems-Information, Safety, and Integration*,. doi:10.1061/9780784413036.220.

53.   Beurier, G. (2012) Analysis of the discomfort feeling of standing bus passengers on the TEOR T1 Rouen bus lane. *Procedia - Social and Behavioral Sciences*, *48*, 425–434. doi:10.1016/j.sbspro.2012.06.1022.

54.   Maternini, G., & Cadei, M. (2014) A comfort scale for standing bus passengers in relation to certain road characteristics. *Transportation Letters-the International Journal of Transportation Research*, *6*, 136–141. doi:10.1179/1942787514y.0000000020.

55.   Suzuki, H. (1998) Research trends on riding comfort evaluation in Japan. *Journal of Rail and Rapid Transit*, *212*, 61–72. doi:10.1243/0954409981530689.

56.   Gangadharan, K. V., Sujatha, C., & Ramamurti, V. (2004) Experimental and analytical ride comfort evaluation of a railway coach. In: *Proceedings of the A conference & exposition on structural dynamics (SEM ORG IMAC XXII)*. Dearborn, Michigan, pp 1–15.

57.   Barbosa, R. S. (2011) Vehicle dynamic safety in measured rough pavement. *Journal of Transportation Engineering*, *137*, 305–310. doi:10.1061/(ASCE)TE.1943-5436.0000216.

58.   Kim, B. S., & Yoo, H. H. (2013) Ride comfort uncertainty analysis and reliability design of a passenger vehicle undergoing random road excitation. *Proceedings of the Institution of Mechanical Engineers, Part D: Journal of Automobile Engineering*, *227*, 433–442. doi:10.1177/0954407012458754.

59.   Wang, F., & Easa, S. (2015) Analytical evaluation of ride comfort on asphalt concrete pavements. *Journal of Testing and Evaluation*, *44*,. doi:10.1520/JTE20140339.

60.   Ueckermann, A., & Oeser, M. (2015) Approaches for a 3D assessment of pavement evenness data based on 3D vehicle models. *Journal of Traffic and Transportation Engineering (English Edition)*, *2*, 68–80. doi:10.1016/j.jtte.2015.02.002.

61.   Sayers, M. W. (1995) On the calculation of international roughness index from longitudinal road profile. *Transportation Research Record*, *1501*, 1–12. doi:10.1080/10643389.2012.728825.

62.   prEN 13036-5 (2015) Road and airfield surface characteristics – Test methods. Part 5: Determination of longitudinal unevenness indices. *European Committee for Standardization*, Brussels.

63.   ASTM E1926-08 (2015) Standard practice for computing international roughness index of roads from longitudinal profile measurements. *ASTM International*, West Conshohocken, PA.

64.   Múčka, P. (2017) International roughness index specifications around the world. *Road*

Materials and Pavement Design, *18*, 929–965. doi:10.1080/14680629.2016.1197144.

65. Ihs, A. (2004) The influence of road surface condition on traffic safety and ride comfort. In: *6th International Conference on Managing Pavements: The Lessons, The Challenges, The Way Ahead*. Swedish National Road and Transport Research Institute, Queensland, Australia.

66. Shen, X., Feng, S., Li, Z., & Hu, B. (2016) Analysis of bus passenger comfort perception based on passenger load factor and in-vehicle time. *SpringerPlus*, *5*, 62. doi:10.1186/s40064-016-1694-7.

67. Sekulić, D., Dedović, V., Rusov, S., Šalinić, S., & Obradović, A. (2013) Analysis of vibration effects on the comfort of intercity bus users by oscillatory model with ten degrees of freedom. *Applied Mathematical Modelling*, *37*, 8629–8644. doi:10.1016/j.apm.2013.03.060.

68. Zhang, K., Zhou, K., & Zhang, F. (2014) Evaluating bus transit performance of Chinese cities: developing an overall bus comfort model. *Transportation Research Part A: Policy and Practice*, *69*, 105–112. doi:10.1016/j.tra.2014.08.020.

69. Múčka, P. (2015) Current approaches to quantify the longitudinal road roughness. *International Journal of Pavement Engineering*, 1–21. doi:10.1080/10298436.2015.1011782.

70. Sayers, M. W. (1989) Two quarter-car models for defining road roughness: IRI and HRI. *Transportation Research Record*, 165–172.

71. Mahala, M. K., Gadkari, P., & Deb, A. (2009) Mathematical models for designing vehicles for ride comfort. In: *ICORD 09: Proceedings of the 2nd International Conference on Research into Design*. Bangalore, India, pp 168–175.

72. Mahala, M., Deb, A., & Chou, C. (2015) A comparative study of lumped parameter models for assessing the performance of vehicle suspension systems. *SAE Technical Papers*, *2015-April*,. doi:10.4271/2015-01-0620.

73. Hamersma, H. A. (2017) A comparison of quarter, half and full vehicle modesl with experimental ride comfort data. In: *Proceedings of the ASME 2015 International Design Engineering Technical Conferences & Computers and Information in Engineering Conference*. ASME, Boston, Massachusetts, USA, pp 1–7.

74. Shu, H. B., Shao, Y. M., Lin, W., & Xu, J. (2016) Computation-based dynamic driving simulation for evaluation of mountain roads with complex shapes: a case study. *Procedia Engineering*, *137*, 210–219. doi:10.1016/j.proeng.2016.01.252.

75. Xu, J., Yang, K., Shao, Y., & Lu, G. (2015) An experimental study on lateral acceleration of cars in different environments in Sichuan, Southwest China. *Discrete Dynamics in Nature and Society*, *2015*, 1–16. doi:10.1155/2015/494130.

76. Fernandes, P., & Nunes, U. (2010) Platooning of autonomous vehicles with intervehicle communications in SUMO traffic simulator. In: *13th International IEEE Conference on Intelligent Transportation Systems*. IEEE, Funchal, Portugal.

77. Burnham, J. F. (2006) Scopus database: A review. *Biomedical digital libraries*, *3*, 1–8. doi:10.1186/1742-5581-3-1.

78. Jacsó, P. (2005) Google scholar: The pros and the cons. *Online Information Review*, *29*, 208–214. doi:10.1108/14684520510598066.

79. Badurowicz, M., Cieplak, T., & Montusiewicz, J. (2016) The cloud computing stream analysis sytem for road artefacts detection. In: Gaj P, Kwiecień A, Stera P (eds) *Communications in Computer and Information Science*, CN 2016. Springer, Cham, Brunów, Poland, pp 360–369.

80. Astarita, V., Caruso, M. V., Danieli, G., Festa, D. C., Giofrè, V. P., Iuele, T., & Vaiana, R. (2012) A mobile application for road surface quality control: UNIquALroad. *Procedia - Soc Behav Sci*. https://doi.org/10.1016/j.sbspro.2012.09.828.

81. Astarita, V., Rosolino, V., Teresa, I., Maria, C., P, G. V., & Francesco, D. M. (2014) Automated sensing system for monitoring of road surface quality by mobile devices. *Procedia - Social and Behavioral Sciences*, *111*, 242–251. doi:10.1016/j.sbspro.2014.01.057.

82. Chen, K., Lu, M., Fan, X., Wei, M., & Wu, J. (2011) Road condition monitoring using on-board three-axis accelerometer and GPS sensor. In: *International ICST Conference on Communications and Networking*. China, pp 1032–1037.

83. Du, Y., Liu, C., Wu, D., & Jiang, S. (2014) Measurement of international roughness index by using z-axis accelerometers and GPS. *Mathematical Problems in Engineering*, *2014*, 1–10. doi:10.1155/2014/928980.

84. Dawkins, J., Bevly, D., Powell, B., & Bishop, R. (2011) Investigation of pavement maintenance applications of Intellidrive. Center for Transportation Studies, University of Virginia.

85. Zeng, H., Park, H., Smith, B. L., & Parkany, E. (2018) Feasibility assessment of a smartphone-based application to estimate road roughness. *KSCE Journal of Civil Engineering*, *22*, 3120–3129. doi:10.1007/s12205-017-1008-9.

86. Mohan, P., Venkata N., P., & Ramachandran, R. (2008) Nericell : using mobile smartphones for rich monitoring of road and traffic conditions. In: *SenSys 2008 Proceedings of the 6th ACM conference on Embedded network sensor systems*. Raleigh, NC, USA, pp 357–358.

87. Mohan, P., Venkata N., P., & Ramachandran, R. (2008) TrafficSense: rich monitoring of road and traffic conditions using mobile smartphones. *Tech. Rep. MSR-TR-2008- 59*, Bangalore, India.

88. Chen, K., Lu, M., Tan, G., & Wu, J. (2014) CRSM: crowdsourcing based road surface monitoring. In: *Proceedings - 2013 IEEE International Conference on High Performance Computing and Communications, HPCC 2013 and 2013 IEEE International Conference on Embedded and Ubiquitous Computing, EUC 2013*. IEEE Computer Society, Zhangjiajie, Hunan, pp 2151–2158.

89. Chen, K., Tan, G., Lu, M., & Wu, J. (2016) CRSM: a practical crowdsourcing-based road surface monitoring system. *Wireless Networks*, *22*, 765–779. doi:10.1007/s11276-015-0996-y.

90. Lemke, M. K., Apostolopoulos, Y., Hege, A., Sönmez, S., & Wideman, L. (2016) Understanding the role of sleep quality and sleep duration in commercial driving safety. *Accident Analysis and Prevention*, *97*, 79–86. doi:10.1016/j.aap.2016.08.024.

91. Barton, D. (2010) Guide to road design - Part 3: Geometric design. In: *Guide to Road Design*, Second. Austroads Ltd, Sydney, Australia.

92. Eliou, N., & Kaliabetsos, G. (2014) A new, simple and accurate transition curve type, for use in road and railway alignment design. *European Transport Research Review*, *6*, 171–179. doi:10.1007/s12544-013-0119-8.

93. BS EN 13803:2017 (2017) Railway applications - Track - Track alignment design parameters - Track gauges 1 435 mm and wider. *BSI Standards Publication*, Brussels.

94. Klauder, L. T. (2012) Railroad spiral design and performance. In: *Proceedings of the ASME 2012 joint rail conference JRC2012*. The American Society of Mechanical Engineering (ASME), Philadelphia, Pennsylvania, USA.

95. Nielsen, T. (2014) Train timetable improvement case study: Fehmarn Land North – Ringsted-Storstrømmen. Master thesis. Technische Universität München, Munich, Germany.

96. ARUP (2017) Guided busway construction handbook. *The British In-situ Paving Association*, Camberley, Surrey, UK.

97. ISO8608:2016(en) (2016) Mechanical vibration - Road surface profiles - Reporting of measured data. *International Organization for Standardization*.

98. Ngwangwa, H. M., & Heyns, P. S. (2014) Application of an ANN-based methodology for road surface condition identification on mining vehicles and roads. *Journal of Terramechanics*, *53*, 59–74. doi:10.1016/j.jterra.2014.03.006.

99. Rau, A. ., Jain, M., Meng, X., Nguyen, T., Tao, L., Xiaodong, L., Yuan, Z., & Ul-Abedin, Z. (2019) Planning and design of a new dynamic autonomous public transport system: the DART system in Singapore. In: *26th ITS World Congress*. Singapore.

100. Liu, X., Zhou, Y., & Rau, A. (2018) Smart card data-centric replication of the multi-modal public transport system in Singapore. *Journal of Transport Geography*, 1–11. doi:10.1016/j.jtrangeo.2018.02.004.

101. Ngwangwa, H. M., Heyns, P. S., Labuschagne, F. J. J., & Kululanga, G. K. (2010) Reconstruction of road defects and road roughness classification using vehicle responses with artificial neural networks simulation. *Journal of Terramechanics*, *47*, 97–111. doi:10.1016/j.jterra.2009.08.007.

102. Zhang, Z., Sun, C., Bridgelall, R., & Sun, M. (2018) Application of a machine learning method to evaluate road roughness from connected vehicles. *Journal of Transportation Engineering Part B: Pavements*, *144*, 1–13. doi:10.1061/JPEODX.0000074.

103. Zhang, Z., Sun, C., Bridgelall, R., & Sun, M. (2018) Road profile reconstruction using connected vehicle responses and wavelet analysis. *Journal of Terramechanics*, *80*, 21–30. doi:10.1016/j.jterra.2018.10.004.

104. Zoysa, K. De (2007) A public transport system based sensor network for road surface condition monitoring. In: *Workshop on Networked System for Developing Regions*. NSDR'07, Association for Computer Machinery, New York, Kyoto, Japan.

105. Anaissi, A., Khoa, N. L. D., Rakotoarivelo, T., Alamdari, M. M., & Wang, Y. (2019) Smart pothole detection system using vehicle-mounted sensors and machine learning. *Journal of Civil Structural Health Monitoring*, *9*, 91–102. doi:10.1007/s13349-019-00323-0.

106. Koh, V. (2017) Device on tower transit buses helps cut down bad driving habits, accidents. In: TODAYonline. https://www.todayonline.com/singapore/device-tower-transit-buses-helps-cut-down-bad-driving-habits-accidents. Accessed 14 May 2019.

Appendix 1: Paper I

Nguyen, T., Lechner, B., Wong, Y.D. (2019). Response-type methods to evaluate road roughness: a state-of-the-art review. *European Transport Research Review,* 11(1), 43, doi: 10.1186/s12544-019-0380-6.

REVIEW   **Open Access**

Response-based methods to measure road surface irregularity: a state-of-the-art review

Teron Nguyen[1,2,3,4*] , Bernhard Lechner[1] and Yiik Diew Wong[2,3]

Abstract

Purpose: With the development of smart technologies, Internet of Things and inexpensive onboard sensors, many response-based methods to evaluate road surface conditions have emerged in the recent decade. Various techniques and systems have been developed to measure road profiles and detect road anomalies for multiple purposes such as expedient maintenance of pavements and adaptive control of vehicle dynamics to improve ride comfort and ride handling. A holistic review of studies into modern response-based techniques for road pavement applications is found to be lacking. Herein, the focus of this article is threefold: to provide an overview of the state-of-the-art response-based methods, to highlight key differences between methods and thereby to propose key focus areas for future research.

Methods: Available articles regarding response-based methods to measure road surface condition were collected mainly from "Scopus" database and partially from "Google Scholar". The search period is limited to the recent 15 years. Among the 130 reviewed documents, 37% are for road profile reconstruction, 39% for pothole detection and the remaining 24% for roughness index estimation.

Results: The results show that machine-learning techniques/data-driven methods have been used intensively with promising results but the disadvantages on data dependence have limited its application in some instances as compared to analytical/data processing methods. Recent algorithms to reconstruct/estimate road profiles are based mainly on passive suspension and quarter-vehicle-model, utilise fewer key parameters, being independent on speed variation and less computation for real-time/online applications. On the other hand, algorithms for pothole detection and road roughness index estimation are increasingly focusing on GPS accuracy, data aggregation and crowdsourcing platform for large-scale application. However, a novel and comprehensive system that is comparable to existing International Roughness Index and conventional Pavement Management System is still lacking.

Keywords: Road profile, Pothole detection, Road roughness, Accelerometer, Estimation, Classification

1 Introduction

A rough road gives poor ride quality, increases vehicle fuel consumption and affects vehicle handling. According to a report in Britain, potholes caused more than £1 million damages to vehicles every day in 2010 [1]. Road roughness measurement is vital for transport authorities in the quest to maintain adequate ride quality for vehicles. Knowledge of road profiles also provides information for adjusting control parameters to improve ride

comfort and ride handling, given the development of suspension system from passive to semi-active and active control in the automotive technology.

Generally speaking, road estimation algorithms [2] can be divided into three distinct types, namely contact measurement, non-contact measurement, and system response-based estimation. Conventional contact and non-contact measurements have been used worldwide as major pavement profiling methods. The primary contact measurement includes two categories: manual profilograph such as rods and levels, straight edges, walking profilers, and trailer-towed devices such as the Longitudinal Profile Analyser (LPA). Non-contact measurement includes inertial profilers such as the GM profilometer developed by General Motors (GM), and the Automated

* Correspondence: teron.nguyen@tum.de; teron.nguyen@tum-create.edu.sg
[1]Institute of Road, Railway and Airfield Construction, Technische Universität München, Baumbachstraße 7, 81245 Munich, Germany
[2]TUMCREATE Ltd, 1 Create Way, #10-02 CREATE Tower, Singapore 138602, Singapore
Full list of author information is available at the end of the article

Pavement Profiler (APP). The advantages and disadvantages of these contact and non-contact measurements are discussed in [3–6]. In recent years, road surface monitoring instruments have transcended from dedicated vehicles with special sensors to dedicated sensors mounted on public transport vehicles, and general-purpose sensors on privately-owned vehicles, and most recently, smartphone-enabled automated monitoring of road infrastructure [7]. This development is driven by response-based methods to indirectly assess road roughness condition using measurements of displacements, velocities, and accelerations of vehicle components, resulting in cost reduction for labour and equipment as compared with direct contact/non-contact profiling [8]. This has led to the emergence of Probe Data Performance Management (PDPM) or Vehicle Probe-based Pavement Management (PBPM) for assessing pavement quality through probe data [9]. There are three system structures by way of connected vehicle approach, fleet vehicle approach and smartphone approach. Basically, road excitation can be estimated using onboard sensors (accelerometers, gyroscopes) for individual or a combination of three key functions as follows (see Fig. 1):

1) Road **P**rofile **R**econstruction/estimation or road roughness classification - **PR** (e.g. Power Spectral Density – PSD), in which fast computation (e.g. in second) adapts vehicle parameters to road roughness levels;
2) **P**otholes **D**etection – **PD**, which detects potholes, manholes, road defects where the precise localisation is of importance; and
3) **R**oughness Index **E**stimation – **RE** (e.g. International roughness index – IRI or new index) for pavement maintenance where roughness data is often aggregated for a certain segment length.

A brief overview of approaches using dedicated sensors and smartphone sensors can be found in [10, 11], yet a comprehensive review is lacking. Herein, in this literature review paper, around 130 articles have been reviewed focusing on the methodologies but not on theories, empirical insights or conceptual model [12]. The objectives and contribution of this review are threefold. Firstly, an examination of the state-of-the-art response-based methods is conducted to provide an overview of their developments within the last 10 years. This provides a comprehensive understanding of the diversity of on-going and dominant methodologies being used. Secondly, the key pros and cons of different methods, e.g. signal processing, data-driven, threshold-based, transfer function, are highlighted. Lastly, key focus areas on the estimation of road surface irregularity are proposed as opportunities for further studies such as the inclusion of air-suspension system, improvement of current machine learning algorithms or further development of the fleet vehicle approach. The results of this review serve to shed light and provide orientation for the research community on system response-based estimation.

Figure 2 illustrates a topology of approaches to measure road surface irregularity focusing on system response-based methods with detailed applications for vehicle dynamics control (VDC) in dealing with PR for adjusting vehicle parameters to improve ride comfort and ride handling; and PBPM utilising portable onboard sensors and smartphones for PD and RE in citywide network.

The methodology for gathering "response-based methods literature database" is presented in the next section. PR algorithms for VDC are then described, followed by PD and RE algorithms for PBPM. The discussion, conclusion and outlook section reports the main results of this review study and proposes research and development gaps deserving of further study.
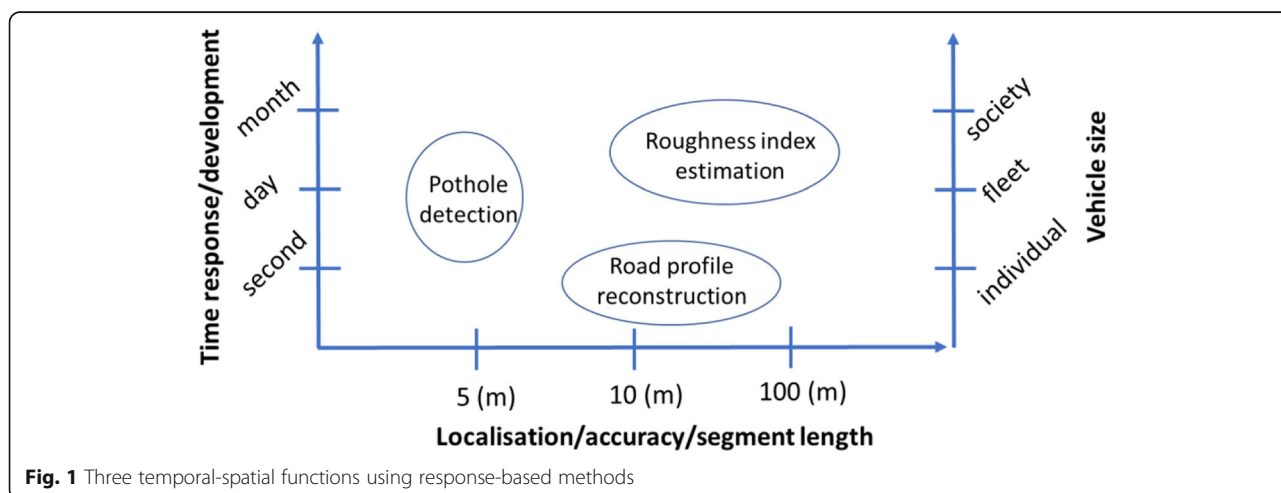

Fig. 1 Three temporal-spatial functions using response-based methods
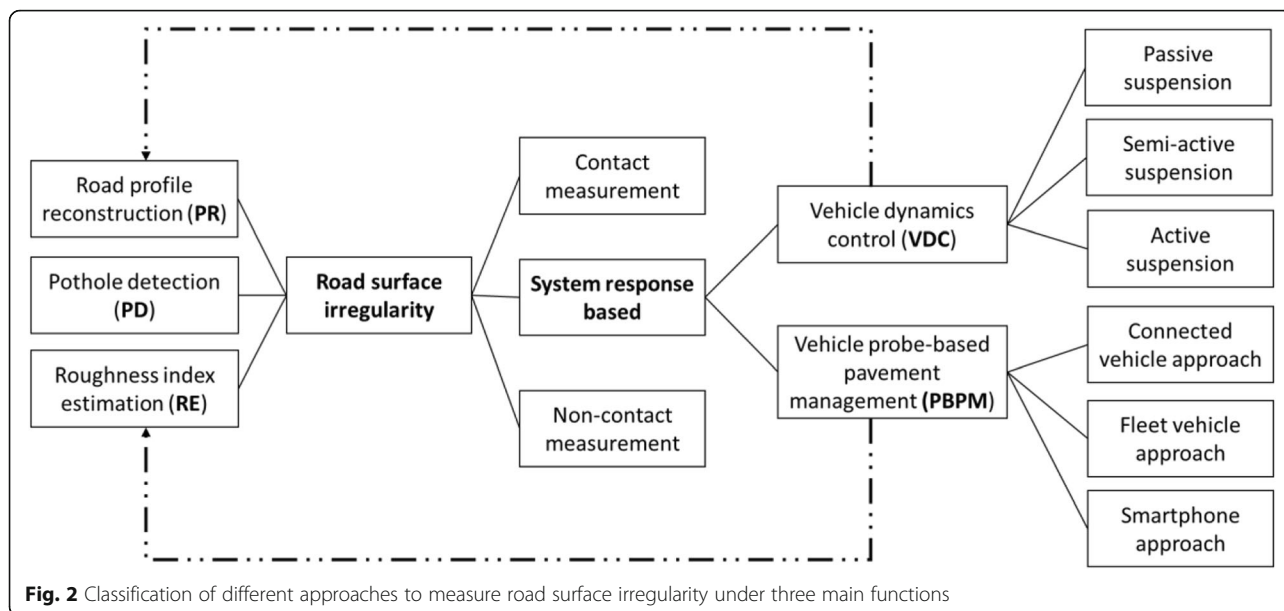
Fig. 2 Classification of different approaches to measure road surface irregularity under three main functions

2 Literature data retrieval method

Available articles regarding response-based methods to measure road surface condition were collected mainly from *"Scopus"* database [13] and partially from *"Google Scholar"* [14]. Articles of focus are those published by international journals and high-quality conferences. The first round of online search was conducted using the following keywords: *(("road roughness" OR "road profile" OR "pothole") AND (accelerometer OR response) AND (estimation OR classification OR detection)) AND PUBYEAR > 2005*, using Scopus' default search settings: article titles, abstracts and/or keywords. The search period is limited to the recent 15 years since an initial investigation found that studies on the topics mostly started at around 2006, with predominant numbers in the past 10 years (see Fig. 3b).

A total of 161 documents were obtained from the various field of studies, of which 86 are published journal articles, 3 are articles in press, 1 is a book chapter and 71 are conference papers. All retrieved documents were further analysed in which 87 documents were removed as being insufficiently related to the main scope of VDC or PBPM nor the main functionalities of system response-based estimation (PR, PD or RE); these rejected documents are mostly related to bridge-vehicle interaction. Relevant references (56) were retrieved and included in the analysis (see Fig. 3a). The additional literature that was missed in the direct search is due to various technical terms being used in these documents such as road anomaly, abnormal section, impact, defect, bump, irregularity, failure, damage (instead of 'pothole') or sensing, measurement (instead of estimation, classification, detection). Among the 130 reviewed documents, 37% are for road
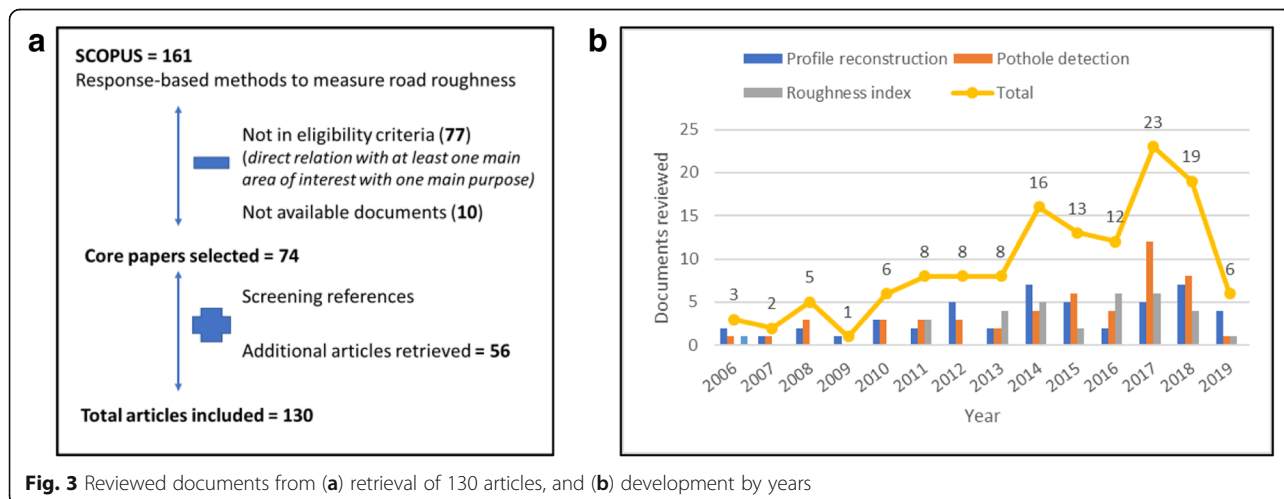

Fig. 3 Reviewed documents from (**a**) retrieval of 130 articles, and (**b**) development by years

profile reconstruction, 39% for pothole detection and the remaining 24% for roughness index estimation.

3 Results

3.1 Road profile reconstruction/estimation for vehicles dynamics control

Profile reconstruction/estimation (PR) is essential for vehicle dynamics control (VDC). However, control algorithms are dependent on vehicle suspension types, be it passive, semi-active or active, to formulate the corrective dynamics behaviours [15]. PR algorithms for VDC can be classified into three main approaches: 1) model-based methods or observers/estimators, 2) data-driven methods/ machine-learning techniques, and 3) frequency response functions/transfer functions and others. These are described in the following sections.

3.1.1 Model-based methods (observers/estimators)

Kalman filter/estimator (KF) and sliding mode observer (SM) are the most commonly-used methods since a long time. Three standard KFs are the linear KF for linear cases, the extended KF for a non-linear relationship, and the unscented KF for strong nonlinearities. Initially in 2011, the linear quarter-car model was developed to implement the KF method [16] that needed measurements of the suspension deflections, the body position and acceleration. In [17], an improved KF was developed to include the vehicle sprung mass change, and in [18] an augmented KF was developed to make use of all the available sensors. The PR is implemented with the modified KF framework in [19] for the non-linear spring-damper system to localise autonomous vehicle position. Unfortunately, for all KF methods, the tuning of the covariance matrix is usually done heuristically which effects the estimation results caused by the deterioration and loss of information. To overcome this drawback, an algebraic estimator was developed in [20], by updating the covariance matrix according to the change of road roughness [21], or by applying the adaptive KF and adaptive super-twisting observer (AKF-ASTO) algorithm in a new estimator [22].

Regarding other *observer* approaches, the most common method is the sliding mode observer (SM) considering the road profile as unknown inputs to be estimated. A 16-DOF full-car model was firstly used to develop the SM based on the vertical motion of the vehicle [5]. A researcher [23] then developed a second-order SM to avoid the assumption of constant velocity, while another model-based observer was developed to compensate for the chassis dynamics for minimising its interaction effect [6]. The higher-order SMs using adaptive super-twisting observer based on a nonlinear quarter-car model were also developed in [24] for PR, and in [25] for PR and tyre friction estimation simultaneously. The combination of sliding mode observer and adaptive Kalman filter for PR related

to tyre dynamics can be found for active suspension control in [26]. Other methods of control theory using an adaptive observer with the Q-parameterisation method have shown their validity and feasibility [27] and the extensions in [28, 29] with detailed synthesis and experimental validation. Compared to other methods such as KF, the Q-parametrization method provides better performance and is suitable for real-time implementation due to less computing cost and implementation complexity.

Another state observer can be found in [30] to use the overall response of the preceding vehicle(s) to generate preview controller information for follower vehicles. An H_∞ observer was adopted and found to be feasible for real-time implementation but required knowledge of many vehicle parameters [31], while a jump-diffusion process estimator can perform PD and PR simultaneously [32]. Although these types of estimators can work effectively for active suspension system control, extensive modelling is required as the main drawback as well as the problem of speed variation.

3.1.2 Data-driven methods/machine-learning techniques

The emergence of machine-learning techniques (MLs) has motivated researchers to focus on various ML algorithms to measure road surface irregularity, as reported in more than half of the reviewed documents. Among them, Neural Network (NN)/Artificial Neural Network (ANN) and Support Vector Machine (SVM) are the most common methods. In 2010, a study [33] used a Bayesian-regularised nonlinear autoregressive exogenous model (NARX) for PR based on the acceleration from a linear half-vehicle model. The ANN-based methodology has been applied for road surface condition identification on mining vehicles and mining roads [34], and for the Land Rover Defender 110 [35]. Similar ANN can be found in [36] using seven vehicle acceleration variables as inputs. To improve estimation efficiency, different techniques/algorithms have been implemented along with ANN. In [8], wavelet analysis was included in similar ANN for the connected vehicle environment. In [37], ANN was used with the mean square of unsprung mass acceleration divided by vehicle speed to classify road Power Spectral Density (PSD) regardless of vehicle speed and suspension parameters.

To classify different road types/terrains (e.g. brick, gravel, grass), ANN and principal component analysis (PCA) were used in combination with image processing [38], or SVM with PCA [39]. To remove the speed dependence from terrain classification, SVM was combined with wavelet analysis of acceleration data [40], or SVM with spatial frequency component analysis by Fast Fourier Transform [41].

Apart from ANN and SVM, other sophisticated MLs were developed and often combined with other techniques for

VDC. Deep Neural Networks [42] and Probabilistic Neural Network classifier [43] were proposed by using measurable system responses. The Adaptive Neuro-Fuzzy Inference System - ANFIS road classification method was proposed using wavelet analysis based solely on sprung mass acceleration [44]. ANFIS classifier was found to be better than other methods in [45], and ANFIS was combined with KF for VDC of semi-active suspension in [21, 46]. PNN classifier using wavelet analysis showed better performance than ANFIS and NARX methods. The combination with PNN classifier and AKF-ASTO [22] adaptively changes the process noise covariances Q and R for the KF, resulted in higher accuracy than existing KF method. Random forest classifier (RF) was used to combine information from both time and frequency domains for a controllable suspension system in [2], while the RF was combined with transfer function to develop a speed independent road classification strategy in [47]. Most recently, independent component analysis as a simple and fast method was developed in [48], and various MLs were compared in [49].

3.1.3 Transfer functions and other techniques

The transfer function (TF) was first used by Gonzalez in 2008 [50] to estimate road PSD based on the relationship between the road surface and vehicle acceleration via a TF as Eq. 1:

$$H(\Omega) = PSD_{acc}(\Omega)/PSD_{road}(\Omega) \tag{1}$$

where $PSD_{acc}(\Omega)$ and $PSD_{road}(\Omega)$ are the PSD for a frequency Ω due to vehicle accelerations and road profile, respectively.

The road can be classified according to ISO 8608 [51] based on PSD_{road} estimated from the PSD_{acc} of the axle or body acceleration measurements [50]. In [52], similar results have confirmed the efficiency of the TF approach, and in [53] the TF was extended to a full-vehicle model to estimate road PSD regardless of vehicle speeds. From another point of view, dynamic tyre pressure sensor was used to estimate road profiles based on an assumption of a linear relationship between road surface profiles and tyre pressure via a TF [54].

Regarding other methods, a numerical optimisation technique can be found in [55] that employs Monte Carlo simulations to obtain the optimal PR, but it is costly for computing. The method of control-constraints was proposed [56] that focuses on tyre dynamics and requires solving differential-algebraic equations. A modulating function technique [57] can fulfil the real-time and noise suppression requirements with the focus particularly on off-road vehicles. In [58], Bayesian estimator was proposed regardless of vehicle models; but a priori information of the road is required. In addition to acceleration measurements, PR can be done by microphones

to measure tyre noise [59]; however, a robustness study is needed to reduce signal contaminations.

3.1.4 Summary of methods for road profile reconstruction/ estimation

Table 1 lists the related *model-based methods* where most of them use a passive suspension system and quarter-vehicle model while fewer use active suspension system. Q-parameterisation has demonstrated its better performance than other methods, with less parameter information required after experimental validation using passive, semi-active and active suspension systems. The pothole detection does not gain much research interest with only 2 relevant studies. Studies on *data-driven methods* are listed in Table 2 and similarly most studies use a passive suspension system and quarter-vehicle model. Together with road profile reconstruction, the functions of pothole detection (2 studies), roughness index estimation (1 study) or terrain classification (4 studies in which 3 are from the same first author) can be found. Since the first ML emerging from NARX in 2010, recent research continues to improve the algorithms by increasing estimation accuracy and using less parameter information such as the ANFIS (only sprung mass). Research related to speed independence has shown the potential for large-scale application with both offline-online phase classification steps such as the speed independent road classification strategy - SIRCS. Studies on *transfer function and other methods* are listed in Table 3 for road profile reconstruction only without consideration of pothole detection or roughness index estimation, in which all the algorithms were developed using the passive suspension system. The sophisticated modelling of other methods has negated them from the real-time or online application.

In summary, various methods have been developed for PR (48 studies) and several include additional functions for PD (4/48 or 8.3%) and RE (1/48 or 2%), in which TF and other methods have focused on PR (9/48 or 19%) only (see Fig. 4). A high number of studies use quarter-vehicle model (29/48 or 60%) and passive suspension system (32/48 or 67%), in which TF and other methods mostly use passive system (8/9 or 89%). Starting from the first developed Kalman filter, sliding mode observer, artificial neural network and transfer function methods in the 2010s which require many vehicle parameters but fewer accuracy levels, recent methods are focusing on fast computation with fewer parameters for online and real-time application. The combination of different techniques has resulted in higher estimation performance such as machine learning and feature extraction, or machine learning and Kalman filters.

Table 1 Summary of model-based methods for road profile reconstruction function

System name/ by	Model-based approach	Additional	Suspension			Vehicle model			Main parameter
			P	SA	A	Q	H	F	
[16]	KF		✓			✓			body position and acc, suspension def
[17]	improved KF		✓			✓			sprung acc, suspension def
[18]	augmented KF		✓			✓		✓	suspension dis, unsprung, sprung acc
[19]	modified KF		✓	✓		✓	✓	✓	vertical dis of the tire-road contact points, longitudinal acc
[5, 23]	SM, second-order SM		✓					✓	wheels and chassis
[6]	SM	PD	✓			✓			chassis
[24]	higher-order SM				✓	✓			sprung mass dis and velocity
[25]	higher-order SM				Tyre	✓			random road profile, the longitudinal friction force, and the engine friction
[26]	SM + AKF				Tyre	✓		✓	spring def, wheel acc, tire road contact acc
[27]	Q-parametrization				✓	✓			sprung mass position
[28]	Q-parametrization			✓		✓(1/5)			
[29]	Q-parametrization		✓			✓			
[20, 30]	Algebraic estimator, state observer		✓			✓			sprung mass and unsprung mass vertical dis, suspension def
[31]	H∞ observer				✓	✓(1/5)			sprung acc, suspension def, unsprung mass motion
[32]	Jump-diffusion estimator	PD	✓				✓		wheel excitation

Table 2 Summary of data-driven methods for road profile reconstruction function

System name/by	Machine learnings	Additional	Suspension			Vehicle model			Main parameter
			P	SA	A	Q	H	F	
[33–35]	ANN (NARX)	PD	✓				✓		sprung, axle, body
[36]	ANN		✓					✓	wheels and chassis
[8]	ANN + wavelet DWT)	RE(IRI)	✓			✓			sprung mass
[37]	ANN + ADV		✓	✓				✓	unsprung mass
[38]	ANN + image processing + PCA	Terrain	✓			✓			wheel acc, speed
[39–41]	SVM+ PCA, FWT, FFT								
DNNs classifier [42]	Deep NNs			✓				✓	sprung, unsprung, rattle space
PNN classifier [43]	PNN + WPT			✓		✓			sprung, unsprung, rattle space
ANFIS classifier [44]	ANFIS			✓		✓			sprung mass
[45]	ANFIS, RLS, GMDH			✓		✓			sprung, unsprung, rattle space
ANFIS+AKF [21]	ANFIS + Kalman filter				✓	✓			sprung mass
AKF-ASTO [22]	PNN + Kalman filter					✓			sprung, unsprung
[46]	ANFIS + MOOP + NSGA-II			✓		✓			sprung mass
[2]	RF + WPT				✓	✓	✓		sprung, unsprung, speed
SIRCS [47]	RF + TF, decision procedure		✓			✓			unsprung mass
[48]	Independent Component Analysis		✓			✓	✓	✓	chassis, suspension
[49]	Various MLs + TF	PD	✓					✓	axle or body, speed

PCA, WPD, WPT, DWT, FWT: Principal Component Analysis, Wavelet Package Decomposition, Wavelet Package Transformation, Discrete Wavelet Transform, Fast Wavelet Transform.

RLS, GMDH, ADV: Recursive Least Square, Group Method of Data Handling, the mean square of unsprung mass acceleration divided by vehicle speed.

Table 3 Summary of TF and other methods for road profile reconstruction function

System name/ by	TF and others	Suspension			Vehicle model			Main parameter
		P	SA	A	Q	H	F	
[50]	TF	✓				✓		axle or body
[52]	TF	✓			✓			unsprung mass acceleration
[54]	TF	✓						tyre pressure
[53]	TF + time span	✓					✓	axle or body
[55]	Cross-entropy	✓			✓			sprung and unsprung acc
[56]	Control-constraints	✓					✓	tire dynamics
[58]	Bayesian parameter							rear wheel acc, veh response, speed
[59]	Microphone	✓			✓			tyre noise and axle acc
[57]	Modulating function technique	✓					✓	accelerometer, spring dis and orientation

3.2 Pothole detection and roughness index estimation

The three approaches in PBPM has been classified as: connected vehicle approach (uses OEM-installed accelerometers, sensor hardware and standardised onboard vehicle) fleet vehicle approach (uses semi-permanent, non-stock accelerometers in a fleet of agency-owned vehicles, supplemented by GPS units) and mobile device approach (uses accelerometer-equipped mobile devices to gather and transmit roughness information to a central database) [9]. The latter approach using smartphone sensors as the concept of "citizen as sensors" in [60] or "citizen engineer" [61] has received much research interest in recent years,

followed by the connected vehicle and the fleet vehicle (which can be grouped into one dedicated sensor onboard approach). Regardless of applications, the methodology can be classified into three groups: acceleration thresholds or threshold-based methods, signal processing and machine-learning techniques.

3.2.1 Threshold-based methods

Threshold-based methods are the most straightforward approaches for PD detection by processing mainly the vertical acceleration (Z-acc) or in combination with

Fig. 4 Method classification for RE, PD and PR
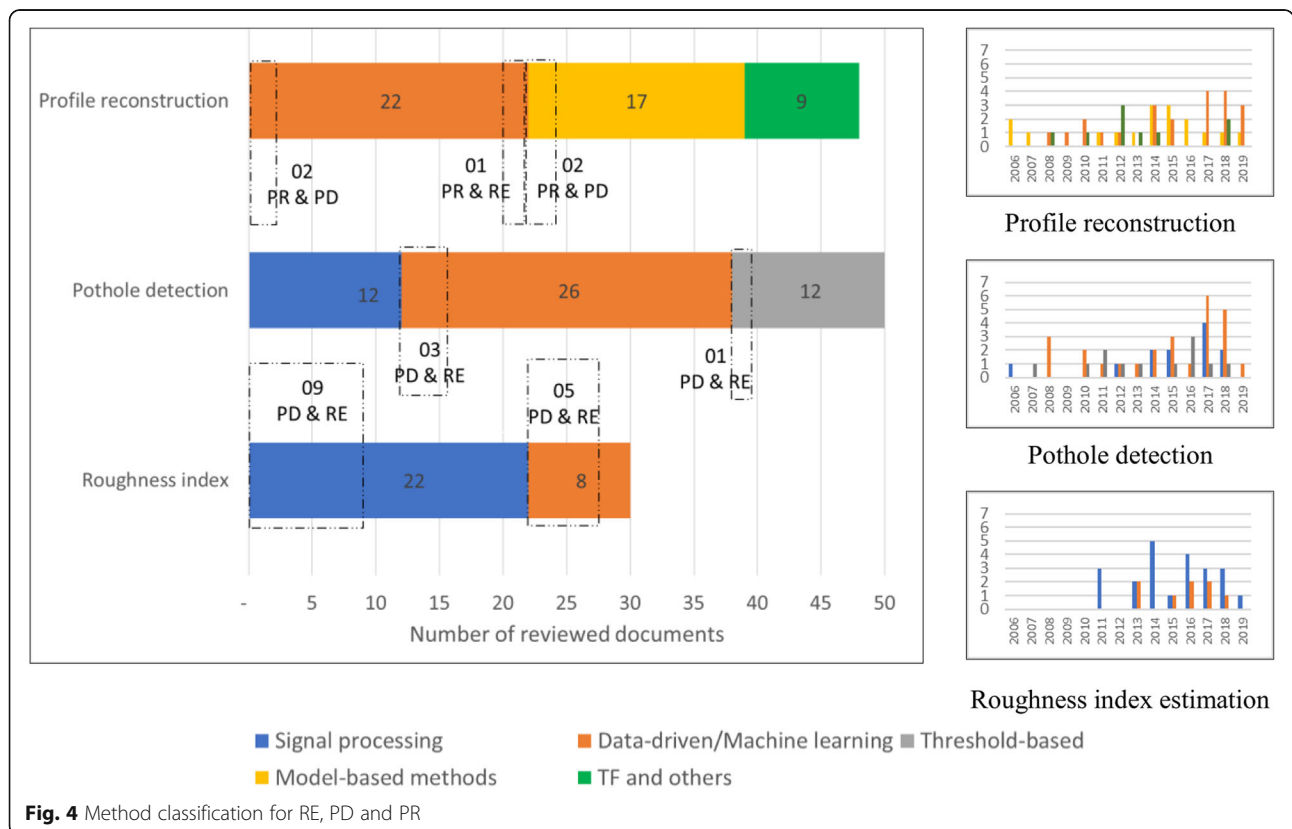
other direction acceleration (x and y) and gyroscopes. A researcher [62] has proposed four indices in which the Z-THRESH was further modified [63] to build a cloud computing system: Z-THRESH (from vertical vibration), Z-DIFF (from the difference of consecutive Z-acc above threshold), STDEV(Z) (as the standard deviation of Z-acc above threshold in a window), and G-ZERO (whether the sensor senses a 0-G vibration). Similar STDEV(Z) can also be found in [64] and to develop a bump index in [65]. Other acceleration thresholds are used to classify three relative rough road levels [66] or severity levels of potholes [67, 68] and to characterise road bumps [69]. Thresholds of Z-acceleration and ultrasonic data were combined in [70] while the Z-jerk as the "rate of change of acceleration" is used in Cyberphysical system [71]. However, how to set up correct thresholds is challenging under the influence of vehicle speeds, suspension parameters as well as sensor location and orientation. Furthermore, only pothole detection alone is not sufficient for real application, as transport authorities care about roughness index estimation as well for road surface maintenance.

3.2.2 Signal processing

To overcome the drawbacks of the threshold-based methods, various signal processing filters have been used. Researcher [72] further processed Z-acc by simple filters and Gaussian model-based algorithm to detect the severity of potholes and differentiate humps and potholes. A study in [73] combined Z-THRESH and G-ZERO and adopted a spatial interpolation method to obtain precisely pothole locations. Fuzzy logic was used to detect and recognise the speed bumps from vehicle speed and Z-acc variance [74]. Time-frequency analysis was used such as the Discrete Wavelet Transform to estimate gravel roads ride quality, detect the location and the severity of surface potholes [75], or the Gabor transform to estimate road roughness condition in combination with image processing for PD [76]. In [77], a greedy heuristic approach for an optimal mobile sensor placement maximises the total length of the road inspected by sensors.

Frequency filter, speed filter and small peaks filter were used to develop the vertical acceleration impulse that corresponds to a "high-energy event" on the road surface in UNIquALroad [78, 79]. Dynamic Time Warping – DTW detects pothole by using the pattern-matching technique independent of time and speed [80]. Similar to DTW, the Smartphone Probe Car system was developed using a new road anomaly indexing heuristic which is adaptive to vehicle dynamics [81].

To evaluate road roughness IRI, the well-known regression relationships between PSD with IRI was investigated in [82, 83], so do the root-mean-squared acceleration (RMS) and IRI in [84, 85]. A compact road profiler and ArcGIS to measure and evaluate road roughness condition was introduced in [86]. Filter and Fast Fourier Transform (FFT) were used to estimate IRI from smartphone data under realistic setting (e.g. inside pockets) based on the approximate proportion of spectrum magnitude and road IRI [87, 88]. The inverse pseudo-excitation method offers a new approach to estimate IRI independent of the travelling speed, road roughness grade, and vehicle type [89]. The RMS acceleration was further studied to detect potholes using speed filter and Z-axis filter in Pothole Patrol, and to develop new roughness index (IRI-proxy) depicting overall road quality [60]. Based on the relationship of PSD between road surface and vertical acceleration, parameters of road profile can be evaluated using Maximum Likelihood-based estimation [90], or using linear predictive coding by averaging the power of the prediction error [91, 92]. In [93], a recursive multiscale Correlation-Averaging algorithm was developed to deal with the uncertainty/noise such as GPS inaccuracies, driving path variation and errors from the distance-measuring devices.

Regarding new roughness index, a speed-independent road impact factor - RIF (individual vehicle) and its corresponding time-wavelength-intensity-transform – TWIT (vehicle groups) for connected vehicles were established using advanced signal processing in [94]. Further studies were conducted intensively to investigate and validate the RIF regarding sampling rate selection [95], localisation [96, 97], RIF-IRI proportionality [98], deterioration forecasts in consideration of suspension parameter variances [99], stop-and-go conditions [100], and wavelength sensitivity [101].

3.2.3 Machine learning techniques

With more data availability, machine learning techniques (MLs) have been utilised in PD and RE functions while noting that most of them were developed for the PD. The abovementioned Z-THRESH is similar but simpler than Z-peak in Pothole Patrol [102], Nericell [103] and TrafficSense [104], which used specific algorithms to filter and to cluster the collected data. Based on Pothole Patrol, further analysis to differentiate pothole and bump-road cases in [105], or to develop the PRISM platform for remote sensing [106]. For the same purpose, a supervised learning approach based on temporal classification was undertaken in [107]. Based on Pothole Patrol, P³ can infer the depth and length of the pothole by adopting a one degree-of-freedom (DOF) vibration model as well as perform a self-learning vibration recovery algorithm [108]. A clustering ML was used to cluster potholes with an adaptive detection threshold and learning rate update in CRSM [109, 110] after using pothole filters in Pothole Patrol. K-mean clustering was used in [111] and additional Random Forest (RF) classifier in [112]. Another study [113] developed an online road roughness classification system using bicycles

instrumented with smartphones embedded with the K-Nearest-Neighbour and Naive Bayes algorithm.

Among MLs, support vector machine (SVM) is used most frequently, and it is often combined with feature extraction methods as multiple classifiers. In [114], SVM was used to detect road anomalies by processing the data collected from a motorcycle-mounted tri-axial accelerometer and further classify road surface condition using unsupervised ML. Recently, SVM and Dynamic Time Warping algorithm were developed in [115] to identify aggressive driving events, road bumps and potholes for cycling. Another improvement was included in [116] where the gyroscope around gravity rotation was used. SVM and wavelet analysis were also used in RoADS [117] to classify the road anomaly into three event classes: severe, mild and span, and in [118] to detect road anomaly based on driver attitudes toward the speeds and turnings. SVM and Fast Fourier Transformation were used in [119] to remove the speed dependence and to label road anomaly. Another study in [120] combined SVM and Wavelet Package Decomposition to detect potholes with low computing cost. In Wolverine [121], the smartphone accelerometer data is used to detect braking events and bumps using K-means clustering and SVM. In [122, 123], SVM was trained using extensive data set from CarSim vehicle simulation as well as experiment, applying for under-sampled vehicles sensor problems and multi-lane pothole detection. In [124], a virtual road network inspector was built based on SVMs to detect potholes using accelerometers mounted to the front and rear axles of the buses.

The comparison of different MLs was conducted in several studies to find the best ML. In [125], a data mining approach was developed to compare the performance of five algorithms for PD. By adopting the framework of this study, a study [126] used RF for its best performance to develop a cloud-based Road Anomaly Service architecture in which PCA was used for feature extraction. PCA was also used in [127, 128] after NN and RF classification were compared to develop a street defect classifier to select NN for its better performance. RMS thresholds were set as a triggering condition for data logging condition and a new street defect level (from 0 to 1) to evaluate the road segment condition. In RoadSense [129], Decision Tree (DT) was designed and compared with SVM and Naïve Bayes algorithm after feature extraction. In Pothole lab [130], a new SVM(Z) and Swarm indices were developed to compare with the four thresholds in [62], Nericell, Pothole Patrol, and PERT [119]. Backward feature elimination was used in [131] to select the optimal set of features for different classification models while in [132] the forward selection and backwards

elimination process was performed showing better performance than existing approaches.

Besides CRSM system for IRI estimation, MLs were used in [133] where the authors used smartphone sensor data for training a feature-based prediction model and compared with the road condition from official IRI measurements of the road surface. Another researcher [134] applied NARX ANN to estimate IRI from the connected vehicle after investigating vehicle suspension characteristics and its speed in [8]. In [7], the mean-absolute-value of the Z-acc for every 100 m was sensed by a smartphone on a motorbike, and a fuzzy classifier from a server was used for RE.

3.2.4 Summary of methods for pothole detection and road roughness estimation

Studies on *threshold-based methods* are listed in Table 4. Given the simplicity of this method based on true positive and false positive of the detection rate, the threshold values may vary due to different factors which make this method not being feasible to be used in real scenarios and large-scale implementation. Table 5 lists the studies on *signal processing methods*, in which not only the methods of accurate PD and RE but also further concerns on GPS data noise/inaccuracy, sensor and smartphone installation/direction, data fusion/aggregation and crowdsensing system/platform were considered. Among them, the adaptive thresholds in Smartphone Probe Car and Smart patrolling, as well as the IRI-proxy, SmartRoadSense and UNIquaALroad system are found to be promising for large scale application. RIF and TWIT are also potential replacements of IRI in the context of connected vehicle environments. As for *ML methods* recent studies are listed in Table 6. MLs have attracted many studies resulting in high performance in which PCA plays an important role in feature extraction for the training process. CRSM [109, 110], the system in [122, 123] and another in [133] are promising systems for large scale application.

In summary, the diversity of methods and systems have been described in over 80 reviewed articles for the main functions of PD (50/80 or 63%) and RE (30/80 or 27%). Many algorithms can perform both PD and RE (20/80 or 20%). The same number of studies use MLs and signal processing (34 each or 41%) whereas threshold-based methods are used mostly for PD (8%). MLs received more research interest than other methods for PD (26/50 or 52%). In contrast, signal processing is preferred for RE (22/30 or 73%) especially for IRI estimation, in which 11/22 studies (50%) are original algorithms while others are further development or application (Fig. 4). Over the studies related to RE, 6/30 (20%) is about the relative roughness index, 14/30 (47%) for IRI estimation, 2/30 (7%) for IRI-proxy estimation

Table 4 Summary of threshold-based methods for pothole detection and roughness index estimation

System name/by	Thresholds	Function		Approach		
		PD	RE	C	F	S
[62], [63]	Z-thresh, Z-diff, Stdev(z), G-zero	✓				✓
BusNet [64]	std of filtered Z-acc	✓			✓	
Bump Recorder [65]	Z-acc, bump index	✓				✓
[66]	Z-acc	✓	Relative			✓
Smart Pune [67]	Z-acc, skid, accident, braking	✓		✓		
[68]	Z-acc for severity levels	✓				✓
[69]	Z-acc pattern	✓				✓
Cyber-physical system [71]	Z-jerk	✓				✓
[135]	0.1 g threshold	✓				✓
PoDAS [70]	Z-acc, ultrasonic	✓		✓		

Relative: Pothole-based roughness index.

and 8/30 (27%) for the new roughness index (RIF and TWIT). There are only 6 studies (7%) related to fleet vehicle approach, 23 studies for the connected vehicle (28%) and 53 studies for smartphone approach (65%). The problems of GPS accuracy, data aggregation and crowdsourcing have been considered in many studies using signal processing (9/21 studies)

and ML (13/30 studies), aiming at supporting the emergence of crowdsourcing-based road surface monitoring.

4 Discussion, conclusion and outlook
Different methods present different levels of complexity, precision and computing intensiveness. Across all the

Table 5 Summary of signal processing methods for pothole detection and roughness index estimation

System name/by	Signal processing	Function		Approach			Additional		
		PD	RE	C	F	S	GPS	Data	Crowd
UNIquaALroad[78, 79]	high-energy events	✓				✓		✓	✓
Smart patrolling [80]	filter + DTW (adaptive)	✓				✓		✓	✓
Smart Probe Car [81]	anomaly index heuristic (adaptive AI)	✓				✓	✓	✓	✓
[72]	Z-acc, Gaussian model	✓				✓			
[73]	Z-thresh, G-zero combined	✓				✓		✓	
[74]	Fuzzy logic	✓				✓			
[75, 76]	time-frequency analysis	✓				✓			
[77]	Greedy heuristic algorithm	✓			✓		✓	✓	
[90]	Maximum Likelihood-based	✓		✓					
RCM-TAGPS [82, 83]	PSD + empirical formula		IRI	✓					
[84]	RMS acceleration		IRI	✓					
[85]	RMS acceleration		IRI			✓			
STAMPER [86]	filter + IRI		IRI	✓					
[87, 88]	Filter + FFT		IRI			✓			
IPEM [89]	Inverse pseudo-excitation method		IRI	✓					
[60]	IRI-proxy	✓	IRI-proxy			✓		✓	✓
SmartRoad Sense [91, 92]	PSD + Linear Predictive Coding		Relative			✓	✓	✓	✓
[93]	Correlation-Averaging Algorithm	✓	✓	✓			✓	✓	
RIF [95–101]	RIF-transform, TWIT	✓	New	✓			✓	✓	

Table 6 Summary of ML methods for pothole detection and roughness index estimation

System name/by	Machine learning	PD	RE	C	F	S	GPS	Data	Crowd
Pothole Patrol [102]	Clustering + training detector	✓		✓					
Nericell [103], TrafficSense [104, 105]	Z-peak method/ Clustering + training detector	✓				✓			
PRISM [106]	Z-peak method + training detector	✓				✓			✓
[107]	supervised ML	✓				✓			
P³ [108]	Clustering + training detector	✓				✓	✓		
PADS [111]	K-mean clustering	✓		✓					
BDS [112]	K-means clustering + RF	✓				✓			
[113]	Naive Bayes algorithm + K-nearest-neighbor		Relative			✓			
[114]	SVM + unsupervised ML	✓	Relative			✓			
D&Sense [115]	SVM + DTW	✓				✓			✓
RoadMonitor [116], RoADS-based [117, 118]	SVM, SVM + SWT	✓				✓			
[119]	SVM + FFT, cross validation	✓				✓	✓		
[120]	SVM + WPD, feature selection	✓				✓			
Wolverine [121]	SVM + K-means clustering	✓				✓			
[122] [123]	SVM + data filter, sliding window, greedy forward feature selection	✓		✓			✓	✓	✓
VRNI [124]	SVM + filter, moving window, feature extraction	✓			✓				
CRISP-DM-based [125, 126]	various algorithms comparison	✓	Relative			✓			
[127, 128]	various algorithms comparison	✓	Relative	✓			✓	✓	
RoadSense [129], Pothole Lab [130]	various algorithms comparison	✓				✓			✓
[131]	various algorithms comparison	✓				✓			
[132]	various algorithms comparison	✓		✓				✓	
CRSM [109, 110]	iGMM clustering	✓	IRI	✓				✓	✓
[133]	SVM + WPD, Random forest		IRI		✓	✓	✓	✓	
[134]	ANN + feature selection		IRI	✓				✓	
[7]	Fuzzy classifier	✓	Relative			✓		✓	✓

Relative: Pothole-based roughness index;
ANN, SVM, RF, DT: Artificial Neural Network, Support Vector Machine, Random Forest, Decision Tree;
PCA, WPD, DWT: Principal Component Analysis, Wavelet Package Decomposition, Discrete Wavelet Transform.

reviewed documents and methods, it is recognised that data-driven methods/MLs are increasingly being used for all the functions in PR, PD and RE (see Fig. 4), as well as the usage of the passive suspension system and quarter-vehicle model due to their modelling simplification. Recent studies have shifted towards RE as shown in the time series graphs, in which signal processing techniques have been preferred for RE given the ability to achieve advanced functionalities such as adaptive thresholds or data fusion. Regarding the function of PR for the individual suspension system, it is more comprehensive to integrate PR for suspension control with variable uncertainty, but more challenges will occur on the knowledge of vehicle dynamic characterisation. Whereas to deal with PD and RE for group of vehicles (fleet or connected vehicle) and "citizen sensor" concept in the large-scale society, the issues of GPS accuracy, data fusion (e.g. the aggregation of sensor data or vehicle suspension types) and crowdsourcing will be challenges to the development of appropriate algorithms/systems. So far, several established algorithms/systems have solved these issues successfully.

In summary, the development of response-based methods to evaluate road surface irregularity has attracted research interests from both automotive technology and pavement engineering, aiming at the three main functions of Road profile reconstruction (PR), pothole detection (PD) and roughness index estimation (RE). The review of about 130 articles on this topic has revealed the diversity of recent approaches mostly within the recent decade. At first, the present study describes the algorithms used for PR including model-based methods, data-driven methods, transfer functions and others. Then, related algorithms for PD and RE are described including the threshold-based,

Table 7 Advantages and disadvantages of response-based methods

Response-based methods	Advantages	Disadvantages
1. Road profile reconstruction		
1.1. Model-based approach	can deal with unforeseen situations that are not included in the data-driven training datasets.	- an accurate model is required - not all required response information is measurable - often only time domains
1.2 Kalman filter/estimator	convenient, fast and simple	- a priori information about model errors - the tuning of the covariance matrix is usually done heuristically
1.1.2 Observer	can include tyre dynamics	generally required knowledge of many vehicle parameters
i. Sliding mode observer	- convergence of the errors	rather complicated for practical application
ii. Q-parameterisation	- less computing cost and complexity for real-time implementation - better performance than KF	- the problem of extensive modelling - the sensitivity to speed variation in almost methods
iii. Algebraic estimator iv. H∞ observer v. State observer vi. Jump-diffusion	- can work effectively in the framework of the active suspension system - overcome the drawbacks of KF	
1.2 Data-driven approach (MLs)	- can use fewer parameters (e.g. only sprung or unsprung mass) - various ML techniques to be applied - does not require excessive system characterisation - required fewer analytical skills than parametric model	- impractical for an online road estimation due to computationally costly training datasets (e.g. 4655 s are required to train the ANN-based moded)
1.2.1 Only MLs (e.g. ANN)	- able to detect potholes	- spatial frequency only - many vehicle parameters - not high accuracy and sensitivity to speed variation
1.2.2 Combined MLs and others	- higher accuracy and performance - feasible for speed independent classifiers	
i. with feature selection (e.g. WPT, FFT, PCA)	- can combine both time and frequency domains - able to classify terrain conditions	further complex modelling and understanding vehicle dynamics control mechanism
ii. with KF	determination of the process noise variance before estimation	
iii. with TF	- speed independent classifier with less training effort - able to detect potholes	
1.3 Transfer function and others	required fewer parameters than the model-based approach	
1.3.1 The transfer function (TF)	- easy, convenient and fast - frequency domain only	- not directly yield the expression of the excitation - limited to a constant speed (can be eliminated when combined TF with small time span)
1.3.2 Others		
i. Cross-entropy	using only sprung and unsprung mass accelerations	too much computing time
ii. Control-constraints	non-linear and complex models	remains costly

Table 7 Advantages and disadvantages of response-based methods *(Continued)*

Response-based methods	Advantages	Disadvantages
iii. Bayesian parameter	low cost regardless of vehicle models	a priori information of the road is required
iv. Microphone	feasible for the combination of techniques	the susceptibility to signal contaminations
v. Modulating function	fulfil the real-time and noise suppression requirements	particularly for off-road vehicles
2. Road roughness estimation and pothole detection		
2.1 Threshold-based methods		
2.1.1 Thresholds only	simplest methods (for PD purpose) with fix thresholds	threshold value varies with different types of smartphones, roads, vehicles, the condition of vehicles.
2.1.2 Combined thresholds and others	overcome drawbacks of the threshold-based methods	
i. with signal processing approaches	- able to detect the severity of potholes, differentiate potholes and humps	
ii. with MLs to train detectors	- clustering of different road anomalies with simple algorithms	training datasets required which are not able to collect in some cases
2.2 Signal processing	- able include both PD and RE in the same system - deal with GPS errors, data aggregation, device installation and orientation, crowdsourcing - higher performance and accuracy - suitable for data aggregation regardless of different configuration (e.g. velocity, orientation, suspension)	complicated analysis
2.2.1 PSD and RMS acceleration	calculate IRI value	not able to detect a pothole
2.2.2 RIF transformation	- feasible for connected vehicles - both PD and RE considering a fleet of vehicles	advanced signal processing
2.2.3 Adaptive threshold (e.g. DWT)	less training effort as compared to MLs	
2.3 Data-driven approach (MLs)	- various techniques to be applied to select the best alternative - easier to implement in the smartphone for crowdsourcing	a huge amount of training datasets required which are not able to collect in some cases
2.3.1 Only MLs (e.g. ANN)	simple using of raw acceleration data and filter	
2.3.2 Combined MLs and feature extraction	- able to eliminate speed dependence, suspension variation - higher accuracy	

signal processing and machine-learning methods. Following this, all reviewed documents and discussion are summarised on their advantages and disadvantages (see Table 7) which should be beneficial for further research in this field.

As for future research, it should be of strong value-add to focus on several potential topics as follows. Firstly, the air-suspension system (as an active-suspension type) has not been investigated by any research for PR whereas most existing studies are about passive suspension system (67%). The reason is probably due to the high modelling complexity of the air-suspension while it is noted that the Macpherson controllable suspension was simulated and simplified in [2]. Secondly, MLs have demonstrated their capability for multiple functions such as ANN algorithms for PR and PD in [33], PR and RE in [8, 134] in which certain limitation in the estimation accuracy, vehicle parameters or speed variance can be further studied to develop comprehensive algorithms.

Thirdly, although fleet vehicle approach seems to be less complicated to deal with, a comprehensive PBPM for PD and RE for the fleet of public transport (e.g. bus fleet) is still missing, except the general concept in [64] or smart PD in [124]. This fleet vehicle approach faces fewer challenges on data aggregation since vehicle fleets are quite identical, with lower GPS errors caused by lane-by-lane difference and without crowdsourcing platform. Such a system, once developed, will be beneficial in maintaining the road condition for public transport such as the citywide bus lane system in Singapore, London or worldwide BRT lane system, in which the road surfaces often deteriorate quickly due to heavy-loading from heavy-duty vehicles [136]. Fourthly, how to localise precise road roughness condition and potholes by lane accuracy (probably less than 0.5 m accuracy) is crucial to make the PBPM comparable to conventional Pavement management system, in which APP instruments currently measure road surface lane-by-lane. Higher GPS localisation of potholes also serves to optimise the trajectories of following vehicles in the connected platooning to avoid road defects by passing the vibration information from the leader to the followers. This can be done with the help of the future development of sensor technology. Lastly, the intensive on-going research on RIF and TWIT [95–101] as the alternatives for IRI in connected vehicle environment will be promising for large-scale implementation.

Abbreviations
acc, def, dis: Acceleration, deflection, displacement; ANFIS: Adaptive neuro-fuzzy inference system; APP: Automated pavement profiler; C, F, S: Connected vehicle, Fleet vehicle, Smartphone approach; DNN: Deep neural networks; DOF: Degree-of-freedom; DTW: Dynamic time warping; DWT: Discrete wavelet transforms; FFT: Fast Fourier transform; GPS, Data, Crowd: GPS accuracy, data fusion/aggregation, crowdsourcing platform; G-ZERO: The sensor senses a 0-g vibration; IRI: International roughness index; KF: Kalman filter; LPA: Longitudinal profile analyser; MLs: Machine-learning techniques; NARX: Bayesian-regularised nonlinear autoregressive exogenous model; NN/ANN: Neural network/artificial neural network; P, SA, A, tyre: Passive, semi-active, active suspension system, tyre dynamics; PBPM: Vehicle probe-based pavement management; PCA: Principal component analysis; PD: Pothole detection; PNN: Probabilistic neural network; PR: Road profile reconstruction/estimation or road roughness classification; PSD: Power spectral density; Q, H, F, 1/5: Quarter, half, full vehicle model, 1/5 vehicle model; RE: Roughness index estimation; RF: Random forest classifier; RIF: Road impact factor; SM: Sliding mode observer; STDEV(Z): The standard deviation of Z-acc above threshold in a window; SVM: Support vector machine; Ter: Terrain classification; TF: Transfer function; TWIT: Time-wavelength-intensity-transform; VDC: Vehicle dynamics control; Z-acc/ Z-thresh: Vertical acceleration/vertical threshold; Z-DIFF: The difference of consecutive Z-acc above threshold

Author details
[1]Institute of Road, Railway and Airfield Construction, Technische Universität München, Baumbachstraße 7, 81245 Munich, Germany. [2]TUMCREATE Ltd, 1 Create Way, #10-02 CREATE Tower, Singapore 138602, Singapore. [3]Centre for Infrastructure System, Nanyang Technological University, N1-01b-51, 50 Nanyang Avenue, Singapore 639798, Singapore. [4]Faculty of Road and Bridge Engineering, University of Science and Technology – The University of Danang, 54 Nguyen Luong Bang Street, Danang City, Lien Chieu District, Vietnam.

References
1. Daily Mail Online (2010) Potholes causing more than £1m damage to cars every day. https://www.dailymail.co.uk/news/article-1168103/Potholes-causing-1m-damage-cars-EVERY-day.html. Accessed 26 Mar 2019.
2. Qin, Y., Wei, C., Tang, X., Zhang, N., Dong, M., & Hu, C. (2018). A novel nonlinear road profile classification approach for controllable suspension system: Simulation and experimental validation. *Mechanical Systems and Signal Processing.* https://doi.org/10.1016/j.ymssp.2018.07.015.
3. ASTM E1364–95. (2017). *Standard test method for measuring road roughness by static level method.* West Conshohocken: American Society for Testing and Materials.
4. Doumiati, M., Victorino, A., Charara, A., & Lechner, D. (2011). *Estimation of road profile for vehicle dynamics motion: Experimental validation* (pp. 5237–5242). San Francisco: Proceedings of the American control conference.
5. Imine, H., Delanne, Y., & M'Sirdi, N. K. (2006). Road profile input estimation in vehicle dynamics simulation. *Vehicle System Dynamics, 44,* 285–303. https://doi.org/10.1080/00423110500333840.
6. McCann, R., & Nguyen, S. (2007). System identification for a model-based observer of a road roughness profiler. In *2007 IEEE region 5 technical conference, TPS* (pp. 336–343).
7. Kumar, R., Mukherjee, A., & Singh, V. P. (2017). Community sensor network for monitoring road roughness using smartphones. *Journal of Computing in Civil Engineering, 31,* 1–11. https://doi.org/10.1061/(ASCE)CP.1943-5487.0000624.
8. Zhang, Z., Sun, C., Bridgelall, R., & Sun, M. (2018). Road profile reconstruction using connected vehicle responses and wavelet analysis. *Journal of Terramechanics, 80,* 21–30. https://doi.org/10.1016/j.jterra.2018.10.004.
9. Sauerwein, P. M., & Smith, B. L. (2011). *Investigation of the implementation of a probe-vehicle based pavement roughness estimation system.* Charlottesville: Center for Transportation Studies.
10. Chugh, G., Bansal, D., & Sofat, S. (2014). Road condition detection using smartphone sensors: A survey. *International Journal of Electronic and Electrical Engineering, 7,* 595–602.
11. Wahlstrom, J., Skog, I., & Handel, P. (2017). Smartphone-based vehicle telematics: A ten-year anniversary. *IEEE Transactions on Intelligent Transportation Systems, 18,* 2802–2825. https://doi.org/10.1109/TITS.2017.2680468.
12. Van Wee, B., & Banister, D. (2016). How to write a literature review paper? *Transport Reviews, 36,* 278–288. https://doi.org/10.1080/01441647.2015.1065456.
13. Burnham, J. F. (2006). Scopus database: A review. *Biomedical Digital Libraries, 3,* 1–8. https://doi.org/10.1186/1742-5581-3-1.
14. Jacsó, P. (2005). Google scholar: The pros and the cons. *Online Information Review, 29,* 208–214. https://doi.org/10.1108/14684520510598066.

15. Tseng, H. E., & Hrovat, D. (2015). State of the art survey: Active and semi-active suspension control. *Vehicle System Dynamics, 53*, 1034–1062. https://doi.org/10.1080/00423114.2015.1037313.

16. Doumiati, M., Victorino, A., Charara, A., & Lechner, D. (2011). Estimation of road profile for vehicle dynamics motion: Experimental validation. In *Proceedings of the 2011 American control conference* (pp. 5237–5242). https://doi.org/10.1109/ACC.2011.5991595.

17. Yu, W., Zhang, X., Guo, K., Karimi, H. R., Ma, F., & Zheng, F. (2013). Adaptive real-time estimation on road disturbances properties considering load variation via vehicle vertical dynamics. *Mathematical Problems in Engineering, 2013*, 1–9. https://doi.org/10.1155/2013/283528.

18. Fauriat, W., Mattrand, C., Gayton, N., Beakou, A., & Cembrzynski, T. (2016). Estimation of road profile variability from measured vehicle responses. *Vehicle System Dynamics, 3114*. https://doi.org/10.1080/00423114.2016.1145243.

19. Gim, J., & Ahn, C. (2018). Imu-based virtual road profile sensor for vehicle localization. *Sensors (Switzerland)*, 18. https://doi.org/10.3390/s18103344.

20. Haddar, M., Baslamisli, S. C., Chaari, R., Chaari, F., & Haddar, M. (2019). Road profile identification with an algebraic estimator. *Proceedings of the Institution of Mechanical Engineers, Part C: Journal of Mechanical Engineering Science, 233*, 1139–1155. https://doi.org/10.1177/0954406218767470.

21. Wang, Z., Dong, M., Qin, Y., Du, Y., Zhao, F., & Gu, L. (2017). Suspension system state estimation using adaptive Kalman filtering based on road classification. *Vehicle System Dynamics, 55*, 371–398. https://doi.org/10.1080/00423114.2016.1267374.

22. Qin, Y., Langari, R., Wang, Z., Xiang, C., & Dong, M. (2017). Road profile estimation for semi-active suspension using an adaptive Kalman filter and an adaptive super-twisting observer. In *Proceedings of the American control conference* (pp. 973–978). https://doi.org/10.23919/ACC.2017.7963079.

23. Rabhi, A., M'sirdi, N. K., Fridman, L., & Delanne, Y. (2006). Second order sliding mode observer for estimation of road profile. In *Proceedings of the 2006 international workshop on variable structure systems* (pp. 161–165). Alghero: VSS'06.

24. Rath, J. J., Veluvolu, K. C., & Defoort, M. (2014). Estimation of road profile for suspension systems using adaptive super-twisting observer. In *2014 European control conference, ECC* (pp. 1675–1680). https://doi.org/10.1109/ECC.2014.6862248.

25. Rath, J. J., Member, S., Veluvolu, K. C., Member, S., & Defoort, M. (2015). Simultaneous estimation of road profile and tire road friction for automotive vehicle. *IEEE Transactions on Vehicular Technology, 64*, 4461–4471. https://doi.org/10.1109/TVT.2014.2373434.

26. Arat, M. A., Taheri, S., & Holweg, E. (2015). Road profile estimation for active suspension applications. *SAE International Journal of Passenger Cars - Mechanical Systems, 8*. https://doi.org/10.4271/2015-01-0651.

27. Doumiati, M., Erhart, S., Martinez, J., Sename, O., & Dugard, L. (2014). Adaptive control scheme for road profile estimation: Application to vehicle dynamics. In *Proceedings of the 19th world congress the International Federation of Automatic Control* (pp. 8445–8450). Cape Town: IFAC.

28. Tudón-martínez, J. C., Fergani, S., Sename, O., Martinez, J. J., Morales-menendez, R., & Dugard, L. (2015). Adaptive road profile estimation in semiactive car suspensions. *IEEE Transactions on Control Systems Technology, 23*, 2293–2305. https://doi.org/10.1109/TCST.2015.2413937.

29. Doumiati, M., Jairo, J., Molina, M., et al. (2017). Road profile estimation using an adaptive Youla- kučera parametric observer: Comparison to real profilers. *Control Engineering Practice, Elsevier, 61*, 270–278.

30. Rahman, M., & Rideout, G. (2012). Using the lead vehicle as preview sensor in convoy vehicle active suspension control. *Vehicle System Dynamics, 50*, 1923–1948. https://doi.org/10.1080/00423114.2012.707801.

31. Tudon-Martinez, J. C., Fergani, S., Sename, O., Morales-Menendez, R., & Dugard, L. (2014). *Online road profile estimation in automotive vehicles* (pp. 2370–2375). Strasbourg: European control conference (ECC).

32. Li, Z., Kalabic, U. V., Kolmanovsky, I. V., Atkins, E. M., Lu, J., & Filev, D. P. (2016). Simultaneous road profile estimation and anomaly detection with an input observer and a jump diffusion process estimator. In *Proceedings of the American Control Conference, 2016-July* (pp. 1693–1698). https://doi.org/10.1109/ACC.2016.7525160.

33. Ngwangwa, H. M., Heyns, P. S., Labuschagne, F. J. J., & Kululanga, G. K. (2010). Reconstruction of road defects and road roughness classification using vehicle responses with artificial neural networks simulation. *Journal of Terramechanics, 47*, 97–111. https://doi.org/10.1016/j.jterra.2009.08.007.

34. Ngwangwa, H. M., & Heyns, P. S. (2014). Application of an ANN-based methodology for road surface condition identification on mining vehicles and roads. *Journal of Terramechanics, 53*, 59–74. https://doi.org/10.1016/j.jterra.2014.03.006.

35. Ngwangwa, H. M., Heyns, P. S., Breytenbach, H. G. A., & Els, P. S. (2014). Reconstruction of road defects and road roughness classification using artificial neural networks simulation and vehicle dynamic responses: Application to experimental data. *Journal of Terramechanics, 53*, 1–18. https://doi.org/10.1016/j.jterra.2014.03.002.

36. Yousefzadeh, M., Azadi, S., & Soltani, A. (2010). Road profile estimation using neural network algorithm. *Journal of Mechanical Science and Technology, 24*, 743–754. https://doi.org/10.1007/s12206-010-0113-1.

37. Li, Z., Yu, W., & Cui, X. (2018). Online classification of road roughness conditions with vehicle unsprung mass acceleration by sliding time window. *Shock and Vibration, 2018*. https://doi.org/10.1155/2018/5131434.

38. Wang, S., Kodagoda, S., Wang, Z., & Dissanayake, G. (2011). *Multiple sensor based terrain classification*. Melbourne: Proceedings of the 2011 Australasian conference on robotics and automation.

39. Wang, S., Kodagoda, S., Shi, L., & Wang, H. (2017). Road-terrain classification for land vehicles: Employing an acceleration-based approach. *IEEE Vehicular Technology Magazine, 12*, 34–41. https://doi.org/10.1109/MVT.2017.2656949.

40. Wang, S., Khushaba, R., & Kodagoda, S. (2012). *Towards speed-independent road-type classification* (pp. 614–619). Guangzhou: 2012 12th International Conference on Control, Automation, Robotics and Vision, ICARCV 2012.

41. Ward, C. C., & Iagnemma, K. (2009). Speed-independent vibration-based terrain classification for passenger vehicles. *Vehicle System Dynamics, 47*, 1095–1113. https://doi.org/10.1080/00423110802450193.

42. Qin, Y., Langari, R., Wang, Z., Xiang, C., & Dong, M. (2017). Road excitation classification for semi-active suspension system with deep neural networks. *Journal of Intelligent Fuzzy Systems, 33*, 1907–1918. https://doi.org/10.3233/JIFS-161860.

43. Qin, Y., Xiang, C., Wang, Z., & Dong, M. (2018). Road excitation classification for semi-active suspension system based on system response. *JVC/Journal of Vibration and Control, 24*, 2732–2748. https://doi.org/10.1177/1077546317693432.

44. Qin, Y., Dong, M., Zhao, F., Langari, R., & Gu, L. (2015). Road profile classification for vehicle semi-active suspension system based on adaptive neuro-fuzzy inference system. In *Proceedings of the IEEE conference on decision and control* (pp. 1533–1538). Osaka: Institute of Electrical and Electronics Engineers Inc.

45. Qin, Y., Langari, R., & Gu, L. (2014). The use of vehicle dynamic response to estimate road profile input in time domain. In *ASME 2014 dynamic systems and control conference, DSCC 2014*. San Antonio: American Society of Mechanical Engineers.

46. Qin, Y., Dong, M., Langari, R., Gu, L., & Guan, J. (2015). Adaptive hybrid control of vehicle semiactive suspension based on road profile estimation. *Shock and Vibration, 2015*, 14–17. https://doi.org/10.1155/2015/636739.

47. Qin, Y., Wang, Z., Xiang, C., Hashemi, E., Khajepour, A., & Huang, Y. (2019). Speed independent road classification strategy based on vehicle response: Theory and experimental validation. *Mechanical Systems and Signal Processing, 117*, 653–666. https://doi.org/10.1016/j.ymssp.2018.07.035.

48. Ben Hassen, D., Miladi, M., Abbes, M. S., Baslamisli, S. C., Chaari, F., & Haddar, M. (2019). Road profile estimation using the dynamic responses of the full vehicle model. *Applied Acoustics, 147*, 87–99. https://doi.org/10.1016/j.apacoust.2017.12.007.

49. Gorges, C., Öztürk, K., & Liebich, R. (2019). Impact detection using a machine learning approach and experimental road roughness classification. *Mechanical Systems and Signal Processing, 117*, 738–756. https://doi.org/10.1016/j.ymssp.2018.07.043.

50. González, A., O'Brien, E. J., Li, Y. Y., & Cashell, K. (2008). The use of vehicle acceleration measurements to estimate road roughness. *Vehicle System Dynamics, 46*, 483–499. https://doi.org/10.1080/00423110701485050.

51. ISO8608:2016(en). (2016). Mechanical vibration - road surface profiles - reporting of measured data. In *International Organization for Standardization*.

52. Qin, Y., Guan, J., & Gu, L. (2012). The research of road profile estimation based on acceleration measurement. *Applied Mechanics and Materials, 226–228*, 1614–1617. https://doi.org/10.4028/www.scientific.net/AMM.226-228.1614.

53. Gorges, C., Öztürk, K., & Liebich, R. (2018). Road classification for two-wheeled vehicles. *Vehicle System Dynamics, 56*, 1289–1314. https://doi.org/10.1080/00423114.2017.1413197.

54. Wang, Q., McDaniel, J. G., Sun, N. X., & Wang, M. L. (2013). *Road profile estimation of city roads using DTPS*. San Diego: Proceedings of SPIE - The International Society for Optical Engineering.

55. Harris, N. K., Gonzalez, A., OBrien, E. J., & McGetrick, P. (2010). Characterisation of pavement profile heights using accelerometer readings and a combinatorial optimisation technique. *Journal of Sound and Vibration, 329*, 497–508. https://doi.org/10.1016/j.jsv.2009.09.035.

56. Burger, M. (2014). Calculating road input data for vehicle simulation. *Multibody System Dynamics, 31*, 93–110. https://doi.org/10.1007/s11044-013-9380-9.

57. Noack, M., Botha, T., Hamersma, H. A., Ivanov, V., Reger, J., & Els, S. (2018). Road profile estimation with modulation function based sensor fusion and series expansion for input reconstruction. In *Proceedings - 2018 IEEE 15th international workshop on advanced motion control, AMC 2018* (pp. 547–552). Tokyo: Institute of Electrical and Electronics Engineers Inc.

58. Heyns, T., Heyns, P. S., & De Villiers, J. P. (2012). A method for real-time condition monitoring of haul roads based on bayesian parameter estimation. *Journal of Terramechanics, 49*, 103–113. https://doi.org/10.1016/j.jterra.2011.12.001.

59. Johnsson, R., & Odelius, J. (2012). Methods for road texture estimation using vehicle measurements. In *Proceedings of the international conference on noise and vibration engineering (ISMA 2012)* (pp. 1573–1582).

60. Li, X., & Goldberg, D. W. (2018). Toward a mobile crowdsensing system for road surface assessment. *Computers, Environment and Urban Systems, 69*, 51–62. https://doi.org/10.1016/j.compenvurbsys.2017.12.005.

61. Harris, D. K., Alipour, M., Acton, S. T., Messeri, L. R., Vaccari, A., & Barnes, L. E. (2017). The citizen engineer: Urban infrastructure monitoring via crowd-sourced data analytics. In S. J.G. (Ed.), *Structures congress 2017: Business, professional practice, education, research, and disaster management - selected papers from the structures congress 2017* (pp. 495–510). Denver: American Society of Civil Engineers (ASCE).

62. Mednis, A., Strazdins, G., Zviedris, R., Kanonirs, G., & Selavo, L. (2011). Real time pothole detection using android smartphones with accelerometers. In *2011 International conference on distributed computing in sensor systems and workshops*. Barcelona: DCOSS'11.

63. Badurowicz, M., Cieplak, T., & Montusiewicz, J. (2016). The cloud computing stream analysis system for road artefacts detection. *Communications in Computer and Information Science, 608*, 360–369. https://doi.org/10.1007/978-3-319-39207-3_31.

64. De Zoysa, K. (2007). A public transport system based sensor network for road surface condition monitoring. In *Workshop on Networked System for Developing Regions. NSDR'07*. New York, Kyoto: Association for Computer Machinery.

65. Yagi, K. (2010). *Extensional smartphone probe for road bump detection* (pp. 1–10). Busan: 17th ITS world congress.

66. Nomura, T., & Shiraishi, Y. (2015). A method for estimating road surface conditions with a smartphone. *International Journal of Informatics Society, 7*, 29–36.

67. Limkar, S., Rajmane, O., Bhosale, A., & Rane, V. (2018). Small effort to build Pune as a smart city: Smart real-time road condition detection and efficient management system. *Smart Innovation, Systems and Technologies, 78*, 609–621. https://doi.org/10.1007/978-981-10-5547-8_63.

68. Rishiwal, V., & Khan, H. (2016). Automatic pothole and speed breaker detection using android system. In *39th international convention on information and communication technology, electronics and microelectronics, MIPRO 2016 - proceedings* (pp. 1270–1273). Opatija: Institute of Electrical and Electronics Engineers Inc..

69. Mukherjee, A., & Majhi, S. (2016). Characterisation of road bumps using smartphones. *European Transport Research Review*. https://doi.org/10.1007/s12544-016-0200-1.

70. Mehta, J., Mathur, V., Agarwal, D., Sharma, A., & Prakasha, K. (2017). Pothole detection and analysis system (PODAS) for real time data using sensor networks. *Journal of Engineering and Applied Sciences, 12*, 3090–3097. https://doi.org/10.3923/jeasci.2017.3090.3097.

71. Syed, B., Pal, A., Srinivasarengan, K., & Balamuralidhar, P. (2012). A smart transport application of cyber-physical systems: Road surface monitoring with mobile devices. In *Proceedings of the international conference on sensing technology, ICST* (pp. 8–12). https://doi.org/10.1109/ICSensT.2012.6461796.

72. Harikrishnan, P. M., & Varun, P. G. (2017). Vehicle vibration signal processing for road surface monitoring. *IEEE Sensors Journal, 17*, 5192–5197.

73. Wang, H.-W., Chen, C.-H., Cheng, D.-Y., Lin, C.-H., & Lo, C.-C. (2015). A real-time pothole detection approach for intelligent transportation system. *Mathematical Problems in Engineering, 2015*. https://doi.org/10.1155/2015/869627.

74. Aljaafreh, A., Alawasa, K., Alja'afreh, S., & Abadleh, A. (2017). Fuzzy inference system for speed bumps detection using smart phone accelerometer sensor. *Journal of Telecommunication, Electronic and Computer Engineering, 9*, 133–136.

75. Aleadelat, W., Wright, C. H. G., & Ksaibati, K. (2018). Estimation of gravel roads ride quality through an android-based smartphone. *Transportation Research Record*. https://doi.org/10.1177/0361198118758693.

76. Grabowski, D., Szczodrak, M., & Czyzewski, A. (2018). Economical methods for measuring road surface roughness. *Metrology and Measurement Systems, 25*, 533–549. https://doi.org/10.24425/123905.

77. Ali, J., & Dyo, V. (2017). Coverage and mobile sensor placement for vehicles on predetermined routes: A greedy heuristic approach. In *ICETE 2017 - proceedings of the 14th international joint conference on e-business and telecommunications* (pp. 83–88).

78. Astarita, V., Caruso, M. V., Danieli, G., Festa, D. C., Giofrè, V. P., Iuele, T., & Vaiana, R. (2012). A mobile application for road surface quality control: UNIquALroad. *Procedia - Social and Behavioral Sciences*. https://doi.org/10.1016/j.sbspro.2012.09.828.

79. Vittorio, A., Rosolino, V., Teresa, I., Vittoria, C. M., & Vincenzo, P. G. (2014). Automated sensing system for monitoring of road surface quality by mobile devices. *Procedia-Social and Behavioral Sciences*. (pp. 111, 242-251).

80. Singh, G., Bansal, D., Sofat, S., & Aggarwal, N. (2017). Smart patrolling: An efficient road surface monitoring using smartphone sensors and crowdsourcing. *Pervasive and Mobile Computing, 40*, 71–88. https://doi.org/10.1016/j.pmcj.2017.06.002.

81. Yi, C.-W., Chuang, Y.-T., & Nian, C.-S. (2015). Toward crowdsourcing-based road pavement monitoring by mobile sensing technologies. *IEEE Transactions on Intelligent Transportation Systems, 16*, 1905–1917. https://doi.org/10.1109/TITS.2014.2378511.

82. Chen, K., Lu, M., Fan, X., Wei, M., & Wu, J. (2011). Road condition monitoring using on-board three-axis accelerometer and GPS sensor. In *International ICST conference on communications and networking*. China (pp. 1032–1037).

83. Du, Y., Liu, C., Wu, D., & Jiang, S. (2014). Measurement of international roughness index by using Z-axis accelerometers and GPS. *Mathematical Problems in Engineering, 2014*. https://doi.org/10.1155/2014/928980.

84. Dawkins, J., Bevly, D., Powell, B., & Bishop, R. (2011). *Investigation of pavement maintenance applications of Intellidrive*. University of Virginia Technical Report: Center for Transportation Studies, University of Virginia.

85. Zeng, H., Park, H., Smith, B. L., & Parkany, E. (2018). Feasibility assessment of a smartphone-based application to estimate road roughness. *KSCE Journal of Civil Engineering, 22*, 3120–3129. https://doi.org/10.1007/s12205-017-1008-9.

86. Abulizi, N., Kawamura, A., Tomiyama, K., & Shun, F. (2016). Measuring and evaluating of road roughness conditions with a compact road profiler and ArcGIS. *Journal of Traffic and Transportation Engineering (English Edition), 3*, 398–411. https://doi.org/10.1016/j.jtte.2016.09.004.

87. Douangphachanh, V., & Oneyama, H. (2014). A study on the use of smartphones under realistic settings to estimate road roughness condition. *EURASIP Journal on Wireless Communications and Networking, 2014*, 1–11.

88. Douangphachanh, V., & Oneyama, H. (2013). A study on the use of smartphones for road roughness condition estimation. *Journal of the Eastern Asia Society for Transportation Studies, 10*, 1551–1564.

89. Li, J., Zhang, Z., & Wang, W. (2019). New approach for estimating international roughness index based on the inverse pseudo excitation method. *Journal of Transportation Engineering Part B: Pavements, 145*. https://doi.org/10.1061/JPEODX.0000093.

90. Ndoye, M., Vanjari, S. V., Huh, H., Krogmeier, J. V., Bullock, D. M., Hedges, C. A., & Adewunmi, A. (2006). Sensing and signal processing for a distributed pavement monitoring system. In *2006 IEEE 12th digital signal processing workshop and 4th IEEE signal processing education workshop* (pp. 162–167). https://doi.org/10.1109/DSPWS.2006.265446.

91. Alessandroni, G., Klopfenstein, L. C., Delpriori, S., et al. (2014). SmartRoadSense: Collaborative road surface condition monitoring. In *UBICOMM 2014 : The Eighth International Conference on Mobile Ubiquitous Computing, systems, services and technologies SmartRoadSense* (pp. 210–215).

92. Alessandroni, G., Carini, A., Lattanzi, E., Freschi, V., & Bogliolo, A. (2017). A study on the influence of speed on road roughness sensing: The SmartRoadSense case. *Sensors (Switzerland), 17*. https://doi.org/10.3390/s17020305.

93. Ndoye, M., Barker, A. M., Krogmeier, J. V., & Bullock, D. M. (2011). A recursive multiscale correlation-averaging algorithm for an automated distributed road-condition-monitoring system. *IEEE Transactions on Intelligent Transportation Systems, 12*, 795–808. https://doi.org/10.1109/TITS.2011.2132799.

94. Bridgelall, R. (2014). Connected vehicle approach for pavement roughness evaluation. *Journal of Infrastructure Systems, 20*, 04013001. https://doi.org/10.1061/(ASCE)IS.1943-555X.0000167.

95. Bridgelall, R. (2015). Inertial sensor sample rate selection for ride quality measures. *Journal of Infrastructure Systems, 21*, 04014039. https://doi.org/10.1061/(ASCE)IS.1943-555X.0000225.

96. Bridgelall, R., Huang, Y., Zhang, Z., & Deng, F. (2016). Precision enhancement of pavement roughness localization with connected vehicles. *Measurement Science and Technology, 27*. https://doi.org/10.1088/0957-0233/27/2/025012.

97. Bridgelall, R., & Tolliver, D. (2018). Accuracy enhancement of roadway anomaly localization using connected vehicles. *International Journal of Pavement Engineering, 19*, 75–81. https://doi.org/10.1080/10298436.2016.1162306.

98. Bridgelall, R., Rahman, M. T., Tolliver, D. D., & Daleiden, J. F. (2016). Use of connected vehicles to characterize ride quality. *Transportation Research Record: Journal of the Transportation Research Board, 2589*, 119–126. https://doi.org/10.3141/2589-13.

99. Bridgelall, R. (2014). Precision bounds of pavement deterioration forecasts from connected vehicles. *Journal of Infrastructure Systems, 21*, 04014033. https://doi.org/10.1061/(asce)is.1943-555x.0000218.

100. Bridgelall, R., Hough, J., & Tolliver, D. (2017). Characterising pavement roughness at non-uniform speeds using connected vehicles. *International Journal of Pavement Engineering, 8436*, 1–7. https://doi.org/10.1080/10298436.2017.1366768.

101. Bridgelall, R., Rahman, M. T., Tolliver, D., & Daleiden, J. F. (2017). Wavelength sensitivity of roughness measurements using connected vehicles. *International Journal of Pavement Engineering, 8436*, 1–7. https://doi.org/10.1080/10298436.2017.1316645.

102. Eriksson, J., Girod, L., Hull, B., Newton, R., Madden, S., & Balakrishnan, H. (2008). *The pothole patrol: Using a mobile sensor network for road surface monitoring* (pp. 29–39). Breckenridge: MobiSys'08 - proceedings of the 6th international conference on Mobile systems, applications, and services.

103. Mohan, P., Venkata, N. P., & Ramachandran, R. (2008). Nericell: Using mobile smartphones for rich monitoring of road and traffic conditions. In *Proceedings of the 6th international conference on embedded networked sensor systems* (pp. 323–336). Raleigh: SenSys 2008.

104. Mohan, P., Venkata, N. P., & Ramachandran, R. (2008). *TrafficSense: Rich monitoring of road and traffic conditions using mobile smartphones*. Tech. Rep. no. MSR-TR-2008–59.

105. Gunawan, F. E., Yanfi, & Soewito, B. (2015). A vibratory-based method for road damage classification. In *2015 international seminar on intelligent technology and its applications, ISITIA 2015 - proceeding* (pp. 1–4). Surabaya: Institute of Electrical and Electronics Engineers Inc.

106. Das, T., Prashanth, M., Venkata, N. P., Ramachandran, R., & Asankhaya, S. (2010). *PRISM : Platform for remote sensing using smartphones*. San Francisco: Proceedings of the 8th international conference on Mobile systems, applications, and services - MobiSys '10.

107. Monteserin, A. (2018). Potholes vs. speed bumps: A multivariate time series classification approach. In I. Lykourentzou, M. G. Armentano, & HFTA (Eds.), *CEUR workshop proceedings* (pp. 36–40). CEUR-WS.

108. Xue, G., Zhu, H., Hu, Z., Yu, J., Zhu, Y., & Luo, Y. (2017). Pothole in the dark: Perceiving pothole profiles with participatory urban vehicles. *IEEE Transactions on Mobile Computing, 16*, 1408–1419. https://doi.org/10.1109/TMC.2016.2597839.

109. Chen, K., Lu, M., Tan, G., & Wu, J. (2014). CRSM: Crowdsourcing based road surface monitoring. In *Proceedings - 2013 IEEE international conference on high performance computing and communications, HPCC 2013 and 2013 IEEE international conference on embedded and ubiquitous computing, EUC 2013* (pp. 2151–2158). Zhangjiajie, Hunan: IEEE Computer Society.

110. Chen, K., Tan, G., Lu, M., & Wu, J. (2016). CRSM: A practical crowdsourcing-based road surface monitoring system. *Wireless Networks, 22*, 765–779. https://doi.org/10.1007/s11276-015-0996-y.

111. Ren, J., & Liu, D. (2017). PADS: A reliable pothole detection system using machine learning. In *Lecture Notes in Computer Science (including subseries Lecture Notes in Artificial Intelligence and Lecture Notes in Bioinformatics), 10135 LNCS* (pp. 327–338). https://doi.org/10.1007/978-3-319-52015-5_33.

112. Ghadge, M., Pandey, D., & Kalbande, D. (2016). Machine learning approach for predicting bumps on road. In M. Aradhya & S. K. N (Eds.), *Proceedings of the 2015 international conference on applied and theoretical computing and communication technology, iCATccT 2015* (pp. 481–485). Davangere: Institute of Electrical and Electronics Engineers Inc.

113. Hoffmann, M., Mock, M., & May, M. (2013). Road-quality classification and bump detection with bicycle-mouted smartphones. In *CEUR workshop proceedings* (pp. 39–43).

114. Tai, Y., Chan, C., & Hsu, J. Y. (2010). Automatic road anomaly detection using smart mobile device. In *2010 15th conference on artificial intelligence and applications (TAAI)* (pp. 1–8).

115. Bose, B., Dutta, J., Ghosh, S., Pramanick, P., & Roy, S. (2018). D&Sense: Detection of driving patterns and road anomalies. In *Proceedings - 2018 3rd International Conference On Internet of Things: Smart Innovation and Usages, IoT-SIU 2018* (pp. 1–7). https://doi.org/10.1109/IoT-SIU.2018.8519861.

116. Mohamed, A., Fouad, M. M. M., & Elhariri, E. (2014). *RoadMonitor: An intelligent road surface condition monitoring system*. Warsaw: 7th IEEE International Conference Intelligent Systems IS'2014.

117. Seraj, F., van der Zwaag, B. J., Dilo, A., Luarasi, T., & Havinga, P. J. M. (2014). RoADS: A road pavement monitoring system for anomaly detection using smart phones. In *1st international workshop on machine learning for urban sensor data, SenseML 2014* (pp. 1–16). Berlin: Springer.

118. Seraj, F., Meratnia, N., Zhang, K., Havinga, P. J. M., & Turkes, O. (2015). *A smartphone based method to enhance road pavement anomaly detection by analyzing the driver behavior* (pp. 1169–1177). Osaka: In proceedings of the UbiComp '15.

119. Perttunen, M., Mazhelis, O., Cong, F., et al. (2011). *Distributed road surface condition monitoring using mobile phones* (pp. 64–78). Banff: International conference on ubiquitous intelligence and computing.

120. Cong, F., Hautakangas, H., Nieminen, J., Mazhelis, O., Perttunen, M., Riekki, J., & Ristaniemi, T. (2013). Applying wavelet packet decomposition and one-class support vector machine on vehicle acceleration traces for road anomaly detection. *Lecture Notes in Computer Science, 7951 LNCS*, 291–299. https://doi.org/10.1007/978-3-642-39065-4-36.

121. Bhoraskar, R., Vankadhara, N., Raman, B., & Kulkarni, P. (2012). Wolverine: Traffic and road condition estimation using smartphone sensors. In *2012 fourth international conference on communication systems and networks (COMSNETS 2012)*. Bangalore: IEEE.

122. Fox, A., Kumar, B. V. K. V., Chen, J., & Bai, F. (2015). Crowdsourcing undersampled vehicular sensor data for pothole detection. In *2015 12th annual IEEE international conference on sensing, communication, and networking, SECON 2015* (pp. 515–523). Seattle: Institute of Electrical and Electronics Engineers Inc.

123. Fox, A., Kumar, B. V. K. V., Chen, J., & Bai, F. (2017). Multi-lane pothole detection from crowdsourced undersampled vehicle sensor data. *IEEE Transactions on Mobile Computing, 16*, 3417–3430. https://doi.org/10.1109/TMC.2017.2690995.

124. Anaissi, A., Khoa, N. L. D., Rakotoarivelo, T., Alamdari, M. M., & Wang, Y. (2019). Smart pothole detection system using vehicle-mounted sensors and machine learning. *Journal of Civil Structural Health Monitoring, 9*, 91–102. https://doi.org/10.1007/s13349-019-00323-0.

125. Silva, N., Soares, J., Shah, V., Santos, M. Y., & Rodrigues, H. (2017). Anomaly detection in roads with a data mining approach. *Procedia Computer Science, 121*, 415–422. https://doi.org/10.1016/j.procs.2017.11.056.

126. Silva, N., Shah, V., Soares, J., & Rodrigues, H. (2018). Road anomalies detection system evaluation. *Sensors (Switzerland), 18*. https://doi.org/10.3390/s18071984.

127. Jang, J., Smyth, A. W., Yang, Y., & Cavalcanti, D. (2015). Road surface condition monitoring via multiple sensor-equipped vehicles. In *Proceedings - IEEE INFOCOM* (pp. 43–44). Hong Kong: Institute of Electrical and Electronics Engineers Inc.

128. Jang, J., Yang, Y., Smyth, A. W., Cavalcanti, D., & Kumar, R. (2017). Framework of data acquisition and integration for the detection of pavement distress via multiple vehicles. *Journal of Computing in Civil Engineering, 31*, 1–15. https://doi.org/10.1061/(ASCE)CP.

129. Allouch, A., Koubaa, A., Abbes, T., & Ammar, A. (2017). RoadSense: Smartphone application to estimate road conditions using accelerometer and gyroscope. *IEEE Sensors Journal, 17*, 4231–4238. https://doi.org/10.1109/JSEN.2017.2702739.

130. Carlos, M. R., Aragon, M. E., Gonzalez, L. C., Escalante, H. J., & Martinez, F. (2018). Evaluation of detection approaches for road anomalies based on accelerometer readings-addressing who's who. *IEEE Transactions on Intelligent Transportation Systems, 19*, 3334–3343. https://doi.org/10.1109/TITS.2017.2773084.

131. Lin, J.-L., Peng, Z.-Q., & Lai, R. K. (2017). Improving pavement anomaly detection using backward feature elimination. *Lecture Notes in Business Information Processing, 288*, 341–349. https://doi.org/10.1007/978-3-319-59336-4_24.

132. Celaya-Padilla, J. M., Galván-Tejada, C. E., López-Monteagudo, F. E., et al. (2018). Speed bump detection using accelerometric features: A genetic algorithm approach. *Sensors (Switzerland), 18*. https://doi.org/10.3390/s18020443.

133. Laubis, K., Simko, V., & Schuller, A. (2016). *Road condition measurement and assessment: A crowd based sensing approach* (pp. 1–10). Dublin: Thirty Seventh International Conference on Information Systems.

134. Zhang, Z., Sun, C., Bridgelall, R., & Sun, M. (2018). Application of a machine learning method to evaluate road roughness from connected vehicles.

Journal of Transportation Engineering Part B: Pavements, 144, 1–13. https://doi.org/10.1061/JPEODX.0000074.

135. Aksamit, P., & Szmechta, M. (2011). *Distributed, mobile, social system for road surface defects detection* (pp. 37–40). Floriana: ISCIII 2011 - 5th international symposium on computational intelligence and intelligent informatics.
136. Nguyen, T., Lechner, B., Wong, Y. D., & Tan, J. Y. (2019). Bus ride index - a refined approach to evaluate road surface irregularities. *Road Mater Pavement Des.* https://doi.org/10.1080/14680629.2019.1625806.

Publisher's Note

Springer Nature remains neutral with regard to jurisdictional claims in published maps and institutional affiliations.

Appendix 2: Paper II

Nguyen, T., Swolana, P., Lechner, B., Wong, Y.D. An Experimental Comparison of Mathematical Heavy-duty City Bus Models to Evaluate Passenger Ride Comfort induced by Road Roughness. *Mathematical and Computer Modelling of Dynamical Systems* (Under Review).

An Experimental Comparison of Mathematical Heavy-duty City Bus Models to Evaluate Passenger Ride Comfort induced by Road Roughness

Teron Nguyen[a,b,c,*], Patrick Swolana[b], Bernhard Lechner[b], and Wong Y.D.[a,c]

[a]*TUMCREATE Ltd., 1 Create Way, #10-02 CREATE Tower, Singapore 138602,*

[b]*Technical University of Munich (TUM), Baumbachstraße 7, 81245 München, Germany*

[c]*Nanyang Technological University (NTU), N1-01b-51, 50 Nanyang Avenue, Singapore 639798, Singapore*

*Corresponding Author: teron.nguyen@tum-create.edu.sg;

An Experimental Comparison of Mathematical Heavy-duty City Bus Models to Evaluate Passenger Ride Comfort induced by Road Roughness

Abstract

Modern developments of road vehicles have allowed the mitigation of ride discomfort induced from excitation of rough roads by various corrective means (e.g. compensatory suspension system). Mathematical models have been used widely to investigate the vehicle-passenger-infrastructure dynamical interaction, however, the responses of various heavy-duty city bus models to estimate ride comfort induced by road roughness are still unknown. In this study, the comparison of dynamical response of buses used in city transport is investigated based on multi-degrees-of-freedom (DOF) bus models developed in MATLAB/Simulink and correlated against passenger ride comfort criteria. The study provides comprehensive insights into dynamics behaviours of a heavy-duty city bus, under conditions of air-suspension configuration, stop-and-go phenomenon and passenger load variation. The results showed that 9-DOF full bus model is the best option to estimate passenger ride comfort within an error of 2%, as compared to 5-DOF half and 3-DOF quarter bus models with 7% and 20% errors using one wheel-track, and 24% and 36% errors using two wheel-tracks, respectively. Based on these results, ride comfort value from quarter-bus-model can be converted to that of higher DOF bus models, or vice versa. These mathematical bus models can be customised for estimating passenger ride comfort and surface roughness of dedicated bus/BRT lanes worldwide.

Keywords: Bus lanes; road roughness; bus dynamics; ride comfort; mathematical model; MATLAB/Simulink

Introduction

The human-centric design approach has emerged in recent decades as the central concept in developing technology and infrastructure for human beings [1, 2]. This trend is also applicable in public transportation, with emphasis on the experience of passengers as they make use of public transport service [3]. Consequently, from the road infrastructure aspect, maintenance of pavement surface to keep in good conditions is vital since excitation from rough road contributes significantly to passenger ride quality. It is of utmost importance in the case of public transport to improve ride quality as a crucial incentive to attract higher ridership.

Vehicle dynamics models have long been developed for different purposes such as to design and optimise suspension system [4, 5], to evaluate passenger ride comfort and vehicle handling [6, 7], and to evaluate road roughness conditions [8, 9]. Multi-body dynamical models have been used intensively [10, 11] but require a massive amount of data and computation efforts. Regarding mathematical models and road roughness evaluation, the most commonly-used vehicle models are quarter-car-simulation (QCS), half-car-simulation (HCS) and full-car-simulation (FCS), of which the QCS has been used most often due to its simplicity. A comprehensive summary in [12] shows that among various indices to evaluate road roughness, there are eight QCS, two HCS and one FCS models. A study in [13] has contributed another six-degrees-of-freedom (6-DOF) FCS model as an evaluation tool for road roughness and whole-body vibration, whereas study [6] provided an HCS model for motorcycle, car, SUV and truck for assessing ride quality on Portland cement concrete pavements. Dynamics models of car and truck, however, would be not applicable to the bus, e.g. heavy-duty city bus which is asymmetric, in larger dimensions, equipped with air suspension, and carrying many passengers on-board.

Regarding bus dynamics, relatively few studies are found in the literature and often focused more on vehicle design such as seat configuration, stiffness and damping parameterisation. A study by [5] has evaluated the bus suspension system based on 3-DOF QCS to optimize the bus vibrational behaviours. In another study [14], a 10-DOFs bus model was developed to investigate the ride comfort of intercity bus users. Recently, the same full bus model was built in [15] using MSC.ADAMS multi-body simulation (MBS) software to establish the "equal oscillatory comfort zones". A much higher DOF low-floor urban-bus model was developed in [16] based on Finite Element Method or in [17] by integrating finite element discretisation into multi-body dynamics. For such complicated multi-body systems, even with high simulation accuracy, it is difficult for transport and pavement engineers to use them to evaluate road roughness condition in a large city network. In this case, the vehicle-infrastructure dynamics interaction can be simulated sufficiently based on the equations of motion of the vehicle [18], such as a 6-DOF half bus model in [19] or a 3-DOF quarter bus model (Bus Ride Index - BRI) to correlate passenger ride comfort with road surface irregularities [20].

The use of BRI, however, is in the question of whether this 3-DOF quarter bus model [20] can deliver reliable results due to information lost during the modelling simplification. Importantly, the effects of roll and pitch motions have been not considered. It is well noted from the literature that the FCS captures the full behaviour of the vehicle body when comparing 2-DOF QCS, 4-DOF HCS and 7-DOF FCS with road input as a step-hump [21, 22], or when comparing 2-DOF QCS, 4-DOF HCS and 15-DOF FCS using a multibody simulation software with experimental ride comfort data from a vehicle travelling on a

Belgian pavement [23]. Surprisingly, the simplified 2-DOF QCS generated non-correlated output as compared to 15-DOF FCS when estimating ride comfort results [23]. These methods, however, have limitations such as constant car speeds and the inclusion of artificial road profiles, or based on a designated road segment/short hump. The use of artificial profiles to evaluate their effects on users is not adequate according to the investigation in [24]. City bus operation is more diversified comprising stop-and-go phenomena along bus corridors and under variable passenger load. More importantly, the inclusion of non-linear air suspension into a mathematical heavy-duty bus model is still limited. The responses of various heavy-duty city bus models to estimate ride comfort induced by road roughness are still unknown.

These research gaps have thus motivated this study to compare different mathematical bus models for calculating passenger ride comfort as based on human-centric design approach in public transport [3]. Multi-degrees-of-freedom (3-DOF quarter, 5-DOF half and 9-DOF full) bus models were built in MATLAB/Simulink and their performances in calculating passenger ride comfort on buses operating along bus lanes were compared. Bus technical parameters were collected from manufacturers while bus lane roughness was sampled using a professional multi-laser road profiler. Vertical acceleration and GPS data were collected from a portable seat-pad accelerometer. This is the first time an experimental comparison between three mathematical bus models has been conducted, providing comprehensive insights into dynamics behaviours of a heavy-duty city bus, under conditions of air-suspension configuration, stop-and-go phenomenon and passenger load variation. By matching GPS data and speed profiles the ride comfort indicator can be compared in time-series domain. These mathematical bus models can be customised for estimating passenger ride comfort and surface roughness of dedicated bus/BRT lanes worldwide.

The remaining paper is structured as follows. In the next section, bus parameters and experimental set-up are then described. Bus dynamics models such as 3-DOF quarter-bus-model (QBM), 6-DOF half-bus-model (HBM) and 9-DOF full-bus-model (FBM) are then formulated and built using MATLAB/Simulink. Findings on the vehicle dynamics and the difference between simulated and measured ride comfort levels are discussed, following by the Conclusion part.

Bus parameters and experimental set-up

To simulate bus dynamics, technical data were referenced to the single-decker bus model Mercedes-Benz Citaro operating in urban areas [25]. The bus body is asymmetric where the front axle can carry up to 7.245t and rear axle can carry 12t when fully laden at 19t. Detailed parameters with the acronym used for bus dynamics are shown in Appendix A. Damping ratio = 0.3 was chosen in favour of passenger ride comfort. Passenger seat characteristics were selected concerning ride comfort optimisation. Mathematical air spring model is rather complicated as the investigated in [26]. Therefore, the simplified configuration and calculation of the non-linear air-spring suspension were referred to the recommendation of the Firestone manufacturer [27] as well as its application in [20].

The experimental set-up, in this study, was conducted with the following steps:

- Selecting bus lane segments with different road roughness levels;
- Scanning the bus lane by a multi-laser road profiler;
- Measuring onboard ride comfort index using a seat-pad accelerometer;

- Developing 3-DOF QBM, 6-DOF HBM and 9-DOF FBM to estimate ride comfort index using the same measured road longitudinal profiles; and
- Comparing the measured and calculated ride comfort levels to evaluate the developed bus dynamics models.

A 2.3km bus lane segment was selected for field measurement, in which the Bus lane 45 is from West to East and Bus lane 44 is from East to West (Fig. 1). This straight segment was chosen to avoid the impact of lateral acceleration on the measurement data. Multi-laser road profiler was used to measure bus lane longitudinal profiles with the sampling rate of 25mm. Bus lane 44 has IRI_{left}=4.4, IRI_{right}=3.51 (m/km), while Bus lane 45 has IRI_{left}=4.85, IRI_{right}=4.21 (m/km). Fig. 2 illustrates the IRI values of the Bus lane 45 for every 100m, ranging from 2 to 7 (m/km) and calculated using ProVal software [28]. It is evident from IRI values that this segment contains different road conditions from smooth to very rough surfaces with different left and right-wheel-track profiles.
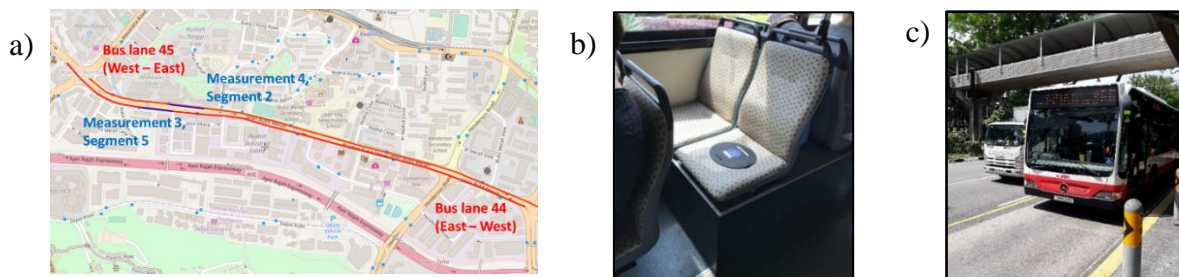

Fig. 1 Field measurement setup a) selected road segment; b) portable accelerometer c) the urban bus
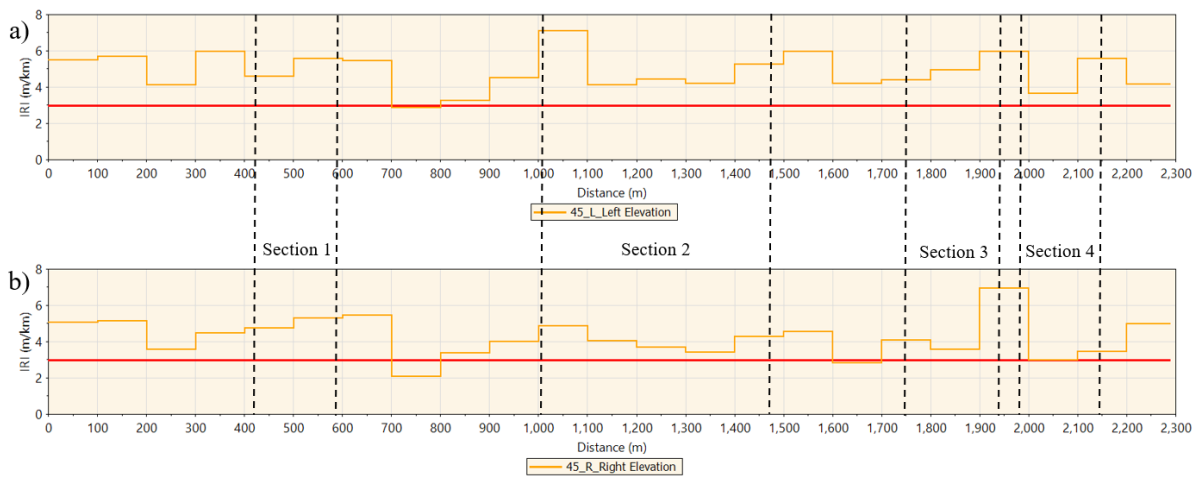

Fig. 2 IRI value of the Bus lane 45 for every 100m with four sections for further investigation (a) left-wheel track; (b) right-wheel track.

A seat-pad accelerometer SV100A, loaded by a 70kg human, was used to measure acceleration data. The rear-axle seat is one of the most critical locations where often higher vertical acceleration was collected [15]. The device is controlled wirelessly by a mobile application and can collect acceleration data at a sampling rate of 750Hz and GPS data at 1Hz, which in turns were used to match the vehicle model's simulation output. This sampling frequency is satisfied as two times greater than the maximum considered frequency of 1~100Hz to be considered primarily [29], according to the Sampling Theorem [30]. Raw vertical acceleration (a_z) is processed to frequency-weighted acceleration ($a_{wz}(t)$) and root-mean-square frequency-weighted acceleration (a_{wz}), as calculated by Equation (2). The relative levels of comfort according to levels of a_{wz} are listed in Table 1.

$$a_{wz} = \left[\frac{1}{T}\int_0^T a_{wz}^2(t)dt\right]^{\frac{1}{2}}$$ (1)

where: $a_{wz}(t)$ is the weighted acceleration (m/s^2); T is the duration of the measurement, in seconds.

Table 1: Levels of Comfort corresponding to RMS Acceleration in ISO 2631-1 [29]

RMS vertical acceleration a_{wz} (m/s^2)	Levels of comfort
less than 0.315	not uncomfortable
0.315 to 0.63	a little uncomfortable
0.5 to 1.0	fairly uncomfortable
0.8 to 1.6	Uncomfortable
1.25 to 2.5	very uncomfortable
greater than 2.0	extremely uncomfortable

Mathematical bus dynamics models

Quarter-bus model (QBM)

The simplest vertical oscillatory QBM consists of three aligned masses, representing the equivalent human-seat mass (m_H), half of the unsprung mass (m_U) and a quarter of the sprung mass (m_S). The vertical alignment assumes that the affected human is sitting right above the suspension system. The smoothed road elevation $z_R(t)$, induces vertical displacement and velocity to the system through the tyre's spring-damper-system. Fig. 3 displays the 3-DOF QBM as well as its free body diagram.

From the free body diagram in Fig. 3(b), the equations of motion (vertical acceleration of human-seat mass, unsprung and sprung mass) can be derived as follows:

$$m_H\,\ddot{z}_H = -k_H(z_H - z_S) - d_H(\dot{z}_H - \dot{z}_S)$$ **(2)**

$$m_S\,\ddot{z}_S = k_H(z_H - z_S) + d_H(\dot{z}_H - \dot{z}_S) - k_S(z_S - z_U) - d_S(\dot{z}_S - \dot{z}_U)$$ **(3)**

$$m_U\,\ddot{z}_U = k_S(z_S - z_U) + d_S(\dot{z}_S - \dot{z}_U) - k_U(z_U - z_R) - d_U(\dot{z}_U - \dot{z}_R)$$ **(4)**
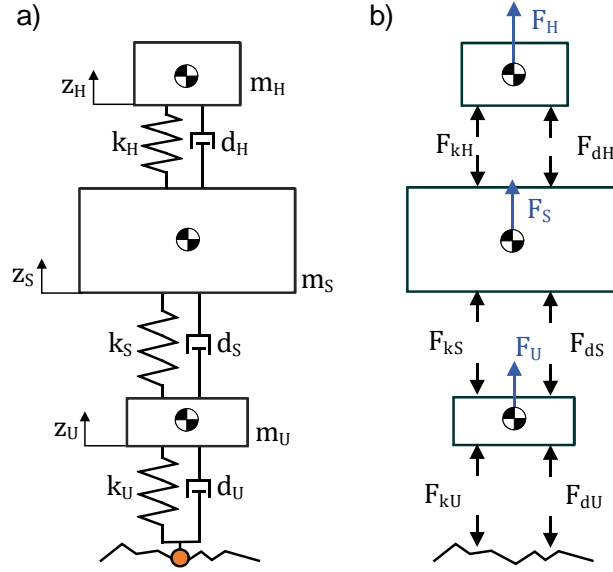
Fig. 3 (a) Quarter-bus model (3-DOF); (b) Free body diagram of the quarter-bus model

Half-bus model (HBM)

A better approximation of reality is achieved by adding the pitch movement to the model. This is attained by modelling the sprung mass as a rigid bar in the longitudinal direction with half of the total sprung mass and half of the moment of inertia (Fig. 4). It is supported, like the QBM, by two suspension systems connecting half of the unsprung masses with the vehicle body, depicting the front and the rear of the bus. Hence, the pitch motion of the sprung mass is introduced. Fig. 4 displays the lumped mass model of the developed longitudinal HBM including the 6 DOFs (vertical acceleration of 2 human-seat masses, 2 unsprung masses, 1 sprung mass, and pitch motion of 1 sprung mass) as highlighted.
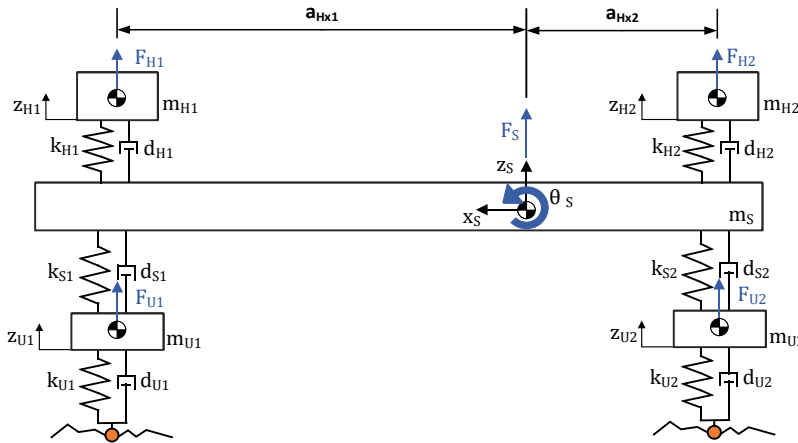

Fig. 4 Half-bus model (6-DOF)

By applying Newton's second law, the equations of motion can be derived as follows:

$$m_{H1} \ddot{Z}_{H1} = -k_{H1} Z_{H1} - d_{H1} \dot{Z}_{H1} \tag{5}$$

$$m_{H2} \ddot{Z}_{H2} = -k_{H2} Z_{H2} - d_{H2} \dot{Z}_{H2} \tag{6}$$

$$m_S \ddot{Z}_S = k_{H1} Z_{H1} + d_{H1} \dot{Z}_{H1} + k_{H2} Z_{H2} + d_{H2} \dot{Z}_{H2} - k_{S1} Z_{S1} - d_{S1} \dot{Z}_{S1} - k_{S2} Z_{S2} - d_{S2} \dot{Z}_{S2} \tag{7}$$

5

$$I_{Sy}\ddot{\theta}_S = -a_{Hx1}k_{H1}Z_{H1} - a_{Hx1}d_{H1}\dot{Z}_{H1} + a_{Hx2}k_{H2}\,Z_{H2} + a_{Hx2}d_{H2}\,\dot{Z}_{H2} + a_{Sx1}k_{S1}\,Z_{S1} + a_{Sx1}d_{S1}\,\dot{Z}_{S1} - a_{Sx2}\,k_{S2}\,Z_{S2} \quad (8)$$
$$- a_{Sx2}\,d_{S2}\,\dot{Z}_{S2}$$

$$m_{U1}\ddot{z}_{U1} = k_{S1}\,Z_{S1} + d_{S1}\,\dot{Z}_{S1} - k_{U1}Z_{U1} - d_{U1}\,\dot{Z}_{U1} \quad (9)$$

$$m_{U2}\ddot{Z}_{U2} = k_{S2}\,Z_{S2} + d_{S2}\,\dot{Z}_{S2} - k_{U2}\,Z_{U2} - d_{U2}\,\dot{Z}_{U2} \quad (10)$$

with

$Z_{H1} = (z_{H1} + a_{Hx1}\theta_S - z_S)$ $\qquad\qquad$ $Z_{H2} = (z_{H2} - a_{Hx2}\theta_S - z_S)$

$Z_{S1} = (z_S - a_{Sx1}\theta_S - z_{U1})$ $\qquad\qquad$ $Z_{S2} = (z_S + a_{Sx2}\theta_S - z_{U2})$

$Z_{U1} = (z_{U1} - z_{R1})$ $\qquad\qquad\qquad\;$ $Z_{U2} = (z_{U2} - z_{R2})$

Full-bus model (FBM)

The FBM developed in this part introduces the roll motion by modelling the sprung mass as a rigid plate, as can be seen in Fig. 5. In total, the developed FBM contains 9 DOFs (vertical displacement of 2 human-seat masses, 2 front unsprung masses, 1 rear unsprung mass, 1 sprung mass; pitch motion of 1 sprung mass; and roll motion of 1 sprung mass and 1 rear unsprung mass). Angles are again assumed to be small for the whole system which is why the small-angle approach is applicable. The 3-dimensional FBM furthermore includes both wheel tracks with a time-shifted road input for the rear axle. The location of both human models can be adjusted in the longitudinal and lateral direction. For comparison purpose, they are located above the axles on the left side of the model by default.
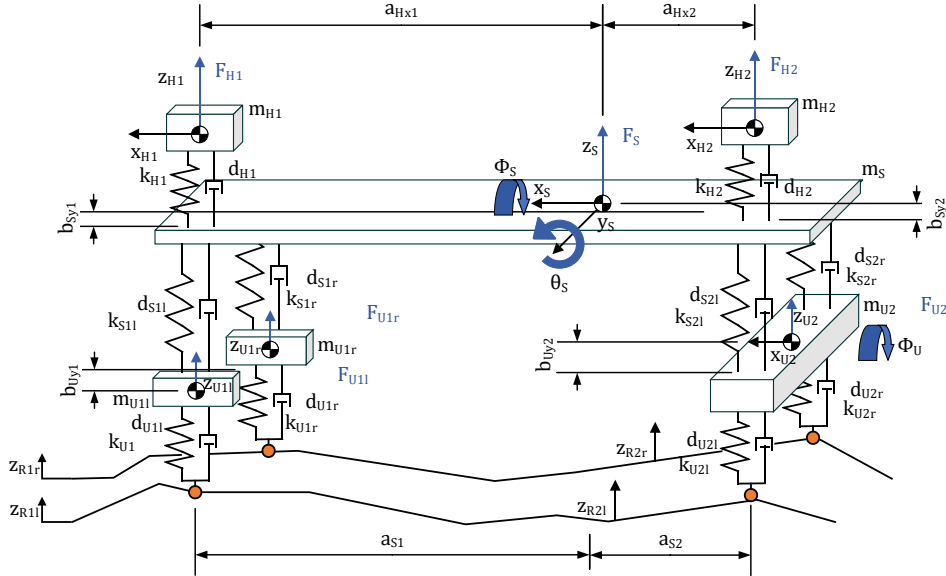

Fig. 5 Full-bus model (9-DOF)

After applying Newton's second law the equations of motion for the full bus model can be derived as follows:

$$m_{H1}\,\ddot{Z}_{H1} = -k_{H1}Z_{H1} - d_{H1}\dot{Z}_{H1} \quad \textbf{(11)}$$

$$m_{H2}\,\ddot{Z}_{H2} = -k_{H2}Z_{H2} - d_{H2}\dot{Z}_{H2} \quad \textbf{(12)}$$

$$m_S\ddot{Z}_S = k_{H1}\,Z_{H1} + d_{H1}\,\dot{Z}_{H1} + k_{H2}\,Z_{H2} + d_{H2}\,\dot{Z}_{H2} - k_{S1r}\,Z_{S1r} - d_{S1r}\,\dot{Z}_{S1r} \quad \textbf{(13)}$$

$$- k_{S1l}\,Z_{S1l} - d_{S1l}\,\dot{Z}_{S1l} - k_{S2r}\,Z_{S2r} - d_{S2r}\,\dot{Z}_{S2r} - k_{S2l}\,Z_{S2l} - d_{S2l}\,\dot{Z}_{S2l}$$

6

$$I_{Sy}\ddot{\theta}_S \quad = -\,k_{H1}\,Z_{H1}\,a_{Hx1} - d_{H1}\,\dot{Z}_{H1}\,a_{Hx1} + k_{H2}\,Z_{H2}\,a_{Hx2} + d_{H2}\,\dot{Z}_{H2}\,a_{Hx2} \tag{14}$$

$$+\,k_{S1r}\,Z_{S1r}\,a_{Sx1} + d_{S1r}\,\dot{Z}_{S1r}\,a_{Sx1} + k_{S1l}\,Z_{S1l}\,a_{Sx1} + d_{S1l}\,\dot{Z}_{S1l}\,a_{Sx1}$$

$$-\,k_{S2r}\,Z_{S2r}\,a_{Sx2} - d_{S2r}\,\dot{Z}_{S2r}\,a_{Sx2} - k_{S2l}\,Z_{S2l}\,a_{Sx2} - d_{S2l}\,\dot{Z}_{S2l}\,a_{Sx2}$$

$$I_{Sx}\ddot{\Phi}_S \quad = k_{H1}\,Z_{H1}\,b_{Hy1} + d_{H1}\,\dot{Z}_{H1}\,b_{Hy1} + k_{H2}\,Z_{H2}\,b_{Hy2} + d_{H2}\,\dot{Z}_{H2}\,b_{Hy2} \tag{15}$$

$$+\,k_{S1r}\,Z_{S1r}\,b_{Sy1} + d_{S1r}\,\dot{Z}_{S1r}\,b_{Sy1} - k_{S1l}\,Z_{S1l}\,b_{Sy1} - d_{S1l}\,\dot{Z}_{S1l}\,b_{Sy1}$$

$$+\,k_{S2r}\,Z_{S2r}\,b_{Sy2} + d_{S2r}\,\dot{Z}_{S2r}\,b_{Sy2} - k_{S2l}\,Z_{S2l}\,b_{Sy2} - d_{S2l}\,\dot{Z}_{S2l}\,b_{Sy2}$$

$$m_{U1r}\ddot{Z}_{U1r} = k_{S1r}\,Z_{S1r} + d_{S1r}\,\dot{Z}_{S1r} - k_{U1r}\,Z_{U1r} - d_{U1r}\,\dot{Z}_{U1r} \tag{16}$$

$$m_{U1l}\ddot{Z}_{U1l} = k_{S1l}\,Z_{S1l} + d_{S1l}\,\dot{Z}_{S1l} - k_{U1l}\,Z_{U1l} - d_{U1l}\,\dot{Z}_{U1l} \tag{17}$$

$$m_{U2}\ddot{Z}_{U2} \quad = k_{S2r}\,Z_{S2r} + d_{S2r}\,\dot{Z}_{S2r} + k_{S2l}\,Z_{S2l} + d_{S2l}\,\dot{Z}_{S2l} - k_{U2r}\,Z_{U2r} - d_{U2r}\,\dot{Z}_{U2r} \tag{18}$$

$$-k_{U2l}\,Z_{S2l} - d_{U2r}\,\dot{Z}_{S2l}$$

$$I_{U2x}\ddot{\Phi}_U \quad = -k_{S2r}\,Z_{S2r}\,b_{Sy2} - d_{S2r}\,\dot{Z}_{S2r}\,b_{Sy2} + k_{S2l}\,Z_{S2l}\,b_{Sy2} + d_{S2l}\,\dot{Z}_{S2l}\,b_{Sy2} \tag{19}$$

$$+k_{U2r}\,Z_{U2r}\,b_{Uy2} + d_{U2r}\,\dot{Z}_{U2r}\,b_{Uy2} - k_{U2l}\,Z_{S2l}\,b_{Uy2} - d_{U2r}\,\dot{Z}_{S2l}\,b_{Uy2}$$

with

$$Z_{H1} = \left(z_{H1} + a_{Hx1}\theta_S - b_{Hy1}\Phi_S - z_S\right) \qquad Z_{H2} = \left(z_{H2} - a_{Hx2}\theta_S - b_{Hy2}\Phi_S - z_S\right)$$

$$Z_{S1l} = \left(z_S - a_{Sx1}\theta_S + b_{Sy1}\Phi_S - z_{U1l}\right) \qquad Z_{S1r} = \left(z_S - a_{Sx1}\theta_S - b_{Sy1}\Phi_S - z_{U1r}\right)$$

$$Z_{S2l} = \left(z_S + a_{Sx2}\theta_S + b_{Sy2}\Phi_S - (z_{U2} + b_{Uy2}\Phi_{U2})\right) \quad Z_{S2r} = \left(z_S + a_{Sx2}\theta_S - b_{Sy2}\Phi_S - (z_{U2} - b_{Uy2}\Phi_{U2})\right)$$

$$Z_{U1l} = \left(z_{U1l} - z_{R1l}\right) \qquad Z_{U1r} = \left(z_{U1r} - z_{R1r}\right)$$

$$Z_{U2l} = \left(z_{U2} + b_{Uy2}\Phi_{U2} - z_{R2l}\right) \qquad Z_{U2r} = \left(z_{U2} - b_{Uy2}\Phi_{U2} - z_{R2r}\right)$$

Findings and discussion

Calibration of the bus models

For the calibration process, the step response (1cm height at a simulation time of 0.5s) was used to investigate the behaviours of the bus dynamics models built in Matlab/Simulink (see Appendix B). The step size for simulation is fixed at 0.001s, for which the used solver is the 'ode3' using Bogacki-Shampine formula integration technique. The bus dynamics behaviour in different cases are described as follows:

- vertical oscillation: the same two responses caused by the step input were observed from HBM and FBM (Fig. 6b), while only one response from QBM (Fig. 6a),
- pitch motion (HBM and FBM): the change of pitch angle theta (θ_S) rotating around the y-axis while encountering the first step by the front tyre (counter-clockwise) and second step by the rear tyre (clockwise) (Fig. 6c), and
- bounce, pitch and roll motion (only FBM): the step of 1cm only occurs under the right tyres, resulting in higher displacement response on the right side than that of the left side (Fig. 6d).

The step response method is an appropriate way to investigate system response of second-order dynamic systems on a small scale. Since each model consists of second-order dynamic

subsystems, they were compared with general second-order dynamic response curves from [31]. All vehicle models show the expected dynamic responses to the step road input of 1cm height. Thus, it can be concluded that all models are adequately set up in the Simulink environment according to their equations of motion.
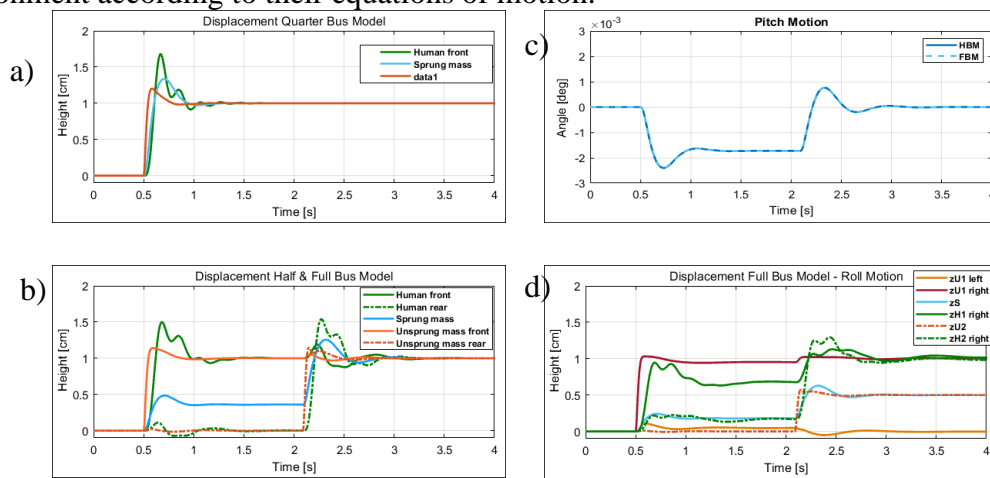

Fig. 6 Step response calibration using road input 1cm step at 0.5 seconds (front tyres) and 2.09 seconds (rear tyres), velocity=10 km/h (a) Displacement of QBM; (b) Displacement of HBM and FBM; (c) Pitch angle of HBM and FBM; (d) Bounce, pitch and roll motion of FBM.

Transfer functions under passenger load change

To investigate the behaviour of the bus dynamics models under passenger load change, the transfer functions (TFs) of QBM vehicle responses are considered and illustrated (Fig. 7a). For comparison, the QCS for International Roughness Index (IRI) [8] is calculated for the TF of sprung mass displacement over unsprung mass, whereas QBM's TF considers the response of the sprung mass to road profile inputs. The dominant peak of the IRI-QCS response is near 1 and 10Hz, while QBM body bounce frequency is near 1.54Hz, in which different passenger loading factors ($n = 0 \div 1$ from unladen to fully laden) do not influence the TFs of QBM. This can be explained by the air suspension characterized by its nonlinear dynamic behaviours. This comparison has shown that the developed bus models have captured and represented the bus dynamics appropriately under passenger loading variation. Fig. 7b shows a similar trend for the wavenumber, travel speed of 80km/h was considered when calculating the transfer functions concerning the spatial frequency. More difference can be expected under the speed change because the heavy-duty city bus is often operated at lower speed levels than cars.
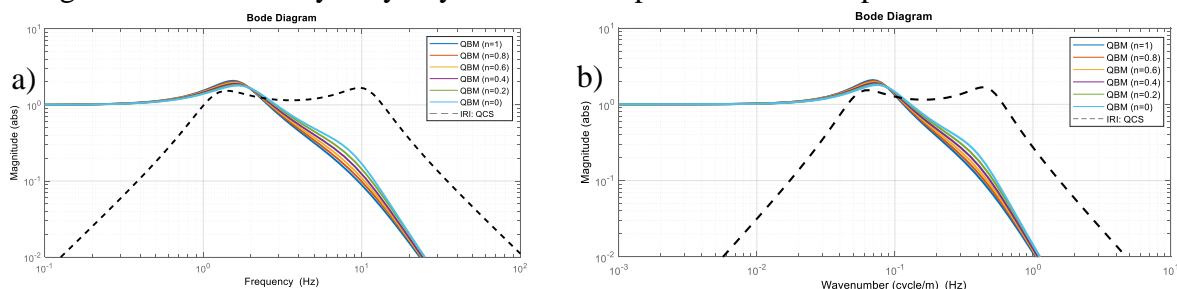

Fig. 7 The difference in response from transfer functions of IRI-QCS and QBM as (a) temporal frequency and; (b) spatial frequency.

8

Comparison of simulation and measurement results

Four measurements with different length were recorded for comparison with simulation results. These sections have the most comparable GPS data between longitudinal road profiles and acceleration measurement using the accelerometer. The dedicated bus lanes help to improve the matching of GPS data between the field-measured bus lane longitudinal profiles and bus wheel trajectories. Fig. 8 shows the comparison of frequency-weighted acceleration $a_{wz}(t)$ in time-series and the RMS a_{wz} between simulation and field-measurement at different velocity (m/s). The illustration shows data comparison only for the right-wheel-track on the rear-axle location of the 3-DOF QBM and 6-DOF HBM. Good matching results are observed from simulation output and measurement data under the speed changes, especially for the peak value. Due to the slight misalignment between bus wheel trajectories and road profiles, perfect matching is not possible to achieve.

Fig. 9a shows the ratio $r = a_{wz\text{-}simulation}/a_{wz\text{-}measurement}$ of all section measurements and the average ratios of r = 136% (std = 16%), r = 124% (std = 15%) and r = 102% (std=6%) as found for the three QBM, HBM and FBM, respectively. Data comparison is based on the average r-ratios of both left-, and right-wheel tracks of the 3-DOF QBM and 6-DOF HBM. The 9-DOF FBM provides the best matching results while 3-DOF QBM overestimates the ratio and 6-DOF HBM is in between. These trends are also observed at individual section measurements; however, they varied over the four measurements. In section 1, the three results across all simulation models are not much different, which can be explained by the similar roughness pattern between two wheel-track profiles. For the remaining sections, the impact of non-uniform roughness level of two wheel-tracks is evident. For example, in section 4, QBM and HBM give almost similar results while FBM output is much lower. In contrast with the study in [23] concluded that QCS does not have "any correlation" with measurement data, this study has shown that QBM results are higher than that of FBM at 36% when using both wheel-track and 24% when using only the right-track, respectively. Whereas, HBM results are higher than that of FBM at 20% when using both wheel-track and 7% when using only the right-track, respectively. Fig. 9b shows similar results for only right-wheel track comparison. Another left-wheel track has accounted for around 10% of result variation compared to the right-wheel track alone where in situ measurement was conducted.

FBM provides the most reliable results, however, its modelling complexity is the highest in terms of data requirement and modelling algorithms. Several main factors made the outputs from QBM and HBM being higher than those of FBM. Firstly, QBM only considers vertical oscillation while HBM and FBM take pitch motion, and both pitch and roll motion, respectively, into account. This helps to reduce vertical acceleration since when rear tyres go over the hump, the front tyres stay on the ground in case of HBM and FBM, which is contrasted to QBM. Secondly, the outputs from the three models can be similar as in section 1 when there are less roll and pitch motions. This means that the right and left road profiles are quite uniform. Regarding different results as compared to [23] (see Table 2), it is noted that this study estimated ride comfort index a_{wz} at human mass on a seat cushion with consideration of optimal seat damping and stiffness configuration. However, the study of [23] does not model the human mass and a_{wz} was calculated based on sprung mass oscillation. As a result, the estimated a_{wz} is overestimated significantly in case of QCS.
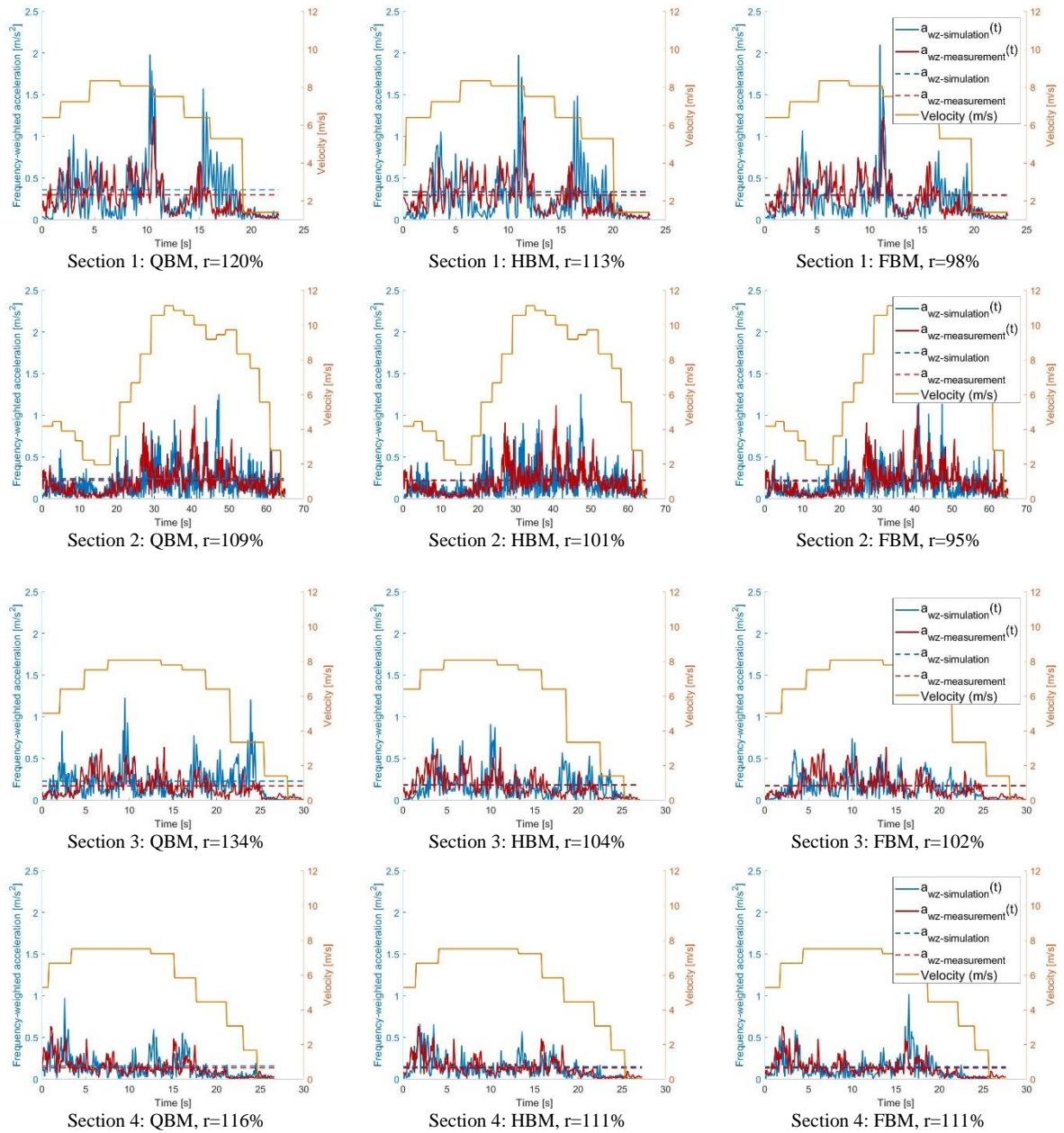
Fig. 8 The frequency-weighted $a_{wz\_simulation(t)}$ and $a_{wz\_measurement(t)}$ at different sections for the right-wheel-track only
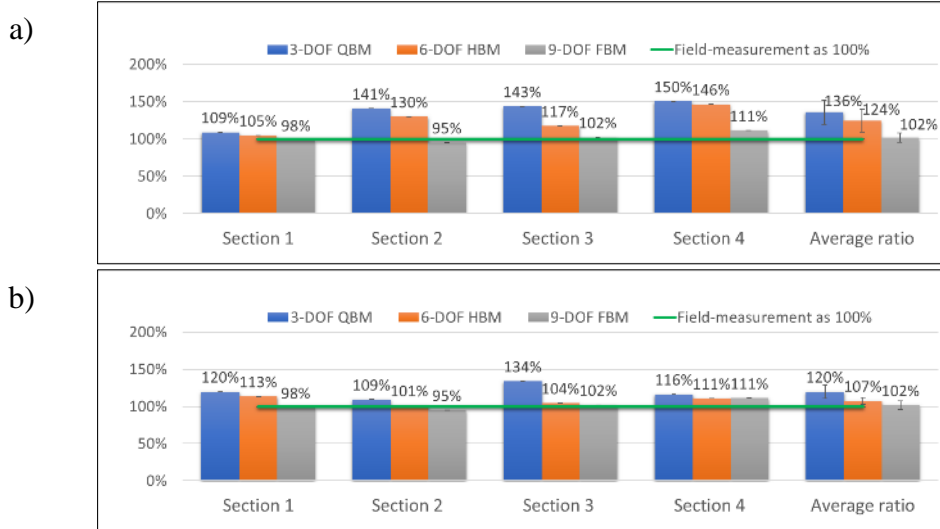
Fig. 9 $a_{wz\_simulation}/a_{wz\_measurement}$ ratios at different sections and the average ratios (standard deviation) (a) using both wheel tracks; (b) using only the right-wheel track where the field measurement was taken

Over the comparison of $a_{wz}(t)$ in the time domain, there is always the trend that simulated results are higher than field-measured results. This can be explained by the tyre being modelled as a point contact of the mathematical bus models which is different from the dual-wheel rear axle. The real dual-wheel helps to reduce the impact of road roughness, for example when one tyre goes over a small pothole while another tyre stays on flat ground to keep the whole dual-wheel in the flat, balanced position.

Table 2: Comparison of output between different vehicle type modelling, in which simulated results from full-vehicle model is equivalent to the field-measured data

Source	Half- vs. full-vehicle model	Quarter- vs. full-vehicle model	Quarter- vs. half-vehicle model	Wheel-track for quarter- and half-vehicle models	Vehicle type
Ride comfort: a_{wz} values [23]	52% error, or FCS = 66% HCS	105% error, or FCS = 49% QCS		one track, Belgian paving road	Car
Roughness index: IRI and HRI [32]			HRI ≈ 80% IRI$_{mean}$ (or r = 25%)	both tracks, HRI derived from IRI	Car
Roughness index: IRI, HRI, FRI [33]	FRI ≈ 76% HRI	FRI ≈ 69% IRI$_{mean}$		both tracks, generated road profiles, HRI, FRI derived from IRI	Car
Ride comfort (recent study)	FBM ≈ 95% HBM FBM ≈ 83% HBM	FBM ≈ 85% QBM FBM ≈ 75% QBM	HBM ≈ 92% QBM HBM ≈ 89% QBM	one track, field-measured profiles both track, field-measured profiles	Bus

Note: QCS, HCS, FCS: quarter-car, half-car and full-car simulation; IRI, HRI, FRI: International roughness index, half- and full roughness index. QBM, HBM, FBM: quarter-bus, half-bus and full-bus model.

From the overall ratio comparison, ride comfort value from QBM can be converted to that of higher DOF vehicle model, such as FBM ≈ 85% QBM for single wheel-track calculation, and FBM ≈ 75% QBM for two wheel-track calculation, or vice versa. Compared to literature, in case of both wheel-tracks calculation the findings of ride comfort ratio of HBM ≈ 0.89 QBM is higher than the case of car dynamics where half-car roughness index HRI ≈ 0.8 IRI$_{mean}$ of quarter-car roughness index [32], or FBM ≈ 0.83 HBM and FBM ≈ 0.75 QBM is higher from the full-car roughness index FRI ≈ 76% HRI or FRI ≈ 69% IRI$_{mean}$ [33], respectively (see Table 2). It is worth emphasising that these HRI and FRI are derived from IRI QCS, instead of simulating the half- and full-car dynamics models. This difference can be explained by the inherent difference between car and bus dynamics, as well as the field-measured road profiles input for adequately evaluating ride comfort as the recommendation in [24]. Once again, the

11

finding results have confirmed the importance of this study and support the usage of Bus Ride Index [20] with the cautions on vehicle dynamical modelling complexity, resulting in different outputs.

Conclusions

This study on bus dynamics provides a detailed investigation of the behaviours of different bus models: 3-DOF QBM, 6-DOF HBM and 9-DOF FBM, from the perspective of passenger ride comfort. This is the first time a comprehensive comparison between three mathematical dynamics models of a heavy-duty city bus (19t) has been conducted, focusing on the actual travelling operation. The RMS acceleration a_{wz} induced on human mass above the rear axle is a primary location for comparison, in which similar trend was observed from different measurements along the selected bus lane segment: $a_{wz}(QBM) > a_{wz}(HBM) > a_{wz}(FBM)$, as a similar trend from literature. However, the output is not that significant in the case of QBM. The FBM well captures the correct behaviours of bus dynamics, but this is the most complex model. Therefore, each bus model can be utilised depending on the specific study purpose such as the widely used QCS as pragmatic approaches to design individual vehicle suspension and to evaluate road roughness. Based on these results, ride comfort value from quarter-bus-model can be converted to that of higher DOF bus models, or vice versa. These mathematical bus models can be customised for estimating passenger ride comfort and surface roughness of dedicated bus/BRT lanes worldwide.

This experimental study has explored a new method to compare between simulation and field-measurement operating on a bus lane. By matching GPS data and speed profiles the frequency-weighted $a_{wz}(t)$ and a_{wz}, ride comfort index can be compared in time-series domain. Importantly, the developed algorithms can incorporate speed changes along the bus corridor that replicates the stop-and-go phenomenon of city bus service, resulting in more reliable outputs. The nonlinear characteristics of air-suspension have been considered in the city bus mathematical models which are often modelled using sophisticated and data-required Multibody dynamics system [15, 34–36]. The findings, thus, contribute to the literature by providing an understanding of the dynamics of different city bus models, applicable for road surface and ride comfort evaluation.

The study, however, contains limitations in its modelling simplification. The effects of other lateral and longitudinal accelerations have not been considered. Moreover, the human body can be modelled as an active mechanical system. The primary purpose of this study is focused on the development and comparison of simple mathematical dynamics models for evaluating road roughness and ride comfort for pavement engineering application, like the investigation in [13]. Regarding the further study, sensitivity analysis can be focused on a greater number of road profiles to establish more precisely the r ratios. Bus models regarding aging, operating speeds and noise variation can also be included.

Declaration of Conflicting Interests: The Authors declare that there is no conflict of interest

References

1. Mitchell, D., Claris, S., & Edge, D. (2016) Human-centered mobility: a new approach to designing and improving our urban transport infrastructure. *Engineering*, *2*, 33–36. doi:10.1016/j.eng.2016.01.030.

2. Bogren, L., Fallman, D., & Henje, C. (2009) User-centered inclusive design: making public transport accessible. In: *International Conference on Inclusive Design–Royal College of Art*. London, UK.

3. Camacho, T., Foth, M., Rakotonirainy, A., Rittenbruch, M., & Bunker, J. (2016) The role of passenger-centric innovation in the future of public transport. *Public Transport*, *8*, 453–475. doi:10.1007/s12469-016-0148-5.

4. Yu, K., Luo, A. C. J., & He, Y. (2002) Stability and vibration of a non-linear vehicle and passenger system. *Proceedings of the Institution of Mechanical Engineers, Part K: Journal of Multi-body Dynamics*, *216*, 109–116. doi:10.1243/14644190260070358.

5. Sekulić, D., & Dedović, V. (2011) The effect of stiffness and damping of the suspension system elements on the optimisation of the vibrational behaviour of a bus. *International Journal for Traffic & Transport Engineering*, *1*, 231–244.

6. Prem, H., & Ayton, G. (2005) Improved techniques for assessing ride quality on concrete pavements. In: *8th International Conference on Concrete Pavements*. Colorado, USA, pp 733–754.

7. Talukdar, S., Mazumdar, A., Mullasseril, M., Kalita, K., & Ujjwal, A. (2012) Mathematical modeling in vehicle ride dynamics. *SAE Tech Pap*. https://doi.org/10.4271/2012-01-0056.

8. Sayers, M. W. (1995) On the calculation of international roughness index from longitudinal road profile. *Transportation Research Record*, *1501*, 1–12. doi:10.1080/10643389.2012.728825.

9. Prem, H., Ramsay, E., & McLean, J. (2000) A road profile based truck ride index (tri). In: *6th International Symposium on Heavy Vehicle Weights and Dimensions*. Saskatoon, Saskatchewan, Canada, pp 483–506.

10. Minaker, B. P. (2015) The tangent stiffness matrix in rigid multibody vehicle dynamics. *Mathematical and Computer Modelling of Dynamical Systems*, *21*, 288–310. doi:10.1080/13873954.2014.953549.

11. Jang, B. C., & Choi, G. (2007) Co-simulation and simulation integration for a full vehicle dynamic system. *Mathematical and Computer Modelling of Dynamical Systems*, *13*, 237–250. doi:10.1080/13873950600759073.

12. Múčka, P. (2015) Current approaches to quantify the longitudinal road roughness. *International Journal of Pavement Engineering*, 1–21. doi:10.1080/10298436.2015.1011782.

13. Cantisani, G., & Loprencipe, G. (2010) Road roughness and whole body vibration: evaluation tools and comfort limits. *Journal of Transportation Engineering*, *136*, 818–826. doi:10.1061/(ASCE)TE.1943-5436.0000143.

14. Sekulić, D., Dedović, V., Rusov, S., Šalinić, S., & Obradović, A. (2013) Analysis of vibration effects on the comfort of intercity bus users by oscillatory model with ten degrees of freedom. *Applied Mathematical Modelling*, *37*, 8629–8644. doi:10.1016/j.apm.2013.03.060.

15. Sekulić, D., Dedović, V., Rusov, S., Obradović, A., & Šalinić, S. (2016) Definition and determination of the bus oscillatory comfort zones. *International Journal of Industrial Ergonomics*, *53*, 328–339. doi:10.1016/j.ergon.2016.04.003.

16. Eriksson, P., & Friberg, O. (2000) Ride comfort optimization of a city bus. *Structural and Multidisciplinary Optimization*, *20*, 67–75. doi:10.1007/s001580050137.

17. Georgiou, G., Badarlis, A., & Natsiavas, S. (2008) Modelling and ride dynamics of a flexible multi-body model of an urban bus. *Proceedings of the Institution of Mechanical Engineers, Part K: Journal of Multi-body Dynamics*, *222*, 143–154. doi:10.1243/14644193JMBD130.

18. Cantero, D., O'Brien, E. J., & González, A. (2010) Modelling the vehicle in vehicle-infrastructure dynamic interaction studies. *Proceedings of the Institution of Mechanical Engineers, Part K: Journal of Multi-body Dynamics*, *224*, 243–248. doi:10.1243/14644193JMBD228.

19. Fichera, G., Scionti, M., & Garescì, F. (2007) Experimental correlation between the road roughness and the comfort perceived in bus cabins. *SAE Tech Pap 2007-01-0325*. https://doi.org/10.4271/2007-01-0352.

20. Nguyen, T., Lechner, B., Wong, Y. D., & Tan, J. Y. (2019) Bus ride index - a refined approach to evaluate road surface irregularities. *Road Mater Pavement Des*. https://doi.org/10.1080/14680629.2019.1625806.

21. Mahala, M. K., Gadkari, P., & Deb, A. (2009) Mathematical models for designing vehicles for ride comfort. In: *ICORD 09: Proceedings of the 2nd International Conference on Research into Design*. Bangalore, India, pp 168–175.

22. Mahala, M., Deb, A., & Chou, C. (2015) A comparative study of lumped parameter models for assessing the performance of vehicle suspension systems. *SAE Technical Papers*, *2015-April*,. doi:10.4271/2015-01-0620.

23. Hamersma, H. A. (2017) A comparison of quarter, half and full vehicle modesl with experimental ride comfort data. In: *Proceedings of the ASME 2015 International Design Engineering Technical Conferences & Computers and Information in Engineering Conference*. ASME, Boston, Massachusetts, USA, pp 1–7.

24. Loprencipe, G., & Zoccali, P. (2017) Use of generated artificial road profiles in road roughness evaluation. *Journal of Modern Transportation*, *25*, 24–33. doi:10.1007/s40534-017-0122-1.

25. Mercedes-Benz (2018) The citaro - technical data and dimensions. https://www.mercedes-benz.com.sg/content/singapore/mpc/mpc_singapore_website/enng/home_mpc/bus/home/new_buses/models/regular_service_busses/citaro/technical_data.html. Accessed 5 Oct 2018.

26. Kat, C. J., & Els, P. S. (2009) Interconnected air spring model. *Mathematical and Computer Modelling of Dynamical Systems*, *15*, 353–370. doi:10.1080/13873950902955783.

27. Firestone (2014) Engineering manual and design guide. *Firestone*.

28. The Transtec Group (2016) ProVal 3.6: profile viewing and analysis software. Austin, Texas.

29. ISO2631-1 (1997) Mechanical vibration and shock - evaluation of human exposure to whole-body vibration (part 1: general requirements). *International Organization for Standardization*, Switzerland.

30. Weik, M. H. (2001) Nyquist theorem. In: *Computer Science and Communications Dictionary*. Springer US, Boston, MA, p 1127.

31. Derek Rowell (2004) Review of first-order linear system transient response. *MIT Dep. Mech. Eng.*

32. Sayers, M. W. (1989) Two quarter-car models for defining road roughness: iri and hri. *Transportation Research Record*, 165–172.

33. Capuruço, R., Hegazy, T., Tighe, S., & Zaghloul, S. (2005) Full-car roughness index as summary roughness statistic. *Transportation Research Record*, *1905*, 148–156. doi:10.3141/1905-17.

34. Kowarska, I., Korta, J., Kuczek, K., & Uhl, T. (2014) Fully equipped dynamic model of a bus. *Shock and Vibration*, *2014*,. doi:10.1155/2014/201952.
35. Teixeira, R. R., Moreira, S. R. D. S., & Tavares, S. M. O. (2015) Multibody dynamics simulation of an electric bus. *Procedia Engineering*, *114*, 470–477. doi:10.1016/j.proeng.2015.08.094.
36. Sekulić, D., Rusov, S., Dedović, V., Šalinić, S., Mladenović, D., & Ivković, I. (2018) Analysis of bus users' vibration exposure time. *International Journal of Industrial Ergonomics*, *65*, 26–35. doi:10.1016/j.ergon.2018.01.017.

APPENDIX A: Bus parameters

Table A1: Bus model parameters human & seat

| Parameter	Acronym	Value [Unit]	Parameter	Acronym	Value [Unit]
Human mass	m_{H1} / m_{H2}	70 [kg]	Equivalent seat stiffness	k_{H1} / k_{H2}	10,000 [N/m]
			Equivalent seat damping	d_{H1} / d_{H2}	330 [Ns/m]
Distance COM (sprung mass) to seat 1 (x-direction)	a_{Hx1}	3.71 [m]	Distance COM (sprung mass) to seat 2 (x-direction)	a_{Hx2}	2.09 [m]
Distance COM (sprung mass) to seat 1 (y-direction)	b_{Hy1}	0.64 [m]	Distance COM (sprung mass) to seat 2 (y-direction)	b_{Hy2}	0.60 [m]

Table A2: Bus model parameters: sprung mass

| Parameter	Acronym	Value [Unit]	Parameter	Acronym	Value [Unit]
Permitted gross weight	m_{PGW}	19,000 [kg]	Kerb weight	m_{KW}	10,770 [kg]
Moment of Inertia (y-axis)	IB_{Sy}	150,000 [kg m^2]	Moment of Inertia (x-axis)	IB_{Sx}	13,000 [kg m^2]
Vehicle width	b_{veh}	2.5 [m]	Wheelbase	l_{WB}	5.8 [m]
Spring coefficient front suspension (max./min. load)	k_{S1}	332,409 [N/m] 189,418 [N/m]	Equivalent spring coefficient rear suspension (max./min. load)	k_{S2}	664,818 [N/m] 378,836 [N/m]
Damping coefficients front suspension (max./min. load)	d_{S1}	50,220 [Ns/m] 29,674 [Ns/m]	Equivalent damping coefficient rear suspension (max./min. load)	d_{S2}	71,023 [Ns/m] 41,965 [Ns/m]
Distance front axle to COM (sprung mass) (x-direction)	a_{Sx1}	3.71 [m]	Distance rear axle to COM (sprung mass) (x-direction)	a_{Sx2}	2.09 [m]
Distance front suspension to COM (sprung mass)	b_{Sy1}	0.64 [m]	Distance rear suspension to COM (sprung mass)	b_{Sy2}	0.60 [m]

Table A3: Bus model parameters suspension & unsprung mass

Parameter	Acronym	Value [Unit]	Parameter	Acronym	Value [Unit]
Unsprung mass front	m_{U1}	662 [kg]	Unsprung mass rear	m_{U2}	1333 [kg]
Tyre stiffness front axle	k_{U1}	1,000,000 [N/m]	Equivalent tyre stiffness rear axle	k_{U2}	2,000,000 [N/m]
Tyre damping front axle	d_{U1}	150 [Ns/m]	Equivalent tyre damping rear axle	d_{U2}	300 [Ns/m]
Distance front tyre to COM (unsprung mass)	b_{U1}	1.39 [m]	Distance rear tyre to COM (unsprung mass)	b_{U2}	1.02 [m]
Moment of Inertia front axle (x-axis)	IB_{Ux1}	350 [kg m^2]	Moment of Inertia rear axle (x-axis)	IB_{Ux2}	620 [kg m^2]
Tyre contact length	$l_{contact}$	0.3045 [m]			

APPENDIX B: Simulink (a) 3-DOF QBM, (b) 6-DOF HBM and (c) 9-DOF FBM
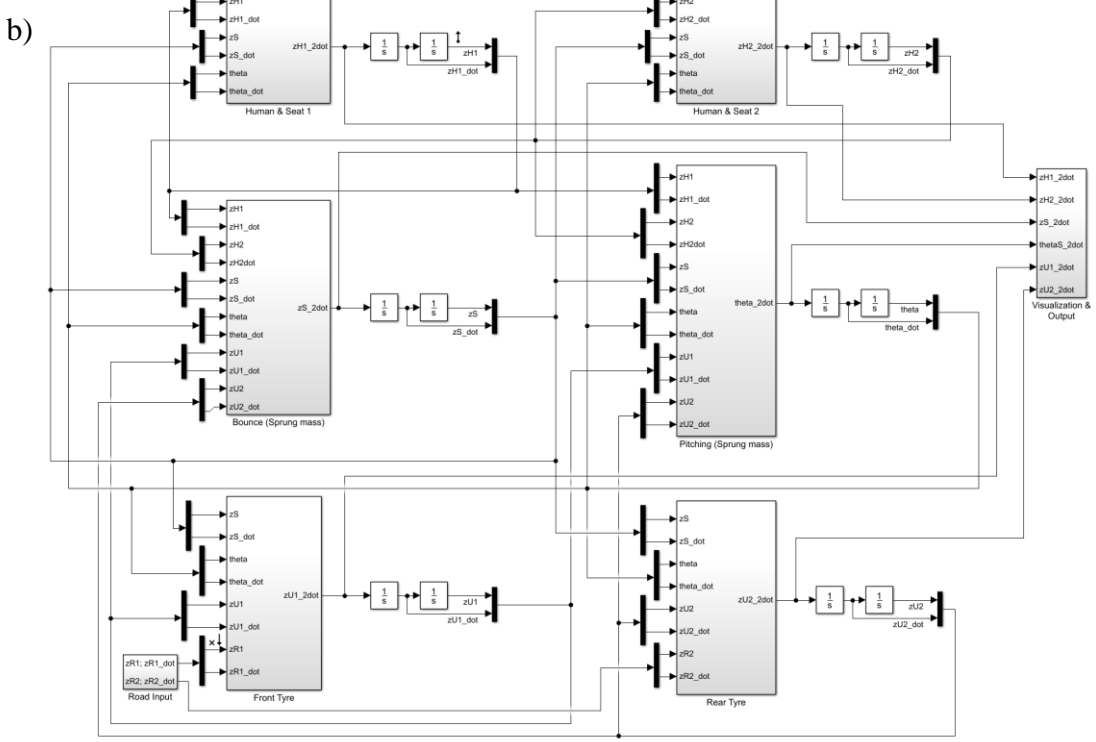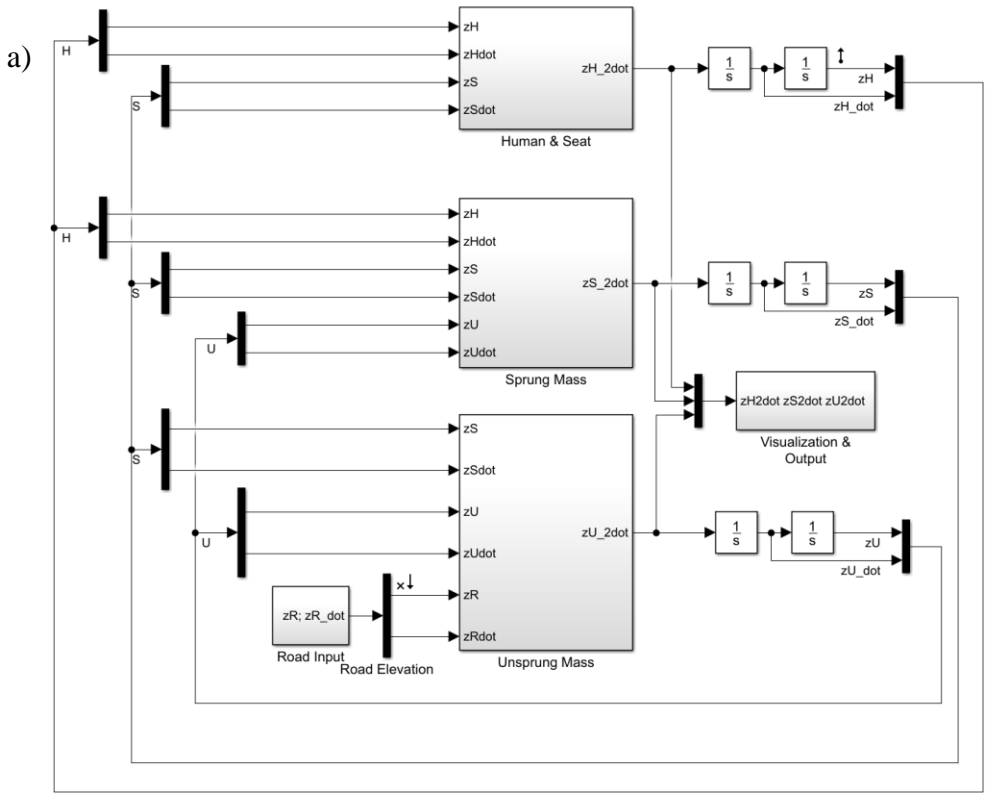
c)
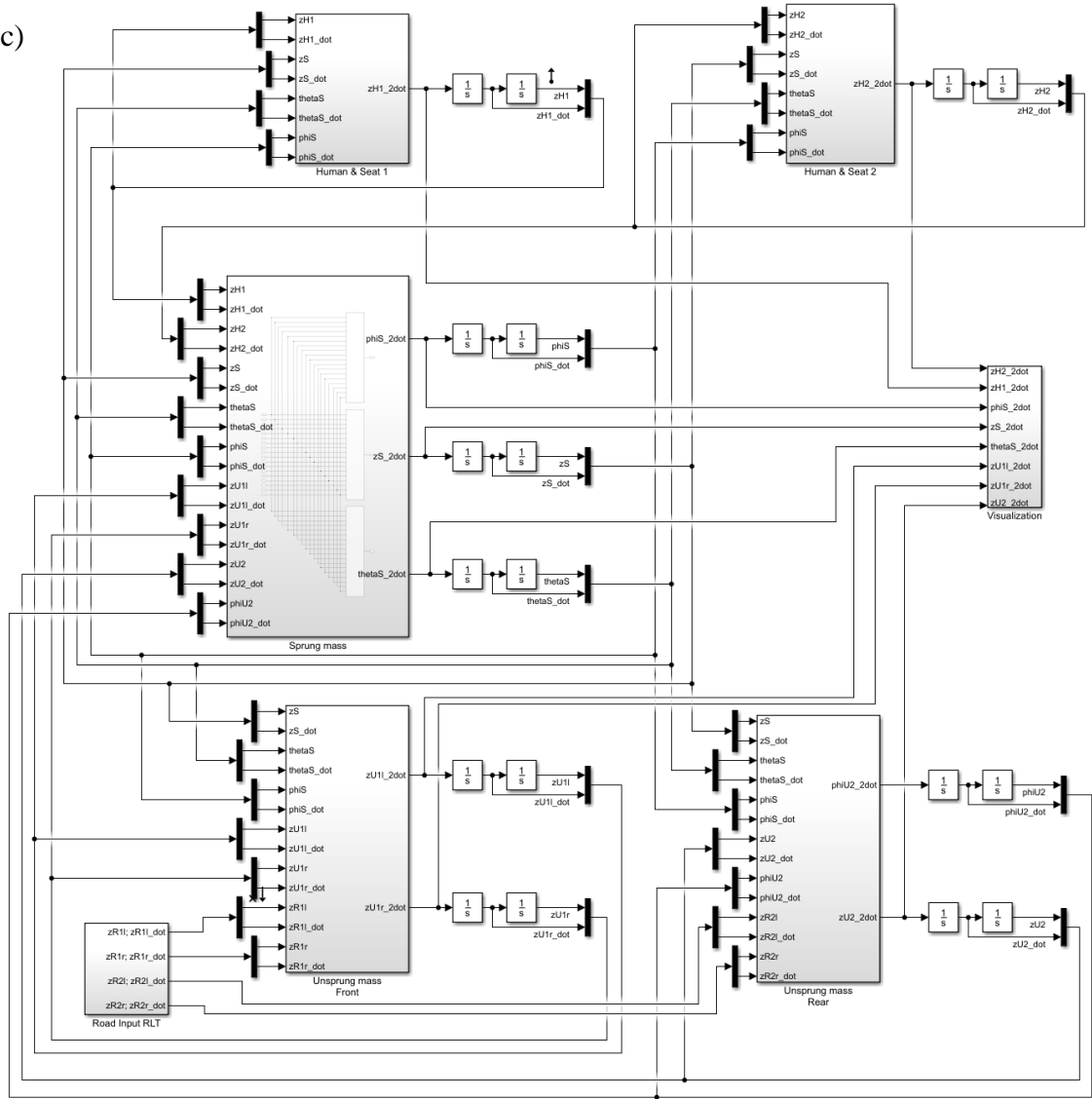
Appendix 3: Paper III

Nguyen, T., Lechner, B., Wong, Y.D. & Jun, Y. T. (2019). Bus ride index - a refined approach to evaluating road surface irregularities. *Road Material and Pavement Design*, doi: 10.1080/14680629.2019.1625806.

Bus Ride Index – a refined approach to evaluating road surface irregularities

Teron Nguyen, Bernhard Lechner, Yiik Diew Wong & Jun Yew Tan

Published online: 12 Jun 2019.

Submit your article to this journal ☑

View Crossmark data ☑

Taylor & Francis
Taylor & Francis Group

Check for updates

Bus Ride Index – a refined approach to evaluating road surface irregularities

Teron Nguyen [a*], Bernhard Lechner [b], Yiik Diew Wong [c] and Jun Yew Tan [d]

[a]*TUMCREATE Ltd, Singapore, Singapore;* [b]*Institute of Road, Railway and Airfield Construction, Technische Universität München (TUM), München, Germany;* [c]*School of Civil and Environmental Engineering, Nanyang Technological University (NTU), Singapore, Singapore;* [d]*Samwoh Innovation Centre, Singapore, Singapore*

The road surface quality can be assessed with ride comfort indices because of their strong correlation. Many studies on ride comfort have focused on cars and trucks, but their results are not applicable to buses, which are characterised by inherently different vehicle dynamics. In this study, a quarter-vehicle simulation concept was used to develop a Bus Ride Index (BRI) for evaluating the effect of road irregularities on bus ride comfort. A BRI model was developed to optimise ride comfort depending on seat configuration and air suspension and validated according to technical data. The results show a good regression relationship between BRI and the International Roughness Index (IRI). New IRI thresholds with regard to ride comfort and bus operating speeds were established to serve as a benchmark to develop better pavement maintenance strategies for bus lanes and to estimate road quality based on acceleration data.

Keywords: ride comfort; road longitudinal profile; quarter-car simulation; bus lane; International Roughness Index

1. Introduction

Road roughness (e.g. unevenness, irregularities) has a strong impact on ride comfort; vehicles cannot operate at high speeds when traversing rough surfaces. Numerous research studies have evaluated the effect of road roughness on vehicle performance and hence ride quality by using quarter-vehicle (Khavassefat, Jelagin, & Birgisson, 2015; Prem, Ramsay, & McLean, 2000; Sayers, 1995), half-vehicle (Múčka & Granlund, 2012; Sayers, 1989) and full-vehicle models (Cantisani & Loprencipe, 2010; Capuruço, Hegazy, Tighe, & Zaghloul, 2005) to represent vehicle system. Each representation has its advantages and disadvantages; the quarter-car simulation (QCS) is the simplest model and is frequently used in many studies. Nonetheless, all vehicle dynamic models to evaluate road roughness so far have been focused on car and truck applications (Múčka, 2016a); therefore, their results are not directly applicable to the vehicle dynamics of buses.

Bus transit can be considered as a form of heavy transport that causes heavy damage to the road surface/pavement. In many cities around the world, a bus rapid transit (BRT) system requires a strong pavement structure and more frequent maintenance than regular car lanes. Global BRT-Data (BRT + Centre of Excellence and EMBARQ, 2018) reported that BRT lanes around the

---

*Corresponding author. Email: teron.nguyen@tum-create.edu.sg

world are surfaced by Portland cement concrete (35%; around 1441 km) or asphalt concrete (65%; around 2635 km). Dense bus networks in cities such as Singapore, London and Hong Kong are continuously loaded with a high number of buses.

Even though buses operate at lower speeds than cars or trucks and bus lanes are maintained well, there continues to be concerns and interest in bus ride comfort in relation to road surface irregularities. The vibrations from road irregularities are transmitted to the bodies of drivers and passengers via their seats, although bus drivers typically have more comfortable seats than passengers. The conventional International Roughness Index (IRI) cannot represent passenger ride comfort directly and is not applicable to lower-speed road categories. This motivated Cantisani and Loprencipe (2010) and Yu, Chou, and Yau. (2006) to develop speed-related ride quality thresholds based on IRI for car rides. However, there have been no studies on bus dynamics or whether their work (Cantisani & Loprencipe, 2010; Yu et al., 2006) applies to bus lanes. Hence, the present study aimed to address this gap in knowledge and meet the following objectives:

- To develop a vehicle dynamics model by calibrating a Bus Ride Index (BRI) for evaluating the bus lane surface roughness and accurately capturing bus passenger ride comfort, and
- To propose new IRI thresholds conditioned on BRI at lower speeds that are more appropriate for bus operation, which will be beneficial for pavement monitoring and maintenance to ensure bus passenger ride comfort.

BRI was analysed for both artificial and field-measured road profiles to find the regression relationships between BRI and IRI.

The remainder of the paper is structured as follows. First, the relevant scientific literature is summarised. The fundamentals of BRI and its characteristics are then described. Road profiles for BRI analysis (i.e. artificial and measured road profiles) are presented. Findings on the relationship between IRI and BRI at different speed levels and the advantages of BRI are discussed. The conclusion sums up the study.

2. Literature review

Existing approaches to evaluate road irregularity can be classified in different categories with various indices (Ueckermann & Oeser, 2015): geometry in the distance domain (e.g. standard deviation, energy content), geometry in the spectral domain (e.g. power spectral density), effect in the distance domain (e.g. IRI, ride number), and geometry and effect in the distance domain (e.g. profilograph, bump integrator). Each approach is related to a specific measurement equipment or specific numerical calculation method. Measurement approaches consider the dynamic response of measurement devices or vehicle components. Hence, they are more appropriate for evaluating specific vehicle-dedicated lanes and the effects related to such vehicles (e.g. ride quality). Numerical calculation methods are more suitable for investigating the road surface itself regardless of the vehicle dynamics.

Among the vehicle response approaches, IRI is recognised and used worldwide as a standard index for road roughness evaluation (Múčka, 2017). It is based on a two-degree-of-freedom (DOF) QCS. The comfortable ride of a car driver has been proposed as the reference roughness at various IRI levels. IRI can be interpreted as the output of an idealised response-type measurement system known as the golden-car driving at 80 km/h. This is expressed by accumulated suspension motions over the distance travelled (e.g. mm/m). The algorithm was proposed by Sayers (1995) and has also been implemented in the proposed standard CEN-PREN 13036-5 (2015) and ASTM E1926-08 (2015).

Given its simplified model, IRI includes several disadvantages, such as being specific to car dynamics, a single calculated speed level of 80 km/h, and an indirect relation to ride comfort (Bridgelall, 2014; Cantisani & Loprencipe, 2010; Múčka, 2016a). Hence, several other approaches to quantifying road irregularity have been developed based on QCS to include other vehicle types (e.g. trucks) and effects (e.g. ride comfort). Some examples are the Truck Ride Index (TRI) for truck driver comfort in cabin (Prem et al., 2000), Heavy Articulated Truck Index (HATI) that accesses poor ride to occupants of heavy articulated trucks (Hassan, McManus, & Cossens, 2006), and Longitudinal Evenness Index (LWI) for evaluating ride comfort, ride safety, dynamic load of road and cargo (Ueckermann, 2002). Yu et al. (2006) developed speed-related ride quality thresholds using IRI for local street application, as given in Table 1. Table 2 presents another IRI threshold at low operating speeds, where similar ranges of values can be observed for vehicle speeds of 30–60 km/h. Cantisani and Loprencipe (2010) conducted this study by using an 8-DOF full-car simulation.

Regarding passenger ride comfort, studies on human subjects have shown that the human body mass has a vibration resonance frequency of 4–8 Hz at which it is most sensitive to acceleration. To include all possible effects of vibration on health, comfort and perception, ISO2631-1 (1997) considers a frequency range of 0.5–80 Hz. The weighted root-mean-square (RMS) acceleration is calculated as follows:

$$a_w = \left[\frac{1}{T} \int_0^T a_w^2(t) \, \mathrm{d}t \right]^{1/2} \tag{1}$$

where $a_w(t)$ is the weighted acceleration as a function of time (m/s^2) and T is the duration of the measurement (s).

The frequency-weighting curves in the vertical direction are applied to calculate the frequency-weighted RMS vertical acceleration (a_{wz}) related to road roughness excitation. Table 3 gives the suggested scale of a_{wz} according to different levels of user ride comfort on public transport vehicles, which is similar to that suggested by British Standard BS6841:1987 (1999). These recommendations have been widely used in numerous studies to evaluate passenger ride comfort

Table 1. IRI thresholds at different speeds 10–60 km/h (Yu et al., 2006).

Ride quality	IRI threshold at different speeds [m/km]					
	10 km/h	20 km/h	30 km/h	40 km/h	50 km/h	60 km/h
Very good	< 11.44	< 5.72	< 3.80	< 2.86	< 2.28	< 1.90
Good	11.44–17.99	5.72–8.99	3.80–5.99	2.86–4.49	2.28–3.59	1.90–2.99
Fair	18.00–22.79	9.00–11.39	6.00–7.59	4.50–5.69	3.60–4.54	3.00–3.79
Mediocre	22.80–32.32	11.40–16.16	7.60–10.80	5.70–8.08	4.55–6.25	3.80–5.40
Poor	> 32.32	> 16.16	> 10.80	> 8.08	> 6.25	> 5.40

Table 2. IRI thresholds at different speeds 30–80 km/h (Cantisani & Loprencipe, 2010).

Ride quality	IRI threshold at different speeds [m/km]					
	30 km/h	40 km/h	50 km/h	60 km/h	70 km/h	80 km/h
Very good	< 4.17	< 3.41	< 2.98	< 1.86	< 1.60	< 1.20
Good/fair	4.17–8.34	3.41–6.83	2.98–5.95	1.87–3.73	1.60–3.20	1.42–2.84
Mediocre	8.34–11.92	6.83–9.75	5.95–8.51	3.73–5.33	3.20–4.58	2.84–4.06
Poor	> 11.92	> 9.75	> 8.51	> 5.33	> 4.58	> 4.06

Table 3.   RMS acceleration and levels of comfort according to ISO 2631-1.

RMS vertical acceleration a_{wz} (m/s^2)	Levels of comfort
Less than 0.315	Not uncomfortable
0.315–0.63	A little uncomfortable
0.5–1.0	Fairly uncomfortable
0.8–1.6	Uncomfortable
1.25–2.5	Very uncomfortable
Greater than 2.0	Extremely uncomfortable

with regard to vehicle dynamics subjected to road excitation (Cantisani & Loprencipe, 2010; Múčka, 2016b; Prem & Ayton, 2005).

Múčka (2016a) summarises current approaches, which include four QCS models (SEI, TRI, LWI, HI) related to ride comfort evaluation and three QCS models (PQI, HATI, VRI) used to measure dynamic suspension load, as given in Table 4. The QCS models are mainly differentiated by the vehicle type, either car (SEI, LWI, HI, PQI, VRI) or truck (TRI, LWI, HATI). Some were derived from IRI model. For urban buses, the ride comfort is crucial because a single vehicle can carry about 100 passengers, which can lead to public concern if any uncomfortable incidents occur because of road irregularities. Increasing bus ride comfort will contribute to the strategy of shifting car users to public transport. A QCS model for buses is necessary to evaluate road surface irregularities associated with ride comfort but has yet to be developed, which was the motivation for the present study.

With regard to bus dynamics, there have been few studies in the literature. Sekulić and Dedović (2011b) used a 3-DOF QCS to evaluate the effects of the stiffness and damping of the suspension system on optimising the vibrational behaviour of a bus. Sekulić, Dedović, Rusov, Šalinić, and Obradović (2013) used a 10-DOF oscillatory bus model to analyse the effects of vibration on the comfort of intercity bus users. However, these models used only one artificially

Table 4.   Summary of road unevenness indices based on QCS (Múčka, 2016a).

No	Unevenness index	Abbreviation	Vehicle model	Velocity (km/h)	Response category
1	Single-number unevenness indicator	SEI	3-DOF QCS car	100 (car); 80 (truck)	- Ride comfort - Ride safety - Road dynamic load - Cargo dynamic load
2	Truck Ride Index	TRI	3-DOF QCS truck	100	Ride comfort
3	Longitudinal Evenness Index	LWI	2-DOF QCS truck; 5-DOF three-axle semi-trailer; 3-DOF QCS car	100 (car) 80 (truck)	- Ride comfort - Ride safety - Road dynamic load - Cargo dynamic load
4	Health Index	HI	2-DOF QCS (IRI)	80	Ride comfort
5	Pavement Quality Index	PQI	2-DOF QCS (IRI)	80	Suspension dynamic load
6	Heavy Articulated Truck Index	HATI	2-DOF QCS truck	100	Suspension dynamic load
7	Vehicle Response Index	VRI	2-DOF QCS (IRI)	Variable	Suspension dynamic load

generated road profile and focused more on the vehicle dynamics instead of evaluating road irregularities. Recently, Sekulić, Dedović, Rusov, Obradović, and Šalinić (2016); Sekulić et al. (2018) built the same full-bus model with MSC.ADAMS and validated it with two road profiles (poor and good asphalt concrete pavement) to establish equal oscillatory comfort zones in which passengers seated in the bus overhang and over the front axle or in the rear overhang and over the rear axle are exposed to a higher level of ride discomfort. These are also the fundamental positions for the proposed BRI in the present study. Overall, there have been limited field surveys on the relationship between a ride comfort index and IRI except for the experimental study by Fichera, Scionti, and Garescì (2007, April), who used three buses (18, 9.46, and 4.6 t) running on 12 public roads to evaluate the driver ride comfort in bus cabins. They also built a 6-DOF half-bus model to represent the system dynamics of an 18 t bus, whose parameters were used as a reference to develop BRI.

In this study, the proposed BRI for road roughness evaluation has several goals:

- to reflect the ride comfort of bus passengers,
- to reflect the speed variation of the bus fleet, and
- to provide a simple calculation procedure.

3. Methodology

A realistic ride comfort index to evaluate road roughness can be obtained by carefully considering the following aspects of vehicle ride dynamics:

- properties of seat dynamics,
- vehicle suspension and associated damping characteristics, and
- human tolerance to whole-body vibrations.

These aspects are considered in the proposed QCS bus model and ride comfort evaluation standard.

3.1. *Development of the BRI QCS bus model*

IRI calculation is based on the rear axle of vehicle-body responses (as illustrated by Cantisani and Loprencipe (2010); Sayers (1998)). IRI can be considered as an indirect indicator of the ride quality, which is not related to human tolerance, seat configuration, and seat properties. In contrast, the proposed BRI takes the occupants vibration response to the rear axle as the ride comfort index. A 3-DOF QCS is proposed for BRI that includes a 2-DOF quarter-bus model and 1-DOF human and seat model, as shown in Figure 1. Instead of the driver seat, which is equipped with a pneumatic elastic suspension and shock absorber, BRI considers a passenger seat, which has higher stiffness and less damping from hard polyurethane foam. The selected parameters are described below; available bus data from bus manufacturers were used (gross vehicle weight, axle weight, air suspension type, and specifications) by referencing previous studies on bus dynamics (passenger weight, seat stiffness and damping, tire stiffness, and damping). Compared to other studies, the technical parameters for BRI consider a comfortable ride for bus passengers, as given in Table 5.

- Sprung and unsprung mass:
  The bus parameters of the 2-DOF quarter-bus model were referenced from the existing bus fleet in Singapore; technical specifications were available for the Volvo B9L,
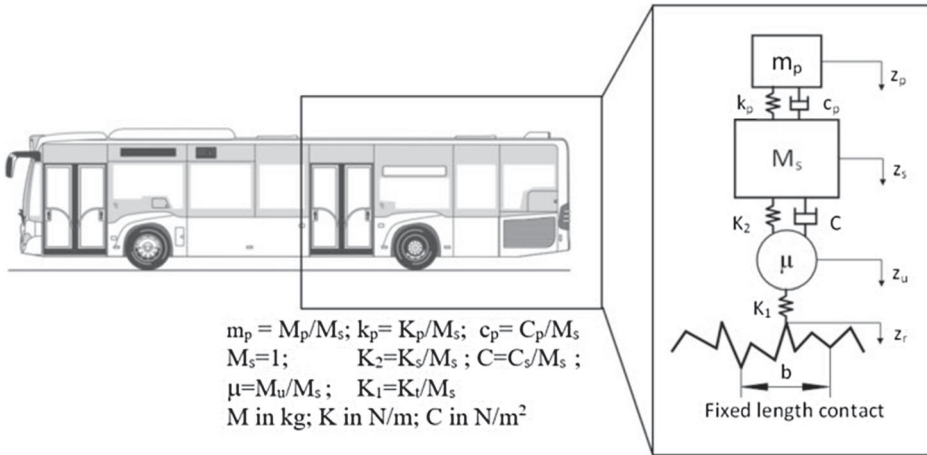
Figure 1.   3-DOF QCS for BRI based on Citaro bus model.

Mercedes Citaro, and MAN NL323F but unavailable for Volo B7RLE and Scania K230UB. These are either low-floor or low-entry buses for urban areas and have similar dimensions and dynamics characteristics. Among these bus types, only the Mercedes Citaro (Mercedes-Benz, 2018) provided enough technical data for reference. This single-decker bus model was used for simulation purposes to build the BRI QCS. The maximum bus weight is 19,000 kg (including the chassis, axles, tyres, wheels, drive train, passengers, interior, and cowlings), while an empty bus weighs 10,770 kg. The bus weight is not distributed evenly; the front axle carries one-third of the gross vehicle weight, while the rear axle carries two-thirds. For BRI, a sprung mass was proposed in the case of a fully loaded bus.

- Suspension and damping:
The Mercedes Citaro bus is equipped with an independent front axle system (RL 82 EC) and rigid rear axle system (AV 133); both are manufactured by ZF GmbH (2009). For the 2-DOF model, only the rear axle parameters are considered. The suspension system is an air spring for ordinary buses in the city, and the double convoluted spring #22 was chosen from the Firestone catalogue (Firestone, 2014) and Enviro 500 bus specifications Alexander (2014). The dynamic spring rate is calculated based on the following equation from Firestone:

$$k = \left[\left[p_{required} + 14.7 \right] \left[A_c \left(\frac{V_1}{V_c} \right)^{1.38} - A_e \left(\frac{V_1}{V_e} \right)^{1.38} \right] - 14.7 \left(A_c - A_e \right) \right] \quad (2)$$

where V_1 is the internal air spring volume (in^3) at the design height, A_e is the effective area (in^2) 0.5 in above design height, A_c is the effective area (in^2) 0.5 in below design height, V_e and V_c are the corresponding inner air volume (in^3), $p_{required}$ is the required inflation pressure (lbs/in^2) ($p_{required} = load_{current}/A_{eff}$ and $A_{eff} = load_{max,default}/p_{default}$), $load_{max,default}$ is the maximum static load (lbs) at default pressure per air spring, and $p_{default}$ is the default pressure (lbs/in^2).

For the damping parameter, a simple approximation of a digressive damping curve has been proposed (Fakultaet fuer Maschinenwesen, 2018; Jazar, 2005) in which the damping ratio for passenger cars should be between 0.25 and 0.3 for the best compromise between safety and comfort while favouring ride comfort. The equivalent stiffness and

Table 5. Parametric review and analysis for quarter-bus model at the rear axle.

	Unit	2-DOF quarter bus[a]	6-DOF half bus 18t[b]	3-DOF quarter bus[c]	10-DOF full bus 18t[d]	65-DOF full bus[e]	Proposed BRI (bus 19t)
Effective mass of seat and passenger	kg	n/a	n/a	100	90	70	70
Seat suspension stiffness	N/m	n/a	n/a	25,000	40,000	20,000	10,000
Seat suspension damping	Ns/m	n/a	n/a	1000	220	220	330
Sprung mass	kg	4000	4355	4500	5300	n/a	5600
Suspension stiffness (equivalent)	N/m	320,000	300,000	300,000	408,650	n/a	664,800
Suspension damping (equivalent)	Ns/m	10,000	5000	20,000	45,973	n/a	63,800
Unsprung mass	kg	550	250	500	677	n/a	660
Tire stiffness (equivalent)	N/m	1,700,000	1,000,000	1,600,000	2,000,000	2,000,000	2,000,000
Tire damping (equivalent)	Ns/m			150	300	300	300

[a]Agostinacchio, Ciampa, and Olita (2014).
[b]Fichera et al. (2007, April).
[c]Sekulić and Dedović (2011a).
[d]Sekulić et al. (2013).
[e]Sekulić et al. (2016), n/a: not available.

damping values of the air suspension were doubled after calculation to represent the dual-wheel rear axle.

- Tyre parameters:
  The Mercedes Citaro bus is equipped with tires and wheels with the dimensions of 275/70 R22.5. Because of their larger diameters and higher axle loads, bus tyres have a larger contact area than passenger car tyres. Gillespie, Karamihas, Sayers, and Hansen (1992, August) suggested using a filter with a length of 304.8 mm (1 ft) to represent a 11R22.5 heavy-duty truck tyre. According to the stated axle loads and suggested tyres by ZF Friedrichshafen AG, a single-decker bus can be compared to a two-axle straight truck with the above tyres. Therefore, the base length of the moving average filter was set to 0.304 m. The tire stiffness and damping were referenced from (Sekulić & Dedović, 2011b; Sekulić et al., 2013) because they had the only available data. The equivalent tire stiffness and damping value were doubled to represent the dual-wheel rear axle.

- Human seat model:
  For the passenger 1-DOF seat model, Patten, Sha, and Mo (1998); Wei and Griffin (1998) demonstrated that the stiffness and damping of a foam cushion are dependent on the load and excitation level. The nonlinearity is accounted for by the preload-dependent parameters of stiffness and damping. Note that those values are for a vehicle passenger foam seat and that the stiffness of urban bus seats may be higher than the proposed values. On the other hand, Sekulić et al. (2016)'s parametric design-of-experiment study showed that the optimal stiffness (K_p) and damping (C_p) for the lowest a_{wz} value of a passenger seat are $K_p = 10,000$ N/m and $C_p = 330$ Ns/m. Hence, these parameters are proposed for BRI model.

Table 5 presents the calculated and proposed BRI parameters based on the above analysis on vehicle dynamics. BRI has similar parameters to other bus models from the literature. For the specific Citaro bus model, its axle configuration, air spring stiffness, and damping are calculated. Figure 1 shows the proposed BRI QCS model with normalised values based on the sprung mass (Ms). Table 6 compares its values to those of IRI and TRI. The calculated undamped natural frequencies of the seat and passenger, sprung mass, and unsprung mass were 1.93, 1.47, and 10.14 Hz, respectively, and the calculated damped natural frequencies were 1.89, 1.26, and 10.14 Hz, respectively. These computed frequencies are close to the oscillation frequencies of a regular bus service (Sekulić & Dedović, 2011b); the air spring helps maintain a nearly constant sprung mass natural frequency (Cao, Song, & Ahmadian, 2011). The tire damping effect is minimal, so it can be ignored in the simulation and calculation. The passenger seat damping effect is also small compared to that of the driver seat from TRI. Table 6 describes all BRI parameters that differ from IRI and TRI. Bus speeds are much lower than the car and truck speeds for calculation; $v = 40$ km/h is the operating speed on urban roads and $v = 60$ km/h is the operating speed on highways. These values are proposed based on field observations and measurements.

The vertical vibration of a bus passenger can be found by solving the differential equation of motion in a matrix expression:

$$[M]\{\ddot{z}\} + [C]\{\dot{z}\} + [K]\{z\} = [A]\{z_r\} \tag{3}$$

where $[M]$, $[C]$, and $[K]$ are the symmetric mass, damping and stiffness matrices; $[A]$ is the stiffness matrix of the input from road roughness; $\{z\}$, $\{\dot{z}\}$, and $\{\ddot{z}\}$ are the column vectors of the generalised coordinates, velocities and acceleration, respectively; $\{z_r\}$ is the column vector of the road roughness vertical motion; and $z = [z_u, z_s, z_p]^T$.

Table 6. Parameter values for BRI compared to IRI and TRI.

Description of parameter	Variables	Value of different vehicle types			Unit
		IRI-car	TRI-truck	BRI-bus	
Effective mass of seat and driver/passenger[a]	m_p		0.067	0.01	—
Seat suspension stiffness[a]	k_p		8.26	1.78	s^{-2}
Seat suspension damping[a]	c_p		0.7	0.06	s^{-1}
Sprung mass[a]	M_s	1	1	1	—
Suspension stiffness[a]	K_2	63.3	250	118.12	s^{-2}
Suspension damping[a]	C	6	30	11.34	s^{-1}
Unsprung mass[a]	μ	0.15	0.15	0.12	—
Tire stiffness[a]	K_1	653	400	355.37	s^{-2}
Tire enveloping (base length)	b	250	300	304	mm
Travel speed	v	80	60 (urban) 100 (rural)	40 (urban) 60 (highway)	km/h
Ride comfort criteria			BS6841:1997	ISO 2631-1	

[a]Values have been normalised by the sprung mass, Ms.

The differentiation of the IRI, TRI, and BRI models can be based on the transfer functions (TFs) of the vehicle responses for both the temporal and spatial frequencies. Fundamentally, IRI is calculated based on the displacement of the sprung mass to the unsprung mass, whereas TRI and BRI consider the response of the sprung mass to road profile inputs. The vibration of the sprung mass is then transferred to a seat and the human body. The similarity and difference between the three TF curves are shown in Figure 2 based on the parameters in Table 6.

In Figure 2(a), the dominant peak of the IRI-car response is near 1 and 10 Hz, while the TRI-truck body bounce frequency is near 2.57 Hz, and the BRI-bus response is near 1.54 Hz. TFs of BRI-bus are almost unchanged over different passenger loading factors ($n = 0--1$) because of the nonlinear dynamics of the air suspension. Figure 2(b) shows a similar trend for the wavenumber: the IRI-car is sensitive to the road roughness for a wavelength range of 30–1 m (a wavenumber range of 0.03–1 cycles/m), while the TRI-truck and BRI-bus are sensitive to wavelengths greater than about 3 m (wavenumber of 0.33 cycles/m). These wavenumber values are equivalent to a magnitude of 0.1 abs. However, the BRI and TRI transfer function gains/magnitude show a clear difference; the gains are higher for BRI from 0.01 to 0.08 cycles/m and higher for TRI from 0.08 to 0.33 cycles/m. The transfer functions for the spatial frequency were calculated at a travel speed of 80 km/h for comparison purposes only. During normal operation, buses travel at much lower speeds, and the stiffer and less damped seat configuration for the BRI calculation results in a greater differentiation between the TRI and BRI outputs.

3.2. *Validation of the BRI model*

To validate the BRI QCS model, field measurements were conducted by using a seat-pad accelerometer (SV100A, Svantek), which was placed on a seat cushion (Figure 3) and preloaded with a 70 kg human, along a 2 km bus lane of Jalan Bukit Merah Street in Singapore. The bus lane longitudinal profile was scanned by using a multi-laser road profiler with a sampling interval of 25 mm and GPS data at 1 Hz. The SV100A seat-pad accelerometer was settled on a seat cushion above the rear axle, controlled wirelessly by a smartphone, and collected vibration

(b)

(c)
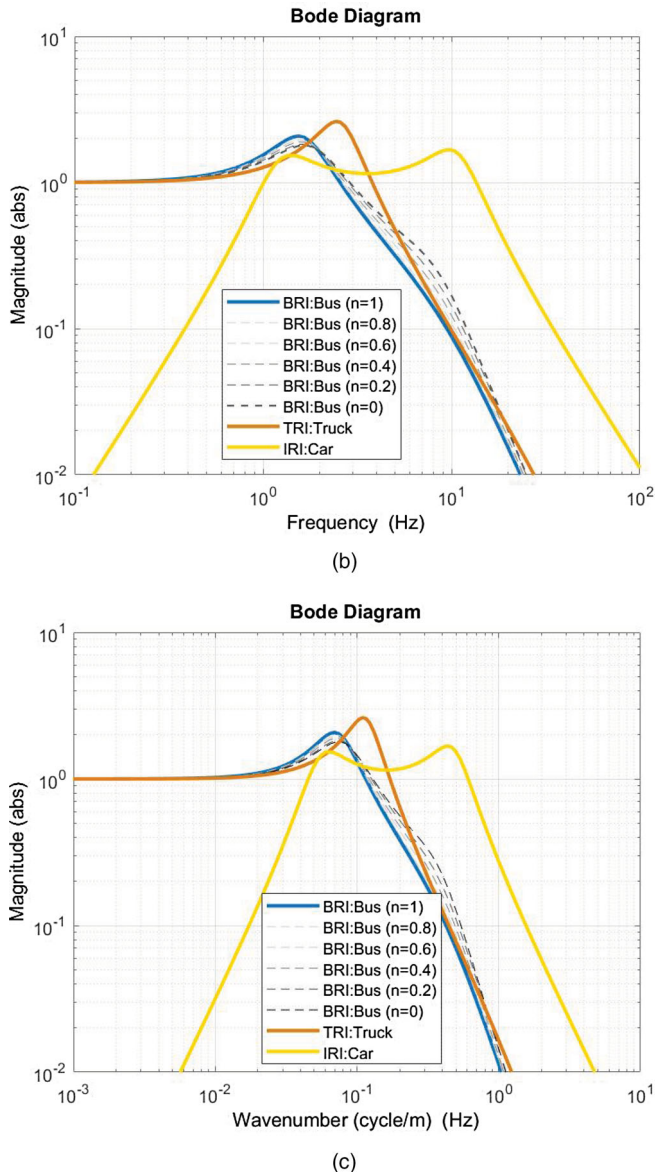
Figure 2.   Transfer functions (TFs) of sprung mass over road input for BRI and TRI, and sprung mass over the unsprung mass of IRI. BRI TFs are similar at different passenger loading factors ($n = 0 - 1$). (a) As functions of temporal frequency. (b) As functions of spatial frequency (travel speed of 80 km/h).

data at a frequency of 750 Hz to calculate a_{wz}, and GPS data at 1 Hz. Bus lanes IRI was 3.5–4.8 m/km. To include different bus models in the city, the measurement was also conducted for the single-decker bus model MAN NL323F driving on the same road segments.

The BRI QCS model was simulated in MATLAB/Simulink using the same road input and bus speed from the field measurement. The developed numerical algorithm included the speed changes along the bus route and matched GPS locations between road profiles and bus vibration measurements. There were 12 road sections with different lengths for an average

Figure 3. Field measurement setup. (a) On-cushion Svantek SV100A. (b) The Citaro single-decker bus. (c) The MAN NL323F.
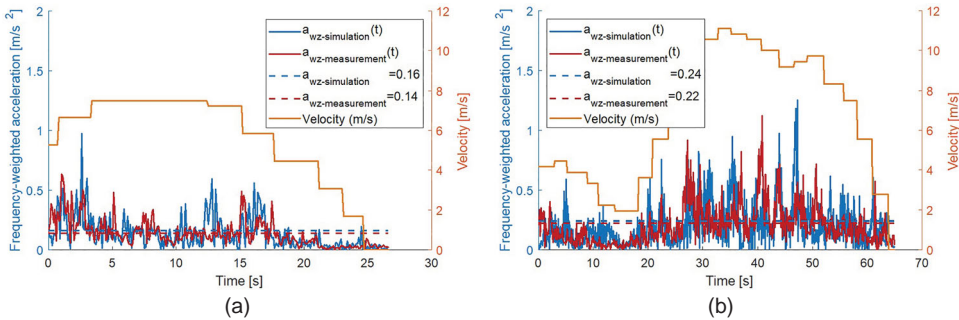
Figure 4. Comparison of the simulated and measured $a_{wz}(t)$ at different road sections. (a) Smooth road (Section 8). (b) Rough road (Section 5).

ratio of $a_{wz\_simulation}/a_{wz\_measurement} = 1.02$ (std = 0.13). Figure 4 compares of time-series frequency-weighted acceleration ($a_{wz}(t)$) and a_{wz} between simulation and measurement at different velocities (m/s); Section 8 was a smooth road and Section 5 was a rough road surface. The graphs show that the simulation output and measurement data matched quite well for different speed changes, especially the peak values. Perfect matching could not be achieved because the speed sampling based on GPS signal did not have a high level of accuracy, and the bus wheel trajectories and road profiles were misaligned.

4. Road profiles for BRI analysis

4.1. *Generation of road profiles*

A road profile is the variation in road elevation with distance as measured by appropriate field devices. If the vertical displacement is assumed to be a centred, homogeneous, and Gaussian function of distance, the road profile can be described as the power spectral density (PSD) of the spatial frequency $G_d(n)$ (m²/cycle/m) or angular spatial frequency $G_d(\Omega)$ (m³/rad). The

roughness profile can be defined as follows:

$$G_d(n) = G_d(n_0) \cdot \left(\frac{n}{n_0}\right)^{-2} \tag{4a}$$

$$G_d(\Omega) = G_d(n_0) \cdot \left(\frac{\Omega}{\Omega_0}\right)^{-2} \tag{4b}$$

Table 7 divides the values of $G_d(n_0)$ and $G_d(\Omega_0)$ according to ISO 8608:2016 (2016) into eight road categories, where their PSDs were calculated based on a spatial frequency n_0 of 0.1 cycles/m and angular spatial frequency Ω_0 of 1 rad/m. The different road classes are illustrated on a log-log scale as straight lines with a constant waviness w of 2 for the lines slope. Múčka (2018) reviewed 27 scientific papers to show that, for simulation purposes, road class A may represent a typical good- or average-quality road (e.g. motorway, expressway, and first-class road), whereas classes B and C may be appropriate for simulating low-quality paved surfaces (second- and third-class roads or local highways). In Germany, road class B is often considered as a basic standard for road roughness evaluation, in which $G_0 = 1, 3$ and $9 \, \text{cm}^3$ are equivalent to the target value, warning value and threshold value, respectively (FGSV-489, 2006; Maerschalk, Ueckermann, & Heller, 2011; Ueckermann & Oeser, 2015).

With ISO 8608:2016, road profiles can be generated from different mathematical algorithms once all necessary parameters are known. Agostinacchio et al. (2014) presented a widely used equation for generating artificial profiles:

$$h(x) = \sum_{i=0}^{N} \sqrt{\Delta n} \cdot 2^k \cdot 10^{-3} \cdot \left(\frac{n_0}{i \cdot \Delta n}\right) \cdot \cos(2\pi \cdot i \cdot \Delta n \cdot x + \varphi_i) \tag{5}$$

where x is the abscissa variable from 0 to L; $\Delta n = 1/L$; $n_{\max} = 1/B$; $N = n_{\max}/\Delta n = L/B$, B is the sampling interval; k is a constant value depending on the ISO road profile classification and is assumed to be an integer value from 3 to 9 corresponding to classes A–H; $n_0 = 0.1$ cycles/m, and φ_i is a random phase angle following a uniform probabilistic distribution within $0–2\pi$.

Equation (5) was used to generate 200 road profiles in MATLAB as the input for vehicle dynamics simulations. The road surface profiles Figure 5 were very good (ISO A–B class with $h_{\max} = 15 \, \text{mm}$), good (ISO B–C class with $h_{\max} = 25 \, \text{mm}$), average (ISO C–D class with $h_{\max} = 50 \, \text{mm}$), and poor (ISO D–E class with $h_{\max} = 100 \, \text{mm}$). Road classes E–H primarily represent rough unpaved roads which were not present in the network covered in this study. On the other

Table 7. $G_d(n_0)$ and $G_d(\Omega_0)$ according to ISO 8608.

Road class	$G_d(n_0) \, (10^{-6} \, \text{m}^3)$		$G_d(\Omega_0) \, (10^{-6} \, \text{m}^3)$	
	Lower limit	Upper limit	Lower limit	Upper limit
A	–	32	–	2
B	32	128	2	8
C	128	512	8	32
D	512	2048	32	128
E	2048	8192	128	512
F	8192	32,768	512	2048
G	32,768	131,072	2048	8192
H	131,072	–	8192	
	$n_0 = 0.1$ cycles/m		$\Omega_0 = 1$ rad/m	
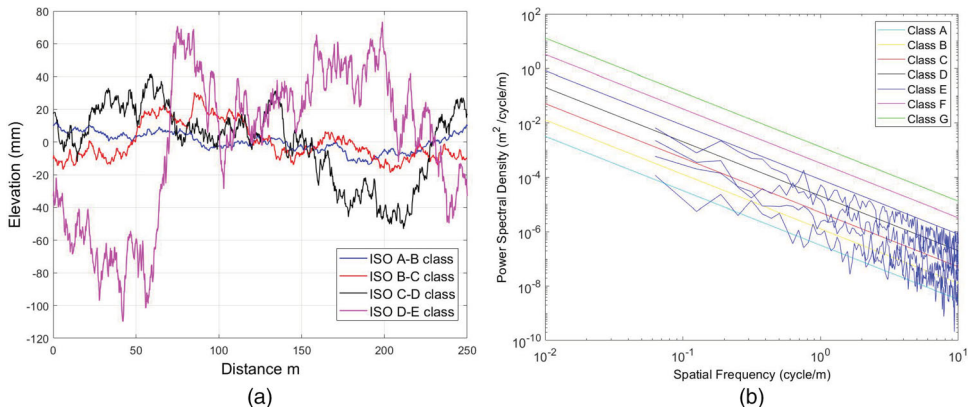
Figure 5.   Examples of four artificial road profiles and their classification. (a) Artificially generated road profiles. (b) Road classification.

hand, since road classes D–H are often associated unpaved roads (Múčka, 2018), only the very good and good road profiles were used to present urban road network in this study.

4.2.   *Field-measured road profiles*

Singapore has a resident population of 5.5 million in a small land area of 719 km^2, bus ridership has a high share of public transit at 3.9 million out of 7.9 million passenger trips per day (PTC, 2016). Figure 6(a) visualises bus lane schemes according to data from Singapore (LTA, 2018) which highlight full-day bus lanes mostly paved with Portland cement concrete in the city centre. Figure 6(b) shows the daily bus volumes generated using the method in (Liu, Zhou, & Rau, 2018). The high daily bus volumes are concentrated along bus lanes, with 1500–3000 buses equivalent to 23–46 million equivalent single axle loads in 10 tons (10t-ESALs) accumulated over a service life of 30 years. These traffic volumes are classified as the highest road class Bk100 (>32 million ESALs) according to German standards (FGSV-499, 2015).

The longitudinal road profiles were collected in May 2018 by using a multi-laser road profiler with a sampling interval of 25 mm. The device has a unique 'Stop & Go' functionality that enables it to collect data efficiently from both urban and rural networks at traffic lights, stop signs, junctions, and roundabouts. Measurements were performed for 31.2 km of normal bus lanes and 17.96 km of mixed traffic lanes in the city, where buses operate regularly and
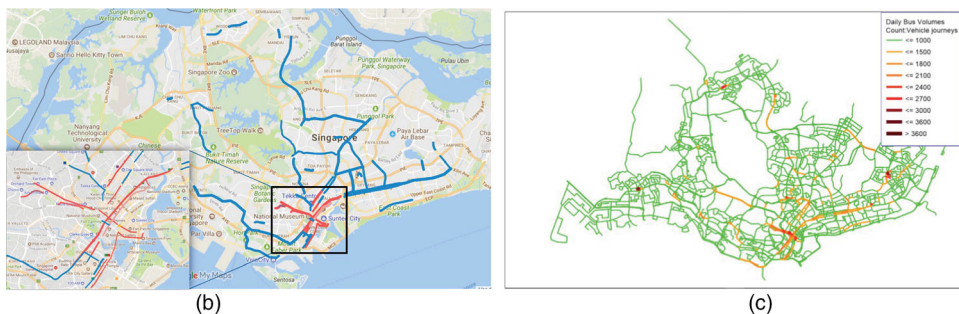
Figure 6.   Singapore road network. (a) Bus lane schemes with the highlight of full-day bus lanes in city centre. (b) Highly concentrated daily bus volumes.
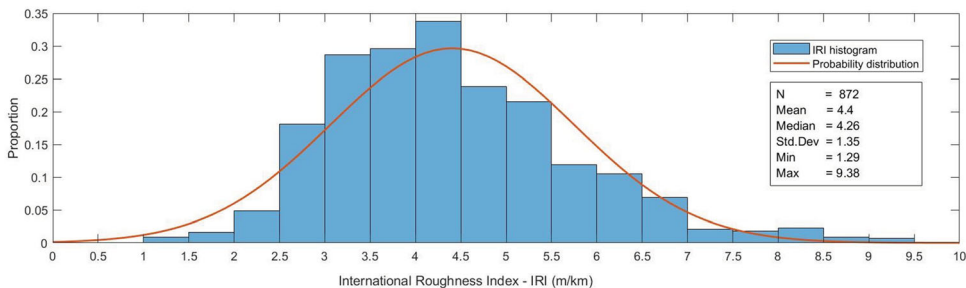
Figure 7.   Distribution of IRI overall measured road profiles.

frequently. However, the full-day bus lanes could not be measured because vehicles excluding public buses are not allowed to drive on them.

IRI was calculated for both the left and right wheel tracks. For each survey lane, elevation data is at an offset of 85 cm left and 85 cm right of the survey vehicle centreline. This is the maximum distance that the measurement device can offer. Figure 7 shows the IRI distribution for a total of 872 profile segments, each 100 m in length. Most of the IRI values were distributed from 2.5 to 6.5. With regard to riding quality, IRI < 2.5 is good, IRI = 2.5–3.5 is average, IRI = 3.5–4.5 is marginal, IRI = 4.5–6.0 is poor and IRI > 6 is bad (LTA, 2009). The field-measured road profiles showed a high proportion of poor bus lane surfaces.

5.   Results and discussion

5.1.   *Correlation between BRI and IRI*

IRI is proportional to the vertical vibration a_{wz} and total three-dimensional vibration a_w. Many studies have been conducted to establish the following relationship between these indices:

$$a_w(a_{wz}) = b_1 IRI + b_2 \qquad (6)$$

where b_1 is the slope of the straight line and b_2 is the intercept.

In Múčka (2016b), the summary of nine experimental studies on different types of vehicles at different speeds showed that b_1 ranges from 0.071 to 0.192 for a_{wz} and from 0.002 to 0.369 for a_w, while the b_2 ranges from 0.005 to 0.49. In particular, for a heavy bus with a weight of 18 t, $a_{wz} = 0.088 IRI + 0.054$ ($R^2 = 0.882$) at the drivers seat according to Fichera et al. (2007, April), although they did not report the speed.

In this study, BRI was calculated for all road profiles with a default length of 100 m based on the above calibrated BRI QCS bus model. The relationships between IRI and BRI at different speeds of 20, 40, 60 and 80 km/h were established for artificially generated road profiles (Figure 8) and field-measured road profiles (Figure 9). The maximum IRI values range around 10 mm/m for both artificial and field-measured road profiles, representing realistically urban city bus lanes in the very good ISO A–B and good ISO B–C road categories.

Lower *R*-squared values were observed for the measured road profiles at a speed of 80 km/h: $BRI_{80} = 0.26 IRI$. For car, Cantisani and Loprencipe (2010) established the relationship $a_{wz} = 0.22 IRI$ at the same speed of 80 km/h based on 124 road profiles with lengths of 320 m each. Table 8 presents the b_1 coefficients of BRI–IRI calculated at 100, 160 and 320 m interval as the most used intervals worldwide (Múčka, 2017) and car a_{wz}-IRI regression at different speeds. The formers were always higher than the latter by around 0.3–0.6, which means that the same IRI can cause greater discomfort to bus passengers than car passengers. For BRI–IRI, similar
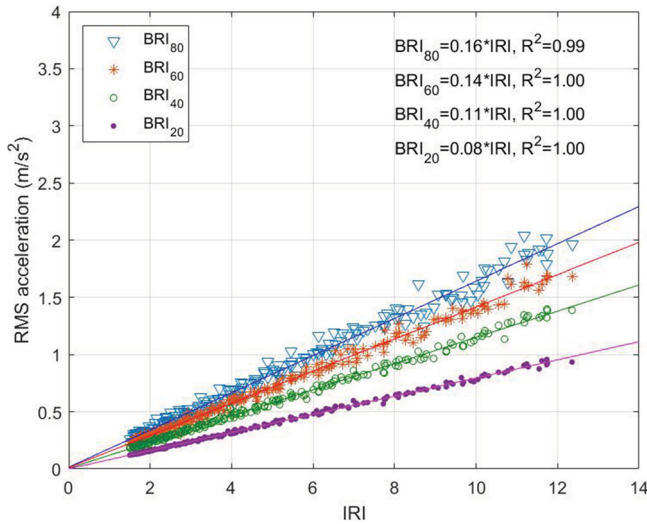
Figure 8. Relationship between IRI and BRI at different speeds for artificially generated profiles.
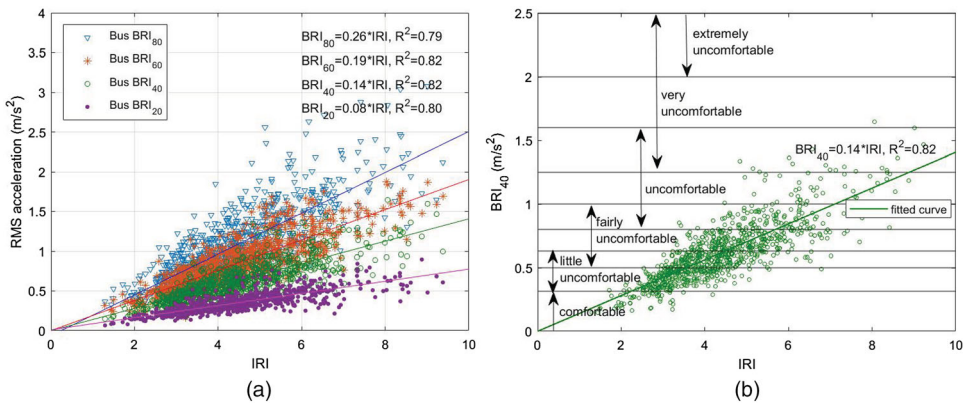
Figure 9. Relationship between IRI and BRI for field-measured road profiles (100 m interval). (a) BRI–IRI correlation at different speeds. (b) The scatter of BRI_{40} at speed of 40 km/h.

results of coefficient b1 are observed between the three alternatives at different speeds, however, longer calculating intervals have improved the correlation (*R*-squared) in the BRI–IRI relationship. While IRI varied at longer interval, BRI could also change accordingly. The significantly high *R*-squared is nearly to 1.0 for IRI–BRI_{80} in the case of artificially generated road profiles can be explained by the relatively homogeneous distribution compared to the field-measured profiles, which contained various local obstacles such as bumps, potholes, and distresses. Herein, a given value of IRI resulted in a range of BRI values (i.e. different ride comfort levels), as clearly shown in Figure 9(b).

    The vehicle speed was found to have a high impact on the users ride comfort, and different linear regression relationships were observed at different speed levels. Given the different correlation *R*-squared values between BRI and IRI in the two datasets, caution must be exercised when relating artificial road profiles to ride comfort. Artificial profiles are useful for vehicle suspension design but are not adequate for correctly evaluating road irregularities and their effects on users.

Table 8.   Different b_1 values for BRI–IRI and a_{wz}–IRI regression in (Cantisani & Loprencipe, 2010).

	Coefficient b_1 of Equation (6) at different speed levels (and R-squared value)							
	10 km/h	20 km/h	30 km/h	40 km/h	50 km/h	60 km/h	70 km/h	80 km/h
Car a_{wz}–IRI (320 m)	–	–	0.08	0.09	0.11	0.17	0.20	0.22
Bus BRI–IRI (100 m)	0.04 (0.73)	0.08 (0.79)	0.11 (0.82)	0.14 (0.82)	0.17 (0.81)	0.19 (0.82)	0.22 (0.82)	0.26 (0.80)
Bus BRI–IRI (160 m)	0.04 (0.73)	0.08 (0.80)	0.11 (0.85)	0.14 (0.80)	0.17 (0.85)	0.19 (0.80)	0.22 (0.84)	0.26 (0.76)
Bus BRI–IRI (320 m)	0.04 (0.73)	0.08 (0.84)	0.11 (0.86)	0.14 (0.86)	0.17 (0.86)	0.19 (0.85)	0.22 (0.85)	0.26 (0.83)

Table 9.   BRI thresholds based on bus speed levels.

	IRI thresholds at different speed levels [m/km]									
Ride quality	10 km/h	20 km/h	30 km/h	40 km/h	50 km/h	60 km/h	70 km/h	80 km/h	Ride comfort levels	BRI (m/s^2)
Very good	< 7.88	< 3.94	< 2.86	< 2.25	< 1.85	< 1.66	< 1.43	< 1.21	Comfortable	< 0.315
Good/fair	7.88–15.75	3.94–7.88	2.86–5.73	2.25–4.50	1.85–3.71	1.66–3.32	1.43–2.86	1.21–2.42	Little uncomfortable	0.315–0.63
Mediocre	15.75–22.50	7.88–11.25	5.73–8.18	4.50–6.43	3.71–5.29	3.32–4.74	2.86–4.09	2.42–3.46	Fairly uncomfortable	0.63–0.9
Poor	> 22.50	> 11.25	> 8.18	> 6.43	> 5.29	> 4.74	> 4.09	> 3.46	Uncomfortable	> 0.9

This finding is consistent to the investigation by Loprencipe and Zoccali (2017) in the difference excitation effects between ISO 8608 approach and in situ measurements of road profiles.

5.2. *Ride quality levels based on IRI and BRI*

Based on the established IRI-BRI regression relationships (Figure 9(a) and Table 8), IRI thresholds were suggested for different speed levels based on the ride comfort thresholds from *comfortable* to *uncomfortable*. The ride quality for bus operation at lower speeds is given in Table 9 and Figure 10. Compared to the recommendations in Table 1 and 2, Table 9 suggests a higher IRI requirement for bus lanes even for the same ride comfort levels established by Cantisani and Loprencipe (2010).

The correlation between BRI, IRI, and the bus speed provides suggestions for bus operation and pavement maintenance to ensure passenger ride comfort. Different stakeholders (bus operators, road transport authorities) can use these suggestions for different applications. Figure 10 serves as a reference for estimating the bus ride comfort from road roughness conditions based on the IRI levels and bus speed. Bus speeds should be regulated at certain levels of IRI to ensure ride quality. Meanwhile, road conditions should be maintained according to the proposed IRI thresholds to align with the designed bus operating speed and passenger ride comfort. For example, under urban conditions where buses operate at 40 km/h, the bus lanes should be maintained at IRI of 2.25–4.5 m/km to ensure good/fair ride quality. However, IRI should be 1.66–3.32 m/km for buses running at higher speeds of 60 km/h on highways.

With regard to other applications, the road roughness of a bus lane network can be inferred from the BRI value, which can be quickly measured by using a portable accelerometer on the passenger seat (e.g. the SV100A accelerometer used in this study). In this manner, the road surface can be assessed, and a maintenance strategy can be proposed for a specific road segment before/without requiring an expensive road profiler instrument (e.g. full-day bus lanes that do not allow vehicles other than buses). As a result, maintenance cost will be reduced as compared to regular scanning of the whole road network. Furthermore, road surface can be up-to-date assessed once every bus is designed as a probe to detect roughness condition automatically. Similar approaches have been proposed (regardless of passenger ride comfort) to detect road anomalies using a smartphone (Alessandroni, Carini, Lattanzi, Freschi, & Bogliolo, 2017;
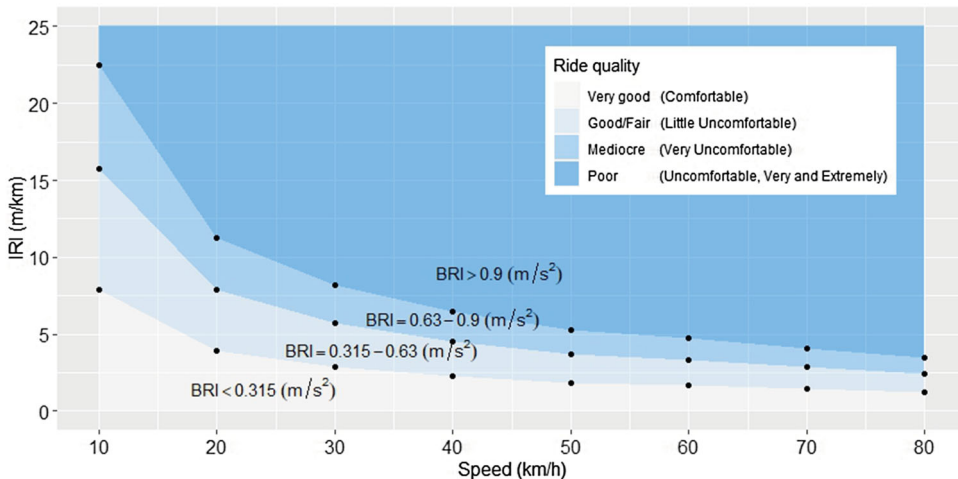
Figure 10. Ride quality based on IRI and BRI.

Eriksson et al., 2008; Seraj, van der Zwaag, Dilo, Luarasi, & Havinga, 2016), to estimate road roughness Power Spectral Density (PSD) (González, O'Brien, Li, & Cashell, 2008) and IRI (Du, Liu, Wu, & Jiang, 2014) from the vehicle acceleration.

6. Conclusion

BRI was developed based on a well-calibrated 3-DOF QCS derived from existing technical parameters for operating buses. The new and simple BRI model can measure directly passenger ride comfort with the inclusion of air suspension stiffness and damping ratio to maximise ride quality. The nonlinear dynamics characteristic of BRI enables it to keep the low vibration frequency (around 1.2 –1.5Hz) regardless of changing the sprung mass by passenger loads. A comparison between the transfer functions of TRI and BRI showed that BRI is more appropriate for evaluating ride comfort with regard to bus/BRT lanes given the inherent difference in vehicle configurations.

Regression relationships were established between IRI and BRI at different speeds for both artificially generated and field-measured road profiles. The analysis of BRI-IRI correlation at two lengths of 100, 160 and 320 m has shown that the correlation coefficients are unchanged, therefore, BRI can be applicable for different calculating intervals. Based on the BRI values from field-measured road profiles, a given input value for IRI can represent a range of ride comfort levels, which means that the concerns of passengers may vary. IRI thresholds according to different speed levels and ride quality are suggested, which will be useful for bus lane pavement maintenance and monitoring. The findings of this study serve as a benchmark to estimate road conditions with an onboard accelerometer, which is an advanced method for monitoring citywide bus lane network more efficiently than the conventional method of using road profiler instrument.

However, this study was based on asphalt pavement field-measured road profiles and passive suspension and damping vehicle dynamics. Further study can involve developing an active suspension QCS bus model to be coupled with the measured profiles of concrete pavement for BRI calculation. Half- and full-bus models should also be developed to consider other dynamic effects such as pitch and roll. The usage of the proposed IRI thresholds certainly deserves careful consideration by transport authorities.

Disclosure statement

No potential conflict of interest was reported by the authors.

ORCID

Teron Nguyen http://orcid.org/0000-0001-6822-0753
Bernhard Lechner http://orcid.org/0000-0002-3014-7463
Yiik Diew Wong http://orcid.org/0000-0001-7419-5777
Jun Yew Tan http://orcid.org/0000-0003-4884-9516

References

Agostinacchio, M., Ciampa, D., & Olita, S. (2014). The vibrations induced by surface irregularities in road pavements – A Matlab approach. *European Transport Research Review*, *6*(3), 267–275.

Alessandroni, G., Carini, A., Lattanzi, E., Freschi, V., & Bogliolo, A. (2017). A study on the influence of speed on road roughness sensing: The smartroadsense case. *Sensors*, *17*(2), 305.

Alexander, D. (2014). *Enviro500-low floor high capacity 12 m double deck bus*. Retrieved from https://www.alexander-dennis.com/products/double-deck-3-axle/

ASTM E1926-08 (2015). *Standard practice for computing international roughness index of roads from longitudinal profile measurements*. ASTM International. Retrieved from http://www.astm.org/cgi-bin/resolver.cgi?E1926-08(2015)

Bridgelall, R. (2014). Connected vehicle approach for pavement roughness evaluation. *Journal of Infrastructure Systems*, *20*(1), 04013001.

BRT + Centre of Excellence and EMBARQ (2018). Global BRT data. Retrieved from https://brtdata.org/

BS6841:1987 (1999). *British standard guide to measurement and evaluation of human exposure to whole-body mechanical vibration and repeated shock*. Retrieved from https://shop.bsigroup.com/Product Detail/?pid = 000000000000171912

Cantisani, G., & Loprencipe, G. (2010). Road roughness and whole body vibration: Evaluation tools and comfort limits. *Journal of Transportation Engineering*, *136*(9), 818–826.

Cao, D., Song, X., & Ahmadian, M. (2011). Editors' perspectives: Road vehicle suspension design, dynamics, and control. *Vehicle System Dynamics*, *49*(1–2), 3–28. doi:10.1080/00423114.2010.532223

Capuruço, R., Hegazy, T., Tighe, S., & Zaghloul, S. (2005). Full-car roughness index as summary roughness statistic. *Transportation Research Record: Journal of the Transportation Research Board*, *1905*(1), 148–156.

CEN-PREN 13036-5 (2015). *Road and airfield surface characteristics – Test methods*. Part 5: Determination of longitudinal unevenness indices. European Committee for Standardization. Retrieved from https://standards.globalspec.com/std/10218779/pren-13036-5

Du, Y., Liu, C., Wu, D., & Jiang, S. (2014). Measurement of international roughness index by using Z-axis accelerometers and GPS. *Mathematical Problems in Engineering*, *2014*. doi:10.1155/2014/928980

Eriksson, J., Girod, L., Hull, B., Newton, R., Madden, S., & Balakrishnan, H. (2008). *The pothole patrol: Using a mobile sensor network for road surface monitoring*. Proceeding of the 6th International Conference on Mobile Systems, Applications, and Services – MobiSys '08. Retrieved from http://dl.acm.org/citation.cfm?id = 1378600.1378605

Fakultaet fuer Maschinenwesen (2018). *Vorlesung Grundlagen des Kraftfahrzeugbaus: Federung und Dämpfung*. Technical University of Munich, Munich.

FGSV-489 (2006). *ZTV ZEB-StB – Zusätzliche Technische Vertragsbedingungen und Richtlinien zur Zustandserfassung und -bewertung von Straßen*. Forschungsgesellschaft für Straßen- und Verkehrswesen. Retrieved from http://www.fgsv-verlag.de

FGSV-499 (2015). *RStO – Guidelines for the standardisation of pavement structures of traffic areas* (English ed.). Road and Transportation Research Association. Retrieved from http://www.fgsv-verlag.de

Fichera, G., Scionti, M., & Garescì, F. (2007). *Experimental correlation between the road roughness and the comfort perceived in bus cabins*. Retrieved from http://papers.sae.org/2007-01-0352/

Firestone (2014). *Engineering manual and design guide*. Retrieved from https://firestoneip.com/-/media/www/fsip/files/ManufacturingIndustrial/Design%20manuals/EMDG_Imperial_2014.pdf

Gillespie, T. D., Karamihas, S. M., Sayers, M. W., & Hansen, W. (1992). *Effects of heavy vehicle characteristics of pavement response and performance* (Technical report). The University of Michigan.

González, A., O'Brien, E. J., Li, Y. Y., & Cashell, K. (2008). The use of vehicle acceleration measurements to estimate road roughness. *Vehicle System Dynamics*, *46*(6), 483–499.

Hassan, R. A., McManus, K., & Cossens, I. (2006). *Development of HATI-heavy articulated truck index*. Research Into Practice: 22nd ARRB Conference, Canberra, Australia.

ISO2631-1 (1997). *Mechanical vibration and shock – Evaluation of human exposure to whole-body vibration – Part 1: General requirements* (pp. 1–30). Retrieved from https://www.iso.org/standard/7612.html

ISO 8608:2016 (2016). *Mechanical vibration – Road surface profiles – Reporting of measured data*. International Organization for Standardization. Retrieved from https://www.iso.org/standard/71202.html

Jazar, R. N. (2005). *Advanced vibrations: A modern approach*. Berlin: Springer.

Khavassefat, P., Jelagin, D., & Birgisson, B. (2015). Dynamic response of flexible pavements at vehicle–road interaction. *Road Materials and Pavement Design*, *16*(2), 256–276. doi:10.1080/14680629.2014.990402

Liu, X., Zhou, Y., & Rau, A. (2018). Smart card data-centric replication of the multi-modal public transport system in Singapore. *Journal of Transport Geography*, *2018*, 1–11. doi:10.1016/j.jtrangeo.2018.02.004

Loprencipe, G., & Zoccali, P. (2017). Use of generated artificial road profiles in road roughness evaluation. *Journal of Modern Transportation*, *25*(1), 24–33.

LTA (2009). *Pavement management system (PMS)*. Land Transport Authority of Singapore.

LTA (2018). *One motoring*. Retrieved from https://www.onemotoring.com.sg

Maerschalk, G., Ueckermann, A., & Heller, S. (2011). *Längsebenheitsauswerteverfahren "Bewertetes Längsprofil": Weiterentwicklung der Längsebenheitsbewertung der Zustandserfassung und-bewertung*. Berichte der Bundesanstalt für Straßenwesen.

Mercedes-Benz (2018). *The Citaro – Technical data and dimensions*. Retrieved from https://www.mercedes-benz.com.sg

Múčka, P. (2016a). Current approaches to quantify the longitudinal road roughness. *International Journal of Pavement Engineering*, *17*(8), 659–679. doi:10.1080/10298436.2015.1011782

Múčka, P. (2016b). Road roughness limit values based on measured vehicle vibration. *Journal of Infrastructure Systems*, *23*(2), 04016029.

Múčka, P. (2017). International roughness index specifications around the world. *Road Materials and Pavement Design*, *18*(4), 929–965.

Múčka, P. (2018). Simulated road profiles according to ISO 8608 in vibration analysis. *Journal of Testing and Evaluation*, *46*(1), 405–418. doi:10.1520/JTE20140493

Múčka, P., & Granlund, J. (2012). Is the road quality still better? *Journal of Transportation Engineering*, *138*(12), 349.

Patten, W. N., Sha, S., & Mo, C. (1998). A vibration model of open celled polyurethane foam automotive seat cushions. *Journal of Sound and Vibration*, *217*(1), 145–161.

Prem, H., & Ayton, G. (2005). Improved echniques for ssessing ride quality on concrete pavements. In *8th International Conference on Concrete Pavements* (pp. 733–754). Colorado, USA.

Prem, H., Ramsay, E., & McLean, J. (2000). *A road profile based truck ride index (TRI)*. 6th International Symposium on Heavy Vehicle Weights and Dimensions, Saskatoon, Saskatchewan, Canada.

PTC (2016). *Commuters at heart on recommendations to improve commuter's journey* (Technical report). Singapore: Public Transport Council. Retrieved from https://www.ptc.gov.sg/

Sayers, M. W. (1989). Two quarter-car models for defining road roughness: IRI and HRI. *Transportation Research Record*, *1215*, 165–172. Retrieved from https://trid.trb.org/view.aspx?id=308315

Sayers, M. W. (1995). On the calculation of international roughness index from longitudinal road profile. *Transportation Research Record*, *1501*, 1–12.

Sayers, M. W. (1998). *The little book of profiling: Basic information about measuring and interpreting road profiles*. University of Michigan, Ann Arbor, Transportation Research Institute.

Sekulić, D., & Dedović, V. (2011a). *Analysis of driver oscillatory comfort by simulation using a model with 6 DOF*. Proceedings of the 23rd International Scientific – Professional Meeting: Science and Motor Vehicles, Special Conference for West Balkans Belgrade.

Sekulić, D., & Dedović, V. (2011b). The effect of stiffness and damping of the suspension system elements on the optimisation of the vibrational behaviour of a bus. *International Journal for Traffic & Transport Engineering*, *1*(4), 231–244.

Sekulić, D., Dedović, V., Rusov, S., Obradović, A., & Šalinić, S. (2016). Definition and determination of the bus oscillatory comfort zones. *International Journal of Industrial Ergonomics*, *53*, 328–339.

Sekulić, D., Dedović, V., Rusov, S., Šalinić, S., & Obradović, A. (2013). Analysis of vibration effects on the comfort of intercity bus users by oscillatory model with ten degrees of freedom. *Applied Mathematical Modelling*, *37*(18–19), 8629–8644.

Sekulić, D., Rusov, S., Dedović, V., Šalinić, S., Mladenović, D., & Ivković, I. (2018). Analysis of bus users' vibration exposure time. *International Journal of Industrial Ergonomics*, *65*, 26–35.

Seraj, F., van der Zwaag, B. J., Dilo, A., Luarasi, T., & Havinga, P. (2016). RoADS: A road pavement monitoring system for anomaly detection using smart phones. In M. Atzmueller, A. Chin, F. Janssen, I. Schweizer, & C. Trattner (Eds.), *Big data analytics in the social and ubiquitous context* (Vol. *9546*, pp. 128–146). Cham: Springer. Lecture Notes in Computer Science.

Ueckermann, A. (2002). The dynamic evenness index. *Forschung Strassenbau und Strassenverkehrstechnik* 839.

Ueckermann, A., & Oeser, M. (2015). Approaches for a 3D assessment of pavement evenness data based on 3D vehicle models. *Journal of Traffic and Transportation Engineering (English Edition)*, *2*(2), 68–80. doi:10.1016/j.jtte.2015.02.002

Wei, L., & Griffin, J. (1998). The prediction of seat transmissibility from measures of seat impedance. *Journal of Sound and Vibration*, *214*(1), 121–137.

Yu, J., Chou, E. Y. J., & Yau., J.-T. (2006). Development of speed-related ride quality thresholds using international roughness index. *Transportation Research Record: Journal of the Transportation Research Board*, *1974*(1), 47–53.

ZF GmbH (2009). *Product overview: Axle and transmission systems for buses and coaches*. 20. Retrieved from https://www.zf.com/products/en/buses/products_40065.html

Appendix 4: Paper IV

Nguyen, T., NguyenDinh, N., Lechner, B., & Wong, Y.D. (2019). Insight into the lateral ride discomfort of young-adult bus passengers at multiple postures: Case of Singapore. *Case Studies on Transport Policy*, 7(3), 617-627, doi: 10.1016/j.cstp.2019.07.002.

Insight into the lateral ride discomfort thresholds of young-adult bus passengers at multiple postures: Case of Singapore

Teron Nguyen[a,b,c,*], Nen NguyenDinh[a], Bernhard Lechner[b], Yiik Diew Wong[a,c]

[a] TUMCREATE Ltd, 1 Create Way, #10-02 CREATE Tower, Singapore 138602, Singapore
[b] Technical University of Munich (TUM), Baumbachstraße 7, 81245 München, Germany
[c] Nanyang Technological University (NTU), N1-01b-51, 50 Nanyang Avenue, Singapore 639798, Singapore

ABSTRACT

Ride comfort is an important serviceability attribute for bus passengers, of which bus operating under the influence of road layout in urban roads is a prominent contributory factor. Passenger posture is another influencing factor that has not yet been investigated comprehensively. In this case study, ride comfort from road-induced lateral acceleration and lateral jerk was assessed by correlating subjective evaluation with bus operation performance parameters as well as road layout in Singapore. In the first bus run, a sample of 26 participants classified in three groups: sitting, leaning and standing postures, rode on the same bus along a 45-min route. Ride comfort was worst-off for standing passengers and least uncomfortable for sitting passengers. A strong statistical correlation was found between participants' subjective ratings with lateral acceleration and duration of turning movement. A second bus run was followed with a sample of 11 participants to collect additional passengers' ratings. Lateral ride discomfort thresholds were thus established for bus negotiating roundabouts, intersections and along links. The three levels of ride discomfort are *Uncomfortable, Very Uncomfortable and Extremely Uncomfortable* with average lateral accelerations of $a_y = 1.5$, 1.75 and 2.0 m/s^2, respectively. The lateral ride discomfort thresholds would be useful for several value-add applications which include better vehicle design including its interiors, and better vehicle handling about the road layout. With the advent of autonomous public transport (APT), the ride discomfort thresholds must also be considered as valuable input for APT vehicle operation.

1. Introduction

Urban bus system plays an important role worldwide for sustainable transportation. Bus services not only contribute to relieving congestion (Nguyen-Phuoc et al., 2018b, 2018a) but also reduce traffic emissions and improve social benefits (Stjernborg and Mattisson, 2016). Improving bus service is one of the key measures to attract more passengers from car transport according to the pull-strategy (Lai and Chen, 2011). Different from intercity bus equipped with all sitting location for long distance travel, e.g. the bus model IK-301 in (Sekulić et al., 2018), urban city bus comprises higher proportion of standing location, e.g. 77 standing over 28 sitting locations on the Citaro bus (Mercedes-Benz, 2002). During peak hours, buses are often crowded, and standing passengers onboard at different locations and orientations would experience lower ride comfort when the bus negotiates sharp turning areas such as small-radius curves and roundabouts or making left-turn and

right-turn at crossroad intersections. Indeed, standing passengers are the most vulnerable groups associated with various risk impacts (Asociación RUVID, 2012; Robert et al., 2007). This issue has called for better design of bus interior as well as improved bus driving behaviour towards passenger ride comfort as a recent human-centric design approach in transportation (Bogren et al., 2009; Mitchell et al., 2016).

Ride comfort is one of the main factors in attracting urban public transport ridership (Morton et al., 2016). However, ride comfort is difficult to evaluate due to various influencing factors: 1) objective factors from ambience such as temperature, air quality, noise, vibration, lighting, ergonomics; and 2) subjective factors like personal perceptions and assessment by Da Silva (2002). The effect of passenger load factor and in-vehicle time on ride comfort can be found in (Imre and Çelebi, 2017; Shen et al., 2016), and an overall bus comfort model can be found in (Zhang et al., 2014). Among the external stimuli, vibration and acceleration are considered as the main factors related to

the effects of road infrastructure and vehicle condition on ride comfort. Evaluation of bus service quality has been often based on interview and questionnaire surveys at the end of the trips, and often without consideration of passengers' onboard position and orientation (Portouli et al., 2017; PTC, 2017). Therefore, information of discomfort might be missed about locations experiencing high acceleration and vibration levels. Better service for passengers is also provided nowadays given the emergence to autonomous public transport (APT) like autonomous bus (AB) worldwide. However, recent research has focused more on the technology development such as platooning control (Lam and Katupitiya, 2013), vehicle concept (Ginn et al., 2017), cost efficiency (Zhang et al., 2019), timetabling and scheduling (Cao and Ceder, 2019), experimental platform for vehicle control (Montes et al., 2017), mapping and path planning (Yu et al., 2018). Empirical evidence from passenger security on AB can be found in (Salonen, 2018), or public attitudes towards AB in (Portouli et al., 2017). There is still little knowledge on the point-of-view of passenger ride comfort to develop these AB systems.

This case study is a part of TUMCREATE project in Singapore to plan and design an innovative AB system not for an individual corridor but a larger part of the city-scale network, where conventional buses will be replaced by fully electrified APT (Rau et al., 2018). Passenger ride comfort is referenced as a benchmarking parameter in bus transport. The study was granted ethics approval by NTU Institutional Review Board IRB-2017-19-058. Specifically, the study focuses on bus passengers' ride comfort in relation to lateral acceleration and lateral jerk while noting that ride comfort thresholds related to vertical acceleration/vibration can be determined in (ISO2631-1, 1997), while ride comfort thresholds related to longitudinal (forward) acceleration have been established by He et al. (2013). Furthermore, ride comfort associated to vertical vibration and road roughness is not a big issue for bus passengers in Singapore since its pavement system is consistently well-maintained in good condition (Tan, 2013), and the modern bus vehicles are well equipped with user-friendly air suspension system that greatly reduces vertical acceleration/vibration (Kowarska et al., 2014). For this case study, a special smart-phone application was designed to collect real-time subjective ride comfort ratings from 26 passengers along the first bus run and 11 passengers along the second bus run. Acceleration data, video recording of passengers' body movements and road conditions were collected and analysed accordingly. The relationship between subjective indicators (passengers' discomfort levels) and objective indicators (lateral acceleration, lateral jerk and duration of turning movement) were established at three levels of lateral ride discomfort: *Uncomfortable, Very Uncomfortable* and *Extremely Uncomfortable*.

The remaining paper is structured as follows. In the Related Works section, the relevant scientific literature is summarised. In the Methodology section, detailed steps in conducting the experiment are described. The Findings section reports the main results of this study, followed by a Discussion section. The study is summed up in the Conclusion and Outlook section.

2. Related Works

Several standards have been established for ride comfort evaluation. For comfort metrics due to whole-body vibration, (ISO2631-1, 1997) suggests a comfort criterion based on the frequency-weighted root-mean-squared acceleration (RMS a_w) of 3-dimension vibration while European standard recommends a comfort scale for train passengers in accordance to (BS EN 12299:2009, 2009). Standards like (BS 6841:1987, 1999; ISO2631-1, 1997) provide approximate indications of likely reactions of passengers to various magnitudes of overall vibration in public transport, but also recommend to use appropriate weighting curves for specific design purposes regarding ride comfort. It should be noted that ISO 2631's comfort criteria are focused mainly on whole-body-vibration with vibration frequency from 0.5 Hz to 80 Hz, which is mainly applicable to vertical acceleration excited by road

roughness. A comprehensive summary of frequency-weighted acceleration and road roughness limit values based on measured vehicle vibration can be found in (Mucka, 2015) study. (Castellanos and Fruett, 2014; Lin et al., 2010) have adapted (ISO2631-1, 1997) approach for their studies on bus ride comfort. In-laboratory experimental study on the discomfort of standing people caused by vibration of a floor can be found in (Nawayseh and Griffin, 2006; Thuong and Griffin, 2012).

Regarding ride discomfort associated with longitudinal acceleration, (He et al., 2013) distributed questionnaires to 35 passengers to find discomfort thresholds due to bus braking and speeding-up, in which bus passengers are found to start to feel uncomfortable when the longitudinal acceleration $a_x > +1.5 \text{ m/s}^2$ and the deceleration/ braking $a_x < -0.75 \text{ m/s}^2$. As for lateral acceleration, (Bodini et al., 2013; Maternini and Cadei, 2014) adapted certain railway ride comfort indicators for comfort evaluation of bus passengers notwithstanding the much different vehicle configuration and operations in rail-based vehicles. Their method was applied in a case study in Italy for ride comfort evaluation of standing passengers for buses negotiating roundabout areas where there are high levels of lateral acceleration. The comfort scale was based on the modified comfort index and transversal movements (or involuntary sway) of standing passengers. Another study in France by Beurier (2012) analysed the discomfort feeling of standing passengers about bus interior design as well as bus lane design. The study recorded passengers' feelings according to their responses (by pressing on buttons mounted on handlebars) at every incident of discomfort; data was collected concurrently on acceleration profiles and GPS locations along the journey. Besides, another ride comfort threshold used in (Shu et al., 2016; Xu et al., 2015) is more appropriate for car passengers, where lateral acceleration $a_y \leq 1.8 \text{ m/s}^2$ is acceptable, $1.8 \text{ m/s}^2 < a_y < 3.6 \text{ m/s}^2$ is bearable, and $a_y > 5.0 \text{ m/s}^2$ exceeds the human's bearing ability.

The recent and typical ride comfort thresholds in different directions and modes of transport are summarised in Table 1. Most of the approaches are based on established standards, guidelines and common practice, whereas to collect bus passenger perception only (He et al., 2013; Prashanth et al., 2013) used questionnaire after the bus run and (Beurier, 2012; Castellanos and Fruett, 2014) used push buttons during a bus run. However, the questionnaire method may not capture the timing of real-time discomfort feelings of bus passengers and push buttons are used on only a small sample, for example, 12 standing passengers (2 bus runs) were investigated based on 10 buttons assembled in 5 handles (Beurier, 2012). Passengers at sitting positions were not well investigated. The comfort scale used in (Maternini and Cadei, 2014) study was based only on passenger movements/sway via video observations but not from direct passengers' ratings.

In summary, there is no existing method that can concurrently collect passenger perceptions in the larger scale of urban bus such as those carrying more than 30 passengers comprising sitting, leaning and standing positions. Table 1 also shows that different ride comfort thresholds are applicable for different transport modes as well as different passenger postures. Therefore, it is necessary to understand the insight of bus passenger ride comfort at different postures. These gaps in the knowledge have provided a strong motivation: (1) to develop a new research method for large scale and real-time onboard survey, (2) to establish ride discomfort thresholds of bus passengers at multiple postures onboard, and (3) to provide recommendation for operating speeds of future AB system. This case study focuses on young-adult passengers and lateral ride comfort, but further application can be extended to larger sample sizes, age groups, and research contexts.

3. Methodology

Public bus service is one of the leading public transport (PT) means in Singapore besides Mass Rapid Transit and Light Rapid Transit. Bus ridership has a high share of 3.9 million passenger trips out of 7.9 million PT passenger trips per day (PTC, 2016), for a resident

Table 1
Ride comfort thresholds at multiple directions.

Source	Longitudinal acceleration a_x (m/s²)	Lateral acceleration a_y (m/s²) / Acceleration rate of change or jerk C (m/s³)	Vertical acceleration a_z (m/s²)	Method to collect passenger ratings	Transport mode	Passenger postures
(ISO2631-1, 1997)	RMS a_{wx}	RMS a_{wy} — RMS a_w includes three RMS a_{wx}, RMS a_{wy}, RMS a_{wz}	RMS a_{wz}	Guidelines	General vibration	Specific method
(BS EN 12299:2009, 2009)		N_{MV}, N_{VA}, N_{VD} include three RMS a_{wx}, RMS a_{wy}, RMS a_{wz}		Guidelines	Rail	Specific method
(Parsons Brinckerhoff, 2012)	$a_x = +1.34$: max acceleration; $a_x = -1.34$: max braking	$a_y = 0.98$–1.47: uncomfortable		Guidelines	Light rail	Not specific
(Parsons Brinckerhoff, 2009)	$a_x = +0.58$: max acceleration; $a_x = -0.54$: max braking	$a_y = 0.49$: uncomfortable		Guidelines	High speed rail	Not specific
(Shu et al., 2016; Xu et al., 2015)		$a_y \leq +1.8$: acceptable, $a_y = +1.8 \div 3.6$: bearable, $a_y > +5.0$: bearing ability		Common practice adaptation	Car	Sitting
(AASHTO, 2011)	$a_x = -3.4$: comfortable braking	$a_y = 0.4$–1.3: safety within spiral curve; $C = 0.3 \div 0.9$: comfortable rate of change		Guidelines	Car	Sitting
(Le Vine et al., 2015)		$a_y = 1.47$: uncomfortable on light rail; $a_y = 0.49$: uncomfortable on high speed rail		Adapting railway	AV	Sitting
(ARUP, 2017)		$a_y = 0.6$–1.0: uncomfortable; $C = 0.3$–0.6: uncomfortable		Guidelines, similar railway	Guided bus	Not specific
(Castellanos and Fruett, 2014)		RMS a_w includes three RMS a_{wx}, RMS a_{wy}, RMS a_{wz}		Adapting ISO2631, button push	Bus	Not specific
(Lin et al., 2010)		RMS a_w includes three RMS a_{wx}, RMS a_{wy}, RMS a_{wz}		Adapting ISO2631, phone sensing	Bus	Not specific
(Bodini et al., 2013; Matemini and Cadei, 2014)		N_{VD} includes three RMS a_{wx}, RMS a_{wy}, RMS a_{wz}		Adapting EN12299, video observation	Bus	Standing
Prashanth et al (2013)		RMS a_w includes three RMS a_{wx}, RMS a_{wy}, RMS a_{wz}; Acceleration thresholds = the average value of the accelerations + their standard deviation		Questionnaire afterwards	Bus	Sitting, activities
(Eboli et al., 2016)		Comfort thresholds = acceleration threshold outliers/the total recorded points		Questionnaire onboard	Bus	Not specific
(He et al., 2013)	$a_x > +1.5$: uncomfortable; $a_x < -0.75$: uncomfortable			Questionnaire afterwards	Bus	Sitting
(Beurier, 2012)	$a_x < -1.4$, $a_x > +1.5$: level 1; $a_x < -2.2$, $a_x > +2.5$: level 2	$a_y < -1.4$, $a_y > +1.6$: level 1; $a_y < -2.0$, $a_y > +2.0$: level 2	$a_x < +8.5$, $a_x > +11.3$: level 1; $a_x < +8.4$, $a_x > +11.6$: level 2	Handlebars buttons	Bus	Standing
Present case study		*Uncomfortable, very uncomfortable and extremely uncomfortable thresholds*		*Mobile app*	*Bus, AB application*	*Sitting, leaning standing*

Note: RMS a_x, RMS a_x, RMS a_x: frequency-weighted root-mean-squared acceleration in vibrational direction x, y, z;
N_{MV}, N_{VA}, N_{VD}: mean comfort standard method; mean comfort complete method: seated passenger; mean comfort complete method: standing passenger;
Level 1, Level 2: uncomfortable and loss of balance; Specific/not specific method: method for individual/not differentiated posture.

population of 5.5 million in the small (719 km^2 land area) island nation. Buses will continue to play a significant role, particularly in serving as feeders to the rail network for the future considering that *"eight in 10 households will be within a 10-minute walk to a train station"* by 2030 (LTA, 2013). Bus interior is designed with a high ratio of standing/ sitting position such as 56/35 (single-deck MAN NL323F model), 51/83 (double-deck Alexander Dennis Enviro500s model) and 90/59 (articulated Mercedes-Benz O405G model) (Land Transport Guru, 2019). There are more than 400 bus services and a total fleet of more than 4000 buses serving the dense residential areas, and their routes include numerous turnings and curves with small radii.

Since passengers' ride comfort is related to both subjective and objective factors, an experimental investigation was carried out involving a relatively large sample of participants. Data was collected over two experimental bus runs. Linear multiple regression and classification methods were used to establish the relationship between various indicators and to classify appropriate ride discomfort levels. It is noted that discomfort is the opposite of comfort; therefore, ride comfort can be inferred from ride discomfort thresholds and vice versa.

3.1. Selection of participants

In the first bus run, a sample of 26 participants (17 female and 11 male) were involved in this study in which 11 were sitting, 8 were leaning, and 7 were standing, which essentially covered various combinations of location (front, middle, rear), posture (sitting, leaning, standing), orientation (facing forwards, backwards, sideways), and standee's support (holding grab-bar/stanchion, celling grip) on board the bus. There is no sideway-facing seat on this bus. Participants were recruited via an online platform as well as traditional distributed advertisements. The initial plan was 30 participants in total, but 4 of them did not show up on the day of the experiment. Participants' ages are in the range of 21–30 years old to ensure stamina of standing subjects on board the bus during the long 45-min round-trip journey. The participants' onboard location, posture, orientation/support and age/gender characteristics are shown in Table 2 and Fig. 1. Participants must keep the same position and orientation (facing), but able to slightly change another hand to hold the handrail for the standing position.

Table 2
Passengers' posture, orientation/support, age and gender.

Posture	Orientation (facing)/support	Code	Age	Gender
Sitting	Forwards	A1	22	Female
	Forwards	A2	27	Male
	Backwards	A3	21	Female
	Forwards	A5	24	Male
	Forwards	A6	21	Female
	Backwards	A7	23	Female
	Backwards	A8	24	Female
	Forwards	A11	22	Female
	Forwards	A12	24	Male
	Forwards	A13	22	Female
	Forwards	A14	26	Female
Leaning	Backwards	B1	22	Male
	Sideways	B2	20	Female
	Forwards	B3	22	Female
	Backwards	B4	24	Female
	Sideways	B5	33	Male
	Backwards	B6	23	Female
	Sideways	B7	23	Female
	Forwards	B8	23	Male
Standing	sideways/ceiling grip	C1	30	Male
	sideways/grab-bar	C2	21	Female
	forwards/ceiling grip	C3	24	Male
	forwards/grab-bar	C4	21	Female
	sideways/ceiling grip	C5	23	Male
	sideways/grab-bar	C6	25	Female
	sideways/grab-bar	C7	29	Female

In this study, the age group is not considered. The initial research idea is to divide the age group into the young and elderly, but it is not necessary since the elderly normally have their priority seat when boarding the bus, and for safety reason, they are only allocated at sitting position if being included in this experiment. However, from the preliminary study results, the sitting position does not expose much discomfort as compared to standing position.

3.2. Measurement instruments

Different from conventional methods used for evaluating the quality of transit services such as SERVQUAL questionnaire (Sam et al., 2018) or in-depth interviews (Mah and Mitra, 2017), in this study a dedicated iOS and Android application "Timestamp datalogger" was designed for easy and portable use for a large number of participants. A 5-point rating scale (*1 – not uncomfortable, 2 – a little uncomfortable, 3 – uncomfortable, 4 – very uncomfortable* and *5 – extremely uncomfortable*) was built into the data-logger. During the 45-min bus ride, real-time subjective ratings on ride comfort were input into the data-logger by the participants. There is not any fixed time interval, and participants would rate their perception at any time of uncomfortable feeling. Then, at the completion of the journey, the participants used the same data-logger to evaluate (on the same 5-point scale) the overall ride comfort with regards to road condition, bus driver's driving performance, and vehicle condition (Fig. 2).

An onboard camera was installed to record the body movements of participants and another out-front camera installed to record road and traffic conditions. A commercial Svantek SV100A seat-pad accelerometer was laid on the seat cushion of participant A05 who was sitting directly above the rear wheel axle, and acceleration data was thus collected above the rear axle location. GPS information was collected by 4G data from a smart-phone. Meanwhile, it was found that a dedicated GPS device using an external antenna was not able to connect well with satellites whenever the bus is under tree and high building shadows, and the GPS device was thus not applied.

3.3. Experimental procedures

The experiment was divided into four parts: (1) Preparatory stage: all participants were required to download and install the mobile application and practise to get used to it beforehand; (2) Briefing: before the onset of on-road experiment, participants were introduced again on the whole experimental process and the associated details; (3) Experiment stage: during 45 min of the bus run, participants pressed on the buttons at any occasion they felt uncomfortable due to vehicle's acceleration, braking, vibration and swerving. Later, these real-time discomfort ratings were matched with acceleration data from the accelerometer; and (4) Ending stage (after bus run): participants evaluated the overall ride comfort of bus run and answered questions regarding the vehicle's interior design.

In the first bus run, the bus route is a round-trip journey of shuttle service between NUS campus (Kent Ridge Terminal – KRT) and BTC campus with speed profile and typical road layout as shown in Fig. 3. The bus is a single-deck low-floor Volvo B9L model in very good condition. The speed values along the AYE highway and Farrer Road arterial are relatively higher than the origin and destination segments. There was no bus resting time at the BTC campus. The bus route includes various urban road horizontal alignments such as 3 small roundabouts (radius R = 6; 10 and 13 m), 22 small-radius curves (radius R < 100 m) and 17 crossroad intersections (where the bus needs to turn left or right). Weather conditions were good with dry and good road surface during the bus run. The bus driver was not informed about the study, and he drove the bus as per normal operation. The bus was not crowded, and traffic was not congested as the experiment was conducted on a Saturday morning. The weekend is better timing for several reasons: 1) easier for the attendance of planned 30 participants;
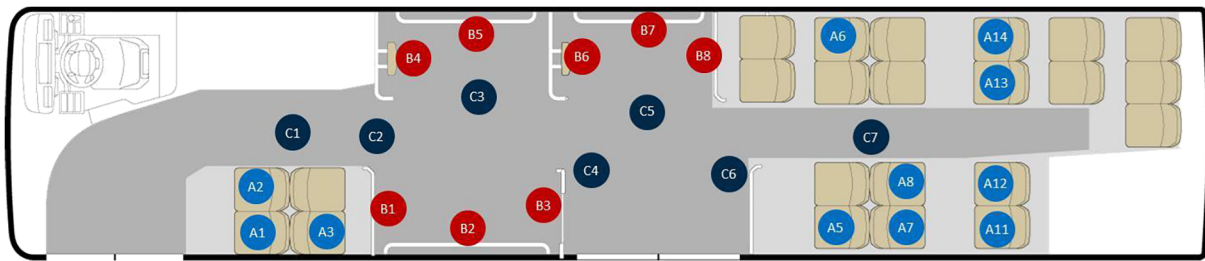
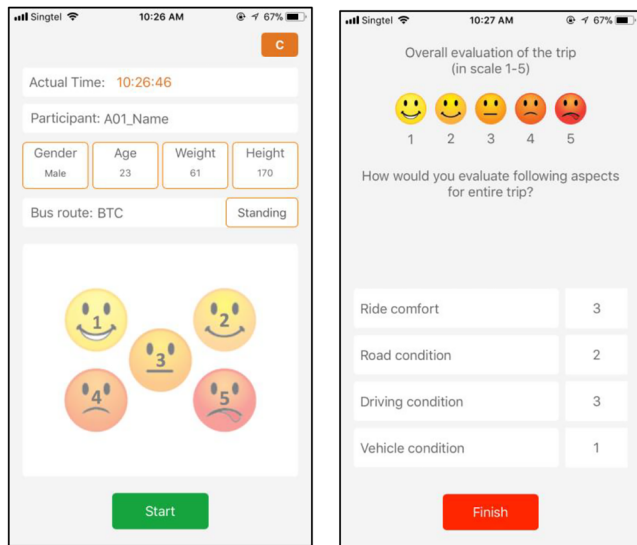Fig. 1. Passengers' location, posture and orientation.

Fig. 2. Two user interfaces of the mobile application.

2) enough available space to allocate all participants with absolute position and posture without much interaction with regular bus passengers; 3) the bus can run faster than on weekdays, resulted in higher levels of lateral acceleration and uncomfortable perception of participants.

4. Findings

After data collection, the locations of turning movements were identified based on the minimum value of lateral acceleration and minimum duration while the bus is turning. The primary subjective indicator is personal ratings of jury panels while objective indicators include lateral acceleration, lateral jerk and duration of turning movement, which was matched based on their timestamps. Linear multiple regression was used to investigate the relationship between various indicators but not to predict the subjective ratings. Thereafter, the classification method was used to classify three ride discomfort ranges according to passengers' ratings on different turning movements.

4.1. Ride comfort ratings concerning passengers' location and posture

The first bus run resulted in 23 plausible datasets for analysis while data was not received from 3 participants (B2, B5, B8) due to errors in the data collection process (participants turned off their iPhone GPS location services accidentally). Real-time subjective ratings were analysed only for levels 3, 4 and 5 in the 5-level scale since level 3 marks onset of discomfort while levels 1 and 2, which covered comfortable feelings such as along straight road links, were included to provide contrast against discomfort feelings. The frequencies of pressing levels

3, 4 and 5, and the overall evaluation on ride comfort of each participant are shown in Fig. 4(a) and (b), respectively. Higher rating frequencies on levels 4 and 5 are seen for the standing group. It is evident that standing passengers experienced a higher level of discomfort compared to those in other postures, that resulted from the bus negotiating sharp turning areas such as small-radius curves and roundabouts or making left-turn and right-turn at crossroad intersections. This finding is consistent to the calculation of N_{VA} and N_{VD} index ($N_{VA} < N_{VD}$) for seated and standing passenger comfort in railway, respectively (BS EN 12299:2009, 2009), as affirmed in (Maternini and Cadei, 2014). Among sitting passengers, those in the rear positions A05, A06, A07 and A08 pressed levels 3 and 4 more frequently as compared to A11, A12, A13 and A14. The reason can be explained that the former ones were seated above the rear wheel axle where higher levels of vertical acceleration are to be expected.

Regarding overall ride comfort evaluation right after the bus run, 5 levels of ride comfort were considered (see Fig. 4(b)). Regression analysis resulted in greater correlation of overall ride comfort with driving condition (R = 0.74) than with road condition (R = 0.59) and vehicle condition (R = 0.46). The overall ride comfort is dependent on posture whereby levels 3 and 4 are seen more in the standing group while levels 1 and 2 in the sitting group, with the leaning group being in between. This is the main reason why 23/26 participants responded to sitting preference when answering the question after the bus run: *Do you prefer to sit, stand or lean when travelling on the bus?* The detailed distribution of the rating is shown in Fig. 4(b), in which the ratings on overall ride comfort are highlighted by the rated numeric levels.

4.2. Correlation between subjective and objective indicators

Turning movements of the bus along the journey were tracked and were classified into: turn left and turn right (at intersections); U-turn, straight and right turn (at roundabouts); curve left and curve right (on curved road segments). Ride comfort thresholds were established for these turning movements, by correlating subjective indicator of passengers' ride comfort ratings with objective indicators of bus lateral acceleration, lateral jerk and duration of turning movement. The maximum values of lateral acceleration and lateral jerk, as well as duration at each turning movement, were obtained from seat-pad accelerometer SV100A. Decimation smoothing was applied to reduce the data to 1 Hz, given the high sampling rate of the accelerometer. The turning movements were double-checked with camera footage to avoid lane change movements which last for a short period from 2 to 3 s.

For the experiment, a participant may press the button on the mobile phone application several times over the duration of a given turning movement. The highest rated discomfort level (i.e. at levels 3, 4, 5) was selected for that participant for the particular turning movement. In this way, the aggregated discomfort level, denoted 'S_i', for each turning movement was derived by summing up the individuals' highest discomfort ratings within that turning movement 'i'. In essence, the 'S' value gives the overall perspective of the discomfort level of the given turning movement. In total, 'S' value was determined at 48 turning movements. In the first bus run, the high 'S' value can be about
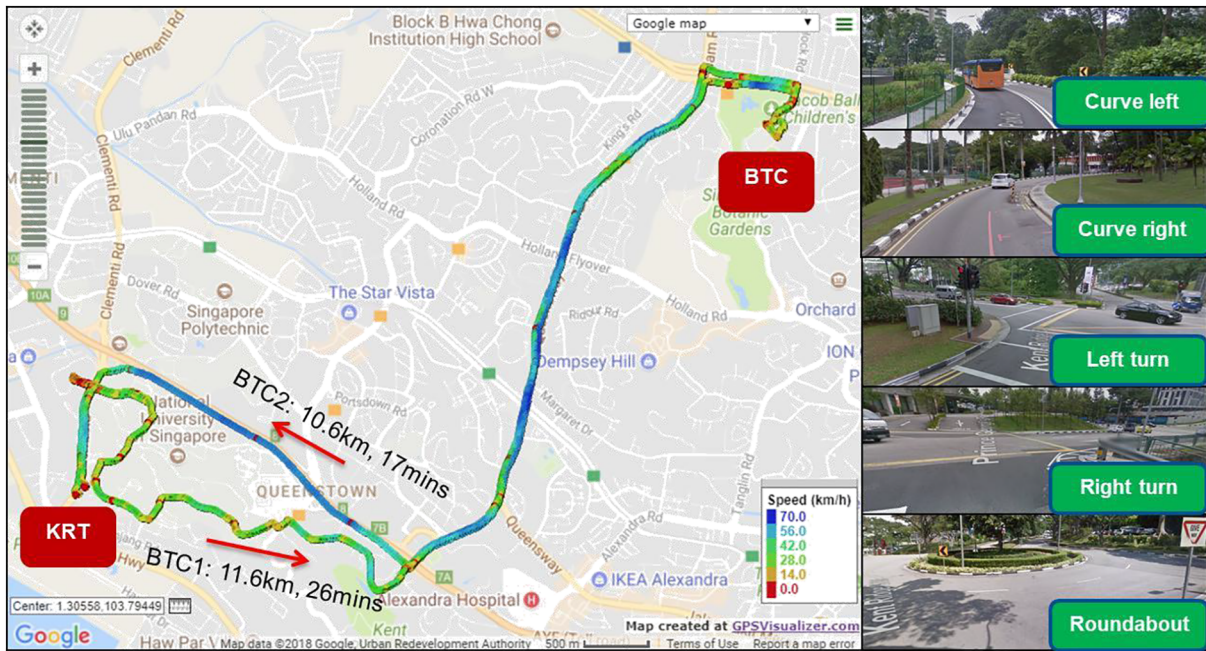
Fig. 3. Speed profile along the bus round-trip journey with typical curves and turning movements.
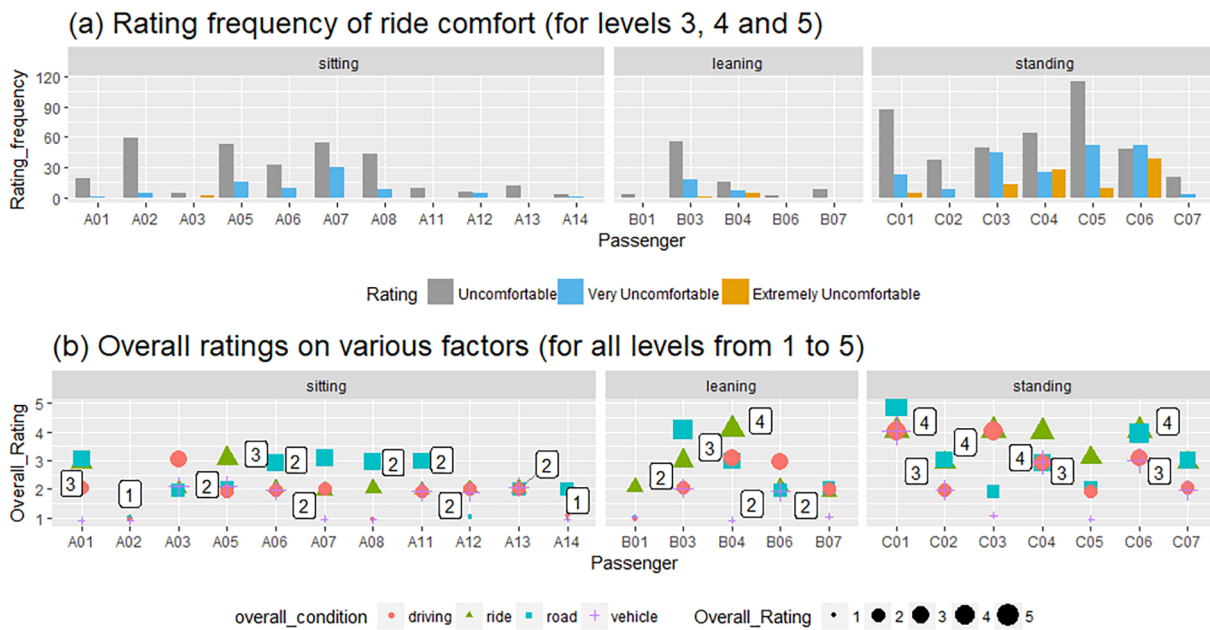

Fig. 4. Subjective ratings of ride comfort levels for entire trip by individual passengers (n = 23).

50, for a rating panel of 23 participants. The greatest uncomfortable situation (S = 53) was for the bus making a U-turn at a roundabout which lasted 13 s. On the other hand, an on-road left turn that persisted over 3 s had a relatively low level of discomfort (S = 6).

Fig. 5a presents the results of linear correlation analysis (showing Pearson's correlation coefficient r) and p-value (two-tailed test) for objective factors (lateral acceleration a_y, lateral jerk, RMS acceleration a_{wY} in lateral direction, a_{wV} in three directions, turning duration, and peed) and subjective factors (sum of comfort ratings of all participants). All variables were standardized (by subtracting its mean then divided by the standard deviation of the variable to have mean = 0 and sd = 1) resulting in the Pearson's r is equivalent to standardized coefficients or

beta coefficients β as the slope of the linear regression line (Asuero et al., 2006; Rodgers and Nicewander, 2006).

In general, p-value is more significant for a_y and duration than jerk, speed and a_{wY}. The strength and positive direction of linear relationship can also be found between SumComfort and a_y and duration (β ≥ 0.5, p < 0.001***). The weaker linear relationship in a positive direction is found between SumComfort with jerk, and a_{wY} (β < 0.5, p < 0.05*). Fig. 5b further shows the results of linear regression between Sum-Comfort (dependent variable) and objective factors (independent variables). Again, the results confirmed that lateral acceleration (coefficient = 2.01, p < 0.001***) has the strongest influence on the discomfort rating of passengers than the duration of turning movements
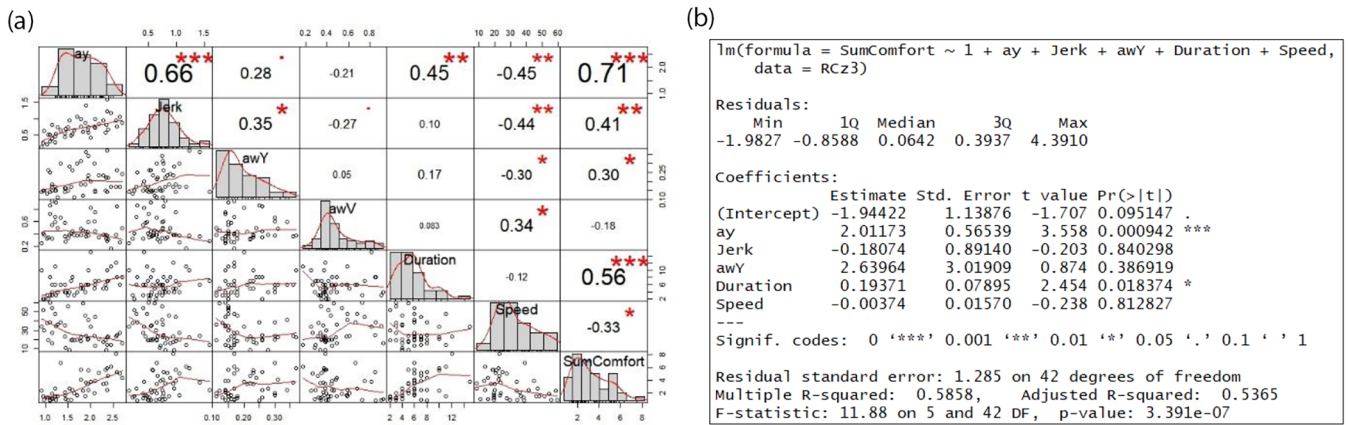
(a)

(b)

```
lm(formula = SumComfort ~ 1 + ay + Jerk + awY + Duration + Speed,
    data = RCz3)

Residuals:
    Min      1Q   Median      3Q     Max
-1.9827 -0.8588  0.0642  0.3937  4.3910

Coefficients:
            Estimate Std. Error t value Pr(>|t|)
(Intercept) -1.94422    1.13876  -1.707 0.095147 .
ay           2.01173    0.56539   3.558 0.000942 ***
Jerk        -0.18074    0.89140  -0.203 0.840298
awY          2.63964    3.01909   0.874 0.386919
Duration     0.19371    0.07895   2.454 0.018374 *
Speed       -0.00374    0.01570  -0.238 0.812827
---
Signif. codes:  0 '***' 0.001 '**' 0.01 '*' 0.05 '.' 0.1 ' ' 1

Residual standard error: 1.285 on 42 degrees of freedom
Multiple R-squared: 0.5858,    Adjusted R-squared: 0.5365
F-statistic: 11.88 on 5 and 42 DF,  p-value: 3.391e-07
```

Fig. 5. (a) Correlation analysis after standardization showing Pearson's r (or beta coefficient β) for objective factors and SumComfort, (b) linear regression between SumComfort and objective factors.

Table 3
Standardized regression coefficient β between subjective factors and objective factors.

	Posture			Gender		Facing			Position		
	Sitting	Leaning	Standing	Female	Male	Forwards	Backwards	Sideways	Front	Middle	Rear
SumComfort	0.68***	0.82***	0.89***	0.87***	0.86***	0.79***	0.85***	0.65***	0.73***	0.86***	0.50***
a_y	0.45*	0.64***	0.61***	0.61***	0.62***	0.70***	0.58***	0.41*	0.48**	0.69***	0.22
Duration	0.40*	0.33*	0.60***	0.47**	0.5**	0.53***	0.35*	0.49**	0.40*	0.47**	0.32*
Jerk	0.23	0.26	0.46*	0.28	0.44*	0.38*	0.24	0.40*	0.38*	0.40*	−0.06

* p < 0.05,
** p < 0.01,
*** p < 0.001.

(coefficient = 0.19, p < 0.05*) and lateral jerks (coefficient = -0.18, p = 0.84 > 0.05). Due to not significant correlation of the intercept, jerk, a_{wY} and speed, they can be left out of the linear regression model.

Furthermore, the factor loading can be interpreted from standardized regression coefficient β for which each subjective factor (comfort rating of individual group: sitting, leaning, standing; gender: female and male; facing: forward, backward, sideways; and location: front, middle, rear of the bus) contributes to the SumComfort. All data related to subjective is normalised per subject by an averaging process to mitigate the cumulative effects of participant number. The results in Table 3 have affirmed that standing is the most uncomfortable posture compared to sitting and leaning with the highest beta with SumComfort (β = 0.89 > 0.82, 0.68; p < 0.001***), duration (β = 0.60 > 0.33, 0.40) and jerk (β = 0.46 > 0.26, 0.23); and second highest with a_y (0.64 > β = 0.61 > 0.45). Also, duration has higher beta and lower p-value (more significant) than jerk across all pairs, which was explored by the linear regression analysis (Fig. 5). There is not different in gender regarding comfortable ratings for almost all correlation factors. Middle position is the least comfortable part onboard the bus (β = 0.86 > 0.73, 0.50; β = 0.69 > 0.48, 0.22 in the correlation with SumComfort and a_y, respectively), which is easily understandable that this is where all standing participants are located. Facing backward is the least comfortable position (β = 0.85 > 0.79, 0.65 in the correlation with SumComfort).

4.3. Ride discomfort threshold for bus passengers

A second bus run, using a different route and on a weekday, was conducted to obtain additional passengers' ratings. In this case, fewer participants (6 sitting, 4 leaning and 1 standing) were included to minimise interaction with crowded passengers during weekday operation. Bus interior is the same design and all the experimental procedures were the same as the first run. From the 2 experimental bus runs,

258 data samples were collected in total from 34 responded participants (17 sitting, 9 leaning and 8 standing) as shown in Table 4 and Fig. 6. These data samples were used for classification analysis using boxplot as described in the following section. Concerning the distribution of age groups, there are in total 20 participants in the "early working age" (from 15 to 21 years old) and 14 participants in the "prime working age" (from 25 to 54 years old), who are frequently travelling and commuting using bus transport service during the peak periods.

As shown in Table 4 and Fig. 6, level 5 rating contains the fewest data samples, but it is understandable that the extremely sharp turning movement does not happen frequently. The discomfort thresholds are slightly different among the 3 posture groups. Standing and leaning participants start to feel uncomfortable at $a_y = 1.5\,\text{m/s}^2$ while sitting participants is at $a_y = 1.55\,\text{m/s}^2$. At $a_y = 1.75\,\text{m/s}^2$, standing participants feel extremely uncomfortable while leaning participants feel very uncomfortable, but sitting participants' perception is still in uncomfortable level. The extremely uncomfortable rating was not observed from sitting participants. The effects of turning duration (range of 5–8 s) and lateral jerk (range of 0.6–0.9 m/s³) are clearly not proportional to different levels of ride discomfort.

The objective indicators were inferred from the median value of the boxplot with the main focus on lateral acceleration which has the most significant correlation with subjective ratings as noted in the investigation in the linear regression model (Fig. 5). The ride discomfort was further characterised by three individual levels: *Uncomfortable, Very Uncomfortable, and Extremely Uncomfortable)*. Average lateral accelerations of $a_y = 1.5$, 1.75 and $2.0\,\text{m/s}^2$ were found for three thresholds, respectively. Fig. 6 shows the boxplots overlain with original data points in which the distribution of data in the box-plot diagram was presented after removing all outliers beyond the upper limit and lower limit.

Table 4
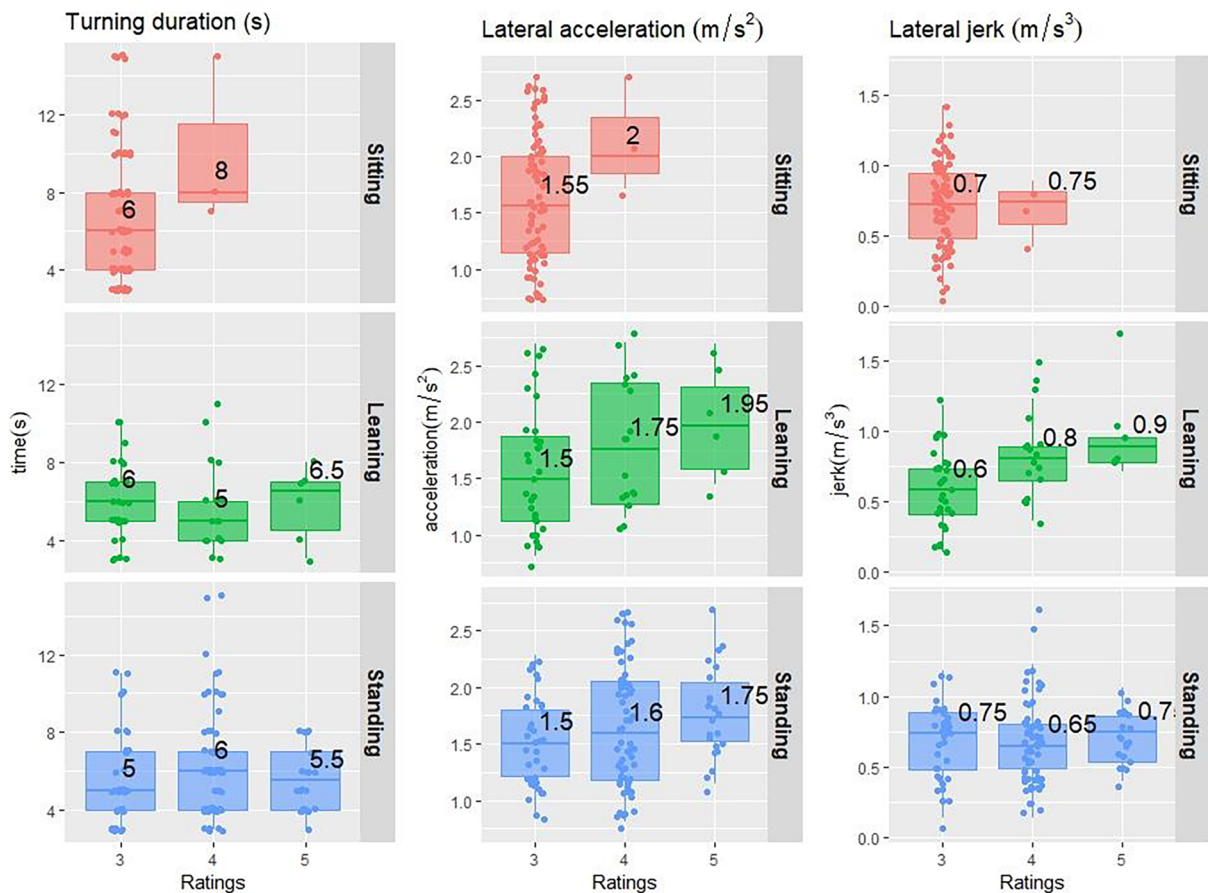Ride discomfort threshold classification.

	Discomfort (3)	Great Discomfort (4)	Extreme Discomfort (5)	Sum of samples
Sitting (samples)	79	3	0	82
Leaning (samples)	31	17	6	54
Standing (samples)	37	63	22	122
Median (standard deviation):				
Turning duration (s)	5 (2)	6 (2.5)	7 (3)	
Lateral acceleration (m/s^2)	1.5 (0.4)	1.75 (0.5)	2.0 (0.5)	
Lateral jerk (m/s^3)	0.6 (0.2)	0.75 (0.3)	0.9 (0.3)	

5. Discussion

The linear regression model (Fig. 5b) expresses the relationship between subjective ratings with lateral acceleration and duration of turning movement, with adjusted $R^2 = 0.54$. This shows that lateral acceleration as well as duration of turning movement are important factors that affect ride comfort of bus passengers. The intercept, jerk, a_{wY} and speed can be left out of model since they are not statistically significant (p-value > 0.05). The low adjusted R^2 can be explained by other human factors that were not taken into account such as: the inconsistency of ratings (even for the same lateral acceleration but a participant mistakenly pressed a different button), the interaction during bus run (normal passengers boarded and interacted with participants), tiredness during the 45-min bus run and other factors. For example, participant A02 pressed 59 times on an uncomfortable level and 5 times on a very uncomfortable level, but he evaluated the overall ride comfort as being not uncomfortable. The main reason is that he compared and considered this bus run as "the best ride in his entire 6 years". This contrasted with C02 when she pressed 40 times on not uncomfortable and little uncomfortable, but the overall ride comfort was uncomfortable. This is the outcome of "tired standing up the whole time" as her comments. In fact, in human behavioural science, R^2 as low as 0.59 is considered good (strong to very strong) since humans are harder to predict than physical processes (Harms and Groen, 2017; Lemke et al., 2016; Sawaya et al., 2017; Van den Bulck et al., 2018). The primary goal for this model is not to predict the dependent variable but it is an intermediate step to investigate the relationship between the subjective factor and objective factors (Moksony, 1990).

Regarding three levels of ride discomfort, the *discomfort* threshold at $a_y = 1.5 \, m/s^2$ is similar to $max(a_y) = 1.4 \, m/s^2$ when passengers feel uncomfortable; and the *extreme discomfort* threshold $a_y = 2.0 \, m/s^2$ is the same as $max(a_y) = 2.0 \, m/s^2$ when there is the start of balance loss, as compared to the study in (Beurier, 2012). The average lateral jerks $d_y = 0.6; 0.75$ and $0.9 \, m/s^3$ in 3 discomfort levels are within the range

Fig. 6. Classification of lateral ride discomfort levels when the bus is turning. The box-plot diagram, after removing outliers beyond the upper and lower limit, is overlaid with original data points.

from 0.3 to 0.9 m/s³ as an empirical value for ride comfort and safety recommended in (AASHTO, 2011) for the design of spiral transition curves. Such consistency has demonstrated the fidelity and relevance of the methodology and devices used in this study. It is noted that the exact S value of subjective ratings of passengers would not be replicable in future experiments due to the inherence of field study. However, the objective indicators (lateral acceleration, later jerk and duration of turning movements) associated with 3 levels of ride discomfort will be unchanged or be only slightly different.

Besides the collected objective indicators (acceleration, jerk and time duration), the maximum root-mean-square value of frequency-weighted lateral accelerations (a_{wy}) within the 48 turning movements were also calculated according to (ISO2631-1, 1997). The $a_{wy} = 0.11–0.37$ m/s² is in the range of "not uncomfortable" to "a little uncomfortable" and did not correspond well with the rated levels of discomfort. Therefore, this a_{wy} index is not suitable for evaluating the ride comfort of bus passengers within the turning movements. The main reason is that lateral sway within turning movements does not occur as frequently as vibration which causes discomfort to passengers (frequency from 0.5 Hz to 80 Hz). The lateral sway at very low-frequency oscillation from 0.1 Hz to 0.5 Hz (or even lower) is, hence, more related to motion sickness. This is probably the reason why (Bodini et al., 2013; Maternini and Cadei, 2014) studied the adaptation of railway ride comfort thresholds for application to roadway public transport. The more appropriate ride comfort scale in (ISO2631-1, 1997) for vertical acceleration rather than longitudinal and transversal directions was also investigation in (Castellanos and Fruett, 2014) or the experiment for bus driver by Fichera et al. (2007).

6. Conclusions and outlook

A full-scale experimental study has been conducted with 34 responded passengers (over 37 invited participants) onboard buses to establish lateral ride discomfort thresholds for bus passengers in an urban road context. Standing passengers experience much more discomfort levels than sitting and leaning groups. Facing backwards and middle location on bus are also associated with high uncomfortable ride. Turning movements are associated with 3 levels of discomfort (*Uncomfortable, Very Uncomfortable and Extremely Uncomfortable*), which were defined based on the relation between passengers' ratings and lateral acceleration, lateral jerk and duration of the turning movements from a linear multiple regression. The a_{wy} index is not consistent with that of (ISO2631-1, 1997) as related to human whole-body vibration. The main findings of the three levels of ride comfort thresholds of bus passengers will assist bus drivers in their driving behaviours to ensure passengers' ride comfort as well as to design the speed and acceleration profiles of autonomous vehicles given the state-of-the-art steering control along vehicle trajectories (Kozłowski et al., 2015; Tan and Huang, 2014).

The three levels of lateral acceleration (a_y) in Table 4 can be used for back-calculation of APT speed (V in km/h) based on turning movements and curved radius (R in m): $V = 3.6\sqrt{a_y R}$. This estimation is inferred from the basic equation that governs vehicle operation on a curve following the laws of mechanics (AASHTO, 2011). The effects of a lateral jerk and turning duration have been neglected in this simple back-calculation (Le Vine et al., 2015). The proposed speeds can be used as the speed limit for APT timetable planning as well as for APT operation along the network to ensure passengers' ride comfort. The logic is that for new innovative APT systems, passengers' locations and orientation can be easily detected by sensors which, coupled with the development of navigation technology, APT will be able to detect road geometry, curves and turning movement trajectory at any location along its route. Therefore, the vehicle speeds at discomfort threshold (uncomfortable at $a_y = 1.5$ m/s²) could be suggested when there is a high number of standing passengers while the vehicle speeds at great discomfort threshold (very uncomfortable at $a_y = 1.75$ m/s²) could be

suggested in case of all seated passengers. In any case, the vehicle speeds at extreme discomfort threshold (extremely uncomfortable at $a_y = 2.0$ m/s²) must be avoided. The lower bound discomfort threshold is similar to railway ride quality (LRT) when considering leisurely or productive activities as for driver and passenger comfort in case of autonomous cars (Le Vine et al., 2015).

The new method of using a smart-phone application to collect passengers' responses has demonstrated its ability to cover a large number of subjects on the same bus run. As a result, the correlation between ride discomfort with lateral acceleration and turning movement duration has been established. This is different from the previous study by Beurier (2012) when pressing buttons were assembled in the bus vehicle body that limits the number of subjects as well as requiring the engineering input of bus manufacturers. Furthermore, the smart-phone application enables the capture of real-time discomfort feelings of passengers which is advantageous than the questionnaire method in the previous study (He et al., 2013). The usage of the portable seat-pad accelerometer in this study does not require the interference with Controller Area Network (CAN bus) system as often used in traditional methods (Bodini et al., 2013; Maternini and Cadei, 2014).

Regarding bus interior design, there are points of improvement towards passenger-centred design such as ergonomics aspects of expansion of seat width and legroom space (Park et al., 2014; UITP, 2008); provision of more leaning surfaces, more accessible grip support in every part of the vehicle as in findings (Beurier, 2012). Furthermore, there are other interior design features that can be configured to improve ride comfort by providing Wifi network, charging ports, and trip information announcements (Beirão and Sarsfield Cabral, 2007; Daimler Global Media Site, 2019).

While this study has provided important insights into the lateral ride discomfort of young-adult bus passenger onboard, several limitations need to be acknowledged. First, the case study was conducted with two bus runs in an urban road context with a small sample size, good vehicle conditions, very good road surface and good driving manoeuvres of the bus driver. The study is at first designed to target the young-adult participants in the "early working age" and "prime working age" groups, who are frequently travelling and commuting using bus transport service during the peak periods (also the more congested periods). The missing "mature working age" group can be a target for further study. Second, the level of passenger ride comfort can vary in other countries, particularly in Europe or America. Further research can be extended to cover larger sample sizes, age groups, and research contexts based on the method developed in this case study. Recently, Volvo launched the "world first" driverless electric bus in Singapore with a capacity of 80 passengers per bus as regular transit (CNA, 2019), which is a potential scenario to extend the experiment once the AB opens for public use. A comparison study between two scenarios: conventional bus and AB, will be expected to gain interesting results on passenger ride comfort on the real AB as the research gap pointed by Le Vine et al. (2015).

Lastly, the further study will also focus more on the application of the three ride discomfort thresholds in other bus routes to detect high uncomfortable locations for diagnosing bus drivers' driving behaviour such as in-vehicle telematics system of Tower Transit (Koh, 2017). Thus, a new ride discomfort warning mobile application can be designed based on the proposed ride discomfort thresholds and the ratio of standing passengers on the bus shall be established as an input, especially during peak hours.

Conflict of interest

The authors declare that they have no competing interests.

Appendix A. Supplementary data

Supplementary data to this article can be found online at https://doi.org/10.1016/j.cstp.2019.07.002.

References

AASHTO, 2011. A Policy on Geometric Design of Highways and Streets, 6th ed. American Association of State Highway and Transportation Officials, Washington, DC.

ARUP, 2017. Guided Busway Design Handbook. The British Cementitious Paving Association, Wokingham, Berkshire.

Asociación RUVID, 2012. Safety of standing passengers in urban buses [WWW Document]. ScienceDaily. URL www.sciencedaily.com/releases/2012/10/121022080357.htm (accessed 5.11.19).

Asuero, A.G., Sayago, A., González, A.G., 2006. The correlation coefficient: an overview. Crit. Rev. Anal. Chem. 36, 41–59. https://doi.org/10.1080/10408340500526766.

Beirão, G., Sarsfield Cabral, J.A., 2007. Understanding attitudes towards public transport and private car: a qualitative study. Transp. Policy 14, 478–489. https://doi.org/10.1016/j.tranpol.2007.04.009.

Beurier, G., 2012. Analysis of the discomfort feeling of standing bus passengers on the TEOR T1 Rouen bus lane. Procedia - Soc. Behav. Sci. 48, 425–434. https://doi.org/10.1016/j.sbspro.2012.06.1022.

Bodini, I., Lancini, M., Pasinetti, S., Vetturi, D., 2013. Techniques for on-board vibrational passenger comfort monitoring in public transport. 12th IMEKO TC10 Work. Tech. Diagnostics New Perspect. Meas. Tools Tech. Ind. Appl. Proc. 3, 118–123.

Bogren, L., Fallman, D., Henje, C., 2009. User-centered inclusive design: making public transport accessible. International Conference on Inclusive Design-Royal College of Art.

BS 6841:1987, 1999. Measurement and Evaluation of Human Exposure to Whole-Body Mechanical Vibration and Repeated Shock. British Standards Institution.

BS EN 12299:2009, 2009. Railway Applications – Ride Comfort for Passengers – Measurement and Evaluation. British Standards Institution.

Cao, Z., Ceder, A., 2019. Autonomous shuttle bus service timetabling and vehicle scheduling using skip-stop tactic. Transp. Res. Part C Emerg. Technol. 102, 370–395. https://doi.org/10.1016/j.trc.2019.03.018.

Castellanos, J.C., Fruett, F., 2014. Embedded system to evaluate the passenger comfort in public transportation based on dynamical vehicle behavior with user's feedback. Meas. J. Int. Meas. Confed. 47, 442–451. https://doi.org/10.1016/j.measurement.2013.08.068.

CNA, 2019. Driverless electric bus launched by NTU and Volvo in "world first" [WWW Document]. CNA. URL https://www.channelnewsasia.com/news/singapore/driverless-electric-bus-launched-by-ntu-and-volvo-in-world-first-11311838 (accessed 4.23.19).

Da Silva, M.C.G., 2002. Measurements of comfort in vehicles. Meas. Sci. Technol. 13, R41–R60.

Daimler Global Media Site, 2019. World premiere:Mercedes-Benz Future Bus with CityPilot – a milestone on the way to the autonomous city bus, and a revolutionary mobility system for the future [WWW Document]. Daimler. URL https://media.daimler.com/marsMediaSite/ko/en/12776336 (accessed 5.14.19).

Eboli, L., Mazzulla, G., Pungillo, G., 2016. Measuring bus comfort levels by using acceleration instantaneous values. Transp. Res. Procedia 18, 27–34. https://doi.org/10.1016/j.trpro.2016.12.004.

Fichera, G., Scionti, M., Garescì, F., 2007. Experimental correlation between the road roughness and the comfort perceived in bus cabins. SAE Trans. https://doi.org/10.4271/2007-01-0352.

Ginn, M., Amuna, F., Colmenares, J.E., Stewart, A., Diong, B., Wang, Y., Yang, J., 2017. Conceptual design and prototyping of a slim semi-autonomous bus rapid transit vehicle. Conf. Proc. – IEEE SOUTHEASTCON. IEEE 1–6. https://doi.org/10.1109/SECON.2017.7925292.

Harms, R., Groen, A., 2017. Loosen up? Cultural tightness and national entrepreneurial activity. Technol. Forecast. Soc. Change 121, 196–204. https://doi.org/10.1016/j.techfore.2016.04.013.

He, Y., Yan, X., Wu, C., Chu, D., Peng, L., 2013. Effects of driver's unsafe acceleration behaviors on passengers' comfort for coach buses. Improv. Multimodal Transp. Syst. Safety, Integr. https://doi.org/10.1061/9780784413036.220.

Imre, Ş., Çelebi, D., 2017. Measuring comfort in public transport: a case study for İstanbul. Transp. Res. Procedia 25, 2441–2449. https://doi.org/10.1016/j.trpro.2017.05.261.

ISO2631-1, 1997. Mechanical Vibration and Shock – Evaluation of Human Exposure to Whole-Body Vibration (Part 1: General Requirements). International Organization for Standardization, Switzerland.

Koh, V., 2017. Device on Tower Transit buses helps cut down bad driving habits, accidents [WWW Document]. TODAY online. URL https://www.todayonline.com/singapore/device-tower-transit-buses-helps-cut-down-bad-driving-habits-accidents (accessed 5.14.19).

Kowarska, I., Korta, J., Kuczek, K., Uhl, T., 2014. Fully equipped dynamic model of a bus. Shock Vib. 2014. https://doi.org/10.1155/2014/201952.

Kozłowski, M., Choromański, W., Kowara, J., 2015. Analysis of dynamic properties of the PRT vehicle-track system. Bull. Polish Acad. Sci. Tech. Sci. 63, 799–806. https://doi.org/10.1515/bpasts-2015-0091.

Lai, W.T., Chen, C.F., 2011. Behavioral intentions of public transit passengers-the roles of service quality, perceived value, satisfaction and involvement. Transp. Policy 18, 318–325. https://doi.org/10.1016/j.tranpol.2010.09.003.

Lam, S., Katupitiya, J., 2013. Modeling and control of a platoon of autonomous buses. IEEE Intell. Veh. Symp., Proc. IEEE 958–963. https://doi.org/10.1109/IVS.2013.6629590.

Land Transport Guru, 2019. Land Transport Guru - Singapore Transport Information at a glance! [WWW Document]. L. Transp. Guru. URL https://landtransportguru.net/ (accessed 5.14.19).

Le Vine, S., Zolfaghari, A., Polak, J., 2015. Autonomous cars: the tension between occupant experience and intersection capacity. Transp. Res. Part C Emerg. Technol. 52, 1–14. https://doi.org/10.1016/j.trc.2015.01.002.

Lemke, M.K., Apostolopoulos, Y., Hege, A., Sönmez, S., Wideman, L., 2016. Understanding the role of sleep quality and sleep duration in commercial driving safety. Accid. Anal. Prev. 97, 79–86. https://doi.org/10.1016/j.aap.2016.08.024.

Lin, C.-Y., Chen, L.-J., Chen, Y.-Y., Lee, W.-C., 2010. A comfort measuring system for public transportation systems using participatory phone sensing. Proceedings of PhoneSense.

LTA, 2013. Land Transport Master Plan 2013. Land Transport Authorithy Singapore, Singapore.

Mah, S., Mitra, R., 2017. The effects of a free bus program on older adults travel behaviour: a case study of a Canadian suburban municipality. Case Stud. Transp. Policy 5, 460–466. https://doi.org/10.1016/j.cstp.2017.05.003.

Maternini, G., Cadei, M., 2014. A comfort scale for standing bus passengers in relation to certain road characteristics. Transp. Lett. Int. J. Transp. Res. 6, 136–141. https://doi.org/10.1179/1942787514y.0000000020.

Mercedes-Benz, 2002. Technical Information The New Citaro, Mercedes-Benz. Mercedes-Benz, Mannheim, Germany.

Mitchell, D., Claris, S., Edge, D., 2016. Human-centered mobility: a new approach to designing and improving our urban transport infrastructure. Engineering 2, 33–36. https://doi.org/10.1016/j.eng.2016.01.030.

Moksony, F., 1990. Small is beautiful: the use and interpretation of R2 in social research. Szociológiai Szle 130–138.

Montes, H., Salinas, C., Fernández, R., Armada, M., 2017. An experimental platform for autonomous bus development. Appl. Sci. 7, 1131. https://doi.org/10.3390/app7111131.

Morton, C., Caulfield, B., Anable, J., 2016. Customer perceptions of quality of service in public transport: evidence for bus transit in Scotland. Case Stud. Transp. Policy 4, 199–207.

Mucka, P., 2015. Road roughness limit values based on measured vehicle vibration. J. Infrastruct. Syst. 23, 1–13. https://doi.org/10.1061/(ASCE)IS.1943-555X.0000325.

Nawayseh, N., Griffin, M.J., 2006. Effect of frequency, magnitude and direction of translational and rotational oscillation on the postural stability of standing people. J. Sound Vib. 298, 725–754. https://doi.org/10.1016/j.jsv.2006.06.027.

Nguyen-Phuoc, D.Q., Currie, G., De Gruyter, C., Kim, I., Young, W., 2018a. Modelling the net traffic congestion impact of bus operations in Melbourne. Transp. Res. Part A Policy Pract. 117, 1–12. https://doi.org/10.1016/j.tra.2018.08.005.

Nguyen-Phuoc, D.Q., Currie, G., De Gruyter, C., Young, W., 2018b. Congestion relief and public transport: an enhanced method using disaggregate mode shift evidence. Case Stud. Transp. Policy 6, 518–528. https://doi.org/10.1016/j.cstp.2018.06.012.

Park, J., Lee, H., Choi, Y., Park, K., Kim, M., You, H., 2014. Development of an ergonomic bus seat profile design guideline. In: Proceedings of the Human Factors and Ergonomics Society, pp. 1825–1828. https://doi.org/10.1177/1541931214581382.

Parsons Brinckerhoff, I., 2012. Transit cooperative research program report #155: track design handbook for light rail transit (Second edition). https://doi.org/10.17226/22800.

Parsons Brinckerhoff, I., 2009. Technical Memorandum: Alignment Design Standards for High-Speed Train Operation. California High-Speed Rail Authority, California.

Portouli, E., Karaseitanidis, G., Lytrivis, P., Amditis, A., Raptis, O., Karaberi, C., 2017. Public attitudes towards autonomous mini buses operating in real conditions in a Hellenic city. IEEE Intell. Veh. Symp. Proc. 571–576. https://doi.org/10.1109/IVS.2017.7995779.

Prashanth, A.S., Saran, V.H., Harsha, S.P., 2013. Study of subjective responses on ride comfort in public transport Uttarakhand State buses. 1st Int. 16th Natl. Conf. Mach. Mech. 236–240.

PTC, 2017. Commuter Satisfaction with Public Transport Continues to Improve. Public Transport Council, Singapore, Singapore.

PTC, 2016. Commuters at Heart on Recommendations to Improve Commuter's Journey. Public Transport Council, Singapore, Singapore.

Rau, A., Tian, L., Jain, M., Xie, M., Liu, T., 2018. Autonomous road transit (DART) for use-case capacity more than bus. Mobil.TUM 2018 "Urban Mobility – Shaping the Future Together" – International Scientific Conference on Mobility and Transport.

Robert, T., Beillas, P., Maupas, A., Verriest, J.P., 2007. Conditions of possible head impacts for standing passengers in public transportation: an experimental study. Int. J. Crashworthiness 12, 319–327. https://doi.org/10.1080/13588260701433552.

Rodgers, J.L., Nicewander, W.A., 2006. Thirteen ways to look at the correlation coefficient. Am. Stat. 42, 59. https://doi.org/10.2307/2685263.

Salonen, A.O., 2018. Passenger's subjective traffic safety, in-vehicle security and emergency management in the driverless shuttle bus in Finland. Transp. Policy 61, 106–110. https://doi.org/10.1016/j.tranpol.2017.10.011.

Sam, E.F., Hamidu, O., Daniels, S., 2018. SERVQUAL analysis of public bus transport services in Kumasi metropolis, Ghana: core user perspectives. Case Stud. Transp. Policy 6, 25–31. https://doi.org/10.1016/j.cstp.2017.12.004.

Sawaya, Y., Sharif, M., Christin, N., Kubota, A., 2017. Self-confidence trumps knowledge:

a cross-cultural study of security behavior. Proc. CHI Conf. Hum. Factors Comput. Syst. 2202–2214. https://doi.org/10.1145/3025453.3025926.

Sekulić, D., Rusov, S., Dedović, V., Šalinić, S., Mladenović, D., Ivković, I., 2018. Analysis of bus users' vibration exposure time. Int. J. Ind. Ergon. 65, 26–35. https://doi.org/10.1016/j.ergon.2018.01.017.

Shen, X., Feng, S., Li, Z., Hu, B., 2016. Analysis of bus passenger comfort perception based on passenger load factor and in-vehicle time. Springerplus 5, 62. https://doi.org/10.1186/s40064-016-1694-7.

Shu, H.B., Shao, Y.M., Lin, W., Xu, J., 2016. Computation-based dynamic driving simulation for evaluation of mountain roads with complex shapes: a case study. Procedia Eng. 137, 210–219. https://doi.org/10.1016/j.proeng.2016.01.252.

Stjernborg, V., Mattisson, O., 2016. The role of public transport in society – a case study of general policy documents in Sweden. Sustainability 8, 1–16. https://doi.org/10.3390/su8111120.

Tan, H.S., Huang, J., 2014. Design of a high-performance automatic steering controller for bus revenue service based on how drivers steer. IEEE Trans. Robot. 30, 1137–1147. https://doi.org/10.1109/TRO.2014.2331092.

Tan, J.Y., 2013. International roughness index – concept and application in Singapore. Singapore Symposium on Pavement Technology (SPT 2013).

Thuong, O., Griffin, M.J., 2012. The vibration discomfort of standing people: relative importance of fore-and-aft, lateral, and vertical vibration. Appl. Ergon. 43, 902–908. https://doi.org/10.1016/j.apergo.2011.12.011.

UITP, 2008. EBSF: Designing the Future of the Bus. The International Association of Public Transport (UITP).

Van den Bulck, S.A., Hermens, R., Slegers, K., Vandenberghe, B., Goderis, G., Vankrunkelsven, P., 2018. Designing a patient portal for patient-centered care: cross-sectional survey. J. Med. Internet Res. 20, e269. https://doi.org/10.2196/jmir.9497.

Xu, J., Yang, K., Shao, Y., Lu, G., 2015. An experimental study on lateral acceleration of cars in different environments in Sichuan, Southwest China 2015.

Yu, L., Kong, D., Yan, X., 2018. A driving behavior planning and trajectory generation method for autonomous electric bus. Future Internet 10. https://doi.org/10.3390/fi10060051.

Zhang, K., Zhou, K., Zhang, F., 2014. Evaluating bus transit performance of Chinese cities: developing an overall bus comfort model. Transp. Res. Part A Policy Pract. 69, 105–112. https://doi.org/10.1016/j.tra.2014.08.020.

Zhang, W., Jenelius, E., Badia, H., 2019. Efficiency of semi-autonomous and fully autonomous bus services in trunk-and-branches networks. J. Adv. Transp. 2019, 1–17. https://doi.org/10.1155/2019/7648735.

Appendix 5: Paper V

Nguyen, T., Xie, M., Liu, X., Arunachalam, N., Rau, A., Lechner, B., Busch, F., & Wong, Y.D (2019). Platooning of autonomous public transport vehicles: The influence of ride comfort on travel delay. Sustainability 2019, 11(19), 5237, doi: https://doi.org/10.3390/su11195237.

Article

Platooning of Autonomous Public Transport Vehicles: The Influence of Ride Comfort on Travel Delay

Teron Nguyen [1,2,3,*] **, Meng Xie** [2] **, Xiaodong Liu** [2] **, Nimal Arunachalam** [2] **, Andreas Rau** [2] **, Bernhard Lechner** [1] **, Fritz Busch** [4] **and Y. D. Wong** [3]

[1] Institute of Road, Railway and Airfield Construction, Technical University of Munich, Baumbachstr. 7, 81245 Munich, Germany; bernhard.lechner@tum.de

[2] Rapid Road Transport, TUMCREATE Ltd., 1 Create Way, #10-02 CREATE Tower, Singapore 138602, Singapore; meng.xie@tum-create.edu.sg (M.X.); xiaodong.liu@tum-create.edu.sg (X.L.); nimal.arunachalam@tum-create.edu.sg (N.A.); andreas.rau@tum-create.edu.sg (A.R.)

[3] Centre for Infrastructure Systems, Nanyang Technological University, N1-01b-51, 50 Nanyang Avenue, Singapore 639798, Singapore; CYDWONG@ntu.edu.sg

[4] Chair of Traffic Engineering and Control, Technical University of Munich, Arcisstr. 21, 80333 Munich, Germany; fritz.busch@tum.de

*** Correspondence: teron.nguyen@tum-create.edu.sg or teron.nguyen@tum.de; Tel.: +65-8376-1636

check for updates

Abstract: The development of advanced technologies has led to the emergence of autonomous vehicles. Herein, autonomous public transport (APT) systems equipped with prioritization measures are being designed to operate at ever faster speeds compared to conventional buses. Innovative APT systems are configured to accommodate prevailing passenger demand for peak as well as non-peak periods, by electronic coupling and decoupling of platooned units along travel corridors, such as the dynamic autonomous road transit (DART) system being researched in Singapore. However, there is always the trade-off between high vehicle speed versus passenger ride comfort, especially lateral ride comfort. This study analyses a new APT system within the urban context and evaluates its performance using microscopic traffic simulation. The platooning protocol of autonomous vehicles was first developed for simulating the coupling/decoupling process. Platooning performance was then simulated on VISSIM platform for various scenarios to compare the performance of DART platooning under several ride comfort levels: three bus comfort and two railway criteria. The study revealed that it is feasible to operate the DART system following the bus standing comfort criterion ($a_y = 1.5$ m/s^2) without any significant impact on system travel time. For the DART system operating to maintain a ride comfort of the high-speed train (HST) and light rail transit (LRT), the delay can constitute up to $\approx 10\%$ and $\approx 5\%$ of travel time, respectively. This investigation is crucial for the system delay management towards precisely designed service frequency and improved passenger ride comfort.

Keywords: autonomous public transport; passenger ride comfort; travel time; horizontal alignment; microscopic traffic simulation

1. Introduction

The emergence of autonomous vehicles (AVs) has engendered innovative solutions for traffic congestion mitigation as well as the improvement of the passenger riding experience. The traveling public can expect level 5 full automation in more than 50% of vehicles by 2030 [1]. Herein, AVs can be readily operated as platoons on the streets with minimum gaps between individual AVs, thereby resulting in a significant increase of road capacity and improving fuel economy [2]. On the other

hand, by eliminating the driving tasks, vehicle occupants (drivers and passengers) can utilize on-board traveling time for activities such as reading, chatting or even working [3,4], which is expected to increase the productivity and enable other activities to be executed within a day [5]. For example, commuter services in motion are designed for NEXT's modular self-driving vehicles with built prototypes of autonomous pods in Dubai [6]. To achieve efficient mobility services, AV platooning in which consecutive vehicles conjugate as a road-train on the street is a good solution.

As for the on-road autonomous public transport (APT) system, which is a public transport mode that can guide itself without human conduction, there is a trend of connecting singular modules to form platoons on the road. This is the latest advance after the well-developed and implemented car platooning [7] and truck platooning [8] where a number of vehicles are traveling together and electronically connected. For example, recent research at TUMCREATE in Singapore is aimed at developing a dynamic autonomous road transit (DART) system at a much higher journey speed of autonomous bus (AB) platoons (at an average speed of 28km/h) than conventional buses (at an average speed of 19km/h) to offer a higher capacity level [9]. With a vehicle module of 6m length, 3.1 m height, 2.7 m width, and capacity of 30 passengers/module, the DART system is designed to flexibly adapt to passenger demand by electronically-linked platoons of the vehicles/modules on shared route segments and to decouple for route divergence. Relevant studies have been conducted focusing on scheduled platoon planning [10], fleet size estimation [11], and the deployment framework [12]. Similar high-speed platooning public transport can be found in Dubai under testing [6,13,14] as well as autonomous rail rapid transit in China (see Figure 1).
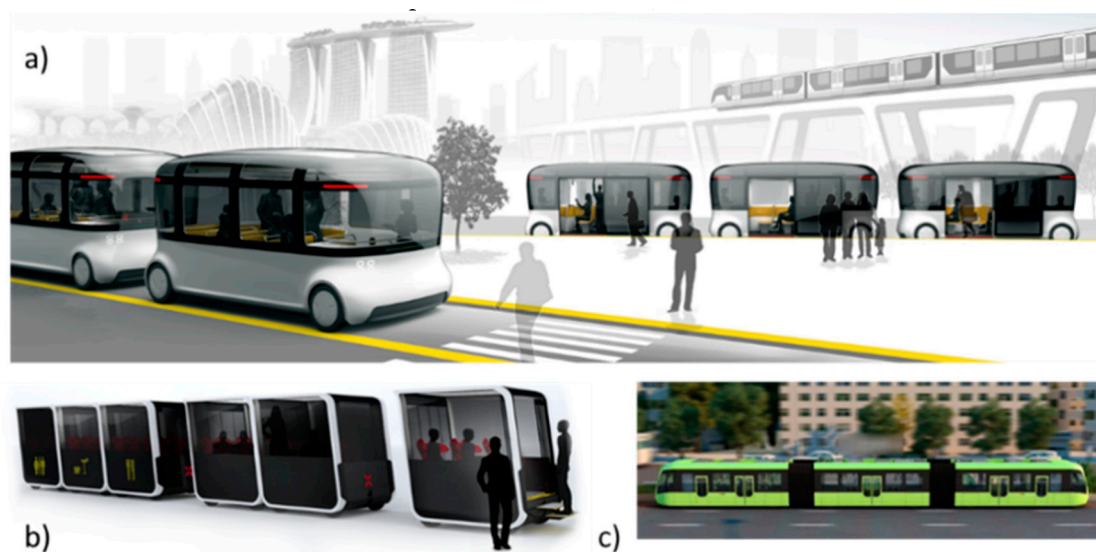
Figure 1. Examples of autonomous public transport (APT) platooning in (**a**) Singapore, source: https://www.tum-create.edu.sg/; (**b**) NEXT's modular self-driving vehicles designed in Dubai, source: http://www.next-future-mobility.com/; and (**c**) Autonomous rail rapid transit in China, source: http://www.crrcgc.cc/zzs.

Although automation may bring down the driver-cost in dense networks such as the urban context, the requirements of the schedule, fleet size, and route optimization are also raised [15]. The application of APT platooning in a large-scale operation has required a new concept in order to maintain a fixed timetabling frequency, e.g., every 5 minutes, for passenger transport. This is different from car platooning for private use or truck platooning for freight transport. Any deviation is expected to affect the system performance regarding travel time and speed, which reduces the whole APT system's reliability. Thus far, recent studies have focused on technological developments and often ignore the human factors which are of utmost importance in attracting car users to use public transport. The vehicle speeds are affected by various factors such as road geometrics, vehicle

performance and environmental conditions [16]. Considerably higher travel speeds are designed for the abovementioned APT systems (see Figure 1). However, there is always the trade-off between vehicle speed against rider comfort induced by the acceleration from the road surface/alignment and braking/accelerating. Hence, it is difficult to achieve ride comfort levels similar to high-speed trains (HST) and light rail transit (LRT), especially in a dense urban network with tight alignment and turning curves along the traveling routes. The comfort consideration is more critical for APT/AB as contrasted to (private) AV whereby AV passengers have greater discretion in their travel schedules and travel routes. They may be able to command the AV to run at the most comfortable speeds as well as along enjoyable routes (e.g., fewer turns or interruptions by intersections). On the other hand, APT/AB passengers often board and alight for shorter travel time and distance, and the APT/AB system must ensure its reliability (e.g., speeds, punctuality, and comfort). The question is raised as to which levels of platooning (e.g., average speed, number of coupling modules) can offer passengers the comfort levels of HST or LRT, or the lower comfort levels of conventional buses?

This study, therefore, aims to investigate the passenger-vehicle-road geometrics interaction to develop a new sustainable transportation system focusing on the user perspective. The platooning operation of the emerging DART system in Singapore city is considered as a case study. This study is part of a larger project at TUMCREATE to plan for a city-scale DART network [9]. The platooning protocol is first developed to simulate the coupling/decoupling process. Platooning performance is then simulated on PTV VISSIM platform for various scenarios to compare the performance of DART platooning under several ride comfort levels: three bus comfort levels [17] and two railway criteria. The horizontal alignment and passenger ride comfort are linked based on the back-calculation of vehicle speeds at different lateral acceleration levels. The study provides a new platooning protocol and comprehensive evaluation on the trade-off between passenger ride comfort against platoon performance e.g., travel time and platoon trajectories.

The remaining paper is structured as follows. In the literature review section, the relevant scientific literature is summarized. In the methods section, detailed steps in conducting the traffic simulation are described. The results and discussion section reports and discusses the main results of this investigation, as well as the outlook for further study.

2. Literature Review

Human factors are always a concern and consideration in the era of AVs [18]. Recent research has focused more on technological development such as platooning control [19], vehicle concept [20], cost efficiency [21], timetabling and scheduling [22], the experimental platform for vehicle control [23], mapping and path planning [24]. Apart from the AV, truck platooning has also attracted much research interest in [7,8,25], but there are very few studies on bus platooning. Regarding passenger perceptions, the empirical evidence from passenger security on the AB can be found in [26], or public attitudes towards AB in [27]. There is still minimal knowledge regarding the points-of-view of passenger ride comfort when developing these AV/AB systems.

Le Vine et al. [28] are perhaps the first researchers who dealt with the ride comfort of AV passengers by assuming that they can enjoy leisure activities as train passengers on a high-speed train (HST) [29] or light rail transit (LRT) [30]. Their assumption is premised on the fact that there is no existing empirical evidence on passenger perception aboard an operational AV. On the other hand, the ride comfort threshold used in [31,32] is more appropriate for car drivers, where lateral acceleration $a_y \leq 1.8\text{m/s}^2$ is acceptable, $1.8\text{m/s}^2 < a_y < 3.6\text{m/s}^2$ is bearable, and $a_y > 5.0\text{m/s}^2$ exceeds the human's bearing ability. It is noted that car passengers feel uncomfortable at lower acceleration levels compared to car drivers because passengers are not involved in active control of the steering wheel.

Indeed, there have been experimental studies on ride comfort and acceleration thresholds on the conventional bus. Regarding ride discomfort associated with longitudinal acceleration, researchers in [33] studied the discomfort thresholds due to the bus braking and speeding-up, in which bus passengers start to feel uncomfortable when longitudinal acceleration reaches $a_x > +1.5\text{m/s}^2$ and the

deceleration/braking $a_x < -0.75 \text{m/s}^2$. Another study in France [34] analyzed the discomfort feeling of standing passengers regarding the bus interior design as well as the bus lane design. There are two levels of ride discomfort: Level 1 (uncomfortable) and Level 2 (loss of balance). Recently, a study in [17] surveyed the ride comfort of passengers at multiple postures aboard buses and suggested comfortable acceleration thresholds for the regular bus as well as for the future AB. The vehicle speeds at the discomfort threshold (uncomfortable at $a_y = 1.5 \text{ m/s}^2$) could be suggested when there is a high number of standing passengers while the vehicle speeds at a great discomfort threshold (very uncomfortable at $a_y = 1.75 \text{ m/s}^2$) could be suggested in case of all seated passengers. In any case, the vehicle speeds at the extreme discomfort threshold (extremely uncomfortable at $a_y = 2.0 \text{ m/s}^2$) must be avoided. The recent literature regarding typical ride comfort thresholds on various modes of transport are summarized in Table 1.

Table 1. Ride comfort thresholds at multiple directions.

Source	Longitudinal Acceleration a_x (m/s^2)	Lateral Acceleration a_y (m/s^2) Acceleration Rate of Change C (m/s^3)	Transport Mode	Passenger Posture
[29]	$a_x = +1.34$: max acceleration $a_x = -1.34$: max braking	$a_y = 0.98$–1.47: uncomfortable	Light rail	Not specific
[30]	$a_x = +0.58$: max acceleration $a_x = -0.54$: max braking	$a_y = 0.49$: uncomfortable	Heavy rail	Not specific
[31,32]		$a_y \leq +1.8$: acceptable, $a_y = +1.8 \div 3.6$: bearable $a_y > +5.0$: bearing ability	Car	Sitting
[35]	$a_x = -3.4$: comfortable braking	$a_y = 0.4$–1.3: safety within spiral curve $C = 0.3 \div 0.9$: comfortable rate of change	Car	Sitting
[28]		$a_y = 1.47$: uncomfortable on light rail $a_y = 0.49$: uncomfortable on heavy rail	AV	Sitting
[36]		$a_y = 0.6$–1.0: uncomfortable $C = 0.3$–0.6: uncomfortable	Guided bus	Not specific
[33]	$a_x > +1.5$: uncomfortable $a_x < -0.75$: uncomfortable		Bus	Sitting
[34]	$a_x < -1.4, a_x > +1.5$: level 1 $a_x < -2.2, a_x > +2.5$: level 2	$a_y < -1.4, a_y > +1.6$: level 1 $a_y < -2.0, a_y > +2.0$: level 2	Bus	Standing
[17]		$a_y \leq 1.5$: comfortable $a_y = 1.5 \div 1.75$: uncomfortable $a_y = 1.75 \div 2.0$: very uncomfortable $a_y > 2.0$: extremely uncomfortable	Bus, AB application	Sitting, leaning standing

Note: Level 1, Level 2: uncomfortable, and loss of balance.

Table 1 shows that only one study [28] investigated passenger ride comfort on the AV versus the levels of service at an intersection, with the study's limitation of a small-scale intersection. Vehicle platooning as the main advantage of AV technology has not been considered, neither was any bus ride comfort criterion included. The attainment of ride comfort levels on a train, a transport mode that has dedicated railway running at higher speed levels, is challenging in an urban context, especially for APT/AB with features of frequent stop-and-go and turning at the intersection. Herein, this study overcomes these limitations by: (1) developing a new platooning protocol for APT coupling/decoupling; (2) simulating a long corridor with several intersections for APT platooning from 3 to 5 modules; and (3) investigating the trade-off between DART platooning performance against passenger ride comfort on the bus and train.

3. Materials and Methods

Researchers have used PTV VISSIM (PTV Group, Karlsruhe, Germany, https://www.ptvgroup.com/en/) as a reliable platform for microscopic traffic simulation and generating plausible results of incidents for evaluating system performance [37–39]. Herein, PTV VISSIM can generate vehicle trajectories for detailed analysis. With the considerable functionality of driving behavior modeling, PTV VISSIM with the external driver model (EDM), was chosen to develop many traffic control strategies for the AV [40] or cooperative adaptive cruise controls [41]. These capabilities have motivated this current study to use EDM for simulating DART platoons in a real road network.

3.1. Development of Coupling/Decoupling Protocol Based on EDM

There is minimal available information on the coupling/decoupling process for APT platooning following a timetable with a fixed frequency and fixed-route that can well cater to passenger demand. The APT platooning was developed and illustrated with its operational dynamics in Figure 2, where vehicles/modules from two different lines/branches (Step 1) couple/merge at a pre-defined stop (Step 2) and run together along their shared-routes/trunks (Step 3) before splitting/decoupling/diverging to their destinations (Step 4). The merged-platoons can also be formulated from shorter platoons, and the merged-platoons split once completing their shared-routes. This merging/splitting process is different from truck platooning problem in [42], in which the trucks are able to merge and split while running at a high speed. The fleet size model was studied by [11] while the deployment planning was investigated in [12], resulting in the timetable input for the system operation.
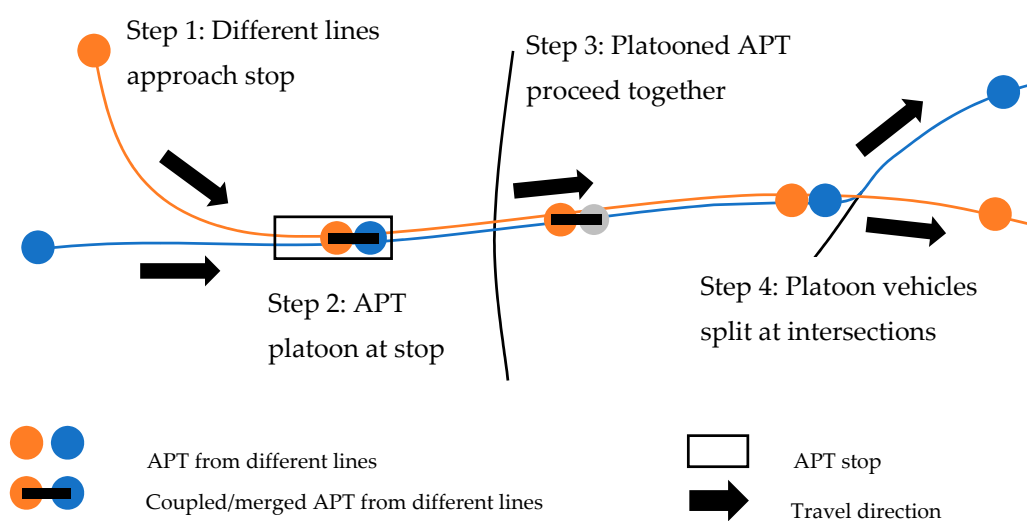

Figure 2. Illustration of the APT coupling based on bus platooning [43].

The coupling/decoupling protocol was developed with three main layers, namely strategic planning, tactical operation, and local behavior. Strategic planning follows the conventional public

transport planning but is extended with a coupling timetable which includes the time, location and line sequence of coupling. The departure times of all lines to be coupled together were adjusted to realize simultaneous arrivals at planned stops for coupling. Tactical operation supervises all APT vehicle operation in the network to guarantee the planed coupling, and to manage the cruising, dwelling of APT vehicles in case of both normal and delayed situation. Local behavior refers to autonomous driving behavior, and it complies to strategic planning and tactical operation. Local behavior corresponds to the consideration of passenger comfort and is developed based on the enhanced intelligent driver model (EIDM).

The local behavior was coded and interfaced with PTV VISSIM via the external driver model (EDM). There are five traffic flow conditions being considered by EIDM, namely free traffic, upstream jam front, congested traffic, downstream jam front and bottleneck sections [44]. The essential behavioral parameters in this study were the desired time gap T = 1.5 s, the desired maximum acceleration a = 1.3 m/s^2 and the desired deceleration b = 1.5 m/s^2. These acceleration and deceleration levels are based on the technical specification of the DART vehicle. Table 2 shows the λ_T, λ_a and λ_b as multiplication factors in different traffic flow conditions for the EIDM.

Table 2. Driving strategy matrix [45].

Traffic Condition	λ_T	λ_a	λ_b	Driving Behavior
free traffic	1	1	1	default/comfort
upstream front	1	1	0.7	increased safety
congested traffic	1	1	1	default/comfort
downstream front	0.5	2	1	high dynamic capacity
bottleneck	0.7	1.5	1	breakdown prevention

3.2. The Effects of Ride Comfort Criteria on DART Performance

After the platooning protocol was established, different scenarios were considered to evaluate the DART performance as follows (see the summary in Table 3). The long corridor included several intersections where the merged-platoons must navigate along sharp turning curves (see Figure 3). Apart from LRT and HSR ride comfort criteria, the other three lateral thresholds regarding passenger posture onboard [17] were also considered. For longitudinal acceleration and comfort, bus deceleration/braking $a_x = -0.75$ m/s^2 [33] was used to define the reduced speed areas, which is much lower than the desired deceleration *b* of the designed vehicle. Each merged-platoon included 3 to 5 modules running from start to end, where the starting point was a pre-defined merging stop, and the ending point was the last stop before decoupling. In this study, vehicle dynamical behavior within curves was the focus by using microscopic traffic simulation, where three scenarios were created with the merged-platoons consisting of 5, 4 and 3 modules. All scenarios were developed without traffic interference which can be considered as an ideal public transport prioritization scenario with no delay caused by the traffic light. The operating speed was 49 km/h on straight segments.

Table 3. Simulation scenarios.

Merged Platoon	Number of Modules	Platoon Formation From		Ride Comfort Criteria and Lateral Acceleration Thresholds					Traffic Conditions
		Platoon A	Platoon B	HST Comfort $a_y = 0.49$ m/s^2	LRT Comfort $a_y = 0.98$ m/s^2	Bus Standing $a_y = 1.50$ m/s^2	Bus Leaning $a_y = 1.75$ m/s^2	Bus Sitting $a_y = 2.0$ m/s^2	Dedicated Lane without Traffic Interference
Platoon 1	5	2	3	✔	✔	✔	✔	✔	✔
Platoon 2	4	2	2	✔	✔	✔	✔	✔	✔
Platoon 3	3	2	1	✔	✔	✔	✔	✔	✔

A small corridor including 3 intersections and 5 turning curves with different radii (Figure 3b,c) was extracted from the more extensive network that consisted of 18 DART lines, 5965 street sections with a total length of over 670km. In the planned DART network (Figure 3a), there are numerous turning curves which are different from the highway whose horizontal alignment is designed with larger curve radii that facilitate the formation of AV platoons. With different levels of lateral acceleration (a_y), vehicle speeds (*V* in km/h) can be back-calculated based on turning movements and curve radius (*R* in m) as Equation (1):

$$V = 3.6 \sqrt{a_y R} \tag{1}$$

This estimation is inferred from the basic equation that governs vehicle operation on a curve following the physical laws of motion [35]. The effects of a lateral jerk and turning duration have been neglected in this simple calculation. The proposed speeds can be used as the speed limit for AB along the corridors (see Table 4) as an important input for the reduced speed areas in VISSIM. The logic is that for new innovative APT systems coupled with the developed navigation technology, APT will be able to detect road geometry, curves and turning movement trajectory at any location along its route. Instead of using ArcGIS to measure distance [46], this study analyzed turning radii in AutoCAD after extracting coordinates of the travel corridor from Google Maps. Indeed, road horizontal alignment can be identified using mobile mapping systems and GIS spatial data as the investigation in [47,48].
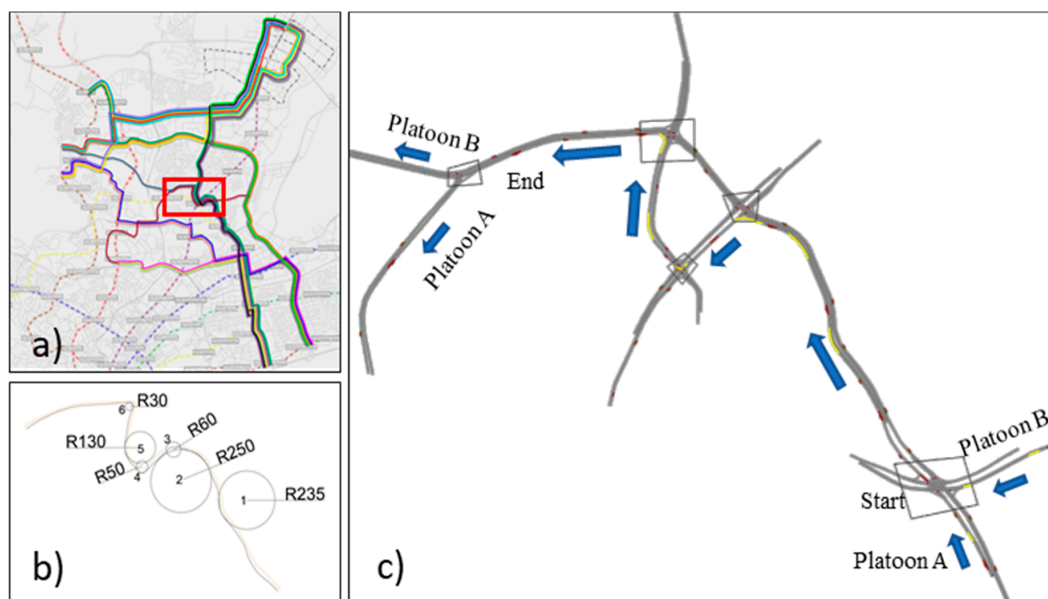
Figure 3. Planned DART network in Singapore (**a**) 18 lines; (**b**) extracted corridor consisting of 6 turning curves with stated radii as 6 reduced speed areas as input for traffic simulation; and (**c**) the formation of merged-platoons from platoon A and platoon B.

Table 4. Reduced speeds within curves, given the designed speed of 49km/h on straight segments.

Curve Order	Radius (m)	HST Comfort a_y = 0.49 m/s²	LRT Comfort a_y = 0.98 m/s²	Bus Standing a_y = 1.50 m/s²	Bus leaning a_y = 1.75 m/s²	Bus Sitting a_y = 2.0 m/s²
1	235	34	48	59 (49)	64 (49)	68 (49)
2	250	35	49	61 (49)	66 (49)	70 (49)
3	60	17	24	30	32	34
4	50	16	22	27	29	31
5	130	25	35	44	47	51(49)
6	30	12	17	21	23	24

Note: value inside the "()" is used once the calculated speed exceeds the designed speed of 49 km/h.

4. Results and Discussion

4.1. Platooning Behaviors and Trajectories

For each simulation scenario among the five ride comfort levels, the three platoon 1, platoon 2, and platoon 3 started at different time steps of 180s, 480s, and 780s, respectively, following a frequency of 5 minutes (see Table 5). In order to meet at the first stop to form platooning along the shared-route/trunk, the two platoons A and B departed much earlier from two branches/lines. Two additional terminals were allocated for individual modules to form platoons A and B (see Figure 4).

The trajectories of each module in platoons at different lateral acceleration levels along the corridor are shown in Figure 4, where the first stop is at the distance = 0 (m). The R software package was utilized for data processing. Two platoons A and B had merged at the first stop and traveled together to the end before splitting into two different destinations. The trajectories are quite similar even with the composition of 3, 4, or 5 modules. This has demonstrated the efficiency of the developed platoon protocol, in which the follower(s) always try to catch up with the leader according to specific conditions of the desired time gap (T = 1.5 s), the desired maximum acceleration (a = 1.3 m/s^2) and the desired deceleration (b = 1.5 m/s^2). Although different from car or truck platooning, APT platoons/modules must frequently dwell at stops for boarding and alighting passengers, as well as at signalized intersections whenever traffic light is not in its favor.

Table 5. Starting time and arrival time of three merged-platoons (unit: time step in second).

Merged Platoon	Start (s)	Arrival (s)				
		HST Comfort	**LRT Comfort**	**Bus Standing**	**Bus Leaning**	**Bus Sitting**
1	180	560	530	520	518	516
2	480	875	843	832	830	828
3	780	1170	1145	1130	1128	1126

Importantly, the effect of 5 levels of passenger comfort on DART travel time is shown based on the platoon trajectories. Due to the constraint of lateral acceleration, the designed speeds within curves are reduced substantially in cases of HST and LRT comfort criteria (see Table 4), especially along curve radii less than 100m (curves 3, 4 and 6). The delay gaps were cumulated by the travel distance after negotiating each curve and reached a maximum value at the ending stop. In Figure 4, a close-look at platoon 1 trajectories within curve 3 (R = 60 m) has shown an identical pattern of 5 modules within the platoon, but large differences between HST, LRT comfort criteria (a_y = 0.49, 0.98 m/s^2) and bus comfort thresholds (a_y = 1.5, 1.75 and 2 m/s^2).

Figure 5 presents the detailed information of 12 modules when they all appeared in the network. At the time-slice C-C, Platoon 1 (No = 1, 2, 3 from platoon B and 4, 5 from platoon A) was decoupled, while platoon 2 (No = 6, 7 from platoon B and 8, 9 from platoon A) were formed (in_platoon = 1) whereas platoon 3 (No = 10 from platoon B and 11, 12 from platoon A) has not been formulated yet (in_platoon = 0). This status is represented in the "speed" information, in which the identical velocity of ≈ 49 km/h is shown for platoon 1, and ≈ 6 km/h for platoon 2, whereas random speed levels are shown for platoon 3.
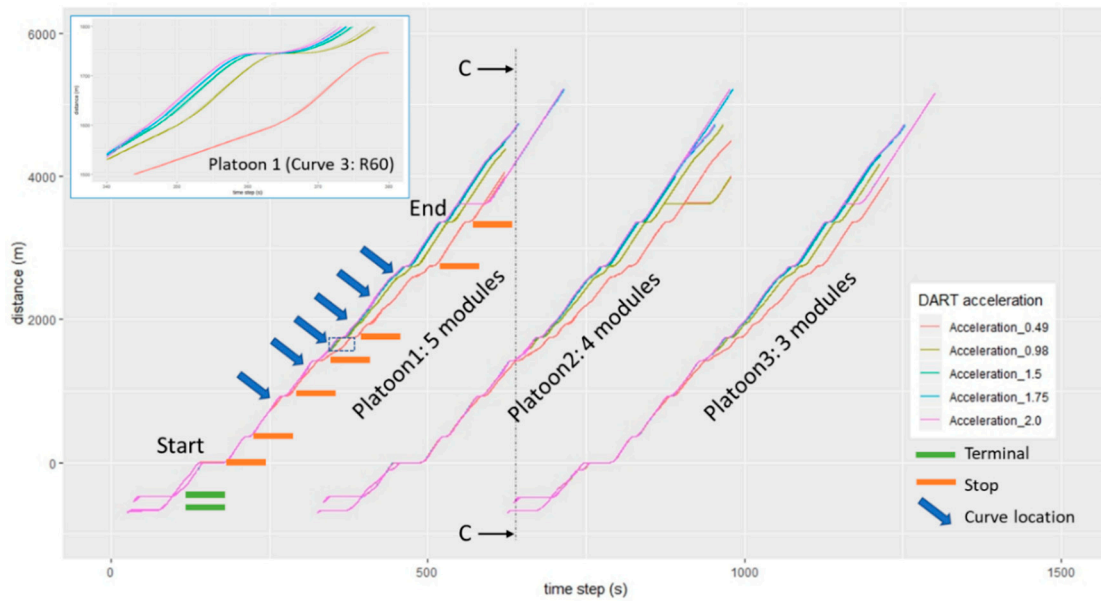
Figure 4. Trajectories of different merged-platoons of 3, 4, 5 modules. The locations of terminals, stops and curves along platoon 1 trajectories are also applied for platoon 2 and platoon 3.

Figure 5. Screenshot from VISSIM shows detailed information of vehicles all appeared at the time-slice C-C in Figure 4. The platooning information is illustrated based on the under-developed coupling/decoupling protocol.

4.2. Travel Time and Delay of DART Platoons

To evaluate the system performance of this APT system, the travel time and delay of the three platoons are summarized in Figure 6. The travel time for each merged-platoon (platoon 1, platoon 2, and platoon 3) is calculated when all modules in the platoon depart from the pre-defined stop (start point) to the final stop (endpoint). For the travel distance of 3.6 km, it takes roughly 340s ÷ 390s (equivalent to travel speeds of 33.23 ÷ 38.11 km/h) for the merged-platoons to finish the shared-route. As for the delay results, the travel time from the ride comfort criterion of a sitting bus is considered as a reference for comparison (see Equation (2)). The simulation scenario without traffic interaction can be considered as an ideal condition of traffic signal prioritization, which enables the platoons to run freely from start to end. The delay ratio is calculated as Equation (3):

$$Delay_i = Travel\ time_i - Travel\ time_{bus\ sitting} \qquad (2)$$

$$Delay\ ratio_i = \frac{Delay_i}{Travel\ time_i} \qquad (3)$$

The platooning protocol has formulated merged-platoons running as designed speeds along the corridor. Overall, the travel time and delay of merged-platoons following the ride comfort levels on the bus (bus standing, bus leaning, and bus sitting) are quite identical, meaning that it is feasible to operate the platoons following the bus standing comfort with lateral acceleration $a_y = 1.5$ m/s^2. On the other hand, the proportion of the delay is significant at ≈10% and ≈5% of travel time of all platoons following HST and LRT comfort criteria, respectively. It is noted that the platooning protocol is designed with maximum waiting time, e.g., of 60s, and the travel delay as 44s for a 3.6 km corridor (as shown in Figure 6) can be extended for a longer travel distance, which can deteriorate the pre-defined platooning sequence. This issue would be scaled up to the larger planned network of 18 lines, resulting in delay effects for the whole system.
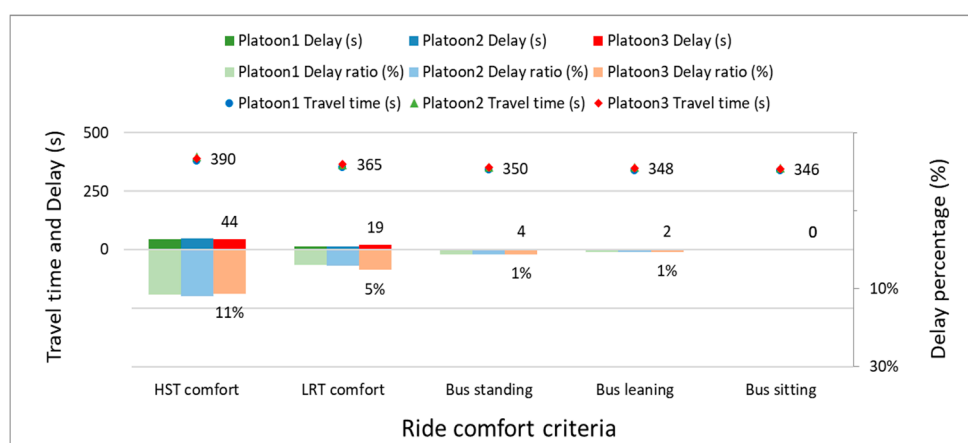
Figure 6. Travel time and delay (bus sitting as reference) of 3 platoons at different ride comfort criteria. The value inside the graphs is the travel time and delay of platoon 3 for reference.

Under different scenarios, the results have shown that the performance of DART platooning is influenced by turning curves, mainly the sharp turning curve with a radius less than 100m with significantly reduced speed constraints. The module number was varied to evaluate the dynamic effects of short and long platoons on the travel time. The results have shown that the number of modules, either 3, 4 or 5 in the merged-platoons, does not affect system performance (e.g., travel time, delay). However, the influence of ride comfort on travel delay is critical in an urban context when operating the DART system following HST and LRT comfort criteria. This investigation in passenger-vehicle-road geometrics interaction is crucial for the delay management of the system, towards the precisely designed timetable/frequency within the trade-off between system performance and passenger ride comfort.

With technological advancements, the emergence of autonomous public transport (APT) is ongoing worldwide towards the finalization of level 5 automation. Autonomous cars can provide many benefits and attract more drivers and passengers. However, this may also promote a car-dependent society. Therefore, how to improve the APT service quality to attract more passengers for using this innovative transport mode is of utmost importance that motivated this study. At first, the platooning protocol was developed in this study to support the new concept of electronically coupling/decoupling of APT platooning from 3 to 5 modules at multiple departures with a frequency of 5 minutes. The VISSIM EDM was utilized as an essential platform to realize the research motivation. Later, this study investigated the trade-off between system performance and rider comfort of APT passengers in an urban condition, in which the DART system was considered as a case study. The different lateral ride comfort thresholds were used in this study since there was no existing empirical evidence of passenger comfort levels on APT/AB, therefore, the literature data was referenced rationally.

This is the first time that APT platooning and passenger factors were investigated in a microscopic traffic simulation using the human-centric design approach. This method has emerged in recent decades

and is considered as the central concept in developing technology and transportation infrastructure for human beings [49,50]. The study has several limitations which can be improved in future research.

1. Firstly, the simulation scenarios allow to ideally prioritize the merged-platoons from start-to-end to improve travel speed and reduce travel time, but the delay impact on private cars have not been evaluated. This delay can be quite severe, as there can be a long waiting time for the whole APT platoon to pass by, especially during peak hours or in case of longer merged platoons e.g., of 10 modules. The trade-off is now expanding to private car drivers' perceptions and the whole network performance for both APT and private cars, which is more challenging to solve.

2. Secondly, due to a single operational corridor in this study, the delay investigation is not comprehensive. A more extensive network with multiple lines practicing coupling and decoupling, and traffic demand inputs are worth investigating for further study. It is noted that the planned DART network includes 18 lines with vast and complicated coupling/decoupling process across these lines. The performance issues may happen and deteriorate the whole system's reliability when the number of modules within each platoon, the number of APT lines and the network are scaled up.

3. Moreover, the effect of road excitation on passenger comfort, which is also an important influencing factor, has not been considered. For the urban bus, air-suspension is often equipped to maintain the high comfort levels at a lower natural frequency as well as the kneeling function by modifying the internal pressure [51]. It is of utmost crucial importance for passengers on APT/AB (also AV) to enjoy their activities onboard, meaning a smoother road surface is required as compared to the conventional bus system. The bus ride index [52] can be one of the potential solutions to solve this problem.

Author Contributions: Conceptualization, T.N.; data curation, T.N. and M.X.; formal analysis, T.N.; funding acquisition, A.R.; investigation, T.N. and M.X.; methodology, T.N.; project administration, T.N., A.R. and W.Y.D.; resources, M.X.; software, N.A.; supervision, B.L., Fritz Busch and W.Y.D.; visualization, T.N. and X.L.; writing–original draft, T.N. and M.X.; writing–review & editing, M.X., A.R., B.L., F.B. and W.Y.D.

Conflicts of Interest: The authors declare no conflicts of interest.

References

1. Kyriakidis, M.; Happee, R.; De Winter, J.C.F. Public opinion on automated driving: Results of an international questionnaire among 5000 respondents. *Transp. Res. Part F Traffic Psychol. Behav.* **2015**, *32*, 127–140. [CrossRef]

2. Miao, C.; Liu, H.; Zhu, G.G.; Chen, H. Connectivity-based optimization of vehicle route and speed for improved fuel economy. *Transp. Res. Part C Emerg. Technol.* **2018**, *91*, 353–368. [CrossRef]

3. Pudāne, B.; Rataj, M.; Molin, E.J.E.; Mouter, N.; van Cranenburgh, S.; Chorus, C.G. How will automated vehicles shape users' daily activities? Insights from focus groups with commuters in the Netherlands. *Transp. Res. Part D Transp. Environ.* **2019**, *71*, 222–235. [CrossRef]

4. Bansal, P.; Kockelman, K.M.; Singh, A. Assessing public opinions of and interest in new vehicle technologies: An Austin perspective. *Transp. Res. Part C Emerg. Technol.* **2016**, *67*, 1–14. [CrossRef]

5. Pudāne, B.; Molin, E.J.E.; Arentze, T.A.; Maknoon, Y.; Chorus, C.G. A time-use model for the automated vehicle-era. *Transp. Res. Part C Emerg. Technol.* **2018**, *93*, 102–114. [CrossRef]

6. Fahmy, T. Dubai Tests Autonomous Pods in Drive for Smart City. Available online: https://www.reuters.com/article/us-emirates-transportation-autonomous/dubai-tests-autonomous-pods-in-drive-for-smart-city-idUSKCN1GD5G6 (accessed on 22 April 2019).

7. Maiti, S.; Winter, S.; Kulik, L. A conceptualization of vehicle platoons and platoon operations. *Transp. Res. Part C Emerg. Technol.* **2017**, *80*, 1–19. [CrossRef]

8. Larsson, E.; Sennton, G.; Larson, J. The vehicle platooning problem: Computational complexity and heuristics. *Transp. Res. Part C Emerg. Technol.* **2015**, *60*, 258–277. [CrossRef]

9. Rau, A.; Tian, L.; Jain, M.; Xie, M.; Liu, T. Autonomous road transit (DART) for use-case capacity more than bus. In Proceedings of the mobil.TUM 2018 "Urban Mobility—Shaping the Future Together"—International Scientific Conference on Mobility and Transport, Munich, Germany, 13–14 June 2018.

10. Liu, T.; Ceder, A.A.; Rau, A. Scheduled platoons of public transport autonomous modular vehicles. In Proceedings of the 7th Symposium of the European Association for Research in Transportation (hEART2018), Athens, Greece, 5–7 September 2018.

11. Tao, L.; Avishai, C.; Rau, A. Public transit fleet size models of single-line autonomous modular system. In Proceedings of the 98th TRB Annual Meeting, Washington, DC, USA, 13–17 January 2019.

12. Liu, T.; Avi, A.; Andreas, C. Deployment planning of single-line modular-vehicle semi- rapid transit system. In Proceedings of the Conference on Advanced Systems in Public Transport and TransitData, Brisbane, Australia, 23–25 July 2018.

13. Radcliffe, D. Driverless Air Taxis, Drones, Pods: Dubai Puts Future Tech at Heart of Transportation. Available online: https://www.zdnet.com/article/driverless-air-taxis-drones-pods-dubai-puts-future-tech-at-heart-of-transportation/ (accessed on 22 April 2019).

14. Debusmann, B. World's First Autonomous Pods Unveiled in Dubai. Available online: https://www.arabianbusiness.com/transport/389656-worlds-first-autonomous-pods-unveiled-in-dubai (accessed on 22 April 2019).

15. De Almeida Correia, G.H.; Wiegmans, B.; Kockelman, K.; Qiang, M. Editorial of the TR Part C special issue on: "Operations with automated vehicles (AVs): Applications in freight and passenger transport". *Transp. Res. Part C Emerg. Technol.* **2018**, *95*, 493–496. [CrossRef]

16. Bassani, M.; Dalmazzo, D.; Marinelli, G.; Cirillo, C. The effects of road geometrics and traffic regulations on driver-preferred speeds in northern Italy. An exploratory analysis. *Transp. Res. Part F Traffic Psychol. Behav.* **2014**, *25*, 10–26. [CrossRef]

17. Nguyen, T.; NguyenDinh, N.; Lechner, B.; Wong, Y.D. Insight into the lateral ride discomfort of young-adult bus passengers at multiple postures: Case of Singapore. *Case Stud. Transp. Policy* **2019**. [CrossRef]

18. Kyriakidis, M.; de Winter, J.C.; Stanton, N.; Bellet, T.; van Arem, B.; Brookhuis, K.; Martens, M.H.; Bengler, K.; Andersson, J.; Merat, N.; et al. A human factors perspective on automated driving. *Theor. Issues Ergon. Sci.* **2019**, *20*, 223–249. [CrossRef]

19. Lam, S.; Katupitiya, J. Modeling and control of a platoon of autonomous buses. In Proceedings of the IEEE Intelligent Vehicles Symposium, Gold Coast, Australia, 23–26 June 2013; pp. 958–963.

20. Ginn, M.; Amuna, F.; Colmenares, J.E.; Stewart, A.; Diong, B.; Wang, Y.; Yang, J. Conceptual design and prototyping of a slim semi-autonomous bus rapid transit vehicle. In Proceedings of the IEEE SoutheastCon, Charlotte, NC, USA, 30 March–2 April 2017; pp. 1–6.

21. Zhang, W.; Jenelius, E.; Badia, H. Efficiency of semi-autonomous and fully autonomous bus services in trunk-and-branches networks. *J. Adv. Transp.* **2019**, 1–17. [CrossRef]

22. Cao, Z.; Ceder, A. Autonomous shuttle bus service timetabling and vehicle scheduling using skip-stop tactic. *Transp. Res. Part C Emerg. Technol.* **2019**, *102*, 370–395. [CrossRef]

23. Montes, H.; Salinas, C.; Fernández, R.; Armada, M. An experimental platform for autonomous bus development. *Appl. Sci.* **2017**, *7*, 1131. [CrossRef]

24. Yu, L.; Kong, D.; Yan, X. A driving behavior planning and trajectory generation method for autonomous electric bus. *Future Internet* **2018**, *10*. [CrossRef]

25. Bhoopalam, A.K.; Agatz, N.; Zuidwijk, R. Planning of truck platoons: A literature review and directions for future research. *Transp. Res. Part B Methodol.* **2018**, *107*, 212–228. [CrossRef]

26. Salonen, A.O. Passenger's subjective traffic safety, in-vehicle security and emergency management in the driverless shuttle bus in Finland. *Transp. Policy* **2018**, *61*, 106–110. [CrossRef]

27. Portouli, E.; Karaseitanidis, G.; Lytrivis, P.; Amditis, A.; Raptis, O.; Karaberi, C. Public attitudes towards autonomous mini buses operating in real conditions in a Hellenic city. In Proceedings of the IEEE Intelligent Vehicles Symposium, Los Angeles, CA, USA, 11–14 June 2017. [CrossRef]

28. Le Vine, S.; Zolfaghari, A.; Polak, J. Autonomous cars: The tension between occupant experience and intersection capacity. *Transp. Res. Part C Emerg. Technol.* **2015**, *52*, 1–14. [CrossRef]

29. Parsons Brinckerhoff, I. *Transit Cooperative Research Program Report #155: Track Design Handbook for Light Rail Transit*, 2nd ed.; Transportation Research Board: Washington, DC, USA, 2012.

30. Parsons Brinckerhoff, I. *Technical Memorandum: Alignment Design Standards for High-Speed Train Operation*; California High-Speed Rail Authority: Sacramento, CA, USA, 2009.

31. Shu, H.B.; Shao, Y.M.; Lin, W.; Xu, J. Computation-based dynamic driving simulation for evaluation of mountain roads with complex shapes: A case study. *Procedia Eng.* **2016**, *137*, 210–219. [CrossRef]

32. Xu, J.; Yang, K.; Shao, Y.; Lu, G. An experimental study on lateral acceleration of cars in different environments in Sichuan, Southwest China. *Discret. Dyn. Nat. Soc.* **2015**, *2015*, 494130. [CrossRef]

33. He, Y.; Yan, X.; Wu, C.; Chu, D.; Peng, L. Effects of driver's unsafe acceleration behaviors on passengers' comfort for coach buses. In *ICTIS 2013: Improving Multimodal Transportation Systems-Information, Safety, and Integration, Proceedings of the Second International Conference on Transportation Information and Safety (ICTIS), Wuhan, China, 29 June–2 July 2013*; American Society of Civil Engineers: Reston, VA, USA, 2013. [CrossRef]

34. Beurier, G. Analysis of the discomfort feeling of standing bus passengers on the TEOR T1 Rouen bus lane. *Procedia Soc. Behav. Sci.* **2012**, *48*, 425–434. [CrossRef]

35. AASHTO. *A Policy on Geometric Design of Highways and Streets*, 6th ed.; American Association of State Highway and Transportation Officials: Washington, DC, USA, 2011.

36. ARUP. *Guided Busway Design Handbook*; The British Cementitous Paving Association: Wokingham, UK, 2017.

37. Salgado, D.; Jolovic, D.; Martin, P.T.; Aldrete, R.M. Traffic microsimulation models assessment—A case study of international land port of entry. *Procedia Comput. Sci.* **2016**, *83*, 441–448. [CrossRef]

38. Nguyen, T.; NguyenDinh, N.; Lechner, B. Traffic microsimulation of roadwork in Singapore, a case study. In Proceedings of the 2nd Conference on Transport Infrastructure with Sustainable Development, Danang, Vietnam, 17–18 September 2016.

39. NguyenDinh, N.; Nguyen, T.; Yang, E.H.; Lechner, B. Life cycle cost assessment of engineered cementitious composite (ECC) precast pavement in Singapore. In Proceedings of the 11th International Conference on Concrete Pavements, San Antonio, TX, USA, 28 August–1 September 2016.

40. Li, Z.; Chitturi, M.V.; Zheng, D.; Bill, A.R.; Noyce, D.A. Modeling reservation-based autonomous intersection control in Vissim. *Transp. Res. Rec. J. Transp. Res. Board* **2013**, *2381*, 81–90. [CrossRef]

41. Zhong, Z. Assessing the Effectiveness of Managed Lane Strategies for the Rapid Deployment of Cooperative Adaptive Cruise Control Technology. Ph.D. Thesis, New Jersey Institute of Technology, Newark, NJ, USA, 2018.

42. Duret, A.; Wang, M.; Ladino, A. A hierarchical approach for splitting truck platoons near network discontinuities. *Transp. Res. Part B Methodol.* **2019**. [CrossRef]

43. Sethuraman, G.; Liu, X.; Bachmann, F.R.; Xie, M.; Ongel, A.; Busch, F. Effects of bus platooning in an urban environment. In Proceedings of the 22nd IEEE Intelligent Transportation Systems Conference (ITSC), Auckland, New Zealand, 27–30 October 2019.

44. Kesting, A.; Treiber, M.; Schönhof, M.; Helbing, D. Adaptive cruise control design for active congestion avoidance. *Transp. Res. Part C Emerg. Technol.* **2008**, *16*, 668–683. [CrossRef]

45. Kesting, A.; Treiber, M.; Helbing, D. Enhanced intelligent driver model to access the impact of driving strategies on traffic capacity. *Philos. Trans. R. Soc. A Math. Phys. Eng. Sci.* **2010**, *368*, 4585–4605. [CrossRef] [PubMed]

46. Shirazinejad, R.S.; Al-Bayati, A.J. Impact of advertising signs on freeway crashes within a certain distance in Michigan. In Proceedings of the Construction Research Congress 2018, New Orleans, LA, USA, 2–4 April 2018; pp. 698–705. [CrossRef]

47. Bassani, M.; Marinelli, G.; Piras, M. Identification of horizontal circular arc from spatial data sources. *J. Surv. Eng.* **2016**, *142*, 1–14. [CrossRef]

48. Marinelli, G.; Bassani, M.; Piras, M.; Lingua, A.M. Mobile mapping systems and spatial data collection strategies assessment in the identification of horizontal alignment of highways. *Transp. Res. Part C Emerg. Technol.* **2017**, *79*, 257–273. [CrossRef]

49. Mitchell, D.; Claris, S.; Edge, D. Human-centered mobility: A new approach to designing and improving our urban transport infrastructure. *Engineering* **2016**, *2*, 33–36. [CrossRef]

50. Bogren, L.; Fallman, D.; Henje, C. User-centered inclusive design: Making public transport accessible. In Proceedings of the International Conference on Inclusive Design–Royal College of Art, London, UK, 5–8 April 2009.

51. Kowarska, I.; Korta, J.; Kuczek, K.; Uhl, T. Fully equipped dynamic model of a bus. *Shock Vib.* **2014**, *2014*, 201952. [CrossRef]
52. Nguyen, T.; Lechner, B.; Wong, Y.D.; Tan, J.Y. Bus ride index—A refined approach to evaluate road surface irregularities. *Road Mater. Pavement Des.* **2019**. [CrossRef]

About the author

Te Ron Nguyen Van (or Teron Nguyen) was born in Hue, Vietnam. He obtained Engineer degree at Danang University of Science and Technology, Vietnam during 2004-2009. Subsequently, Teron completed the Master of Science in Transportation Systems at Technical University of Munich (TUM), Germany in the period 2011-2014 with the full scholarship from Vietnam government. In January 2015 he joined TUMCREATE, Singapore and had been working as a Research Associate. Teron started his PhD in April 2016 until the defence in Feb 2020, following the TUM-NTU joint PhD program between TUM and Nanyang Technological University, Singapore.

Teron is passionate about doing research on Road Design & Construction as well as Traffic & Transport Engineering. Particular research interests are Pavement design and maintenance, Life cycle cost analysis, Vehicle dynamics, Human factor, Public transport and Intelligent Transportation System.

Recent Publications:

1. Nguyen-Phuoc, D. Q., Oviedo-Trespalacios, O., **Nguyen, T.**, & Su, D. N. (2020). The effects of unhealthy lifestyle behaviours on risky riding behaviours – A study on app-based motorcycle taxi riders in Vietnam. *Journal of Transport & Health*, *16*, 100666, doi https://doi.org/10.1016/j.jth.2019.100666

2. **Nguyen T.**, Swolana P., Lechner B., Wong Y.D. (2020) A Comparison of Different Mathematical Bus Dynamics Models to Evaluate Road Roughness and Ride Comfort. In: Klomp M., Bruzelius F., Nielsen J., Hillemyr A. (eds) Advances in Dynamics of Vehicles on Roads and Tracks. IAVSD 2019. *Lecture Notes in Mechanical Engineering.* Springer, Cham, doi: https://doi.org/10.1007/978-3-030-38077-9_191

3. **Nguyen, T.**, Xie, M., Liu, X., Arunachanlam, N., Rau, A., Lechner, B., Busch, F. & Wong, Y.D. (2020). Platooning of Autonomous Public Transport Vehicles: A Trade-off between System Performance and Passenger Ride Comfort. TRB 2020 Annual Meeting, Washington DC, 12-16 Jan 2020.

4. **Nguyen, T.**, Lechner, B., Wong, Y.D. & Jun, Y. T. (2019). Bus ride index - a refined approach to evaluating road surface irregularities. *Road Material and Pavement Design*, doi: 10.1080/14680629.2019.1625806

5. **Nguyen, T.**, Lechner, B., Wong, Y.D. (2019). Response-type methods to evaluate road roughness: a state-of-the-art review. *European Transport Research Review, 11(1), 43*, doi: 10.1186/s12544-019-0380-6

6. **Nguyen, T.**, NguyenDinh, N., Lechner, B., & Wong, Y.D. (2019). Insight into the lateral ride discomfort of young-adult bus passengers at multiple postures: Case of Singapore. *Case Studies on Transport Policy*, 7(3), 617-627, doi: doi.org/10.1016/j.cstp.2019.07.002

7. **Nguyen, T.**, Xie, M., Liu, X., Arunachalam, N., Rau, A., Lechner, B., Busch, F. & Wong, Y.D. (2019). Platooning of Autonomous Public Transport Vehicles: The Influence of Ride Comfort on Travel Delay. *Sustainability* 2019, 11(19), 5237, doi: https://doi.org/10.3390/su11195237

8. **Nguyen, T.**, Swolana, P., Lechner, B., Wong, Y.D.,. An Experimental Comparison of Mathematical Heavy-duty City Bus Models to Evaluate Passenger Ride Comfort induced by Road Roughness. *Mathematical and Computer Modelling of Dynamical Systems* (Under Review, submitted September 2019).

9. Nguyen-Phuoc, D., Q., Gruyter, C., D., Nguyen, H., A., **Nguyen, T.**, Su, D., N., Kim, I., . Risky behaviours associated with traffic crashes among app-based motorcycle taxi drivers in Vietnam. *Transportation Research Part F: Psychology and Behaviour* (submitted Oct 2019).